Universidade de São Paulo -

Instituto de Geociências

Crystallization conditions and magmatic evolution of the Pedra Branca syenite based on the chemistry of accessory minerals

Victor Brugnera Camassari de Gonzaga

Orientador: Prof. Dr. Valdecir de Assis Janasi

Dissertação de Mestrado

Programa de Pós-Graduação em Mineralogia e Petrologia

São Paulo

2022

Universidade de São Paulo -

Instituto de Geociências

Crystallization conditions and magmatic evolution of the Pedra Branca syenite based on the chemistry of accessory minerals

Victor Brugnera Camassari de Gonzaga

Orientador: Prof. Dr. Valdecir de Assis Janasi

Tese apresentada ao Programa Geociências (Mineralogia e Petrologia) para obtenção do título de Mestre em Ciências

Área de concentração: Petrologia Ígnea e Metamórfica

Orientador: Prof. Dr. Valdecir de Assis Janasi

São Paulo

2022

Autorizo a reprodução e divulgação total ou parcial deste trabalho, por qualquer meio convencional ou eletrônico, para fins de estudo e pesquisa, desde que citada a fonte.

Serviço de Biblioteca e Documentação do IGc/USP
Ficha catalográfica gerada automaticamente com dados fornecidos pelo(a) autor(a)
via programa desenvolvido pela Seção Técnica de Informática do ICMC/USP

Bibliotecários responsáveis pela estrutura de catalogação da publicação:
Sonia Regina Yole Guerra - CRB-8/4208 | Anderson de Santana - CRB-8/6658

Brugnera C. de Gonzaga, Victor
Crystallization conditions and magmatic evolution of the Pedra Branca syenite based on the chemistry of accessory minerals / Victor Brugnera C. de Gonzaga; orientador Valdecir de Assis Janasi. -- São Paulo, 2022.
156 p.

Dissertação (Mestrado - Programa de Pós-Graduação em Mineralogia e Petrologia) -- Instituto de Geociências, Universidade de São Paulo, 2022.

1. Minerais Acessórios. 2. Plúton Pedra Branca. 3. Condições de Cristalização. I. Janasi, Valdecir de Assis, orient. II. Título.

UNIVERSIDADE DE SÃO PAULO
INSTITUTO DE GEOCIÊNCIAS

Crystallization conditions and magmatic evolution of the Pedra Branca syenite based on the chemistry of accessory minerals

VICTOR BRUGNERA CAMASSARI DE GONZAGA

Orientador: Prof. Dr. Valdecir de Assis Janasi

Dissertação de Mestrado

Nº 893

COMISSÃO JULGADORA

Dr. Valdecir de Assis Janasi

Dra. Sandra Andrade

Dr. Adejardo Francisco da Silva Filho

SÃO PAULO

2022

Acknowledgments

Foremost, I would like to express my sincere gratitude to my advisor Prof. Dr. Valdecir de Asis Janasi, for the continuous support, the patience, the discussions, for the incredible knowledge and guidance he provided.

I would like to thank Dra. Sandra Andrade, the conversations, and the insights into zircon thermometry and, specially, the lattice strain model were immensely helpful. Thanks to the NAP GeoAnalítica staff, with a special thanks to José Vinicius Martins, for guiding and helping me through all the days of analysis.

I would like to thank all the professors that, in one way or another, helped through this journey, such as Prof. Silvio Vlach, Renato Moraes, Adriana Alves, Rogério Azzone.

A special thanks to FAPESP (2019/17550-0), and the Coordenação de Aperfeiçoamento de Pessoal de Nível Superior (CAPES) for the financial support provided.

Finally, I must express my gratitude for my family and friends, for the continuous support and encouragement throughout the years. Thank you!

Resumo

O Sienito Pedra Branca, localizado na porção sul do Domínio Guaxupé, é um plúton neoproterozoico (594±6 Ma), composto por quatro unidades sieníticas principais, cada qual apresentando características mineralógicas distintas, porém composições químicas muito semelhantes. Com o objetivo de melhor entender a origem da variação mineralógica, foi proposto um estudo de detalhe a respeito das condições de cristalização, especificamente temperatura e fugacidade de oxigênio, que controlaram o desenvolvimento de cada unidade do plúton.

Como as fases acessórias são abundantes em todas as unidades do Pedra Branca, e registram as principais fases de cristalização (precoce, principal e tardia), decidiu-se realizar a caracterização, tanto das temperaturas de cristalização quanto da fugacidade de oxigênio, com base na química de apatita, titanita e zircão, que são as fases acessórias mais abundantes ao lado dos óxidos de Fe-Ti (ferri-ilmenita e magnetita).

Para a caracterização das temperaturas de cristalização foram adotados dois geotermômetros distintos; Ti em zircão (Ferry & Watson, 2007) e Zr em titanita (Hayden et al 2008). Obteve-se temperaturas de cristalização de zircão entre 750ºC e 800ºC, para os sienitos laminados saturados em sílica (unidade LSS) e 870 a 950ºC, para as unidades de sienitos supersaturados em sílica. Contrariamente, as temperaturas de titanita são mais altas (820 – 860ºC) na unidade LSS, e mais baixas (720 – 780ºC) nos sienitos supersaturados, onde este mineral é intersticial, sobrecrescendo os óxidos de Fe-Ti.

Para a caracterização da fugacidade de oxigênio foi adotado o método de Ce em zircão (Smythe & Brenan, 2016), em conjunto com o modelo de *lattice strain*, e foram obtidas condições de fO_2 distintas para cada unidade; as mais reduzidas registrando cristalização em torno do buffer NNO e as mais oxidadas entre NNO+1.0 e NNO+2.0

A partir dos resultados dos métodos aplicados é possível concluir que as diferentes unidades do plúton Pedra Branca registram condições de cristalização distintas, possivelmente sendo um dos fatores que explicam a variação mineralógica, característica do plúton.

Palavras-Chave: Sienito; Condições de cristalização magmática; Apatita; Zircão; Titanita.

Abstract

The Pedra Branca Syenite, located in the southern portion of the Guaxupé Domain, is a Neoproterozoic pluton (594±6 Ma) comprised of four main syenitic units, each with distinct mineralogical characteristics, but similar chemical compositions. To better understand the origin of the mineralogical variation, a detailed study was proposed regarding the crystallization conditions, specifically temperature and oxygen fugacity (fO2), which controlled the development of each unit.

As the accessory phases are abundant in all units of the Pedra Branca pluton, and they record the main stages of crystallization (early-, main- and late-stage), it was decided to carry out the characterization of both the crystallization temperatures and the oxygen fugacity based on the chemistry of accessory minerals, namely, apatite, titanite and zircon.

To characterize the crystallization temperatures, two different geothermometers were used; Ti in zircon (Ferry & Watson, 2007) and Zr in titanite (Hayden et al 2008). Zircon crystallization temperatures between 750ºC and 800ºC were obtained for the silica-saturated laminated syenites (LSS unit) and 870ºC to 950ºC for the silica-supersaturated syenite units. In contrast, titanite crystallization temperatures are higher (820-860ºC) in the LSS unit, and lower (720-780ºC) in supersaturated syenites, where this mineral is interstitial, occurring as an overgrowth of Fe-Ti oxides.

For the characterization of oxygen fugacity, the Ce in zircon geobarometer (Smythe and Brenan, 2016) and the lattice strain model, were adopted. Based on the results obtained it was possible to determine that the Pedra Branca pluton records increasingly more oxidizing conditions towards the border of the pluton, with values around the NNO+1 and NNO+2, whereas the oversaturated units present around the core of the pluton record values around the NNO buffer.

From the results obtained it was possible to determine that the different units of the Pedra Branca pluton record different crystallization conditions, which can explain the mineralogical differences observed in the pluton.

Keywords: Syenite, Magmatic crystallization conditions, Apatite; Zircon; Titanite.

Summary

Chapter I 14
1.1 Introduction 14
1.2 Materials and Methods 15
1.2.1 LA-ICP-MS 15
1.2.2 Electron Microprobe 16
1.3 Regional Geology 17
1.3.1 Mantiqueira Province 17
1.3.2 Socorro-Guaxupé Nappe 18
1.4 Syenitic Plutons 20
1.4.1 Capituva Syenite 20
1.4.2 Pedra Branca Syenite 22
Chapter II 25
2.1 Petrography 25
2.1.1 CSO 25
2.1.2 ESO 27
2.1.3 LSO 28
2.1.4 LSS 29
2.1.5 Crystal Size Distribution (CSD) in apatite 32
Chapter III 35
3.1 Results 35
3.1.1 Mineral Chemistry 35
3.1.2 Thermometry 67
3.1.3 Oxygen Fugacity (*f*O2) 76
Chapter IV 87
4.1 Discussion 87
4.1.1 Factors controlling zircon crystallization in the LSS unit 87
4.1.2 Apatite Homogeneity 88
4.1.3 Proposed crystallization sequence based on mineral crystallization temperatures 89
4.1.4 Conclusion 91
References 93
Appendix I - LA-ICP-MS Results 96
Appendix II – WDS and structural results 126
APPENDIX III – Thermometry 152
Appendix IV – SEM Images and Mineral Maps 155

APPENDIX V – CSD Files 159

Table of figures

Fig 1: Mantiqueira Province and orogens that compose it (Heilbron et al, 2004). Extracted from "Geologia do Continente Sul-Americano: Evolução da Obra de Fernando Flávio Marques de Almeida, Chapter XIII: Província Mantiqueira, pg. 207). 17
Fig 2: Geological map of the Socorro-Guaxupé Nappe and São Roque Domain. Extracted from Heilbron et al 2004 (A Província Mantiqueira. Geologia do Continente Sul-Americano: Evolução da obra de Fernando Flávio Marques de Almeida, São Paulo, Beca, pág 220). 19
Fig 3: Geological map of the Capituva Syenite and host rocks. 1- Gnaisses; 2- Granulites; 3- "Pink" equigranular granites; 4- Mangerite suíte; 5- Calc-alkaline porphyritic granites; 7- Poços de Caldas Massif; 8 – Coarse grained layered syenite (MCS); 9- Melasyenite (MS); 10- Fine to médium grained porphyritic syenite; 11- Layered syenite; 12-Fine grained quartz-syenite (FQS); 13- Coarse grained layered syenite; 14 – fine to medium grained quartz-syenite (FMQS); 15- Leucosyenite. Extracted from de Carvalho (2011). 21
Fig 4: Geological map of the Pedra Branca pluton, highlighting the different syenitic units that compose it. Legend: 4 and 5 – Pinhal-Ipuiúna Batholith (biotite granites and hornblende-biotite-quartz monzonites, respectively); 6- Anatectic biotite granites; 7- Saturated to unsaturated laminated syenite (LSS), 8- Laminated oversaturated syenite (LSO); 9- External oversaturated syenite (ESO); 10- Central silica-oversaturated syenite (CSO); 11- Poços de Caldas Alkaline Massif 23
Fig 5: Concordia diagram, with age of 594.7 ± 5.7 Ma, obtained, by Gonzaga (2018) by U-Pb SHRIMP for the saple PB-123 24
Fig 6: A) Photomicrograph of sample PB-09 depicting an alkali feldspar crystal with altered core, inclusions of pyroxene and opaque minerals and highlighting a myrmekite. B) General aspect of sample PB-09, showing the presence of two types of pyroxenes; enstatite (brown) and diopside (green). 26
Fig 7: Photomicrographs of sample PB-06 depicting pyroxene cores bordered by amphibole crystals. 27
Fig 8: Photomicrograph of sample PB-92B highlighting amphibole replacing diopside. 29
Fig 9: Photomicrograph of altered alkali-feldspar with acicular inclusions. B) Photomicrograph of sample PB-185 depicting actinolite associated with aegirine-augite. 30
Fig 10: A) Photomicrograph of sample PB-181, indicating the association between biotite, pyroxene, and amphibole. B) Photomicrograph of sample PB-185, highlighting the presence of large apatite crystals. C) Photomicrograph of sample PB-181 showing titanite bordering a hematite crystal 31
Fig 11: Pie-charts representing the proportion of fully included apatite crystals 32
Fig 12: Pie-charts representing in which mineral phase apatite is more likely to be included. . 33
Fig 13: Frequency versus crystal length histogram, with the cumulative curve plotted. A) PB-09 (CSO unit); B) PB-181A (LSS unit) 34
Fig 14: CSD plots of the population density (ln (n)) versus crystal length (L) obtained for apatite 34
Fig 15: Photomicrographs of pyroxene from the four different units: A) Sample PB-09 (CSO); clinopyroxene (diopside) and orthopyroxene (enstatite); B) Sample PB-123 (LSO); clinopyroxene associated (diopside) associated with amphibole (hornblende) and ilmenite; C)

Sample PB-06 (ESO); replacement of clinopyroxene (diopside) with amphibole (hornblende); D) Sample PB-181 (LSS); calcic-sodic pyroxene (aegirine-augite) associated with phlogopite and hematite. 37
Fig 16: Morimoto's classification diagrams (Morimoto, 1989); a) QJ diagram, where Q=Ca+Mg+Fe^{2+}, J=2*Na, "QUAD" is delimited by J/(Q+J) =0.2 and "Na" is delimited by J/(Q+J) =0.8. b) WEF-Jd-Ae and Wo-En-Fs classification diagrams, respectively. 38
Fig 17: $[Na]^{+}$ x Mg# diagram 39
Fig 18: Compositional variation diagrams representing the two major cationic exchanges on pyroxene. 40
Fig 19: Pyroxene REE pattern distribution in relation to whole rock analysis, gray lines represent the entire population analyzed, while colored lines represent the average results for each unit. 41
Fig 20: [Na]B x [Ca]B classification diagrams by Leak et al., (1997) 43
Fig 21: $[Si]^{T}$ x Mg# classification diagrams by Leak et al (1997). A) Classification for calcic-amphiboles with $[Na+K]^{A} < 0.5$; b) classification for calcic-amphiboles with $[Na+K]^{A} \geq 0.5$; c) classification for sodic-calcic amphiboles with $[Na+K]^{A} < 0.5$; d) classification for sodic-calcic amphiboles with $[Na+K]^{A} \geq 0.5$ 44
Fig 22: A) [Na]A x [K]A correlation diagram in amphibole; B) [Ti] x Mg# correlation diagram, in amphibole 45
Fig 23: Amphibole images from sample PB-181 depicting amphibole crystals under two different textural contexts 45
Fig 24: Amphibole cationic exchange diagrams from Pedra Branca pluton. A) Ti-Tschermakitic substitution; B) Tschermakitic substitution; C) Edenitic substitution 47
Fig 25: A) [Ti] versus REEs compositional diagrams; B) [Ti] versus [Zr] compositional diagram. 47
Fig 26: A) Comparison between the normalized REE distribution patterns between the different units. B) (Ce/Ce*) versus (Eu/Eu*) diagram; C,D,E) REE normalized distribution pattern for each unit, in relation to whole-rock data. 48
Fig 27: Photomicrographs of biotite from. A) Sample PB-09 (CSO unit); b) sample PB-123 (LSO unit); c) sample PB-181 (LSS unit); d) sample PB-185 (LSS unit). 49
Fig 28: Biotite classification diagrams by Deer et al (1992) 50
Fig 29: A) Fe2+ vs Mg# correlation diagram; B) [F] vs Mg# correlation diagram 50
Fig 30: A) Biotite cationic exchange diagram with Si-rich crystals highlighted. B) $[Al^{3+}]^{VI}$ x $[Si^{4+}]^{IV}$ diagram. C)[Ti] x $[Al]_{tot}$ diagram. 52
Fig 31: a) Typical apatite occurrence, small subhedral to euhedral crystals (sample PB-09; CSO unit); b) Large euhedral apatite crystal (sample PB-181; LSS unit) 53
Fig 32: Correlation diagrams representing two of the major substitution mechanisms for REE in apatite. 54
Fig 33: Whole-rock REE pattern normalized by chondrite 55
Fig 34: A and B) Cl x F correlation diagrams. C and D) Correlation diagrams between whole-rock SiO_2 and apatite Fluorine and Chlorine content. 56
Fig 35: A) SO^{3} x SiO^{2} correlation diagram; B) Si^{4+} + S^{6+} x P^{5+} correlation diagram 56
Fig 36: Apatite REE normalized distribution patterns for each unit, in relation to whole-rock data; A) PB-09 (CSO unit); B) PB-123 (LSO unit); C) PB-181 (LSS unit); D) PB-185 (LSS unit) 57
Fig 37: Ce/Ce* x Eu/Eu* diagram 58
Fig 38: Photomicrographs showing titanite in two different textural relation in sample PB-181 (LSS unit*)* 59
Fig 39: Photomicrographs showing titanite in two different textural relation in sample PB-181 (LSS unit) 59

Fig 40: Different correlation diagrams obtained from titanite data; A) Fe x Al diagram; B) Ti x Fe+Al diagram; C) Ti x F diagram; F x Al+Fe^{3+} diagram 60
Fig 41: Compositional correlation diagrams for titanite; a) U x Th; b) U x ∑REE; c) Zr x ∑REE; d) Zr x Sr. 61
Fig 42: a) Eu/Eu* x Ce/Ce* diagram; b) U x Zr/Hf correlation diagram 62
Fig 43: Chondrite-normalized REE patterns for titanite in relation to whole rock. Marked lines represent the sample average 63
Fig 44: Photomicrographs of zircon on different samples; A) Sample PB-09 (CSO unit); B) Sample PB-92B (LSO unit); C) Sample PB-185 (LSS unit; not analyzed); D) Cathodoluminescence image of the concentrated zircon from sample PB-123 (LSO unit). 64
Fig 45: Chondrite-normalized REE patterns for zircon. A) Comparison between the normalized REE distribution patterns between the different units. B) Sample PB-09 (CSO unit); C) Sample PB-22 (ESO unit); D) Sample PB-92B (LSO unit); E) Sample PB-123 (LSO unit); Sample PB-181 (LSS unit). Colored lines represent sample averages and gray lines represent the entire population of crystals analyzed 66
Fig 46: Correlation diagrams for zircon; arrow indicate core and rim analysis (core → rim); A) Th x U (ppm); B) ∑REE+Y x Hf (ppm); C) Zr/Hf x Eu/Eu*; D) Ti x Th/U 67
Fig 47: Ti-in-zircon crystallization temperatures for the Pedra Branca syenites 69
Fig 48: Tzircsat x Ti-in-zircon temperature 72
Fig 49: Zr-in-titanite temperatures calculated for the LSO (green) and LSS (yellow) units. 73
Fig 50: Ti in Amphibole and Ti in Biotite temperatures obtained for all units 75
Fig 51: Combination of obtained crystallization temperatures for all units, including zircon, titanite, amphibole and biotite temperatures. 76
Fig 52: Ce/Ce* x Eu/Eu* diagram for apatite 78
Fig 53: Logarithm of zircon-melt partition coefficients plotted versus the lattice-strain term for trivalent (A) and tetravalent cations (B) 80
Fig 54: Natural logarithm of the distribution coefficients plotted versus the effective radius of trivalent and tetravalent elements 81
Fig 55: REE^{3+} distribution coefficients plotted in relation to the lattice-strain term, showing the possible different lines for $Log\ DCe3 + zrc/melt$ interpolation; blue line represents the linear regression including all REEs, except Eu and Ce; the orange line represents the linear regression made using the REEs from Nd to Lu, excluding Eu, Pr, Ce and La; and gray line represents the linear regression made using only HREEs, from Gd to Lu. B) Distribution coefficients of tetravalent elements plotted versus the lattice strain term, showing the line used for $Log\ DCe4 + zrc/melt$ interpolation. 83
Fig 56: Compiled fO2 results for every unit, in relation to zircon-crystallization temperature .. 86
Fig 57: SEM image of a full thin-section of sample PB-181, superimposed with a mineral map, where it is highlighted with a red rectangle the presence of a mafic "strip"; composed of apatite (green), amphibole+biotite (purple), pyroxene (orange) and zircon(red), whrere the only crystals of zircon described in the LSS unit, highlighted in red circles, were identified. 88
Fig 58: Diagram illustrating the proposed crystallization sequence; the rectangles represent the range of crystallization temperatures obtained for each mineral phase 90

List of tables

Table 1: Beam parameters adopted for the analysis. 15
Table 2: Analytical conditions used for the WDS analysis..... 16
Table 3: Standards and calibration parameters adopted for each element, for the analysis of every mineral studied 16
Table 4: Sample used for each unit studied. 25
Table 5: Proposed crystallization sequence for the CSO unit. 27
Table 6: Proposed crystallization sequence for the ESO unit. 28
Table 7: Proposed crystallization sequence for the LSO unit. 29
Table 8: Proposed crystallization sequence for the LSS unit 32
Table 9: Values for SiO_2 and TiO_2 activity assumed for calculation of Ti-in-zircon geothermometry for the different units of the Pedra Branca Syenite. 68
Table 10: Summarized values for the parameter M. 71
Table 11: Compositional parameters (M and G) and estimated temperatures of zircon saturation (in degrees C) based on calibrationns by Gervasoni et al. (2016). 71
Table 12: Effective ionic radius (Å) of cations, in octahedral coordination with oxygen, which can replace Zr in zircon (Shannon, 1976). 84

Chapter I

1.1 Introduction

The Pedra Branca (Carvalho, 2011) and Capituva (Janasi, 1993) syenites are considered as records of the last magmatic event related to the neoproterozoic evolution of the northern part of the Socorro-Guaxupé Nappe region.

For a long time, the Pedra Branca syenite was interpreted as gneisses that were fenitized by alkaline fluids related to the intrusion of the Cretaceous alkaline massif of Poços de Caldas. Winters (1981) was the first to carry out a study completely dedicated to the Pedra Branca pluton, identifying its magmatic character and Neoproterozoic age. Subsequently, Carvalho (2011) carried out the first semi-detail mapping, showing that it consists of at least three different magmatic pulses of slightly different compositions, and presented a genetic model for the pluton (Carvalho et al, 2014).

The present work aims to further detail the key compositional differences that define each syenitic unit of the Pedra Branca Syenite, and to quantify the crystallization conditions of each unit, though the use of accessory minerals as the main tool.

The use of accessory minerals is in full development in several areas of geological interest, whether in geochronology, or in the characterization of magmatic or metamorphic conditions. The possibility of using *in situ* methods of analysis of trace elements and their isotopes, in solid material, has opened numerous possibilities in these fields.

The present work focuses on the understanding and application of the main methods of characterization of magma crystallization conditions, aiming to quantify crystallization temperatures, and oxygen fugacity (fO_2), using as a tool the chemistry of the accessory minerals, zircon, apatite and titanite.

Currently zircon is the main accessory mineral used in studies of geological interest, due to a series of chemical and structural properties that preserve the chemical characteristics of the moment of its crystallization. In the present work, two zircon-based methods are studied and examples of each method in natural samples are presented, namely, the Ti in zircon thermometer (Ferry & Watson, 2007) and the Ce in zircon oxybarometer (Smythe & Brenan, 2016).

Apatite is a mineral that has received a lot of attention recently due to its ability to incorporate large amounts of trace elements, mainly LREEs, in its composition, while being resistant to physico-chemical processes post-crystallization, in such a way that, similarly to zircon, it may be used to infer the composition of the melt from which it crystallized. Apatite saturation can be used as a thermometer (Harrison & Watson,

1984), and its composition can be is mainly used to qualitatively estimate redox conditions of magmas, based on the study of the Ce and Eu anomalies.

Amongst the accessory minerals discussed in the present work, titanite is the least used in the characterization of crystallization conditions, despite sharing many of the same characteristics mentioned for zircon and apatite, such as the ability to incorporate a series of trace elements in its composition, while being resistant to post-crystallization processes. The Zr in titanite geothermomether (Hayden et al, 2008), allows it to be used to estimate the crystallization temperature of granitic magmas.

1.2 Materials and Methods

1.2.1 LA-ICP-MS

Chemical analysis of the minerals of interest (pyroxene, amphibole, biotite, apatite, titanite and zircon) were obtained by LA-ICP-MS, *in situ*, in the Geoanalitica Core Facility, at Institute of Geosciences, University of São Paulo. On average, 10 to 15 crystals of each mineral, per sample, was analyzed by Laser Ablation sampler (New Wave Up-213) coupled with a mass spectrometer (model iCAP Q – Thermo Scientific). NIST-610 glass was used as an external reference material and was also run every 30 minutes for drift correction. The Ca content was used as an “internal standard” for all Ca-bearing minerals. Ca contents were previously obtained by electron microprobe; in the case of apatite and titanite, where these values remain essentially constant, stoichiometric values were used. The parameters adopted for each type of analysis are compiled in table 1. Each run consisted of ~30-60s “blank” (detector on without firing the sample) and ~50-60s “sample signal” (with laser on), totaling 80-120s. The software Glitter 4.5 was used for data treatment, specifically to remove signals related to mineral inclusions during the analyses.

Type	**Size**	**Beam speed**	**Beam Potency**	**Frequency**	**Duration**
Raster	55 µm	2 µm/s	80%	15Hz	80-120s
Spot	15 – 20 µm	-	80%	15 Hz	80-120s

Table 1: Beam parameters adopted for the analysis.

1.2.2 Electron Microprobe

Chemical analysis of different minerals, such as pyroxene, amphibole, biotite, apatite and titanite of the 7 samples were obtained by Electron Probe Microanalyzer JEOL – JXA – FE – 8530, in the electronic microprobe laboratory of the Geoanalitica Core Facility, Institute of Geosciences of the University of São Paulo. The parameters adopted for the different analysis are compiled in table 2 and 3.

Mineral	Voltage	Beam current	Beam diameter
Amphibole	15 kV	20 nÅ	5 – 10 µm
Apatite	15 kV	20 nÅ	5 – 10 µm
Biotite	15 kV	20 nÅ	5 – 10 µm
Pyroxene	15 kV	20 nÅ	5 – 10 µm
Titanite	15 kV	20 nÅ	5 – 10 µm

Table 2: Analytical conditions used for the WDS analysis

Table 3 compiles the standards used for the calibration of the different elements analyzed.

Element	X-Ray	Crystal	Standard Amphibole	Standard Apatite	Standard Biotite	Standard Pyroxene	Standard Titanite
Na	Ka	TAP	Albite	Albite	Albite	Albite	Albite
Si	Ka	TAP	Hornblende	Anorthoclase	Diopside	Augite	Diopside
Y	La	TAP	-	Y-phosphate	-	-	Y-phosphate
Fe	Ka	LIFL	Fayalite	Ilmenite	Fayalite	Fayalite	Fayalite
Mn	Ka	LIFL	Fayalite	Fayalite	Fayalite	Fayalite	Fayalite
La	La	LIFL	-	La-phosphate	-	-	La-phosphate
S	Ka	PETJ	-	Meionite	-	-	-
P	Ka	PETJ	-	Fluorapatite	-	-	-
Sr	La	PETJ	-	Strontianite	-	-	-
Ti	Ka	PETJ	-	Rutile	-	-	Rutile
Cl	Ka	PETJ	Sodalite	Sodalite	Sodalite	-	-
Ca	Ka	PETJ	Wollastonite	Fluorapatite	Wollastonite	Wollastonite	Wollastonite
Ce	La	PETJ	-	Ce-phosphate	-	-	Ce-phosphate
F	Ka	TAPH	Fluorapatite	Fluorapatite	Fluorapatite	-	Fluorapatite
Mg	Ka	TAPH	Diopside	Diopside	Diopside	Diopside	Diopside
Al	Ka	TAPH	Hornblende	Corundum	Anorthoclase	Augite	Anorthite
K	Ka	PETJ	Orthoclase	-	Orthoclase	Orthoclase	Orthoclase

Table 3: Standards and calibration parameters adopted for each element, for the analysis of every mineral studied

1.3 Regional Geology

1.3.1 Mantiqueira Province

The Mantiqueira Province represents a Neoproterozoic orogenic system, located in the S-SE regions of Brazil, composed of the Araçuaí, Ribeira, Brasília Sul, Apiaí, Dom Feliciano and São Gabriel orogens (Fig.1), and can be subdivided into three large segments, namely: Northern (which corresponds to the Araçuai Orogen), Central (corresponding to the Ribeira orogen and Apiaí, São Roque and Embu terrains) and Southern (corresponding to the Dom Feliciano and São Gabriel orogens). The Mantiqueira orogenic system developed during the Pan-Africa/Brasiliano orogeny, which resulted in the amalgamation of the paleocontinent of western Gondwana (Heilbron et al, 2004). The following simplified stratigraphic subdivision was proposed by Heilbron et al, applicable to all segments of the Mantiqueira Province (Northern, Central and Southern):

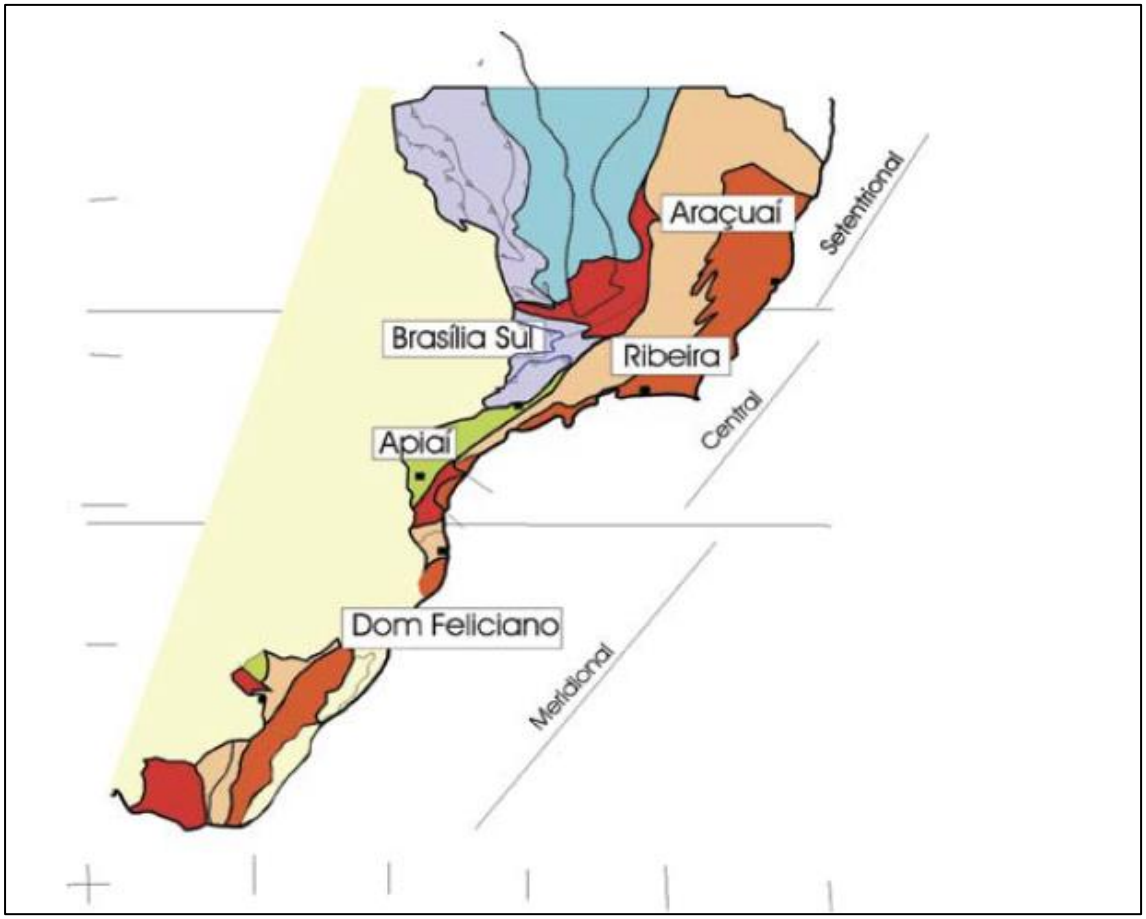

Fig 1: Mantiqueira Province and orogens that compose it (Heilbron et al, 2004). Extracted from "Geologia do Continente Sul-Americano: Evolução da Obra de Fernando Flávio Marques de Almeida, Chapter XIII: Província Mantiqueira, pg. 207).

- Presence of Archean and/or Paleoproterozoic basement, older than 1.7 Ga.
- Metasedimentary sequences deposited in Paleoproterozoic to Mesoproterozoic intracontinental basins.
- Neoproterozoic metasedimentary and metavulcanossedimentary sequences that include passive margin sequences, sequences related to ocean closure and continental collision.
- Pre-collisional Neoproterozoic granitoids, generated in intra-oceanic magmatic arcs or active continental margins.
- Syncolisional Neoproterozoic granitoids.
- Late-orogenic sedimentary basins and post-collisional magmatism

The Araçuaí orogen can be subdivided into three main tectonic domains, being the external domain, characterized as a band of folds and thrusts, the internal domain, which represents the metamorphic-anathetic core of the orogen, and the northern inflection, which contains segments of the two previous domains, but has its own tectonic features (Campos Neto et al, 2004).

The São Gabriel orogen is considered an accretionary orogen, recording the most complete record of juvenile crust formation in the Mantiqueira province, while the Dom Feliciano orogen is comprised of Neoproterozoic passive margin sequences, in addition to magmatic arcs and remains of the Paleoproterozoic-Archean basement (Campos Neto et al, 2004).

The southern portion of the Brasilia orogen consists of a sequence of nappes, with vergence towards the São Francisco craton, which records Neoproterozoic subduction and collision episodes. The nappes of the southern portion of the Brasília orogen can be subdivided into two groups; upper nappes, which record high-grade metamorphism (granulite facies), and lower nappes, which record low-grade metamorphism, with a large presence of calc-alkaline granitoid plutons, in part, interpreted as remnants of a magmatic arc. Three distinc tectonic domains were defined in the region, namely, Nappe Socorro-Guaxupé, which is a domain composed mainly of magmatic arcs, developed in an active continental margin; Andrelândia terrain, which represents a subducted continental terrain; and the Lima Duarte nappes (Campos Neto et al, 2004).

1.3.2 Socorro-Guaxupé Nappe

The Socorro-Guaxupé Nappe (SGN) is an allochthonous terrain, interpreted as being formed in a continental magmatic arc, during a Neoproterozoic collisional event

(Campos Neto & Caby, 1999). According to Campos Neto & Caby (2000), the Socorro-Guaxupé Nappe is composed of three distinct allochthonous terrains, which represent differenct crustal levels; the Lower Granulitic Unit, the Intermediat Diatexitic Unit and the Upper Migmatitic unit, The SGN is further divided into two regions, the Guaxupé lobe, to the north, and the Socorro lobe, to the south (Fig. 2).

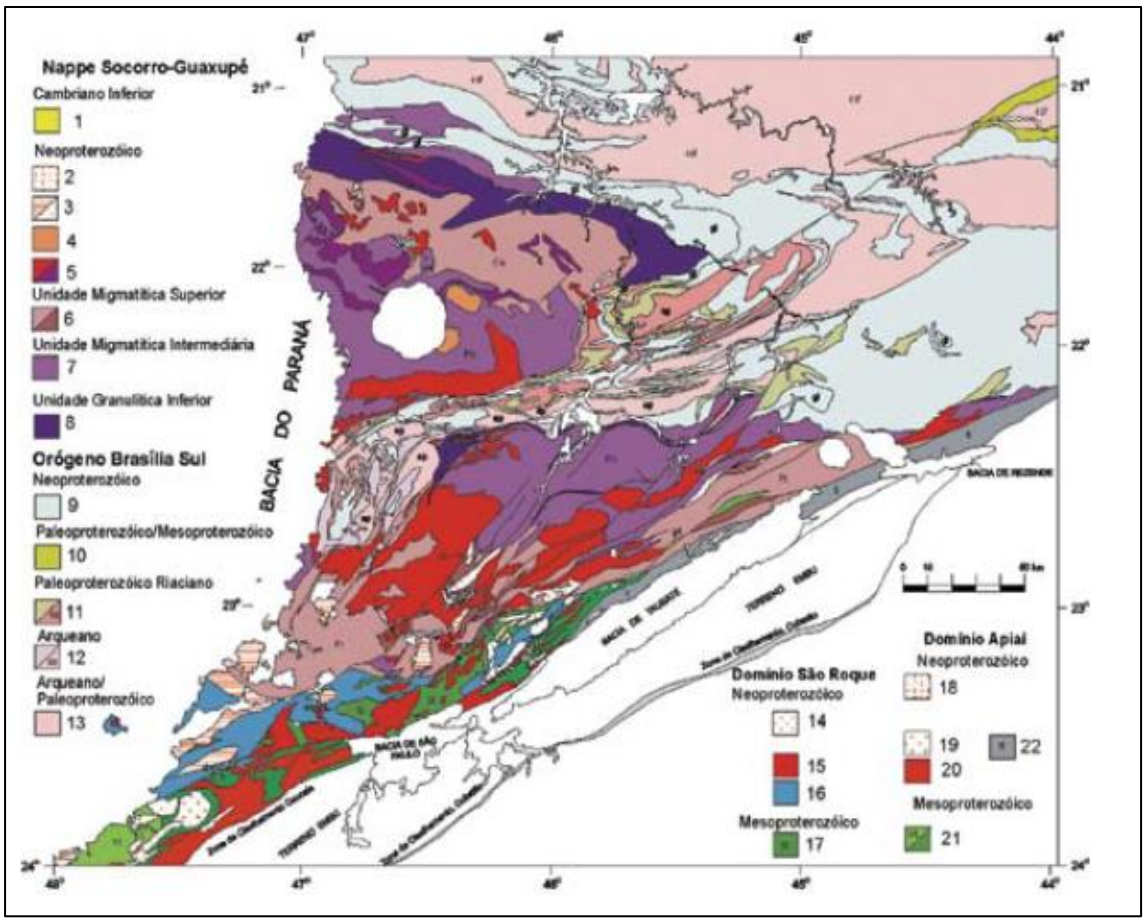

Fig 2: Geological map of the Socorro-Guaxupé Nappe and São Roque Domain. Extracted from Heilbron et al 2004 (A Província Mantiqueira. Geologia do Continente Sul-Americano: Evolução da obra de Fernando Flávio Marques de Almeida, São Paulo, Beca, pág 220).

The lower Granulitic unit is composed mainly of granulite and gneisses of enderbitic to charnockite-enderbite compositions, with gabbro-noritic and tholeiitic gneisses occurring locally (Campos Neto et al, 2004). The Intermediate Diatexitic unit is named Pinhal Complex, in the Guaxupé lobe (Wenick & Penalva, 1980), being composed mainly of metaluminous orthogneisses, in the form of stromatic migmatites, with kinzingite gneisses and calc-silicate gneisses xenoliths occurring locally. The Upper Migmatitic Unit is characterized by the presence of a wide variety of metasedimentary rocks, generally in the form of banded gneisses (sillimanite-garnet-biotite-gneisses), with intercalations of quartzite and quartz-gneisses.

Janasi (1997) characterized three syn-orogenic granitic units present in the Socorro-Guaxupé Nappe, interpreted as being formed from partial melting of continental

crust, dated between 630 and 620 Ma, namely, the São José do Rio Pardo Suite and the Pinhal and Nazaré Paulista granites. The São José do Rio Pardo Suite is mainly composed of mangerites and quartz-mangerites, formed under high temperature conditions (~1000ºC), with associated pink hololeucocratic granites and syenits. The Pinhal granites are characterized by their association with migmatites, and correspond mainly to nebulitic biotite-granites, derived from tonalitic to granodiorite protoliths. The Nazaré Paulista granites, of peraluminous composition, derive from metasedimentary protoliths and were formed under milder temperature conditions, in relation to the other granite units. It is interpreted that the formation of these three granite units occurred in a short period of time(~10Ma) suggesting the presence of an intense thermal anomaly in the region, causing large-scale anatexis (Janasi, 1997).

The Guaxupé lobe is delimited by two shear zones and a sedimentary basin, named, Campo do Meio belt, to the northeast (Morales, 1993), and Ouro Fino belt, to the southeast (Ebert et al, 1991) and the Paraná basin, to the west, respectively (Fig.2).

The predominant lithology found in the Guaxupé lobe is comprised of granulitic-gneiss, of charnokitic to enderbitic composition, often interspersed with mafic granulites and ultramafic rocks (metagabronorites, metanorites and metapyroxenites).

The charnockitic suites found in the Socorro-Guaxupé Nappe, occur mainly in the Guaxupé lobe, in the form of linear bodies, of varied compositions, from norites to enderbite-charnockites, characterized by high potassium content. They represent the Nappe's basal units, containing some of the oldest records of Neoproterozoic magmatism in the area, with ages ranging between 667 to 643 Ma (Campos Neto & Caby, 2000; Basei et al, 1995).

In addition to the granulites described, a wide variety of granitic rocks occur throughout the Guaxupé lobe, with occurrences of plutonic and metaplutonic rocks of different compositions, where four main sets of granitoids are characterized, namely, the São José do Rio Pardo suite, comprised of mangerites and charnokites, the K-rich calc-alkaline granitoids, the syenitic plutons (Pedra Branca and Capituva) and the "pink" granites, associated with regional migmatization (Janasi, 1992).

1.4 Syenitic Plutons

1.4.1 Capituva Syenite

The Capituva syenite is a pluton of Neoproterozoic age (~610 Ma; Carvalho & Janasi, 2012), intrusive in high-grade metamorphic rocks of the northern portion of the Socorro-Guaxupé Nappe and, together with the Pedra Branca syenite, represent the last Neoproterozoic magmatic events in the region.

The ellipsoidal pluton is approximately 180km^2 and, according to Janasi (1993), was formed from four distinct magmatic pulses of similar composition.

The first three pulses formed well-defined, medium to coarse grained syenitic bodies, where the coarse (porphyritic) variety is located at the edges, while the layered, medium to coarse grained variety occurs in the pluton's core. The textural variation described reflects the increase in matrix grain size, associated with a decrease in the concentration of alkali feldspar megacrystals. The fourth pulse formed a core comprised of mela-syenites, bordered by coarse-graned layered syenites, which often occur associated with fine to medium-grained quartz-syenite bodies (Janasi, 1993).

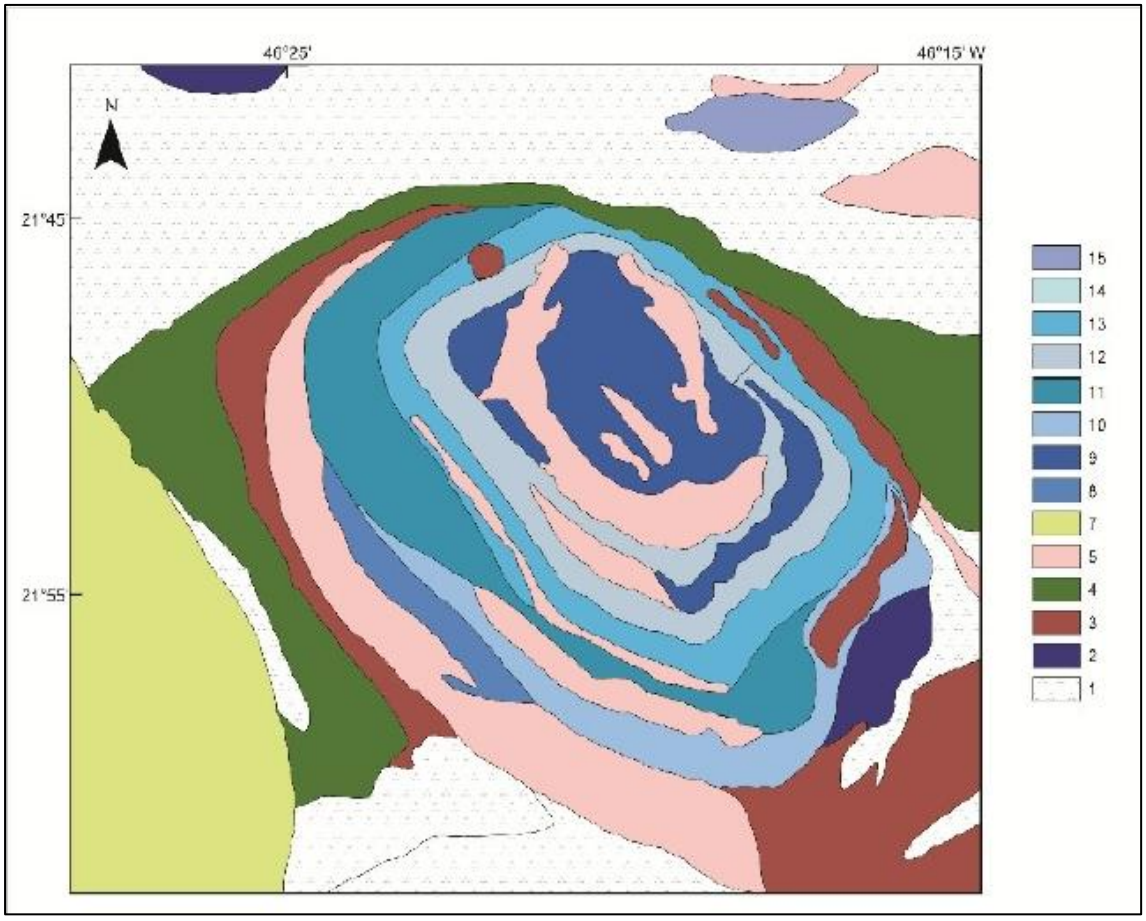

Fig 3: Geological map of the Capituva Syenite and host rocks. 1- Gnaisses; 2- Granulites; 3- "Pink" equigranular granites; 4- Mangerite suíte; 5- Calc-alkaline porphyritic granites; 7- Poços de Caldas Massif; 8 – Coarse grained layered syenite (MCS); 9- Melasyenite (MS); 10- Fine to médium grained porphyritic syenite; 11- Layered syenite; 12-Fine grained quartz-syenite (FQS); 13- Coarse grained layered syenite; 14 – fine to medium grained quartz-syenite (FMQS); 15- Leucosyenite. Extracted from de Carvalho (2011).

The occurrence of host-rock xenoliths is quite common and is interpreted as the result of the collapse of the roof and walls of the former magmatic chamber. The xenoliths composition varies from calc-alkaline granitoids, in the older units, to porphyritic

syenogranites, in the more recent syenite unit. The contacts between the Capituva syenite and the host rocks are truncated, where the difference between the tectonic foliation, present in the host rocks, and the magmatic foliation from the syenites, indicates the occurrence of a forced intrusion (Janasi, 1993).

The different units of the Capituva pluton are compositionally similar, with the main differences occurring between the quartz-syenite (FQS) and layered syenites (MCS) units; the FQS unit is enriched in SiO_2 and CaO but impoverished in Al_2O_3 and Na_2O, in relation to the MCS unit. It is interpreted that the Capituva syenite is derived from lamprophyric melts, formed from partial melting of enriched lithospheric mantle, during subduction events (Janasi, 1993).

1.4.2 Pedra Branca Syenite

The Pedra Branca pluton is in the southern region of Minas Gerais, Brazil, covers an area of approximately 90 km^2 and is truncated by the Poços de Caldas Massif, which is comprised of almost exclusively nepheline-syenites of Cretaceous age (Carvalho, 2011).

The Pedra Branca pluton is comprised of four distinct syenite units (Fig. 4), three of them presenting similar composition, Si-oversaturated syenites, with slight textural differences. The fourth unit constitutes the majority of the pluton's border, comprised of Si-undersaturated to saturated syenite (Carvalho & Janasi, 2012).

Mafic to ultramafic rocks are often found in the different units of the Pedra Branca pluton, occurring mainly in the form of lenses and enclaves, generally concordant with the main magmatic foliation (Carvalho & Janasi, 2012).

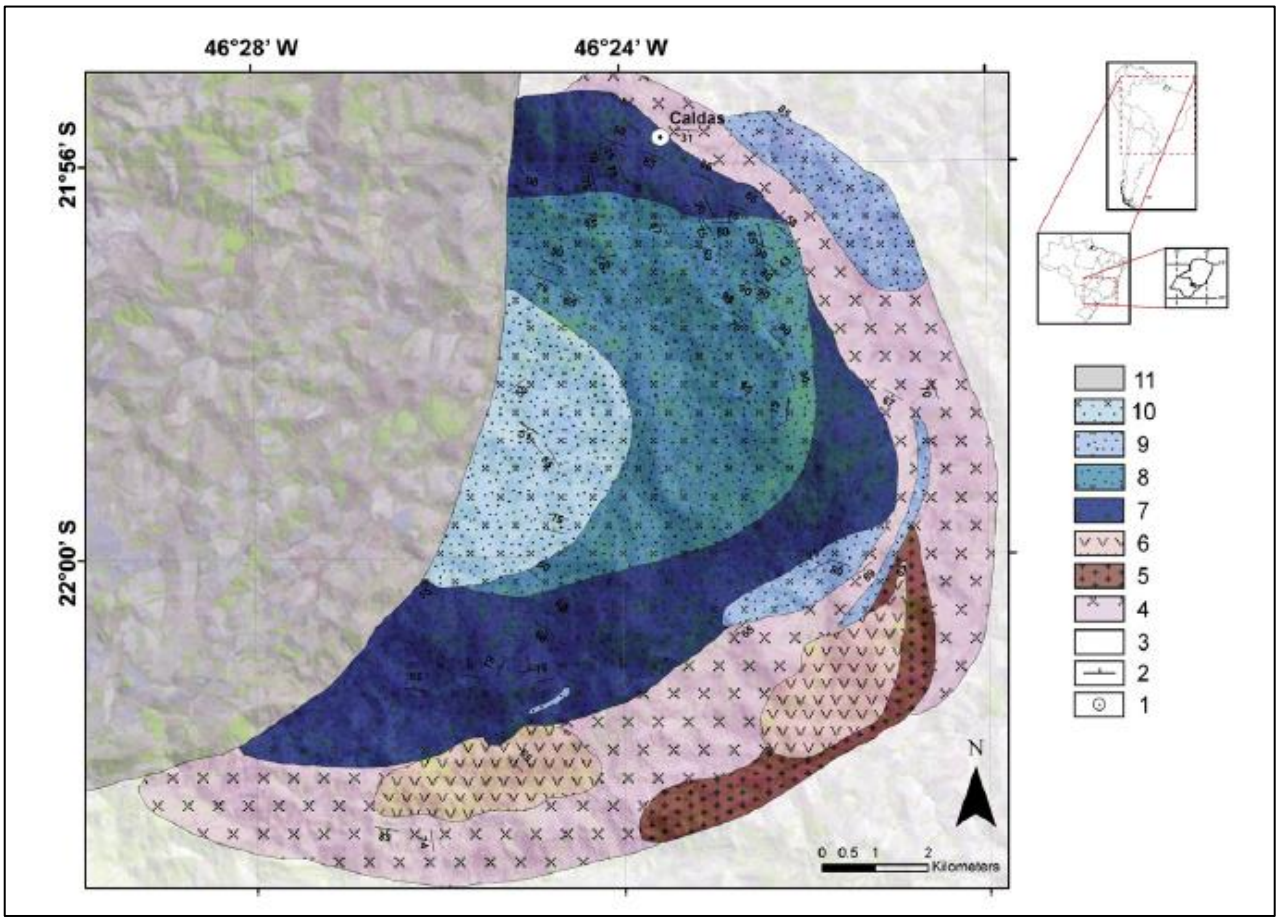

Fig 4: Geological map of the Pedra Branca pluton, highlighting the different syenitic units that compose it. Legend: 4 and 5 – Pinhal-Ipuiúna Batholith (biotite granites and hornblende-biotite-quartz monzonites, respectively); 6- Anatectic biotite granites; 7- Saturated to unsaturated laminated syenite (LSS), 8- Laminated oversaturated syenite (LSO); 9- External oversaturated syenite (ESO); 10- Central silica-oversaturated syenite (CSO); 11- Poços de Caldas Alkaline Massif

1.4.2.1 Previous works

Winters (1981) was the first author to propose the magmatic origin and Neoproterozoic age for the Pedra Branca pluton. Prior to his work the pluton was interpreted as basement gneisses metasomatized by alkaline fluids from the Cretaceous Poços de Caldas intrusion.

Semi-detail mapping (Janasi, 1997; Carvalho, 2011; Carvalho & Janasi, 2012) revealed that the pluton is formed by four distinct units, all K-rich nature and enriched in some trace-elements such as the REE, and further studies characterized the key compositional differences between the units (Carvalho & Janasi, 2012; Carvalho et al, 2014). Carvalho (2011) also provided a description of the main features of each unit, and detailed key mineralogical differences between them.

Carvalho & Janasi (2012) showed that the Pedra Branca pluton crystallized under high temperature (1060 – 1090ºC; apatite saturation temperature) and oxidizing conditions, based on the composition of high mafic minerals and in the high proportion of Fe^{3+} in the Fe-Ti oxides.

Gonzaga (2018) presented a new U-Pb zircon age by SHRIMP, for a sample from the silica oversaturated syenite unit (see below) and obtained the age of 594.7 ± 5.7 Ma (Fig. 5), younger than the result obtained by Topfner (1993) for a silica saturated syenite from the LSS unit (~610 Ma).

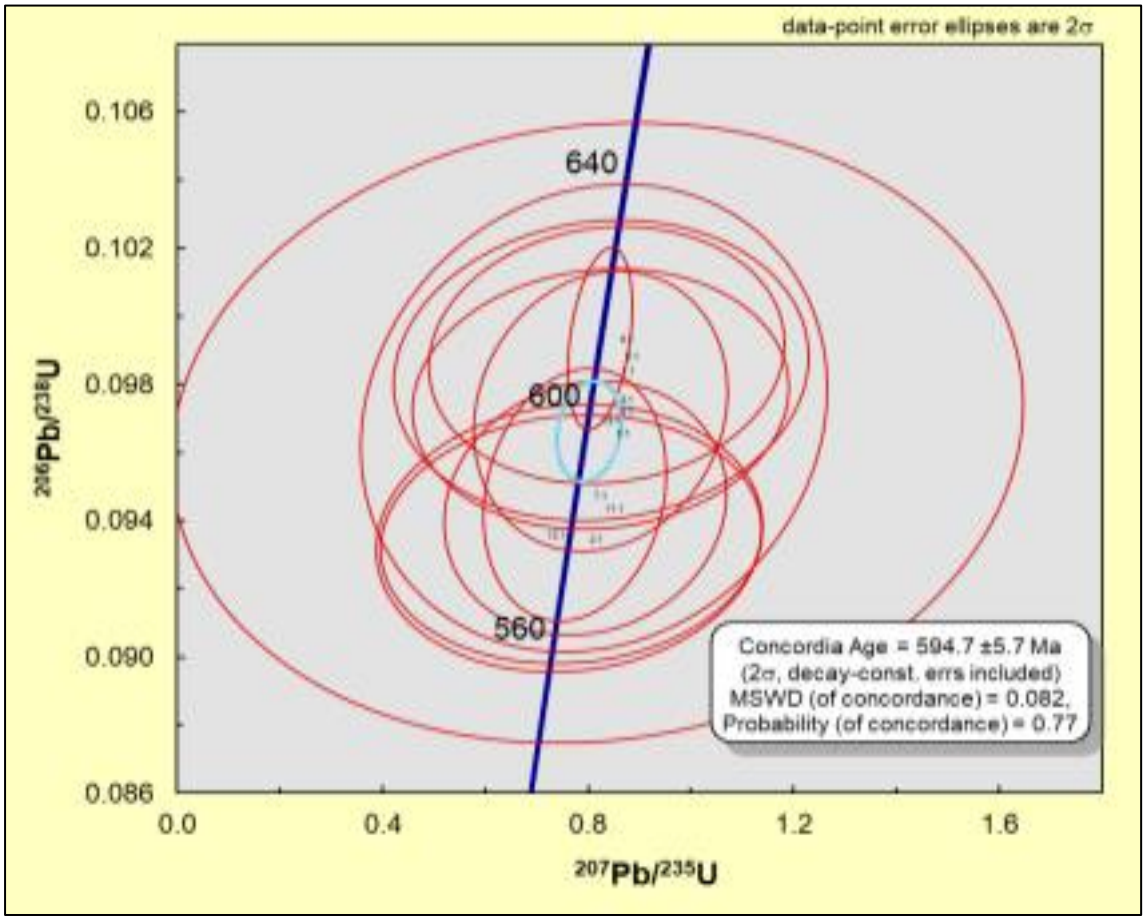

Fig 5: Concordia diagram, with age of 594.7 ± 5.7 Ma, obtained, by Gonzaga (2018) by U-Pb SHRIMP for the saple PB-123

Chapter II

2.1 Petrography

A total of 7 samples, representative of each unit of the Pedra Branca pluton, chosen from the large set of samples collected by Carvalho (2011), were used in presented work. Table 4 compiles the samples chosen for each unit.

Sample	Unit
PB-09	CSO
PB-06	ESO
PB-22	ESO
PB-92B	LSO
PB-123	LSO
PB-181	LSS
PB-185	LSS

Table 4: Sample used for each unit studied.

In all syenitic units, alkali feldspar makes up the main mineral phase, representing 50 to 70% in volume of the rock, while mafic minerals such as pyroxene (10 – 25%), Fe-Ti oxides (2 – 5%) and biotite (~5%), occur as in the interstices, between the tabular feldspar crystals.

Although all units share common characteristics, each unit has petrographic peculiarities that were used by Carvalho (2011) to define them, which will be discussed separately in the following items.

2.1.1 CSO

The CSO unit is fine to medium grained, with crystals up to 5.0mm, inequigranular, with macrocystals of alkali feldspar. Its mineralogy is mainly composed of alkali feldspar (~65%), diopside (~10%), amphibole (~5%), biotite (~5%), enstatite (~5%), ilmeno-hematite (~3%), quartz (~2%) and the accessory minerals apatite (~2%), titanite (<1%) and zircon (<1%).

Alkali feldspar is the main mineral phase, comprising 55 to 65% in volume of the rock, occurring as euhedral to subhedral crystals, commonly recording compositional zoning, and multiple inclusions of different mineral phases, mainly pyroxene, apatite, and opaque minerals. Altered plagioclase can be found as relic cores in alkali feldspar. Plagioclase can also occur as a late-stage crystallization phase, alongside quartz, in the form of myrmekite (Fig. 6a).

Diopside comprises the main mafic phase (~10%), occurring as subhedral to euhedral crystals, beige to green in color, often fractured and altered. Biotite is commonly found replacing diopside crystal cores.

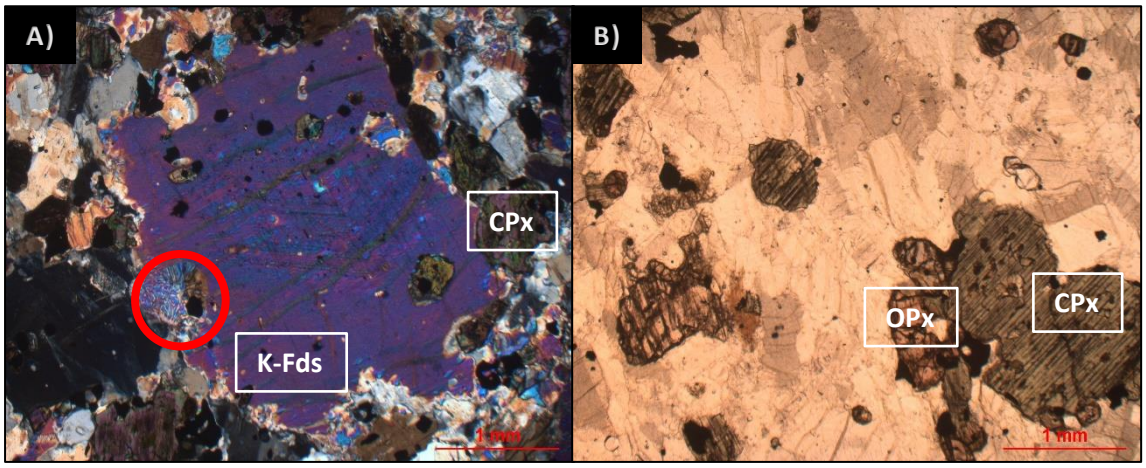

Fig 6: A) Photomicrograph of sample PB-09 depicting an alkali feldspar crystal with altered core, inclusions of pyroxene and opaque minerals and highlighting a myrmekite. B) General aspect of sample PB-09, showing the presence of two types of pyroxenes; enstatite (brown) and diopside (green).

The presence of amphibole is not very common, occurring mainly as dark green to brownish crystals, described as hornblende, it is often found associated with, and replacing pyroxene rims.

Quartz is often found in the CSO unit, occurring as late-stage, interstitial crystals, or as symplectites with biotite.

Apatite is the most common accessory mineral in the CSO unit, occurring as small subhedral to euhedral crystals (0.1 – 0.5mm), are often heavily fractured and are found included, mostly, in alkali feldspar and diopside, indicating its early-stage crystallization.

Zircon is a common accessory phase found in the CSO unit, occurring as small subhedral to euhedral crystals (up to 0.2mm), found in the interstices between feldspar or pyroxene crystals.

The most common opaque mineral described was ilmeno-hematite, broadly found in the sample studied (3 - 5%), often occurring as interstitial crystals, generally associated with other mafic phases, mainly diopside and biotite.

Table 5 provides an estimated crystallization sequence for the CSO unit.

Mineral	Early-stage	Main-stage	Late-stage
Apatite	-----	----------	----------
Zircon		----------	----------
K-Feldspar	----------	----------	----------
Diopside	----------	----------	----------
Hornblende			----------

Opaque minerals		----------	----------
Biotite			----------
Quartz			----------
Enstatite	----	----------	----------

Table 5: Proposed crystallization sequence for the CSO unit.

2.1.2 ESO

Similarly, to the other units, alkali feldspar represents the most abundant mineral phase, comprising up to 70% in volume of the rock, occurring as large (up to 7mm in size) tabular crystals, often heavily altered, recording corrosion textures and strong compositional zoning. The alkali feldspar crystals incorporate a variety of fine inclusions, mostly comprised of apatite and pyroxene crystals, sometimes the inclusions define former crystal borders which were later overgrown (Appendix V; Fig 3).

Diopside is the main mafic phase in the unit (~10%), occurring as light green subhedral to anhedral crystals. It is often found heavily fractured and bordered by amphibole and biotite crystals (Fig 7).

Hornblende is more commonly found in the ESO unit, in relation to the other units, comprising up to 10% in volume. Often described as dark green, anhedral crystals, mostly bordering, and replacing diopside crystals. Biotite is also present, but scarcely throughout the samples studied (~2%), often associated with other mafic phases.

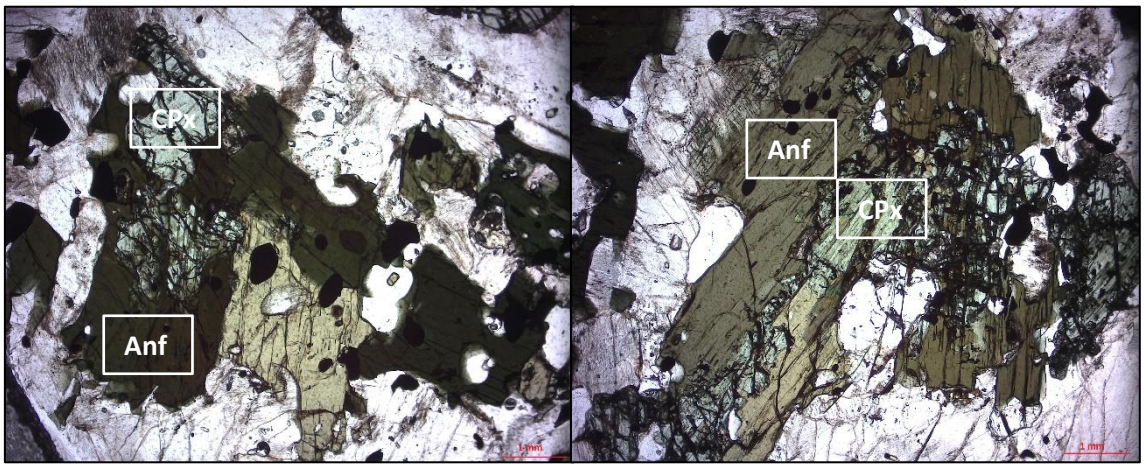

Fig 7: Photomicrographs of sample PB-06 depicting pyroxene cores bordered by amphibole crystals

Apatite is the most abundant accessory phase (~3%), occurring as subhedral to anhedral crystals, found in the interstices between feldspar crystals. Apatite described are often homogenous, heavily fractured and do not record any form of inclusions of different mineral phases. Titanite is present in both samples studied (<1%), but only occurs in the form of thin reaction borders around opaque minerals. Zircon is another

important accessory mineral described, occurring in the form of small subhedral to euhedral crystals, often interstitial but sometimes occurring as inclusions in diopside and alkali feldspar.

The opaque minerals were described as ilmeno-hematites, occurring as anhedral crystals, often associated with hornblende and diopside (Fig. 7).

Table 6 provides an estimated crystallization sequence for the ESO unit

Mineral	**Precoce**	**Principal**	**Tardio**
Apatite	-----	----------	----------
Zircon	-----	----------	----------
K-Feldspar	----------	----------	----------
Diopside	-----	----------	----------
Hornblende		----------	----------
Opaque minerals		----------	----------
Biotite			----------
Quartz			-------
Titanite			------

Table 6: Proposed crystallization sequence for the ESO unit.

2.1.3 LSO

Characteristically, the LSO unit is comprised of single type of pyroxene, being diopside, which corresponds to 10 to 15% in volume of the rock. Diopside often occurs as medium size (0.2 – 1.0 mm), subhedral to anhedral crystals, heavily altered and partially, or sometimes totally, replaced by amphibole and biotite (Fig. 8).

Amphibole, described as hornblende, and biotite often occur associated, the prior, composing up to 10% of the rock, presents a brownish to light green color, occurring as late-stage, interstitial crystals, often found bordering and replacing diopside crystals. Biotite (~5%) are often light to dark brown in color, occurring as anhedral, interstitial crystals, often associated with opaque minerals and amphibole.

Alkali feldspar is the main mineral phase, comprising up to 60% of the rock, usually occurring as euhedral to subhedral crystals, with the common presence of perthite and acicular inclusions of apatite, pyroxene, and opaque minerals. The feldspar crystals are often homogeneous but sometimes records diffuse compositional zoning. The alignment of feldspar and pyroxene crystals, defining a weak magmatic foliation was described in sample PB-92B but absent in sample PB-123.

Quartz can be found as small anhedral crystals, comprising up to 2% of the rock.

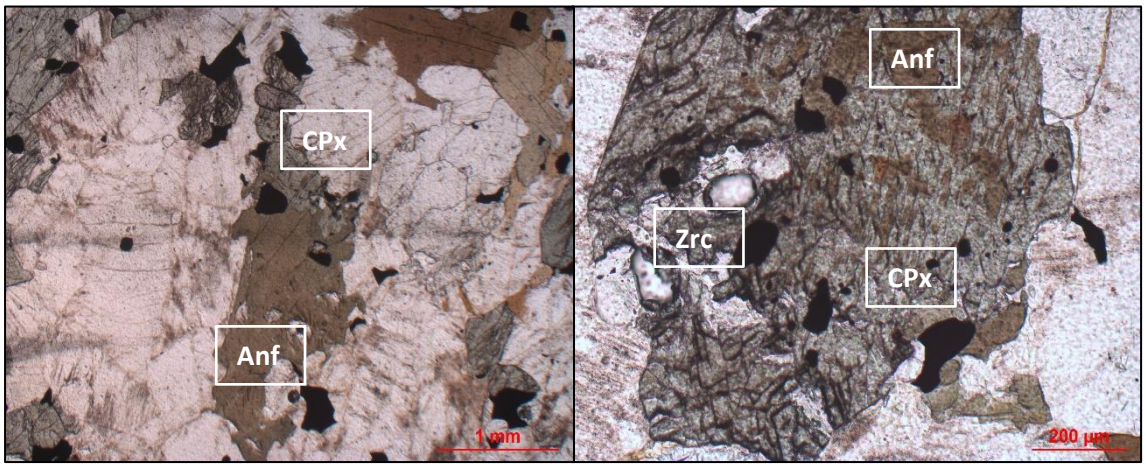

Fig 8: Photomicrograph of sample PB-92B highlighting amphibole replacing diopside.

Apatite is the main accessory phase described (up to 3%), occurring as small to medium size subhedral crystals (0.1 to 0.5 mm), often occurring in the interstices in between tabular feldspar crystals (Fig. Hb). Titanite (<1%) was also described, rarely occurring as independent crystals, but often as thin reaction halos around opaque minerals. Zircon is also a common accessory phase present in the samples studied (~1%), occurring as subhedral to euhedral crystals, often associated with, or included in, diopside or alkali feldspar, indicating a possible early-stage crystallization.

Table 7 seeks to provide an estimate crystallization sequence for the LSO unit.

Mineral	Precoce	Principal	Tardio
Apatite	---	----------	----------
Titanite			----------
Zircon		----------	----------
K-Feldspar	----------	----------	----------
Diopside	---	----------	----------
Amphibole		--------	----------
Opaque minerals		----------	----------
Biotite			----------
Quartz			----------

Table 7: Proposed crystallization sequence for the LSO unit.

2.1.4 LSS

The syenite samples from the LSS unit have a medium to coarse phaneritic texture, with the presence of alkali feldspar (2.0 – 5.0mm) and clinopyroxene (up to 2mm) macrocrystals, slightly oriented, defining a weak magmatic foliation, characteristic of the unit.

Alkali feldspar is the most abundant mineral phase, comprising 50 to 65% in volume of the rock, presenting tabular habit (euhedral to subhedral crystals), strongly altered, with intense presence of fine acicular inclusions of apatite, pyroxene, and hematite (Fig.

9a). Alkali feldspar crystals often show compositional zoning, in addition to the presence of *Carlsbad* germination.

Albite (<1%) can be found in the form of anhedral, interstitial crystals, always associated with alkali-feldspar, being interpreted as exsolution lamellae in alkali feldspar, forced out of the crystals into the interstices.

The main characteristic of the LSS unit is the presence of a dark-green pyroxene, of sodic-calcic character, described as aegirine-augite, composing about 10 to 20% in volume. The crystals are typically euhedral to subhedral, and may record compositional zoning, with dark green cores and light green rims.

Two types of amphiboles have been described; one of dark green color, described as hornblende, which is more abundant, occurring as subhedral to anhedral crystals (0.5 to 1.0mm), often associated with pyroxenes but sometimes occurring as independent crystals. The second amphibole described has a light green to light blue color, occurring in the form of substitution rims in pyroxene crystals, described as riebeckite (Fig 9).

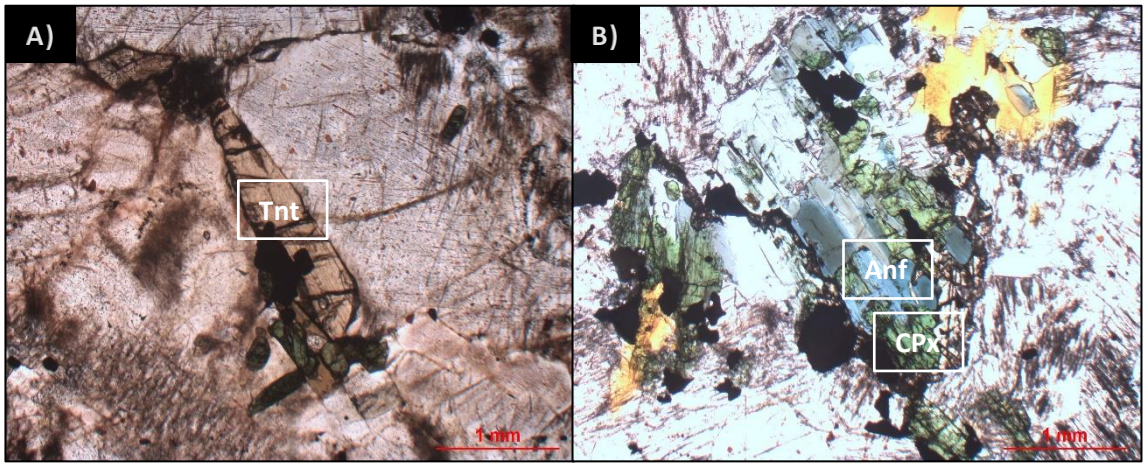

Fig 9: Photomicrograph of altered alkali-feldspar with acicular inclusions. B) Photomicrograph of sample PB-185 depicting actinolite associated with aegirine-augite.

Biotite occurs in the form of anhedral crystals, typically interstitial, indicative of late-stage crystallization, often associated with other mafic phases, mainly pyroxenes and opaque minerals. (Fig 10).

Apatite is the main accessory mineral of the LSS unit, occurring in the form of large euhedral to subhedral crystals (up to 4mm in size), moderately altered, usually fractured and without the presence of inclusions of other mineral phases, which indicates early crystallization. Apatite also occurs in the form of small acicular crystals, included in alkali feldspar.

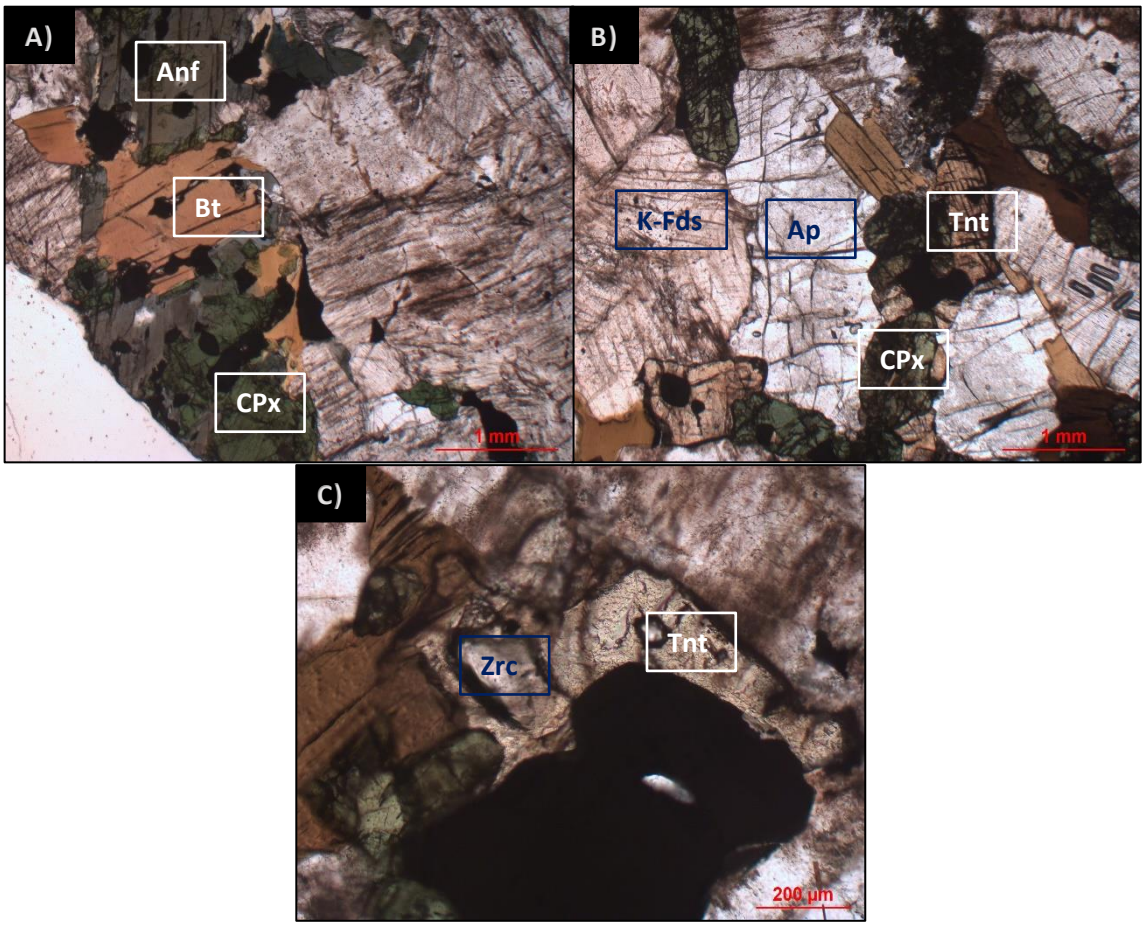

Fig 10: A) Photomicrograph of sample PB-181, indicating the association between biotite, pyroxene, and amphibole. B) Photomicrograph of sample PB-185, highlighting the presence of large apatite crystals. C) Photomicrograph of sample PB-181 showing titanite bordering a hematite crystal

Titanite is also an important accessory phase present, where two distinct populations of crystals have been described; a population of large (up to 1.0mm), independent, subhedral crystals, often occurring associated with other mafic phases, and a population composed of small interstitial, anhedral, crystals, always associated with Fe-Ti oxides, in the form of reaction halos, indicating late-stage crystallization (Fig. 10c).

The presence of zircon is rare in the unit, occurring in the form of small, scattered crystals, throughout the samples studied (Fig. 10c).

Opaque minerals are typically magnetite and hematite, making up 1 to 5% in volume of the rock. Magnetite, being the most common, occurs in the form of interstitial crystals, typically associated with pyroxene. Ilmenite often has hematite lamellae, and occurs in the form of anhedral, interstitial crystals, sometimes bordered by titanite.

Quartz has not been previously described in the LSS unit, and its absence was often mentioned as an important, defining characteristic of the unit. With the use of SEM generated mineral map, quartz was described, and it occurs as very sparse interstitial crystals, indicating a late-stage crystallization (Appendix IV – Fig. 2)

Table 8 seeks to provide an estimate crystallization sequence for the LSS unit.

Mineral	Precoce	Principal	Tardio
Apatite	----------	----------	----------
Titanite		----------	----------
Zircon		----	----------
K-Feldspar	----------	----------	----------
Aegirine-augite	----------	----------	----------
Amphibole		--------	----------
Opaque minerals		----------	----------
Biotite			----------
Quartz			----------

Table 8: Proposed crystallization sequence for the LSS unit

2.1.5 Crystal Size Distribution (CSD) in apatite

To further investigate the crystal relations of apatite, MLA (Mineral Liberation Analysis) data was obtained for two different samples studied, one from the CSO unit (PB-09) and one from the LSS unit (PB-181). The samples chosen, represent the biggest possible difference in apatite texture and form of occurrence within the Pedra Branca pluton.

Based on the results obtained it was possible to determine a few detailed characteristics of apatite from the two units, such as the proportion of apatite crystals included in other mineral phases, the most likely mineral phase to include apatite, and information regarding average crystal size and distribution, which will later be discussed.

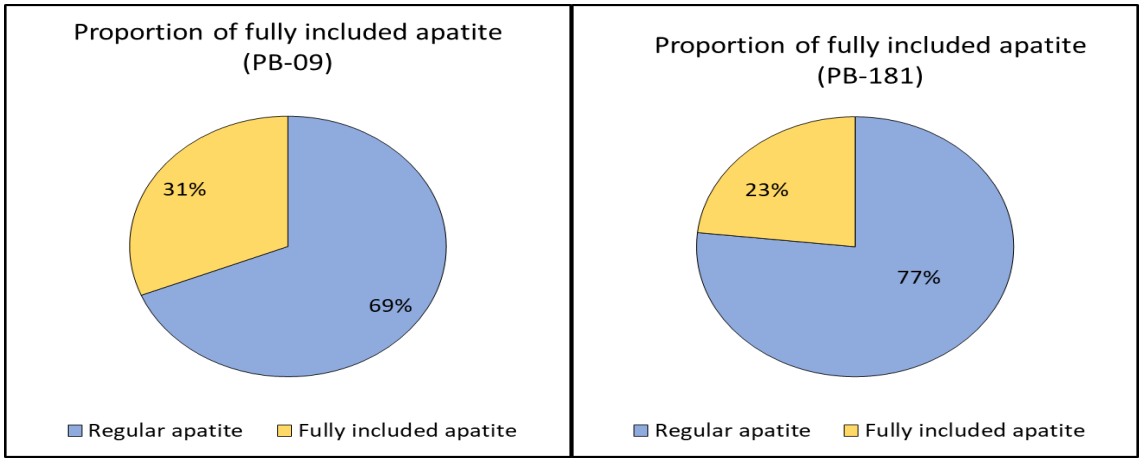

Fig 11: Pie-charts representing the proportion of fully included apatite crystals

Fig 11 shows that the proportion between independent crystals and fully included crystals of apatite, in both units studied are similar, with the LSS unit recording a slightly higher proportion of independent crystals.

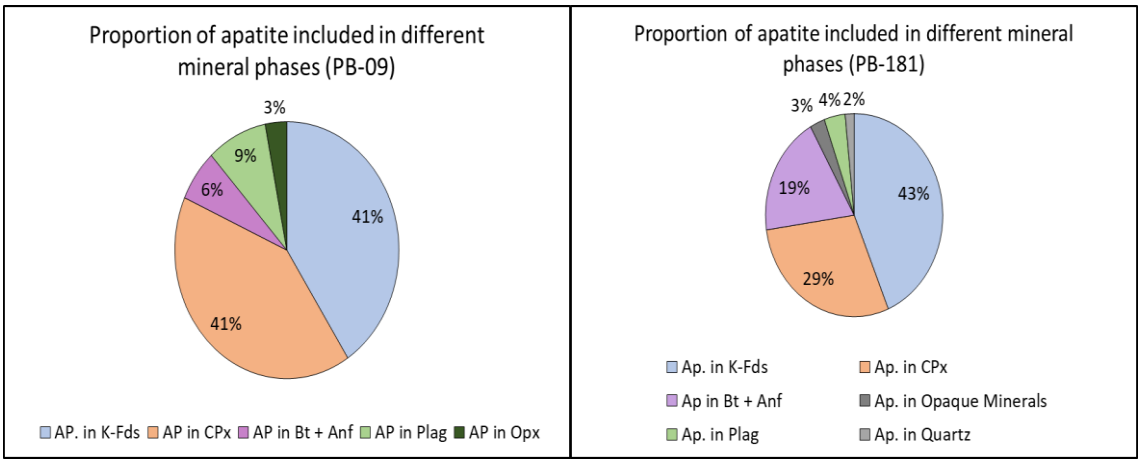

Fig 12: Pie-charts representing in which mineral phase apatite is more likely to be included.

The pie charts from figure 12 show that apatite is more likely to be included by the two most common mineral phases in both units, alkali feldspar and pyroxene, which was the expected result, with the major difference being the significantly higher proportion of apatite included in amphibole and biotite in the LSS unit, relations that were not described during the petrography study.

To characterize the crystal size distribution of apatite, a few CSD curves were produced, using the program CSDcorrections 1.4.0, which converts 2D data (obtained by MLA) to 3D crystal size distributions. The program requires an estimation of the sample fabric, crystal roundness and a 3D crystal shape model. A roundness factor of 0.3 was chosen for the LSS unit, and a value of 0.5 was chosen for the CSO unit, based on petrography. The 3D crystal shape model was estimated using the CSDSlice 5 spreadsheet (Morgan & Jerram, 2006) which compares the aspect ratio of the measurements with those from a database of known crystal shapes and determines the best fit crystal habits for the observed population.

Figure 13 shows the frequency versus crystal length histogram, with the cumulative curve plotted, indicating that although the CSO unit has a higher population of apatite analyzed, it is comprised of, generally, smaller sized crystals, in relation to the LSS results. The results obtained agree with the petrographic descriptions of apatite from both units.

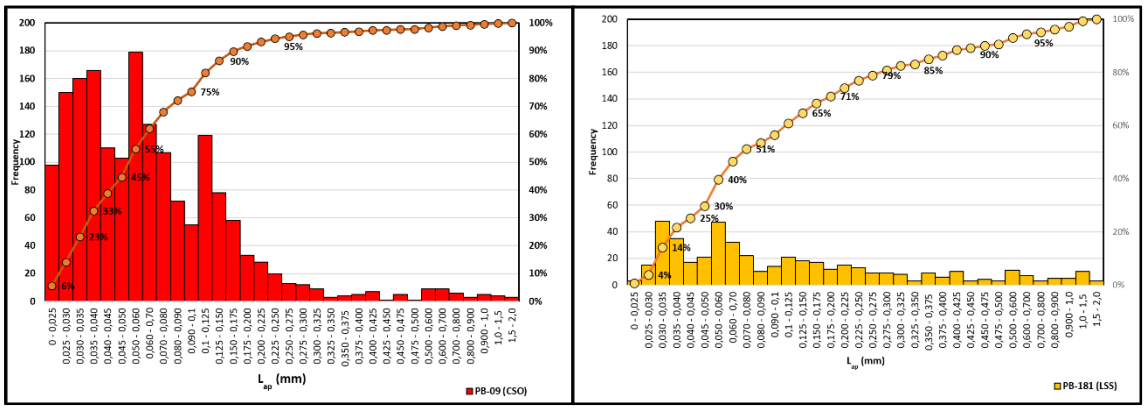

Fig 13: Frequency versus crystal length histogram, with the cumulative curve plotted. A) PB-09 (CSO unit); B) PB-181A (LSS unit)

The CSD curves for apatite obtained from the two units studied are presented in figure 14. Both lines are similar, being concave up and not following the linear trend, obtained by linear regression.

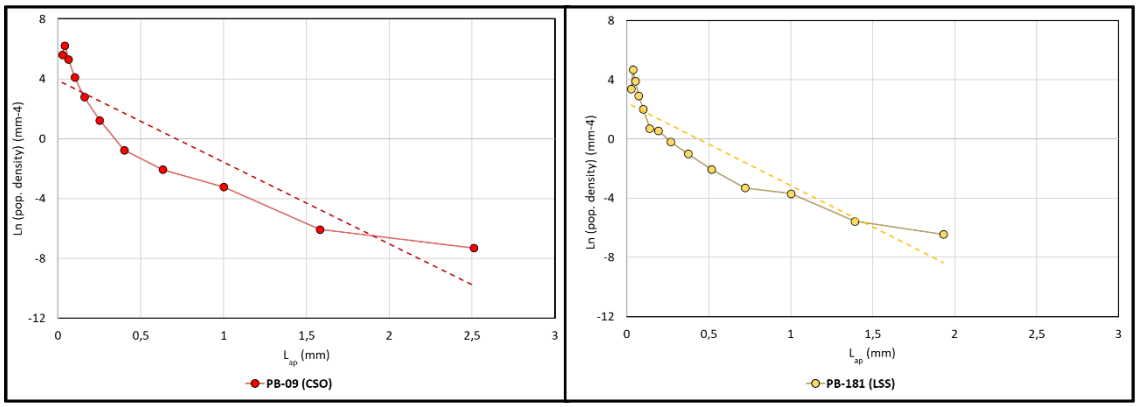

Fig 14: CSD plots of the population density (ln (n)) versus crystal length (L) obtained for apatite

CSD studies in the literature have proposed interpretations on magma cooling and magma evolution processes based on CSD curves, such as the association of linear CSD curves to simple cooling process, in steady-state systems, whereas and non-linear CSD curves would be associated with the occurrence of physic-chemical processes during crystallization, such as magma mixing, crystal coarsening, accumulation or fractionation processes (Cashman & Marsh, 1988; Higgins 1996, 2000). Based on the proposed CSD model, by Vinet & Higgins (2010), the apatite results obtained would be indicative of magma mixing during crystallization, due to the slope variations and concave up shape of the curves obtained.

Chapter III

3.1 Results

3.1.1 Mineral Chemistry

3.1.1.1 Pyroxene

Pyroxenes from the four main units of the Pedra Branca pluton were analyzed by electron microprobe and by LA-ICP-MS, and the results indicate important compositional variations between each unit and, in some cases, significant compositional variations within the same geological unit.

Two units that are Si-oversaturated, ESO and LSO (samples: PB-06, PB-22 and PB-92B, PB-123 respectively) are characterized by the presence of a single type of pyroxene, of greenish color (light green to yellowish tones) and calcic character, being described as diopside, typically occurring associated with other mafic mineral phases, such as amphiboles, titanite and ilmenite. Pedra Branca's central unit, CSO (sample PB-09), which is also quartz-oversaturated, is characterized by the presence of two types of pyroxenes, a clino- and an orthopyroxene, the clinopyroxene being remarkably similar, in terms of appearance and occurrence, to the one described previously in the ESO and LSO units, while the orthopyroxene occurs as small granular crystals of reddish to brown color, described as enstatite.

The LSS unit, which is quartz-saturated, is also characterized by a single type of pyroxene, different from the ones described in other units. It occurs as large crystals, of strong green color (green to bluish tones), indicating a sodic composition (aegirine augite), and is often associated with different mineral phases such as apatite, biotite, titanite and opaque minerals (Fig.15).

The Wo-En-Fs classification diagram by Morimoto (1989) was used to classify and identify compositional variances between pyroxenes of all units. The clinopyroxenes from the central unit (CSO; sample PB-09) are mainly located in the augite field, with a compositional range of $Wo_{40-44}En_{38-45}Fs_{15-19}$, while the orthopyroxenes are all located in the enstatite field, recording a small compositional range of $Wo_{01}En_{59-60}Fs_{38-39.}$ Pyroxenes from the ESO unit (samples PB-06 and PB-22) record a large compositional variation, ranging from the augite to the diopside field ($Wo_{40-46}En_{37-42}Fs_{16-18}$). Pyroxenes from the LSO unit (samples PB-92B and PB-123) are compositionally like the ones from the ESO

unit, but with a smaller compositional diversity, where almost all the crystals analyzed are located right on top of the division between the diopside and augite.

The LSS unit records a large compositional variation between pyroxenes from the two samples analyzed (PB-181 and PB-185). Pyroxenes from sample PB-181 have, overall, higher Na_2O content, ranging from 2.4 to 3.7%, compared to pyroxenes from sample PB-185, with 1.4 to 2.0% Na_2O. The “sodic” character of the pyroxenes from this unit can be observed using the QJ and WEF-Jd-Ae diagrams by Morimoto (1989, Fig. 16). Based on the QJ diagram, all the pyroxenes analyzed from the sample PB-185 are in the “QUAD” area of the diagram, which represents Ca-Mg rich pyroxenes, alongside all of the analysis from the other units, while a portion of the pyroxenes from the sample PB-181 are placed on the “Ca-Na” area of the diagram, which represents sodic-calcic pyroxenes. This difference can also be seen in the WEF-Jd-Ae diagram, where all pyroxenes from sample PB-185 plot in the “augite” field, with a compositional range of $Ae_{7\text{-}15}Jd_{0\text{-}12}$ $WEF_{85\text{-}88}$, while the pyroxenes from the sample PB-181 range from the augite to the aegirine-augite field, recording a compositional variation of $Ae_{15\text{-}29}Jd_{0\text{-}4}$ $WEF_{70\text{-}82}$, where WEF represents the sum of wollastonite, enstatite and ferrosillite molecules (Fig 16.).

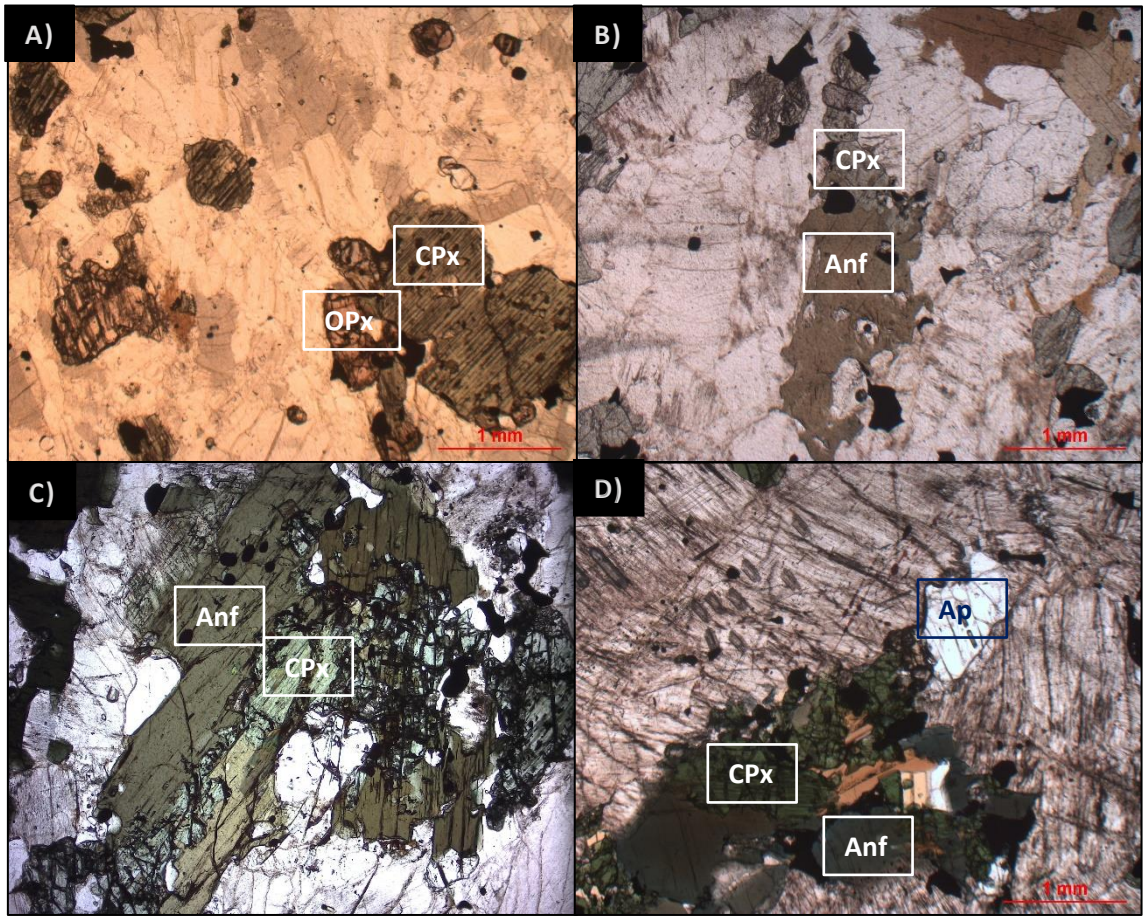

Fig 15: Photomicrographs of pyroxene from the four different units: A) Sample PB-09 (CSO); clinopyroxene (diopside) and orthopyroxene (enstatite); B) Sample PB-123 (LSO); clinopyroxene associated (diopside) associated with amphibole (hornblende) and ilmenite; C) Sample PB-06 (ESO); replacement of clinopyroxene (diopside) with amphibole (hornblende); D) Sample PB-181 (LSS); calcic-sodic pyroxene (aegirine-augite) associated with phlogopite and hematite.

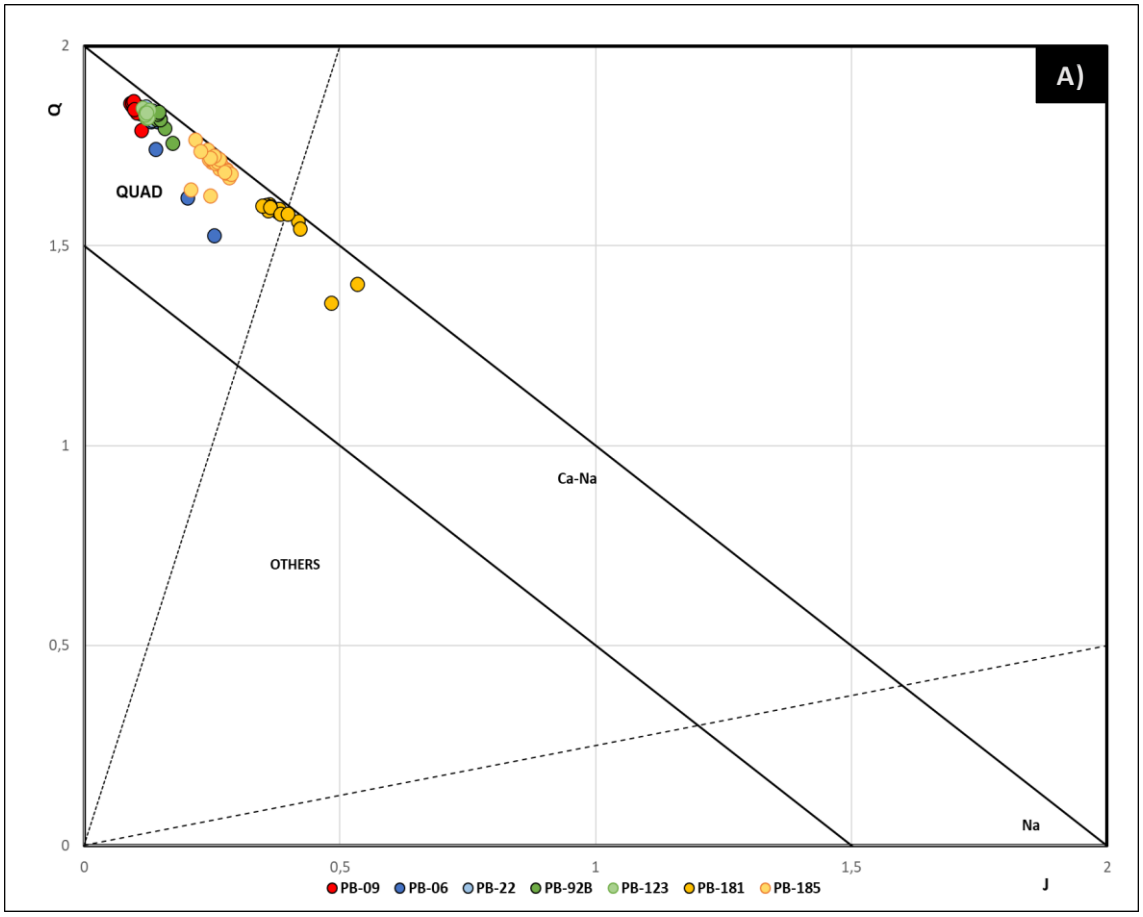

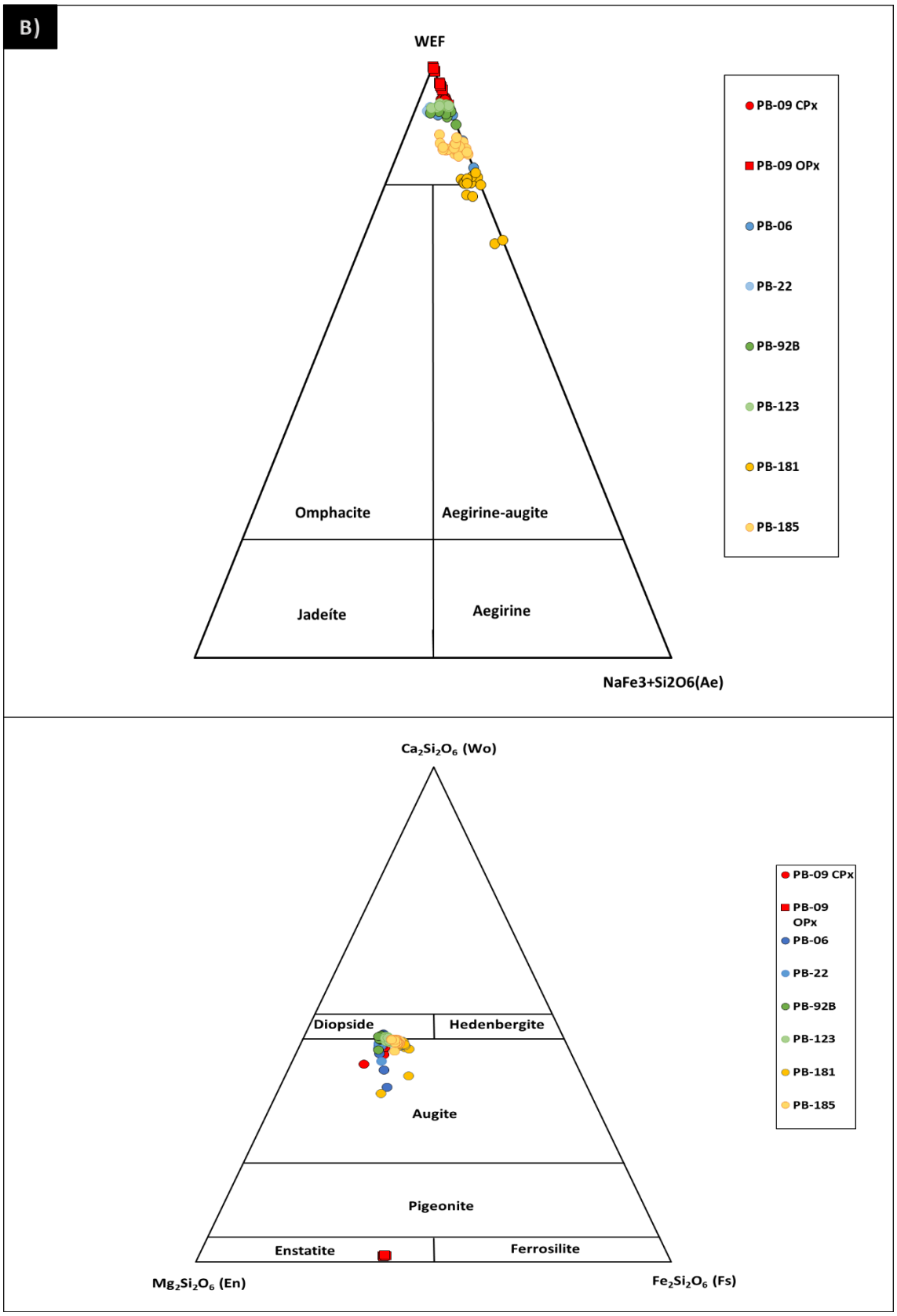

Fig 16: Morimoto's classification diagrams (Morimoto, 1989); a) QJ diagram, where Q=Ca+Mg+Fe^{2+}, J=2*Na, "QUAD" is delimited by J/(Q+J) =0.2 and "Na" is delimited by J/(Q+J) =0.8. b) WEF-Jd-Ae and Wo-En-Fs classification diagrams, respectively.

3.1.1.1.1 Major Elements and Substitutions

Besides the enrichment in Na, clinopyroxenes from the LSS unit are, overall, enriched in trace elements, such as V, Zr and Sr, with concentrations up to seven times higher when compared to the other units. The most notable enrichments are in Zr and Sr, with contents ranging from 241 to 501 and 575 to 1500 ppm respectively, when compared to the Si-oversaturated units with contents ranging from 100 to 165 ppm Zr and 73 to 153 ppm Sr, respectively (fig. 17).

The Mg# for both types of pyroxenes was calculated, where Mg# = Mg/(Mg/Fe^{2+}), and it is noteworthy that all the clinopyroxenes analyzed record a similar interval of Mg#, ranging from 70 to 81, with every unit's average around 74, while the orthopyroxenes, that occur only in the CSO unit, record a lower Mg#, ranging from 61 to 63 (Fig. 17).

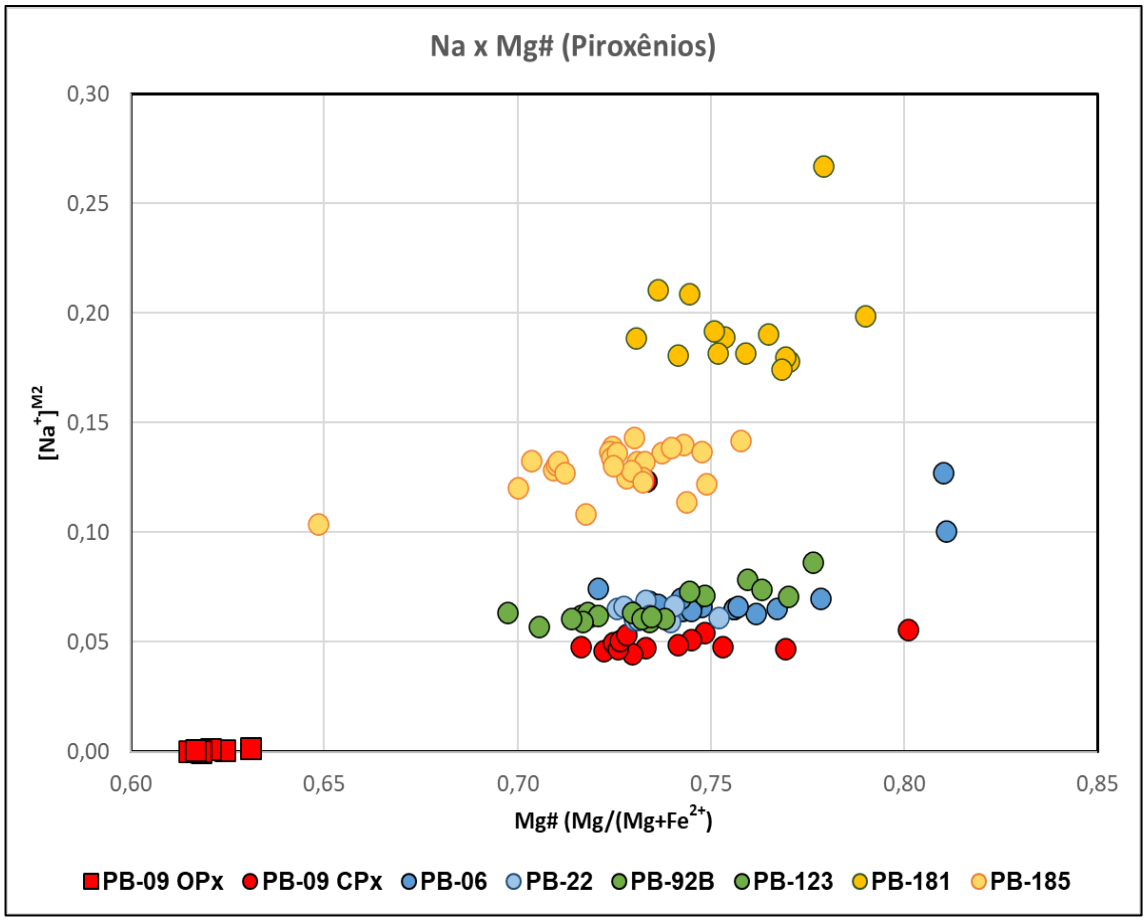

Fig 17: $[Na]^+$ x Mg# diagram

Given the strong negative correlation observed in both diagrams from figure 18, it is plausible to associate the significant compositional variance between pyroxenes from different geological units to two major cationic exchanges:

$$[Na^{+}]^{M2}\,[Fe^{3+}]^{M1} \leftrightarrow [Mg^{2+}]^{M2}[Mg^{2+}]^{M1}$$

$$[Na^{+}]^{M2}[Fe^{3+}]^{M1} \leftrightarrow [Ca^{2+}]^{M2}\,[Mg^{2+}]^{M1}$$

Where Ca^{2+} and Mg^{2+}, on the M2 and M1 sites respectively, are exchanged by Na^{+} and Fe^{3+}.The occurrence of this cationic exchange could explain the crystallization of aegirine-augite and augite, with higher Na content in its composition, in the LSS unit.

The classification, based on Morimoto's diagrams, as well as the compositional variations on pyroxene between different units presented, corroborate with the results published by Carvalho (2011).

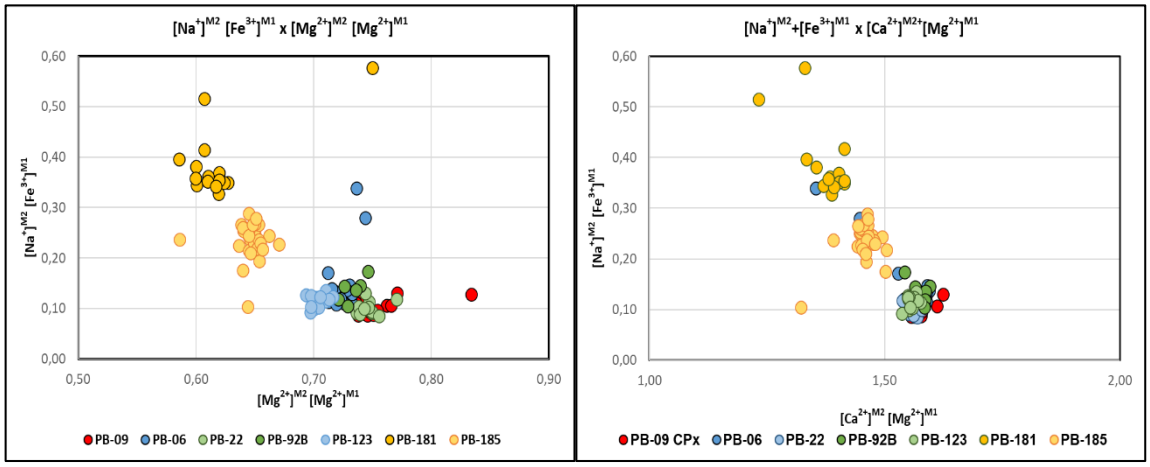

Fig 18: Compositional variation diagrams representing the two major cationic exchanges on pyroxene

3.1.1.1.2 Rare Earth Elements (REE's)

The REE distribution patterns from figure 19 show that the clinopyroxenes from the Si-oversaturated units are enriched in LREE, which show a curved pattern, with a peak in Pr and Nd; the HREE are also fractionated from Gd to Ho, and flat from Er to Lu. The clinopyroxene from sample PB-181 of the LSS unit has lower REE content, with a flatter LREE pattern (Pr > Nd = Ce > La) and a convex pattern at the HREE portion, with a minimum at Tm. The clinopyroxene of the oversaturated units also record a negative Eu anomaly, with $(Eu/Eu^{*})_{N}$ ranging from 0.6 to 0.8, where rim analysis record a more predominant Eu anomaly (Eu/Eu* = 0.60 on average) in relation to core analysis (Eu/Eu* = 0.65 on average), while those from the LSS unit lack any significant Eu anomaly, with $(Eu/Eu^{*})_{N}$ ranging from 0.85 to 1.2 (fig. 19). Every unit record a slight positive Ce anomaly, with the oversaturated units recording the highest values, ranging between 1.0 and 1.2 (~1.1 avg) while the saturated unit record values ranging between 0.95 and 1.1 (~1.05 avg.), it is observed a slight increase in Ce/Ce* values from core to rim in the oversaturated units, while no significant variation is observed in pyroxene from the

saturated units (Fig. 19d). It is noteworthy to mention that, in relation to the respective whole rock analysis, the pyroxenes from the Si-oversaturated units are enriched in LREEs and impoverished in HREEs, while pyroxenes from the saturated unit are heavily impoverished in REEs in general (Fig. 19).

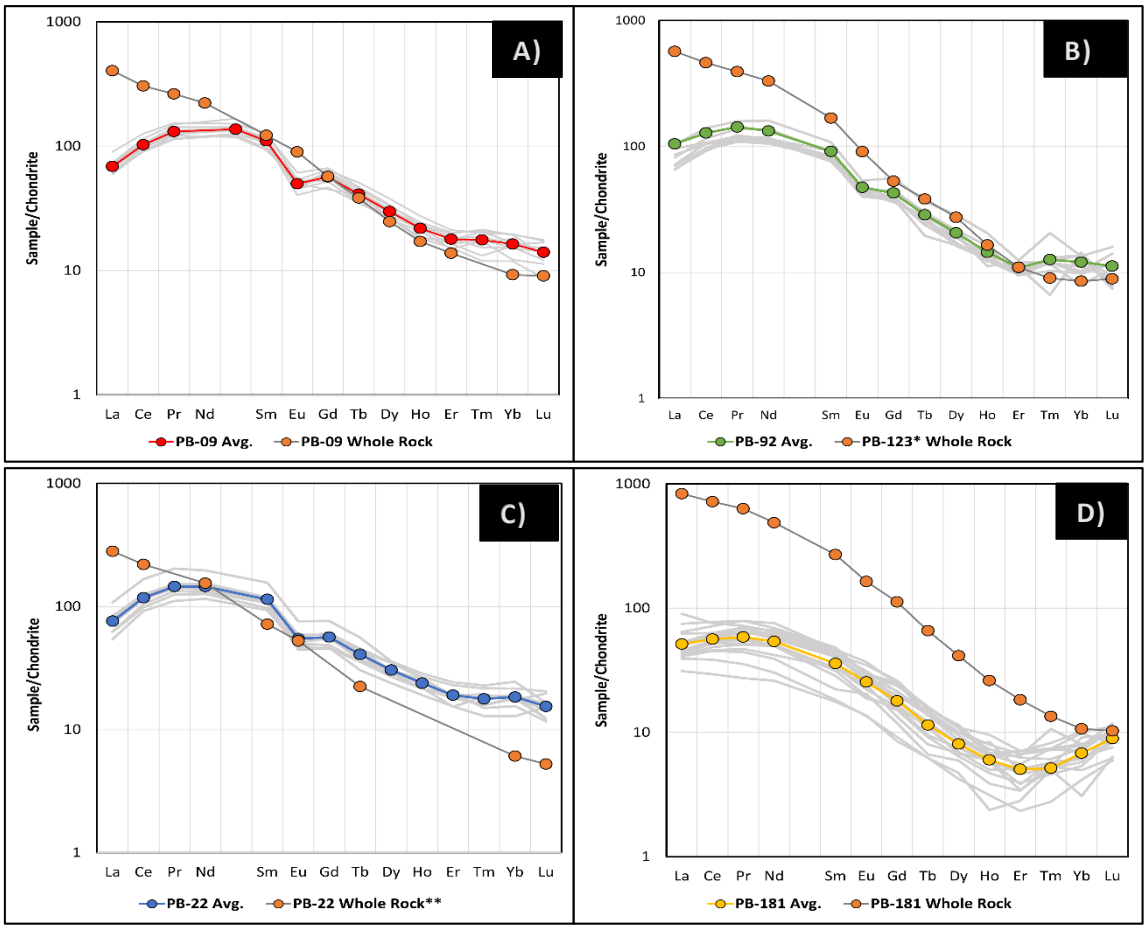

Fig 19: Pyroxene REE pattern distribution in relation to whole rock analysis, gray lines represent the entire population analyzed, while colored lines represent the average results for each unit.

**Whole rock REE data of sample PB-92B was not acquired, whole rock data of sample PB-123, from the same unit, was used for simple comparison.*

***Whole rock REE data of sample PB-22 is not complete, missing the results for the following elements: Pr, Dy, Ho,Er,Tm and Yb.*

3.1.1.2 Amphibole

A total of six samples were analyzed for amphibole by electron microprobe, representative of every geological unit from the Pedra Branca pluton: two samples from the LSS unit (PB-181A and PB-185A), two from the LSO unit (PB-92B and PB-123), one from the CSO unit (PB-09) and one sample from the ESO unit (PB-06). The elements chosen for analysis were as following: Si, Al, Fe, Mn, Cl, Ca, K, Ti, Cr, F, Na and Mg.

Three samples were analyzed for amphibole by LA-ICP-MS: one sample from the LSS unit (PB-181A), one sample from the LSO unit (PB-123) and one sample from the CSO unit (PB-09).

The structural formulas for the amphiboles were calculated based on a total of 23 oxygens, assuming the general formula $A_{0-1}B_2C_5T_8O_{22}(OH,F,Cl)$. All the results obtained from the analysis and formula calculations are presented as supplementary data sheets in Appendix II.

Amphiboles from the silica-oversaturated units (CSO, LSO and ESO) share similar characteristics, such as greenish tones in color (from light to dark green), occurring as anhedral to subhedral crystals, measuring up to 2 mm. Amphibole crystals replacing, or associated with, other mineral phases such as pyroxenes and opaque minerals, are common, especially in the LSO unit (sample PB-92B).

The abundance of amphibole in the LSS unit is smaller and it corresponds to a different type of amphibole, blueish in tone (from light blue to light green color), occurring both as euhedral to subhedral crystals, measuring up to 1 mm, and commonly associated with or replacing other mineral phases, mainly pyroxenes cores, as small anhedral crystals.

3.1.1.2.1 Chemical Classifications

Compositionally, all the silica-oversaturated units have amphiboles of calcic character, while the amphiboles in the LSS unit are sodic-calcic (fig. 20). Based on the classification diagrams by Leake *et. al* (1997), the amphiboles from the LSS unit were classified as two different types; amphiboles from sample PB-181 are winchite ($\square(Ca,Na)(Mg_4,Al)(Si_8O_{22})(OH)_2$), while the ones from sample PB-185 are magnesiokatophorite ($Na(Ca,Na)Mg_4(Al,Fe^{3+})Si_7AlO_{22}(OH)_2$). Two different types of calcic amphiboles were also identified in the different silica-oversaturated units; with crystals from the ESO (sample PB-06) and LSO units (samples PB-92B and PB-123) classified as edenite ($NaCa_2Mg_5(Si_7Al)O_{22}(OH)_2$), while the CSO unit records a compositional variation, ranging from edenite to Mg-hornblende($Ca_2(Mg_4(Al,Fe^{3+})(Si_7O_{22})(OH)_2$) (fig. 21).

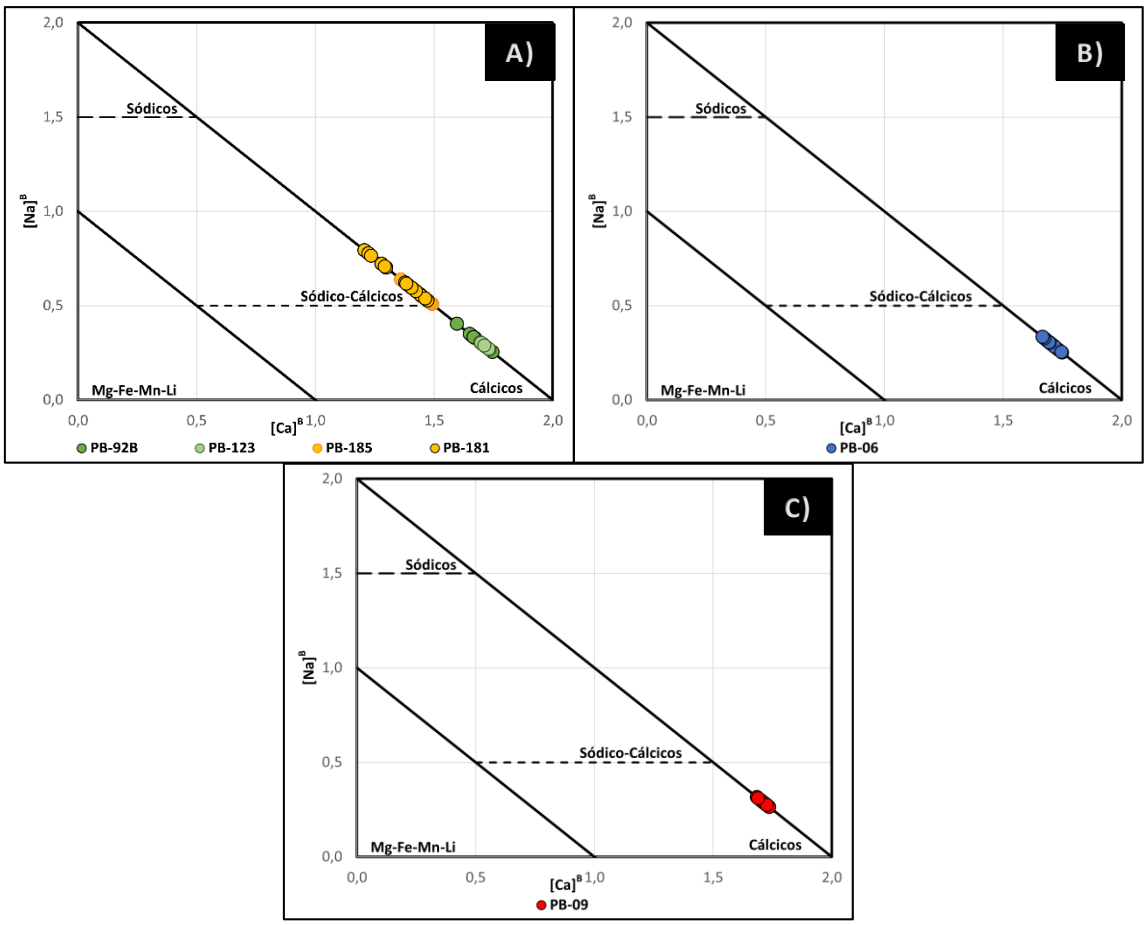

Fig 20: [Na]B x [Ca]B classification diagrams by Leak et al., (1997)

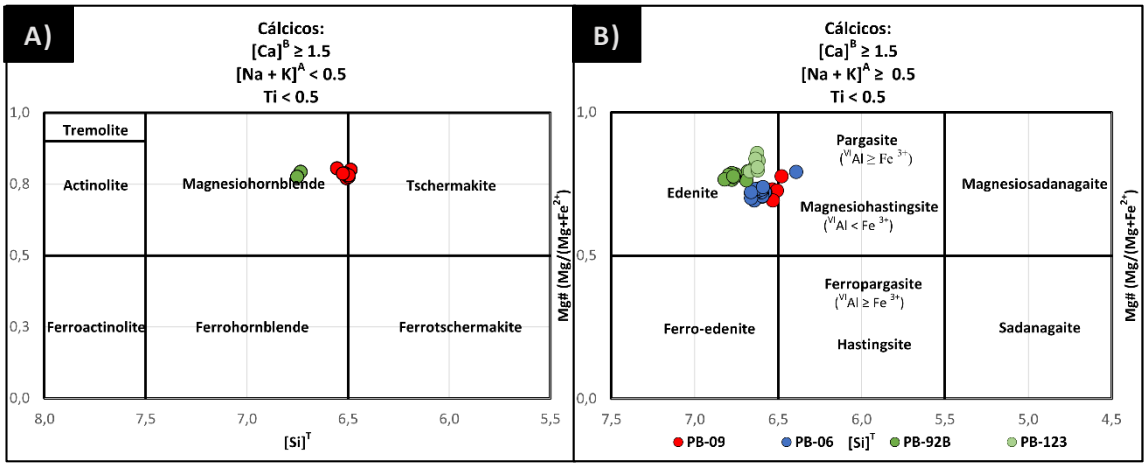

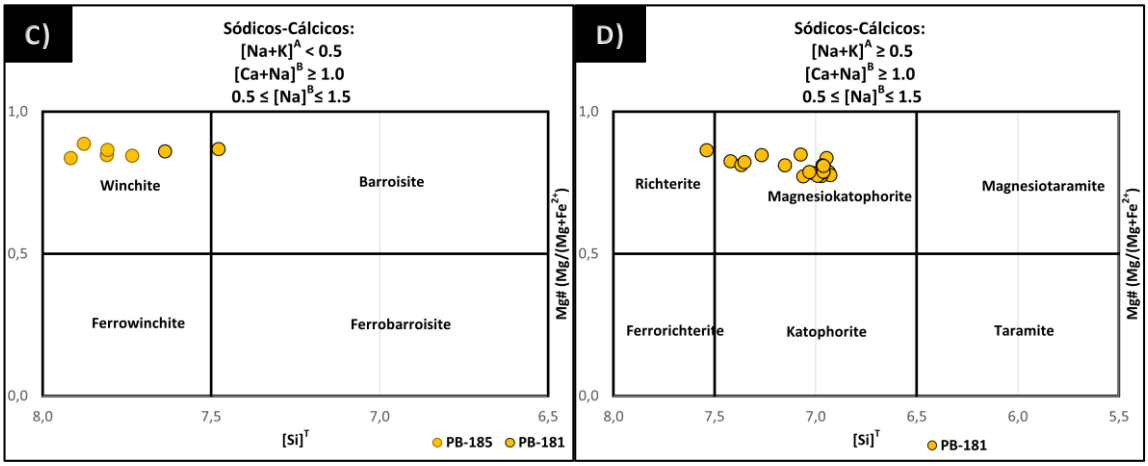

Fig 21: $[Si]^T$ x Mg# classification diagrams by Leak et al (1997). A) Classification for calcic-amphiboles with $[Na+K]^A$ < 0.5; b) classification for calcic-amphiboles with $[Na+K]^A \geq 0.5$; c) classification for sodic-calcic amphiboles with $[Na+K]^A$ < 0.5; d) classification for sodic-calcic amphiboles with $[Na+K]^A \geq 0.5$.

3.1.1.2.2 Major Elements

The silica-oversaturated units are, in general, enriched in Al and Ti in relation to the LSS unit, with Al_2O_3 and TiO_2 contents ranging from 7.8 to 10.3% and 0.9 to 2.1%, respectively, while amphiboles from the LSS unit record Al_2O_3 and TiO_2 contents ranging from 0.9 to 6.8% and 0.04 to 1.5%, respectively.

As indicated by the classification diagrams presented in figure 21, the LSS unit is characterized by the presence of two sodic-calcic amphiboles, winchite and magnesiokatophorite, therefore denoting higher Na content in its composition, with values ranging from 1.98 to 4.19% Na_2O, while the silica-oversaturated units record Na_2O contents ranging from 1.74 to 2.24%. Although the enrichment in Na, the LSS unit records the largest variance in Na content amongst all units, with values fluctuating up to 100% between lowest and highest recorded values. This large variance is largely due to the two different types of sodic-calcic amphiboles present in the LSS unit. Magnesiokatophorite, present exclusively in the sample PB-181, records higher Na content in its composition, ranging from 3.53 to 4.19% Na2O, while winchite, present mostly on the sample PB-185 (fig. 22), record Na2O values ranging from 1.98 to 2.23%, similar values to the amphiboles from the silica-oversaturated units (1.74-2.24% Na_2O). Winchite, from sample PB-185, is also impoverished in Al and K (0.89 – 2.13% Al_2O_3; 0.36-0.66% K_2O, respectively), in relation to magnesiokatophorite, from sample PB-181 (2.36 – 6.84 Al_2O_3 e 0.97 – 1.74% K_2O) and in relation to the calcic-amphiboles from the silica-oversaturated units (7.77 – 10.31% Al_2O_3;1.14 – 1.44% K_2O; Fig. 22).

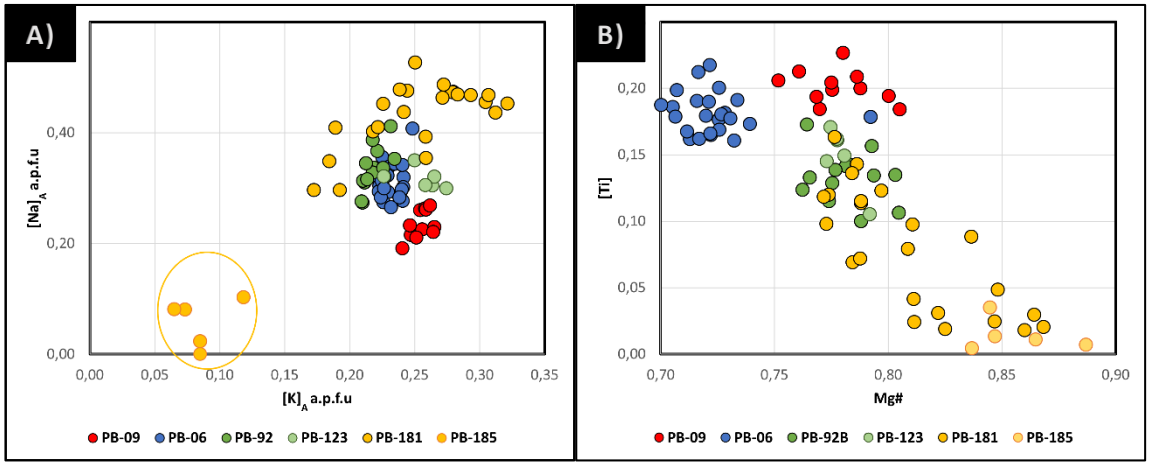

Fig 22: A) [Na]A x [K]A correlation diagram in amphibole; B) [Ti] x Mg# correlation diagram, in amphibole

Mg# diagram (fig. 22b), it is possible to note that Mg# for the CSO (sample PB-09) and LSO units (samples PB-92B and PB-123) are similar, ranging between 75 and 81, while the ESO unit (sample PB-06) record the lowest values, ranging between 70 and 74. The LSS unit is quite unique, with a high variance in Mg#, ranging between 75 and 89, where the Mg# from winchite, from sample PB-185, is the highest amongst all of the amphiboles analyzed, ranging between 85 and 89.

The results from the LSS unit, especially from the sample PB-181, show high variance (fig. 22), and such variance can be associated with analysis of amphibole crystals under different textural relations; for instance, large “independent” euhedral crystals (fig. 23a) and smaller, anhedral crystals associated with different mineral phases (fig. 23b). Overall, there is two sets of results that can be distinguished; a “enriched” and a “impoverished” set of analyzed crystals, that are highlighted in the first diagram from figure 24. The “enriched” set represents analysis of larger euhedral to subhedral amphibole crystals, while the “impoverished” set represent analysis of smaller and anhedral crystals from sample PB-181 (Fig.23).

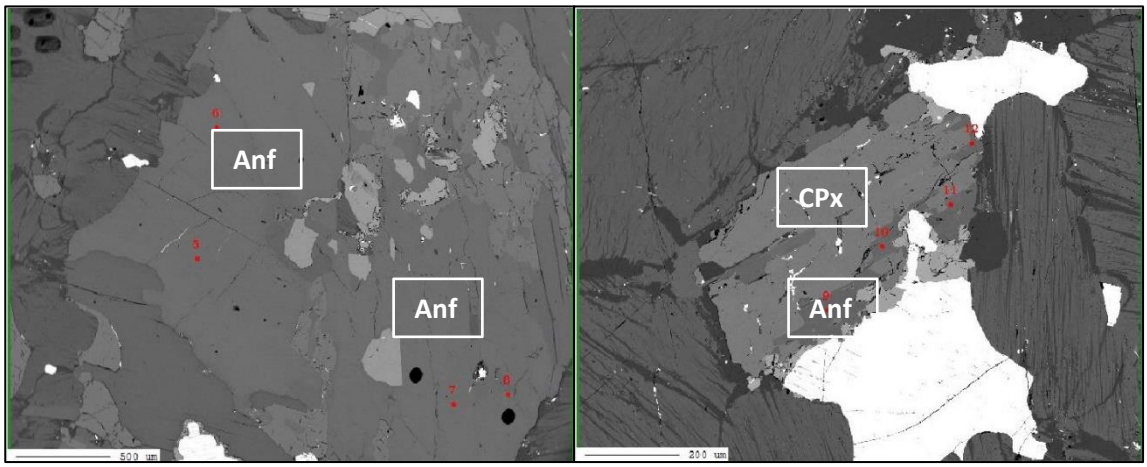

Fig 23: Amphibole images from sample PB-181 depicting amphibole crystals under two different textural contexts

Based on the diagrams presented in figure 10, the main compositional differences observed between amphiboles from the different geological units studied can be associated with two major cationic substitutions that occur in amphibole; Tschermakitic , or Ti-Tschermakitic substitution, and Edenitic substitution, respectively:

$$[Al^{3+}]^T + [Al^{3+}]^C \leftrightarrow [Si^{4+}]^T + [(Mg, Fe, Mn)^{2+}]^C$$

$$2[Al^{3+}]^T + [Ti^{4+}]^C \leftrightarrow 2[Si^{4+}]^T + [(Mg, Fe, Mn)^{2+}]^C$$

$$[Al^{3+}]^T + [(Na, K)^{+}]^A \leftrightarrow [Si^{4+}]^T + \square^A$$

The enrichment in Al and Ti, observed in the units with calcic-amphibole, ESO, LSO and CSO (or silica-oversaturated units), can be attributed to the Tschermakitic, or Ti-Tschermakitic, cationic exchange, given the substitution of silica, in the tetrahedral site, and elements such as Mg and Fe^{2+}, at the octahedral site, by Al and Ti, respectively (Fig. 24).

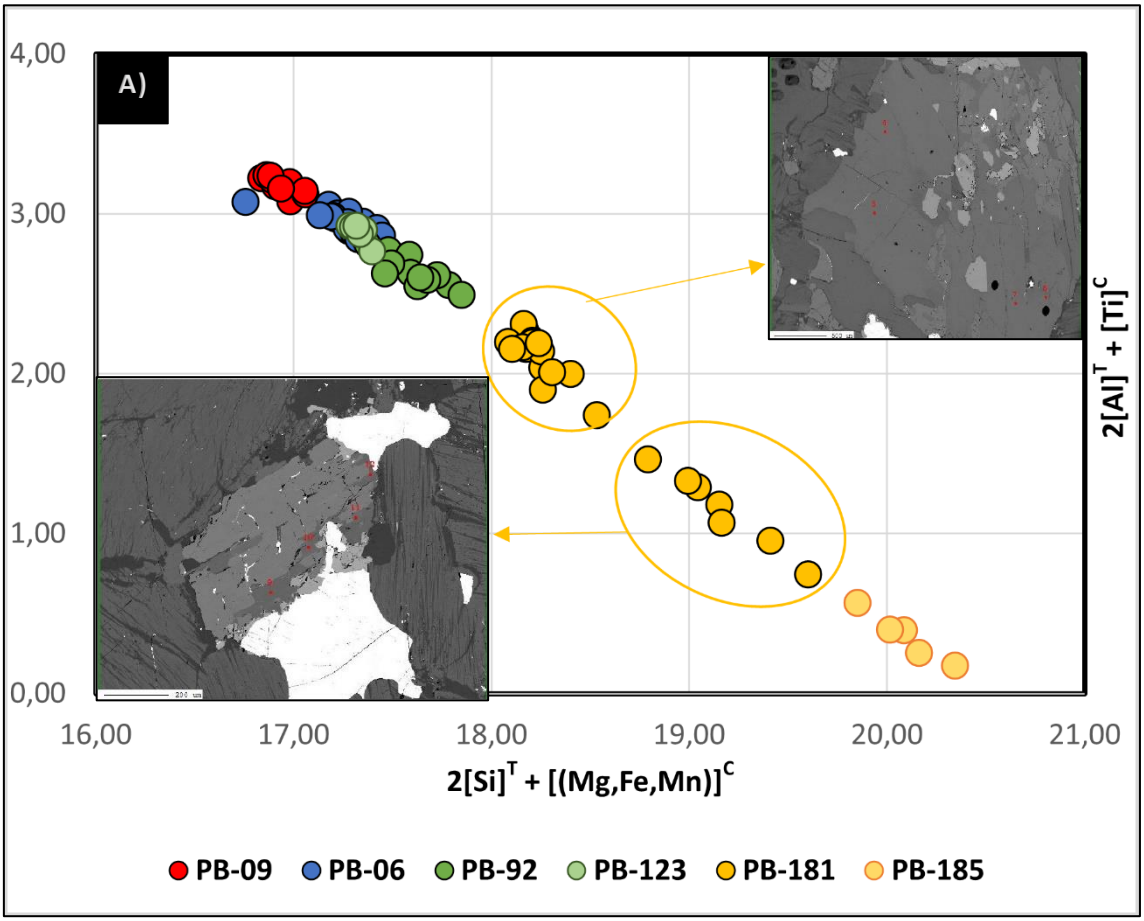

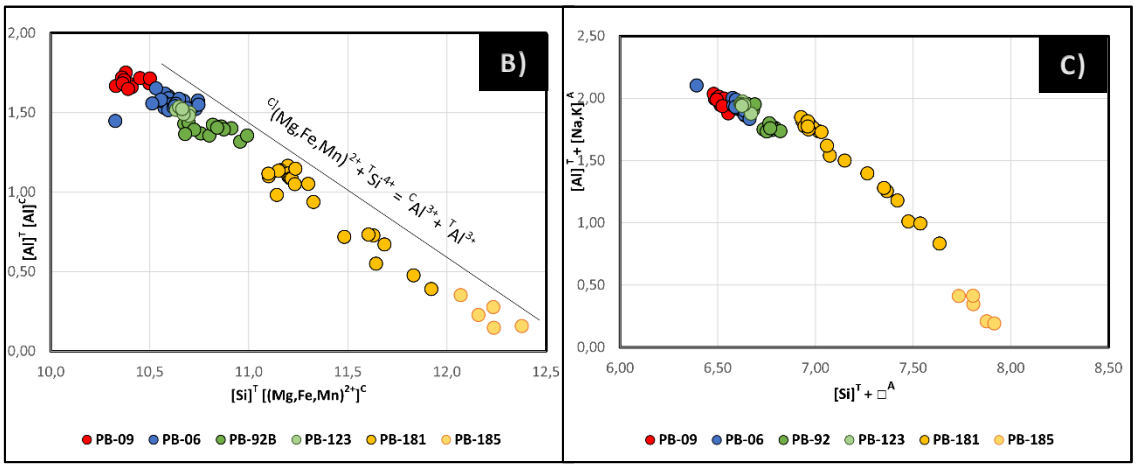

Fig 24: Amphibole cationic exchange diagrams from Pedra Branca pluton. A) Ti-Tschermakitic substitution; B) Tschermakitic substitution; C) Edenitic substitution

3.1.1.2.3 Trace Elements

The CSO unit record the highest contents of different trace elements, in amphibole, such as Ti, V, P and REEs, in relation to the other units studied. They are, in general, compositionally very homogeneous, recording slight correlation between Ti and REEs (Fig. 25a) and are enriched in REEs, in relation to, not only the whole rock data but in relation to the other units as well (fig 26a), with La(N)/Lu(N) ratios ranging between 11.2 and 14.1. Amphibole from the CSO unit record a strong negative Eu anomaly, with Eu/Eu* values ranging between 0.50 and 0.77, despite such anomaly being absent in the whole rock data (fig. 26a).

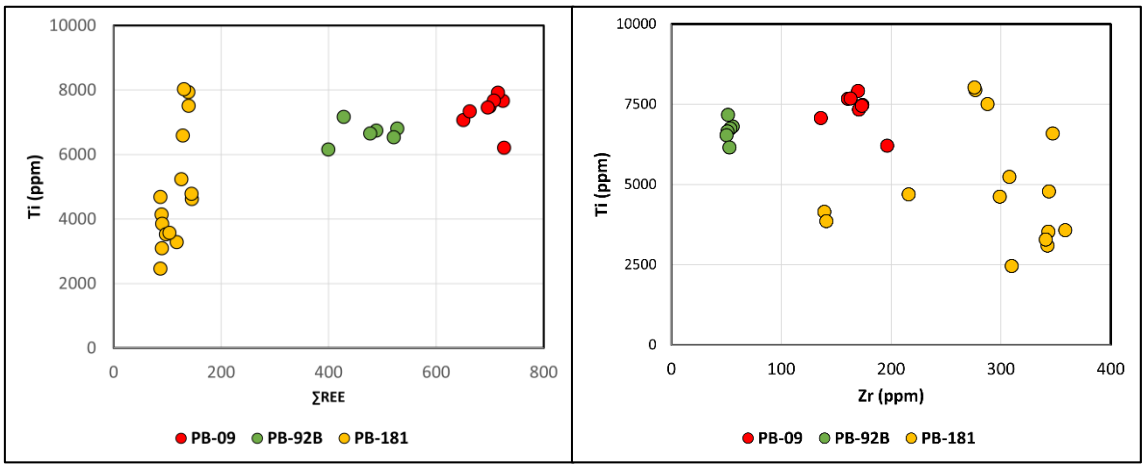

Fig 25: A) [Ti] versus REEs compositional diagrams; B) [Ti] versus [Zr] compositional diagram

Amphibole from the LSO unit are impoverished in LREEs but slight enriched in HREEs, in relation to whole rock, and record a slight negative Eu anomaly, with Eu/Eu* values ranging between 0.67 and 0.77. Similarly, to the crystals from the CSO unit, they are homogeneous in composition, not recording big compositional differences within the same crystal or group of crystals analyzed.

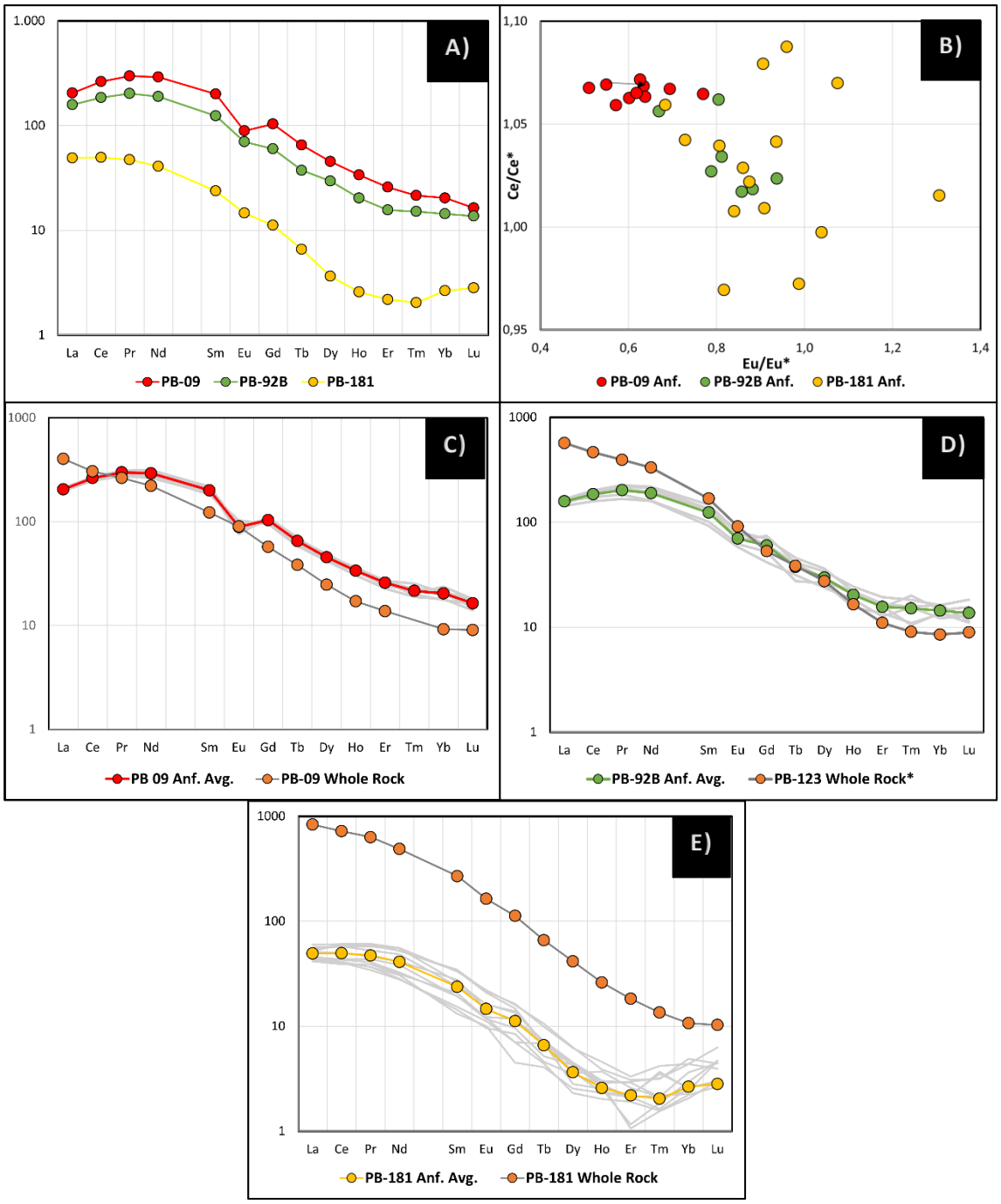

Fig 26: A) Comparison between the normalized REE distribution patterns between the different units. B) (Ce/Ce*) versus (Eu/Eu*) diagram; C,D,E) REE normalized distribution pattern for each unit, in relation to whole-rock data.

Amphibole from the LSS unit differs from the other units; they are characterized by the heavy REEs impoverishment, in relation to the whole rock data and in relation to the other units (Fig 24c and Fig 24a, respectively), and lack any significant Eu anomaly, with Eu/Eu* values ranging from 0,7 to 1,3 (Fig. 12b). They are also enriched in Zr, with content ranging from 150 to 360 ppm Zr, values that are three to six times higher than the ones recorded in the silica-oversaturated units. and show a strong correlation

between Ti and REEs content in its composition, correlation that is not observed in such a degree in the other units studied.

3.1.1.3 Biotite

Biotite is one of the most abundant mafic minerals present in all units of the Pedra Branca pluton, occurring in the form of anhedral to subhedral crystals, usually interstitially and often associated with other mineral phases such as pyroxenes, amphiboles, and opaque minerals (Fe-Ti oxides; fig. 27). A total of seven different samples were used to analyze biotite by electron microprobe, representing all the geological units of interest, aiming to characterize major compositional differences between them. The samples used are as follows: two samples from LSS unit (PB-181 and PB-185), two from the LSO unit (PB-92 and PB-123), two samples from the ESO unit (PB-06 and PB-22) and a single sample from the CSO unit (PB-09). All results obtained and the calculated structural formulas are presented as supplementary data sheets in Appendix II.

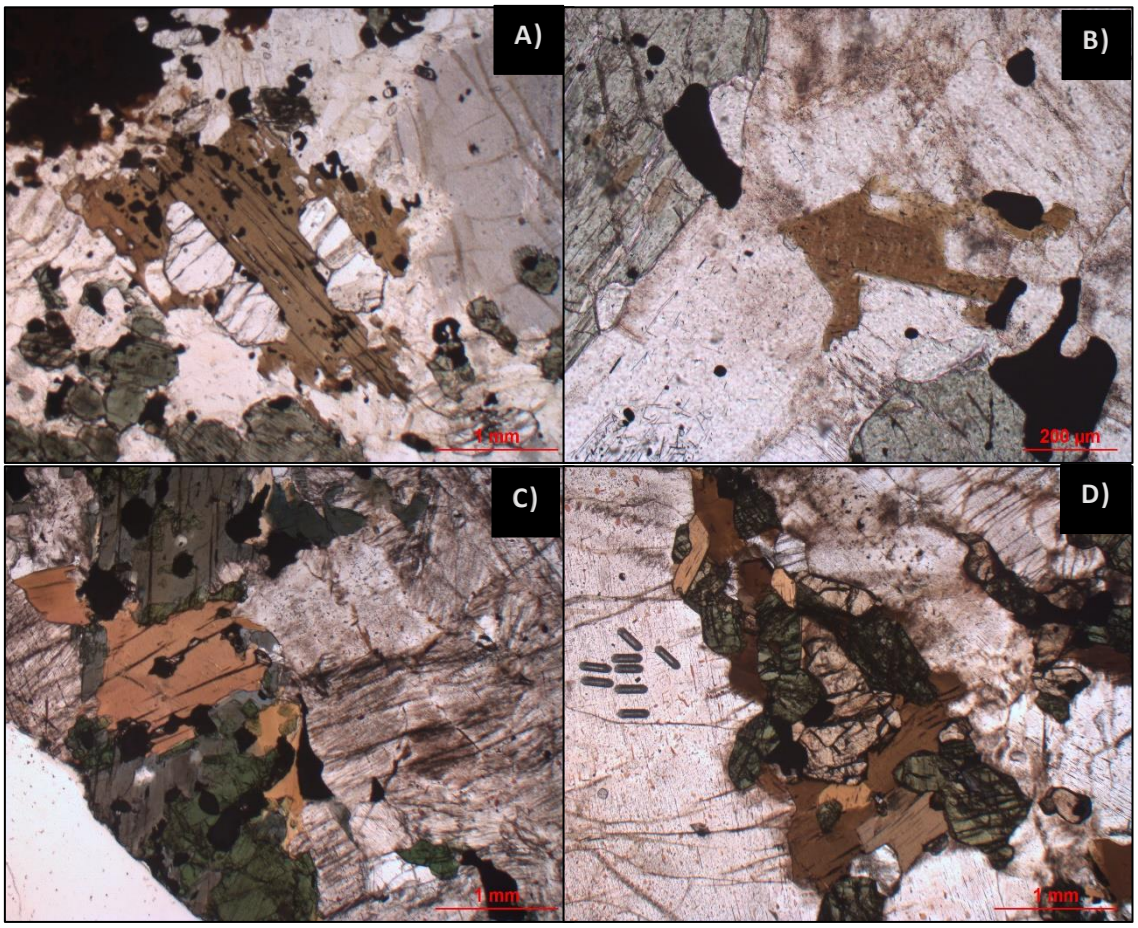

Fig 27: Photomicrographs of biotite from. A) Sample PB-09 (CSO unit); b) sample PB-123 (LSO unit); c) sample PB-181 (LSS unit); d) sample PB-185 (LSS unit).

The classification diagrams by Deer *et al*., (1992) (fig. 28) show that all the biotite crystals are Mg-rich, being classified as phlogopite. Also, the silica-oversaturated units (ESO, LSO and CSO) record a significantly lower Mg#, ranging between 64 and 76, when compared to the silica-saturated unit (LSS), that record Mg# between 72 and 83.

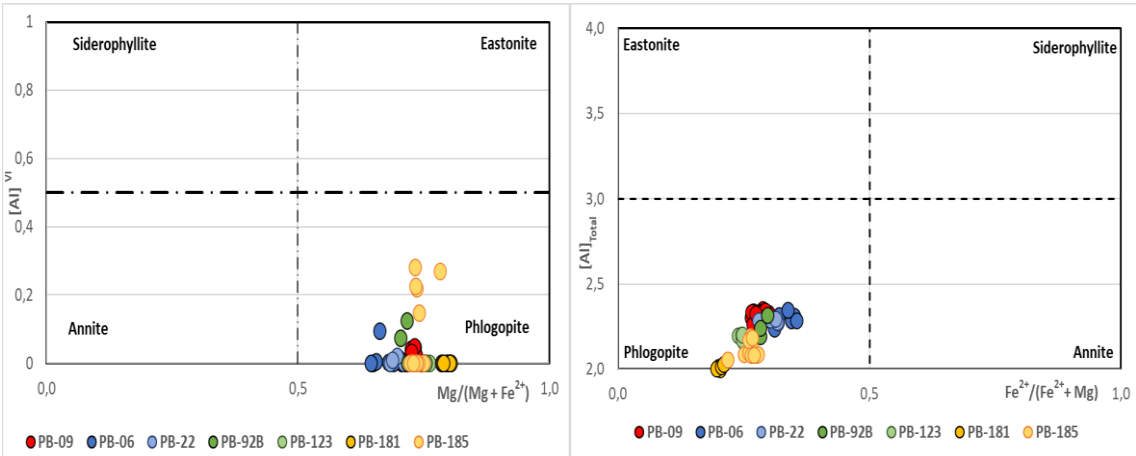

Fig 28: Biotite classification diagrams by Deer et al (1992)

An important negative correlation between Fe^{2+} and Mg# is observed in Figure 28a, where the silica-oversaturated units are, in general, Fe^{2+}-rich in composition (ranging from 1.33 to 1.90 a.p.f.u), while the LSS unit shows more variation, with crystals from the sample PB-181 being Fe^{2+}-poor (1.16 to 1.23 a.p.f.u), and crystals from the sample PB-185 recording Fe^{2+} values similar to the ones from the LSO and CSO units (1.31 – 1.57 a. p.f.u).

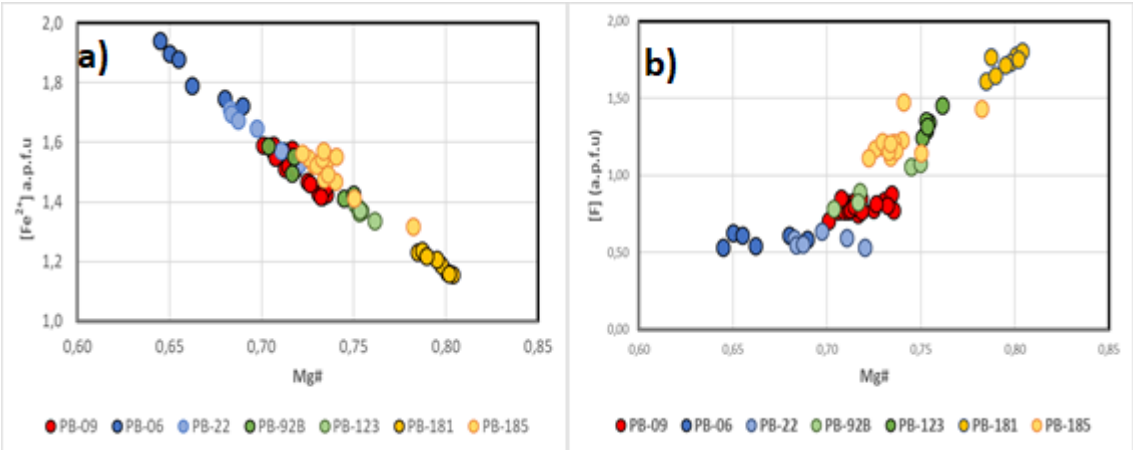

Fig 29: A) Fe2+ vs Mg# correlation diagram; B) [F] vs Mg# correlation diagram

F has the opposite behavior to Fe^{2+} (Fig. 29b); there is a strong positive correlation between F content and Mg#, where biotite from the silica-oversaturated units, such as ESO and CSO units, record the lowest F content, while those from the LSS unit record the highest, with values ranging from 1.1 to 1.8 wt% (0.53 – 0.85 a.p.f.u) and 2.3 to 3.9 wt% (1.11 - 1.8 a.p.f.u) respectively. It is noteworthy that biotite from both the LSS and LSO samples record the highest variation of F contents. Sample PB-181, from the LSS unit, has the highest F content amongst all samples analyzed, ranging between 3.5 and 3.9% F (1.61 – 1.80 a.p.f.u), while sample PB-185 record F content, ranging from 2.3 to 3.0% (1.11 – 1.47 a.p.f.u). For the LSO unit, sample PB-123 show results similar to PB-185, with F content ranging from 2.7 to 3.0% F (1.24 – 1.45 a.p.f.u), while sample PB-92B results closer resembles the values from the other silica oversaturated units, with F content ranging from 1. 7 to 2.3% F (0.78 to 1.07 a.p.f.u).

In general, biotites from the silica-oversaturated units are enriched in Al and Ti when compared to the silica-saturated unit (fig. 30), with the CSO unit recording the highest contents for both elements, with values ranging from 12.9 to 13.5% Al_2O_3 (2.28 – 2.34 a.p.f.u) and 3. 6 to 4.4% TiO_2 (0.39 – 0.48 a.p.f.u) respectively, while the LSS unit record the lowest Al and Ti contents, with values ranging from 11.5% to 12.26% Al2O3 (2.0 – 2.12 a.p.f.u) and 1.1% to 3.2% TiO2 (0.12 - 0.34 a.p.f.u) respectively.

The cationic exchange mechanisms which act in biotite are varied, but based on figure 30a, it is possible to assume that one of the most important is given by the following:

$$[\mathrm{Al}]^{\mathrm{IV}} + [\mathrm{Al}]^{\mathrm{VI}} \leftrightarrow [\mathrm{Si}]^{\mathrm{IV}} + [(\mathrm{Mg}, \mathrm{Fe}, \mathrm{Mn})^{2+}]^{\mathrm{VI}}$$

where biotites from the silica-saturated unit (LSS) are Si and Mg-rich (and consequently Al-poor) compositions. A small group of crystals from the PB-185 sample stands out by their Si-rich character, and a possible cationic exchange would be:

$$2\,[(\mathrm{Fe}, \mathrm{Mg}, \mathrm{Mn})^{2+}]^{VI} + [\mathrm{Al}^{3+}]^{IV} \leftrightarrow [\mathrm{Al}^{3+}]^{VI} + [\mathrm{Si}^{4+}]^{IV} + [\ ]^{V}$$

where bivalent elements such as Fe, Mg and Mn, in the octahedral site, are replaced by Al^{3+}, alongside with Si^{4+} in the tetrahedral site, to balance charges, resulting in the enrichment of Si and Al, as observed in the diagram b from figure 30.

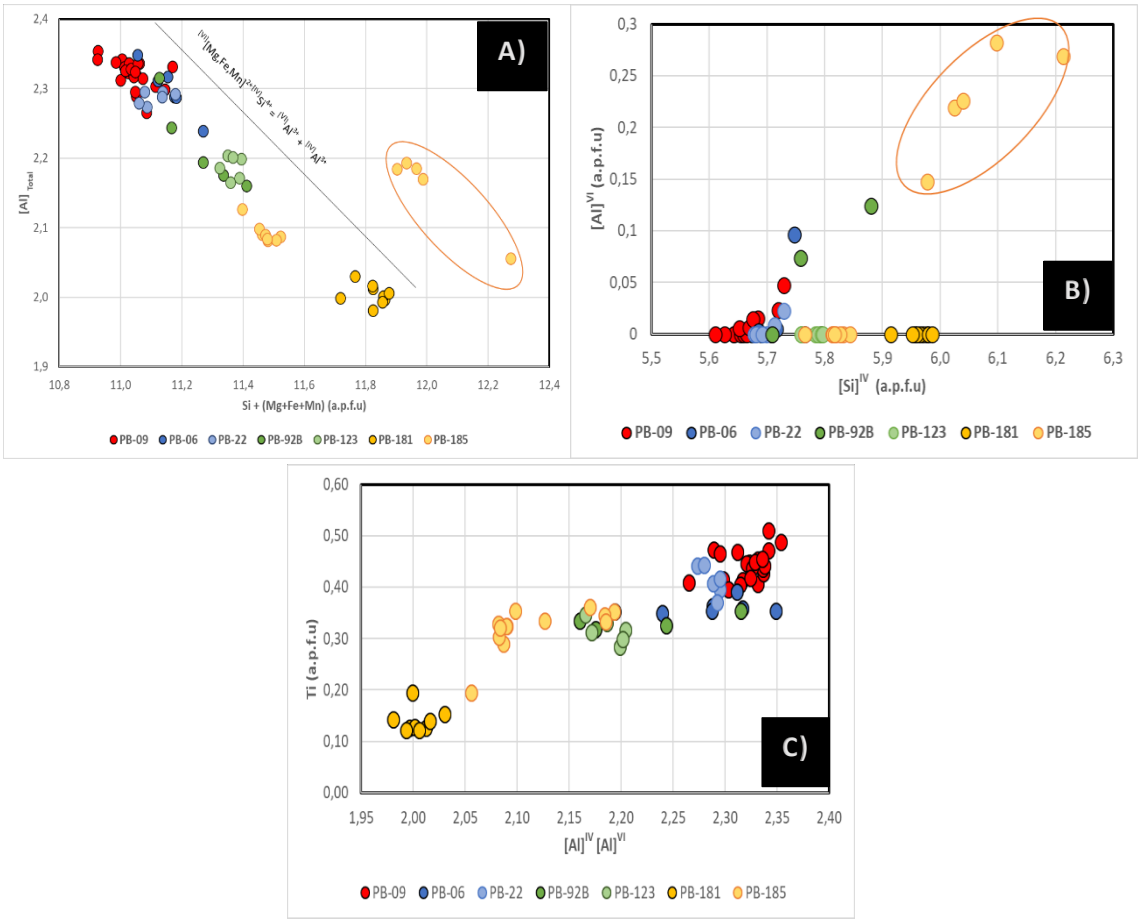

Fig 30: A) Biotite cationic exchange diagram with Si-rich crystals highlighted. B) $[Al^{3+}]^{VI}$ x $[Si^{4+}]^{IV}$ diagram. C)[Ti] x $[Al]_{tot}$ diagram.

3.1.1.4 Acessory Minerals

3.1.1.4.1 Apatite

Apatite ($Ca_5(PO_4)_3(OH,F,Cl)$) is the most common accessory phase in all units from the Pedra Branca pluton. It occurs as small subhedral to euhedral crystals (averaging 70 µm), often associated with, and included in, different mineral phases, such as K-feldspar, pyroxene, amphibole, and opaque minerals, such as ilmenite and hematite. A few exceptionally large crystals occur in every unit (> 1.0 to ~2.0 mm, fig. 31), often euhedral and commonly associated with K-feldspar. Apatite crystals from every sample are often fractured and do not present inclusions of any kind, which could be an indicator of early saturation and crystallization, in relation to the other mineral phases.

All the analyses made on apatite were done by electron microprobe and LA-ICP-MS. The structural formula calculations that were based on a total of 25 anions (counting O, OH, Cl and F), and all the data obtained, as well as the structural formulae, are presented in the form of tables in Appendix I. The samples used are as follows: one sample from the CSO unit (PB-09), two samples from the ESO unit (PB-06 and PB-22), two samples from the LSO unit (PB-92B and PB-123) and two samples from the LSS unit (PB-181 and PB-185).

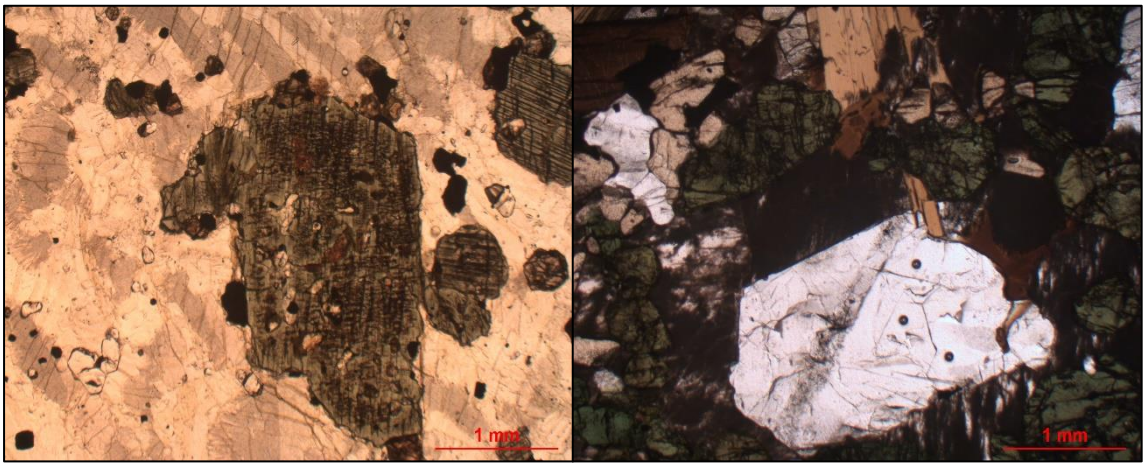

Fig 31: a) Typical apatite occurrence, small subhedral to euhedral crystals (sample PB-09; CSO unit); b) Large euhedral apatite crystal (sample PB-181; LSS unit)

Compositionally, apatite from the four different units are similar, especially in relation to major elements such as Ca and P, with P_2O_5 content ranging from 38 to 41 wt.% (which corresponds to 5.5 to 5.8 a.p.f.u of P), while CaO ranges between 51 and 53 wt.% (9.3 to 9.6 a.p.f.u of Ca), with small differences between core and rim, with the core usually enriched in both elements in relation to the rims, but not by a significant margin (<0.5%). Compared to the stoichiometric values for fluorapatite ($Ca_{10}(PO_4)_6F_2$), apatite from all units are Ca-poor in composition, averaging 9.5 a.p.f.u of Ca, but are enriched in a few different elements, such as REE, Si, Na, and S, depending on the unit, which suggests a high degree of substitution in the Ca-site.

Apatite from the LSO unit (samples PB-92B and PB-123) are enriched in Si and REEs when compared to the other units, with contents averaging around 0.13 and 0.19 a.p.f.u of Si and REE respectively, while apatite from the other units ranges from 0.6 to 0.9 a.p.f.u of Si and 0.9 to 0.13 a.p.f.u of REEs. Depletion in Ca with an associated enrichment of Si and REE in apatite suggests a high degree of substitution in the Ca and P-sites, by REE and Si respectively, and the mechanism that better explain such enrichment is given by the following equation: (Pan & Fleet, 2002; fig. 32).

$$[REE]^{3+} + [SiO4]^{4-} \leftrightarrow Ca^{2+} + [PO4]^{3-}$$

Apatite from the LSS unit are enriched in Na and LREEs, with contents ranging from 0.07 to 0.13 and 0.1 to 0.2 a.p.f.u of Na and LREEs, respectively. Na^{+} and $LREEs^{3+}$ are often incorporated in the apatite structure through a variety of coupled substitutions, such as the equation below, where they prefer the Ca1 and Ca2 sites, respectively.

$$[Na]^{+} + [REE]^{3+} \leftrightarrow 2[Ca]^{2+}$$

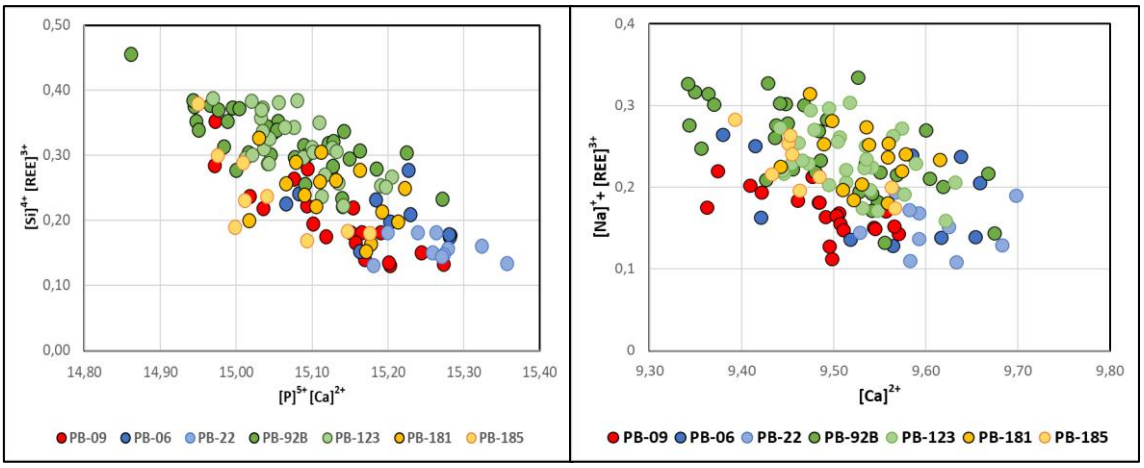

Fig 32: Correlation diagrams representing two of the major substitution mechanisms for REE in apatite.

Although there are multiple mechanisms that incorporate REEs into the apatite structure, the enrichment in REEs on apatite from the LSS unit, is most likely related to the parental magma composition rather than associated to a major substitution mechanism, since the LSS unit whole magma composition is enriched in REEs, especially LREEs, in relation to the other units, as shown in fig. 33, and hence apatite being a really early stage crystallization mineral, in Pedra Branca, it probably inherited its higher REE content from the its parental magma.

All the studied apatite were categorized as fluorapatite, which is the most common type of apatite in igneous rocks, with fluorine contents ranging from 2.7 to 4.6 wt.%, which corresponds to 1.5 to 2.4 a.p.f.u. In general, fluorine has a slight negative correlation with the whole rock SiO_2 content (fig. 34c), such that apatite from the silica oversaturated units has lower F compared to apatite from LSS. It was also noted that fluorine content increases from core to rim, especially in larger crystals.

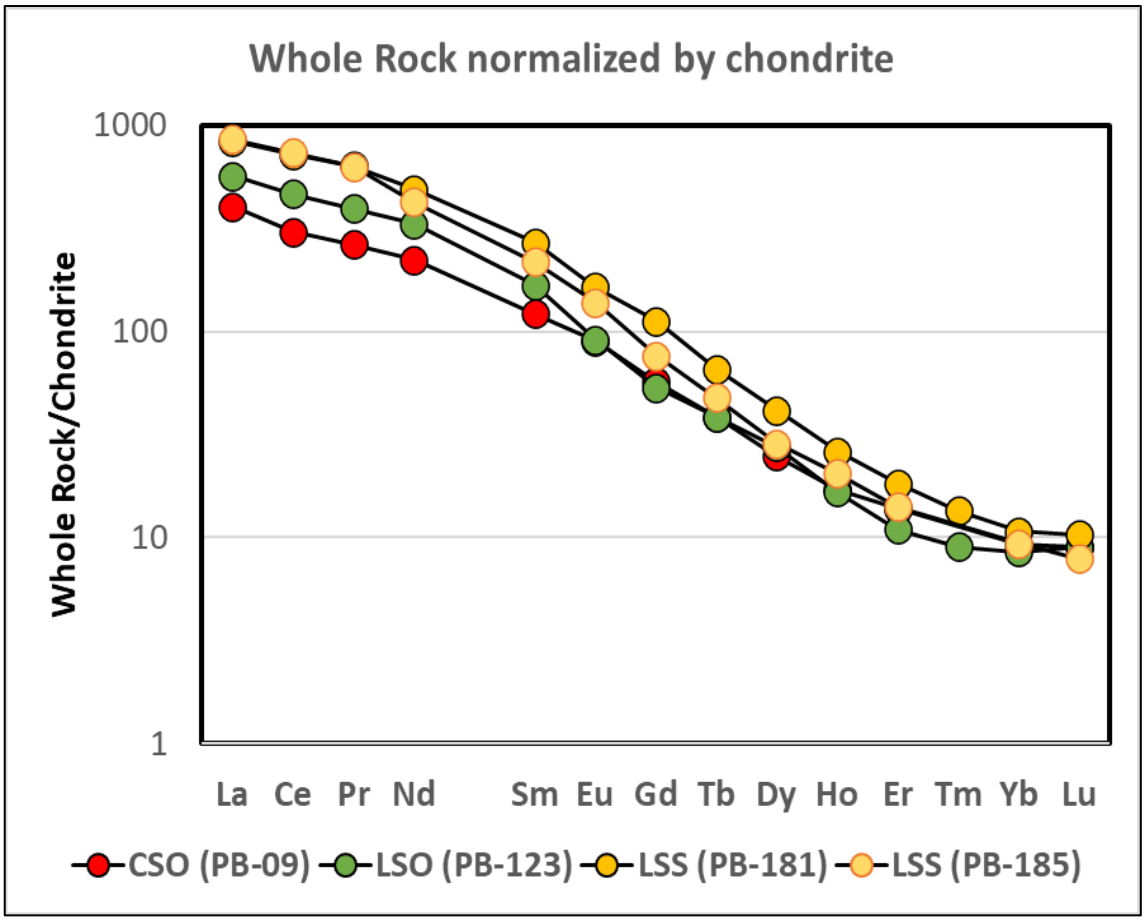

Fig 33: Whole-rock REE pattern normalized by chondrite

There is a large difference in Cl content in apatite from the different units, where apatite from the silica oversaturated units has contents up to thirty times higher than those of LSS (0.2-0.7 wt.% versus 0.01-0.1 wt%, fig. 34a).

Chlorine contents of the studied apatite show a positive correlation with whole rock SiO_2 content (fig. 34d) and no significant variation between core and rim.

The EPMA data show that the oversaturated units are S-poorer compared to the saturated unit, with SO_3 contents ranging from 0.32 to 0.47 wt.%, and 0.5 to 0.9 wt.% respectively (fig 35). Also, large apatite crystals, from oversaturated units, record a slight enrichment in S content in the rims in relation to the core, while the apatite from the saturated unit does not record such enrichment. Since sulfur is a multivalent element, the differences in S content should be related to different oxidation conditions during crystallization, where more oxidizing conditions would facilitate the incorporation of S^{6+} by apatite as $[SO_4]^{-2}$, substituting $[PO_4]^{-2}$ in its structure, according to the following mechanism (Pan & Fleet, 2002); fig. 35.

$$[SO4]^{2-} + [SiO4]^{4-} \leftrightarrow 2\,[PO4]^{3-}$$

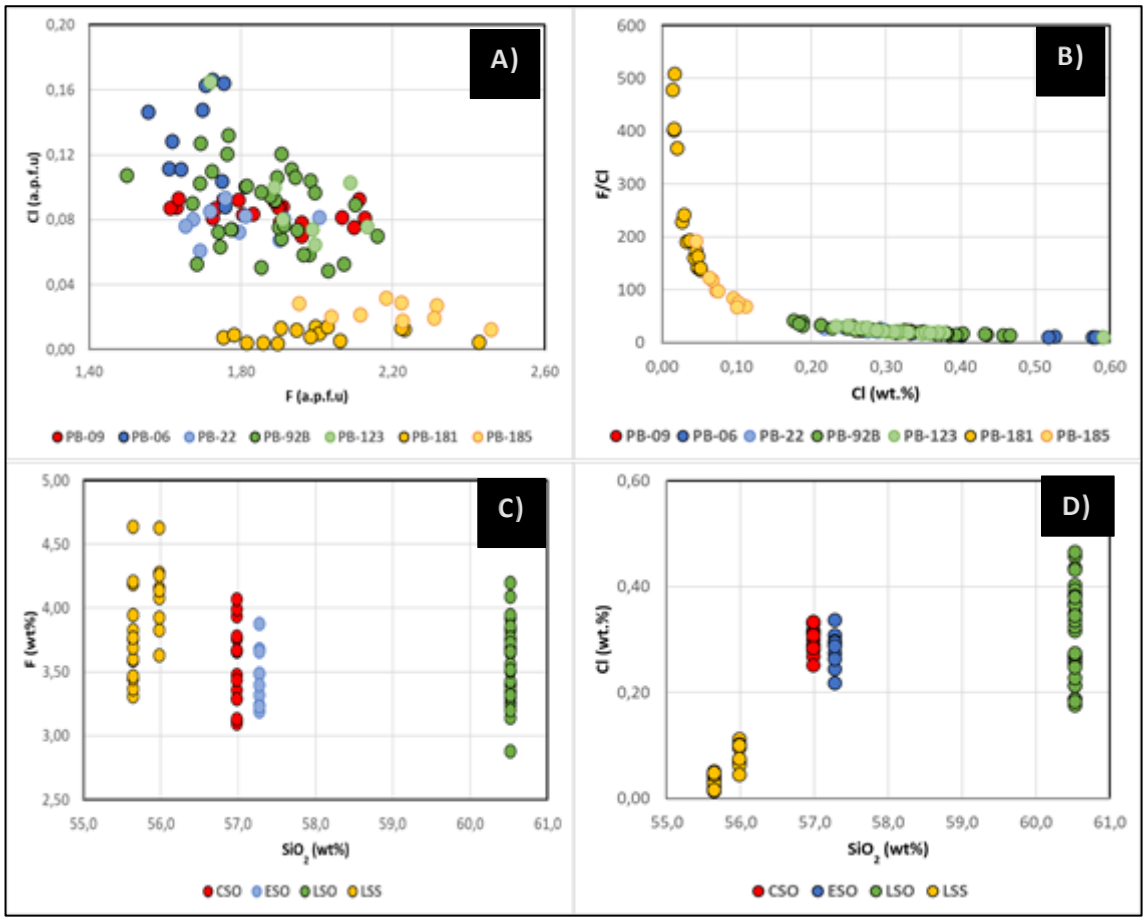

Fig 34: A and B) Cl x F correlation diagrams. C and D) Correlation diagrams between whole-rock SiO_2 and apatite Fluorine and Chlorine content.

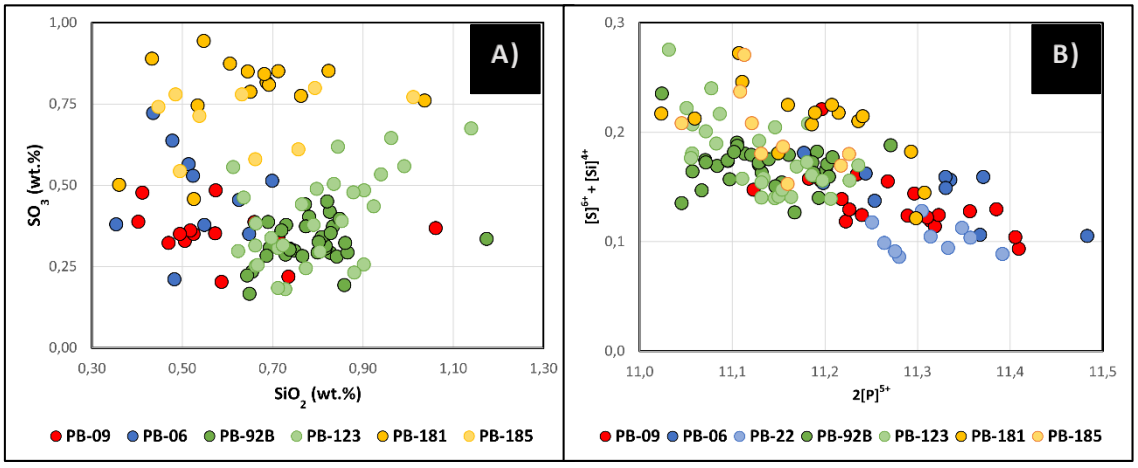

Fig 35: A) SO^3 x SiO^2 correlation diagram; B) Si^{4+} + S^{6+} x P^{5+} correlation diagram

Apatites from LSS unit (samples PB-181 and PB-185) have the highest LREE enrichment amongst apatite from all units, with La ranging between 3000 and 5500 ppm (4130ppm avg.) and (La/Yb) ratio ranging from 155 to 470 (312 avg.). They also have a slightly positive Ce anomaly, with Ce/Ce* (Ce* = $([La]_N \times [Pr]_N)^{1/2}$) ranging from 1.0 to

1.14, and no significant Eu anomaly, with Eu/Eu* (Eu* = $([Sm]_N \times [Gd]_N)^{1/2}$) ratios between 0.87 and 1.1 (figs.36 and 37)

Apatite from the oversaturated units show a weaker enrichment in LREEs, with La values ranging from 1950 to 3900 ppm (2860 avg.) and (La/Yb) ratios between 100 and 230, which are values roughly two times lower than in LSS apatite. Figure 36 shows that the whole rock composition from the LSS unit is enriched in LREEs when compared to the other units, and since apatite is an early crystallization phase in the Pedra Branca pluton, the variations in REE content in apatite from the different units could reflect the differences in parental magma compositions.

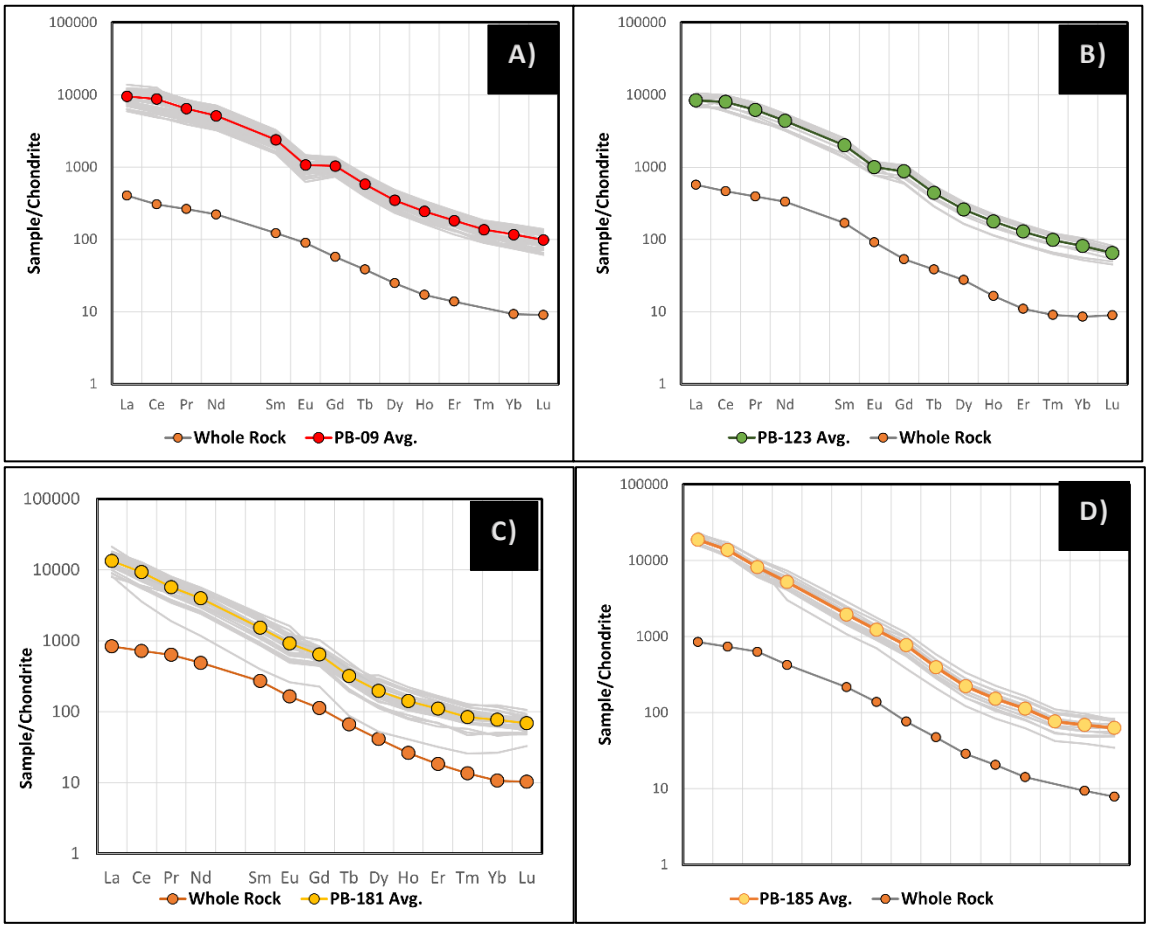

Fig 36: Apatite REE normalized distribution patterns for each unit, in relation to whole-rock data; A) PB-09 (CSO unit); B) PB-123 (LSO unit); C) PB-181 (LSS unit); D) PB-185 (LSS unit)

It is important to highlight that despite apatite from the oversaturated units recording a more modest enrichment in LREEs, when compared to the LSS unit, they are, on average, enriched in HREEs; especially apatite from the CSO unit, with $Yb_{(N)}$ and $Lu_{(N)}$ values ranging from 80 to 160 (~110 avg.), compared to $Yb_{(N)}$ and $Lu_{(N)}$ values between 35 and 100 (~73 avg) from the LSS unit.

Apatite from the oversaturated units shows a positive Ce anomaly, with Ce/Ce* values ranging between 1.0 and 1.3 (fig. 37), and a negative Eu anomaly, with Eu/Eu* values ranging from 0.65 to 0.86. The presence of a negative Eu anomaly in association with the differences in S content, described previously, suggests a difference in oxidation conditions during the crystallization of apatite in the different units, a feature explored in Chapter III.

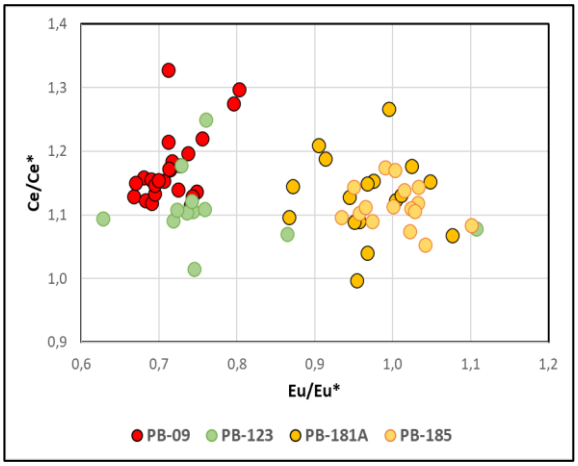

Fig 37: Ce/Ce* x Eu/Eu* diagram

3.1.1.4.2 Titanite

Titanite ($CaTiSiO_5$) is one of the main accessory minerals in syenites of the Pedra Branca pluton, but its abundance and form of occurrence vastly differs between the different units. Out of the four major units studied (CSO, LSO, LSS and ESO), only two of them record the crystallization of titanite, the two units being LSO and LSS. Titanite crystals, under different textural relations, were analyzed using electron microprobe and LA-ICP-MS, and all the data obtained as well as the structural calculations made are present in the form supplementary data sheets in Appendix I and II. The samples used are as follows: using the electron microprobe the samples chosen were PB-92B from the LSO unit and samples PB-181 and PB-185 from the LSS unit, while using LA-ICP-MS the samples chosen were PB-92B and PB-123 from the LSO unit and PB-08A, PB-181 and PB-185 from the LSS unit.

In the LSS unit, titanite occurs both as large euhedral to subhedral crystals, measuring up to 1.5 mm, light to dark brown in color (fig. 38a), and as anhedral,

late-stage crystals, riming ilmeno-hematites, typically beige to light brown in color with crystals measuring up to 0.25mm (fig. 38b).

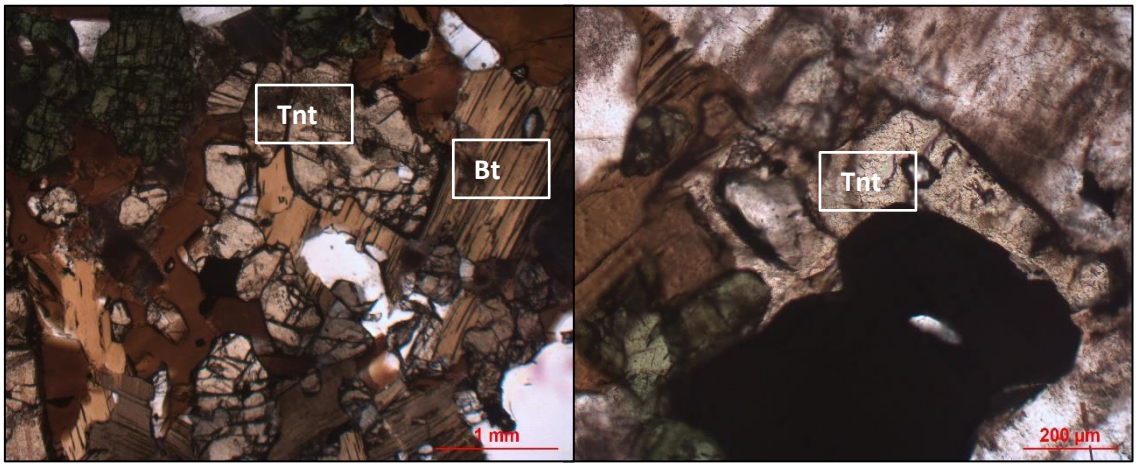

Fig 38: Photomicrographs showing titanite in two different textural relation in sample PB-181 (LSS unit)

The structural formulas for titanite used in the diagrams presented, were calculated based on a total of 05 oxygens. It is noteworthy that the results obtained by LA-ICP-MS, from sample PB-181, were subdivided into two groups named “Pop.1” and “Pop.2”, based on the textural context of each analyzed crystal; where “Pop.1” represents the group of large euhedral to subhedral crystals, “independent” from other mineral phases, while “Pop.2” represents the group of anhedral crystals, associated with other mineral phases, shown in figure 39.

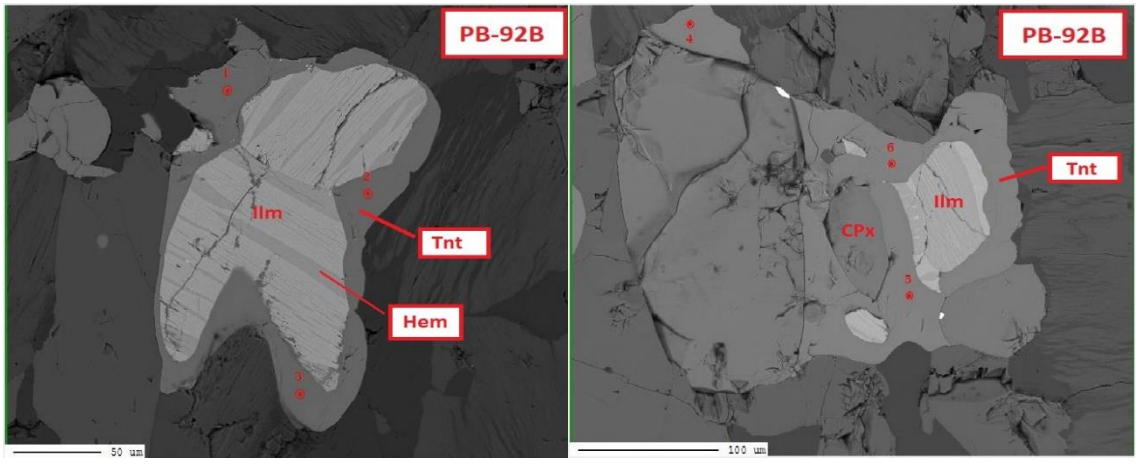

Fig 39: Photomicrographs showing titanite in two different textural relation in sample PB-181 (LSS unit)

The proportion of titanite in the LSO unit is much lower when compared to the LSS unit, and it occurs exclusively as reaction halos around ilmeno-hematite, as can be seen

in figure 39b. In the studied samples from the CSO and ESO units titanite is rare or absent.

Titanites from the LSS unit are Al-poor (0.7 – 1.0% Al_2O_3) when compared with those from the LSO sample, with Fe/Al ratios averaging around 2.0 (Fe/Al_{LSS}= 1.6 – 2.8), which is characteristic of silica-undersaturated peralkaline magmas (Kowallis et al 2008), while those from LSO unit show higher Al content (1.4 – 2,6% Al_2O_3), with Fe/Al ratios averaging around 1.1 (Fe/Al_{LSO} = 0.9 – 1.2), which is characteristic of titanites from silica-saturated magmas (fig. 40a).

Al^{3+} and Fe^{3+} are often elements incorporated into titanite structure through coupled substitutions of Ti for Al or Fe;

$$(\mathrm{Al,Fe})^{3+} + (\mathrm{OH,F})^{-} \leftrightarrow [\mathrm{Ti}]^{4+} + \mathrm{O}^{2-}$$

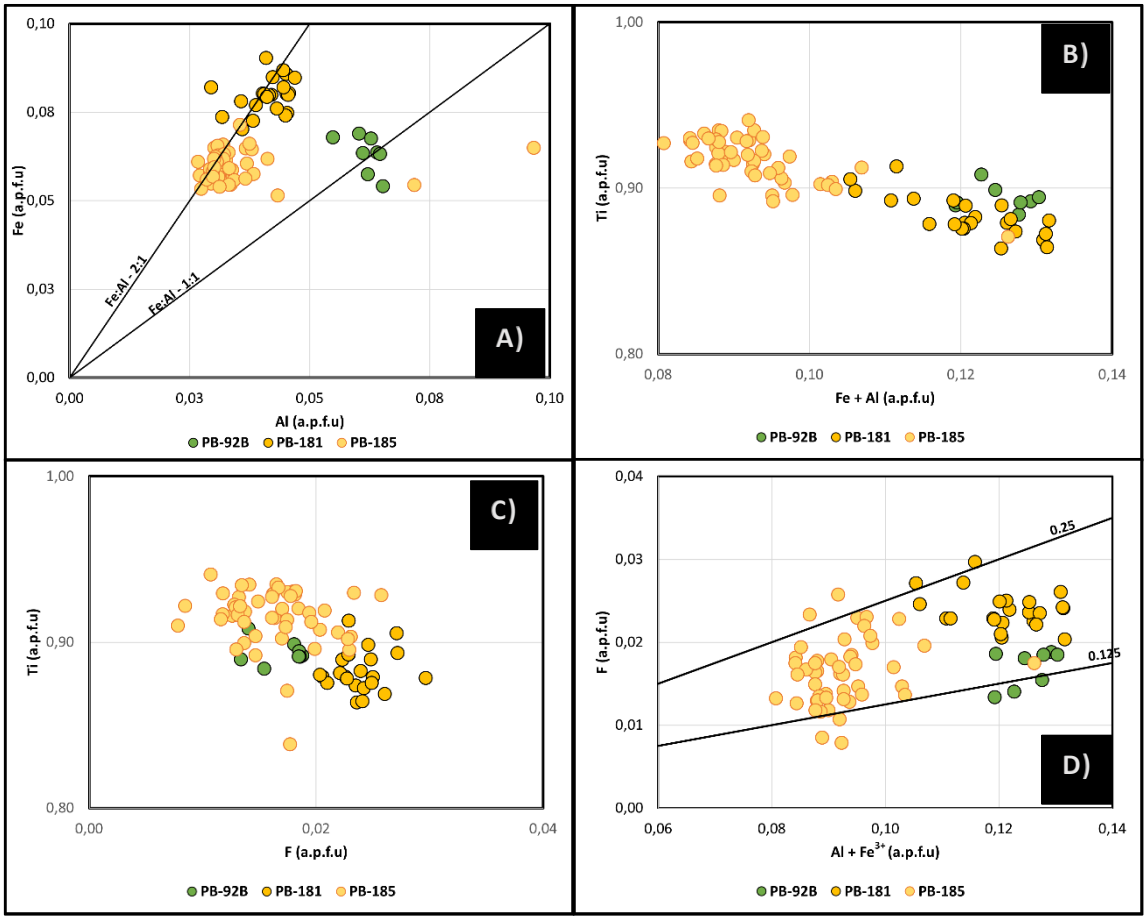

Fig 40: Different correlation diagrams obtained from titanite data; A) Fe x Al diagram; B) Ti x Fe+Al diagram; C) Ti x F diagram; F x Al+Fe^{3+} diagram

In general, titanite from both units studied are F-poor, with F content ranging between 0.10 to 0.28 wt% F (0.01 to 0.03 a.p.f.u). Despite the small fluorine content, both units record a weak correlation between F and Ti (fig. 40c).

Titanite from the LSO unit are characterized by the enrichment in elements such as REEs, U, Th and Y, in relation to the LSS unit (fig 41). These elements are often incorporated into the titanite structure through different mechanisms of coupled substitution; REEs and Y, due to the similar ionic radius and electronic charge, occupy the Ca site in the titanite structure and often involve the coupled substitution of Al^{3+} and Fe^{3+}, which occupy the Ti site, to balance charges.

$$\mathrm{REE}^{3+} + (\mathrm{Al}, \mathrm{Fe})^{3+} \leftrightarrow [\mathrm{Ca}]^{2+} + [\mathrm{Ti}]^{4+}$$

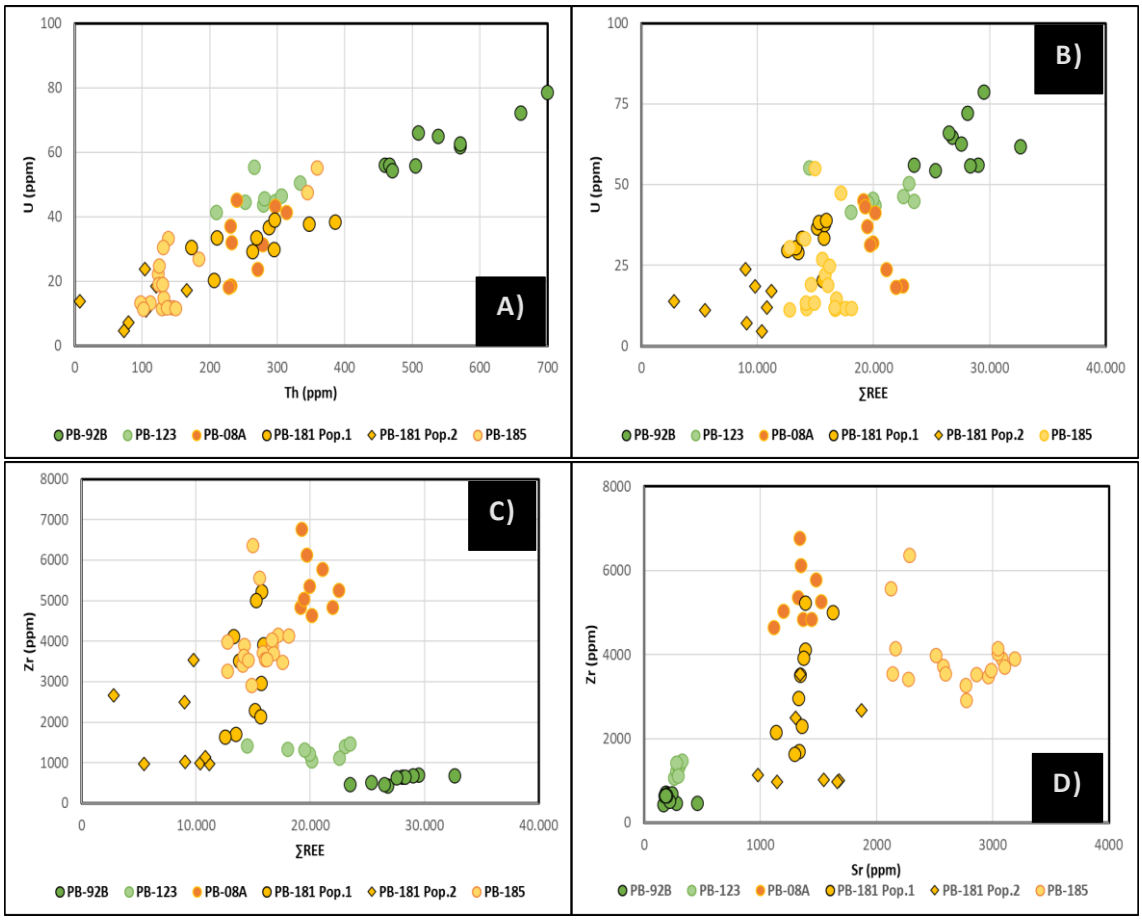

Fig 41: Compositional correlation diagrams for titanite; a) U x Th; b) U x ∑REE; c) Zr x ∑REE; d) Zr x Sr.

Titanite from the LSO unit, show a strong correlation between U and REE contents (fig. 41b; where ∑REE is the sum of La,Ce, Pr, Nd, Sm, Eu, Gd, Tb, Dy, Ho, Er, Tm, Yb and Lu, in ppm), such correlation is observed on sample PB-181, from the LSS unit as well, but only on crystals from the “Pop.1” group, which are analysis from large

titanite crystals, and is absent on the “Pop.2” group, which are the late-stage crystals rims of ilmeno-hematites, as well as in sample PB-185.

The expressive enrichment in Zr and Sr of the LSS unit, in relation to the LSO unit, stands out (fig. 41c and d). Crystals from the LSS unit record Zr content ranging from 0.5 to 1.25 wt% ZrO_2 (up to 6000ppm of Zr, with an average of 3255 ppm) while crystals from the LSO unit record contents ranging between 0.01 to 0.1 wt% ZrO_2 (up to 1500 ppm, with an average of 950 ppm).

Due to the strong enrichment in Zr, the Zr/Hf ratios vary between the two units studied, with the LSS recording higher Zr/Hf ratios, ranging between 25 and 43, while the LSO unit record ratios ranging between 15 and 25 (fig 42b).

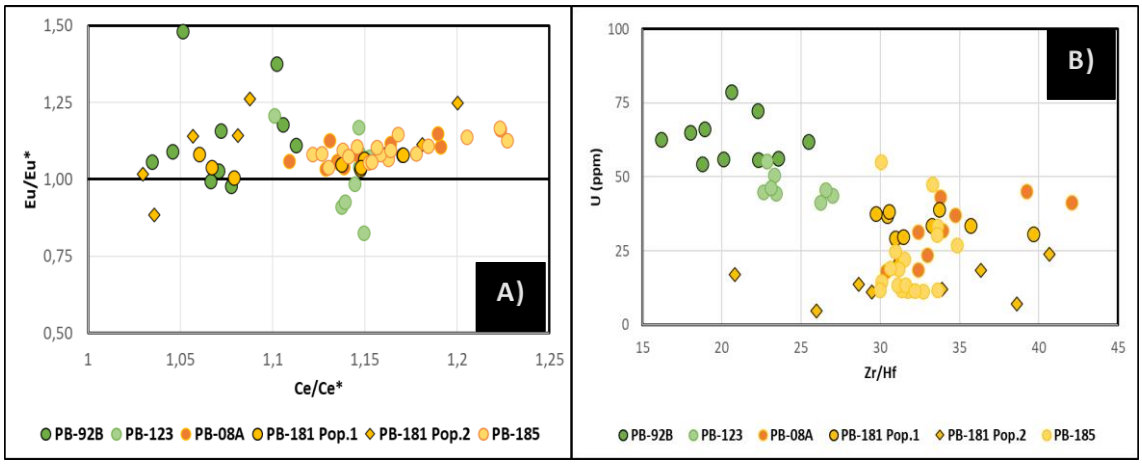

Fig 42: a) Eu/Eu* x Ce/Ce* diagram; b) U x Zr/Hf correlation diagram

Titanite crystals from both units studied show enrichment of LREEs in relation to HREEs, characteristic of the mineral, and predominance of Ce in relation to La and Nd (Ce>La>Nd, fig. 38). The LREE/HREE ratios in the LSO sample average around 33 ($LREE/HREE_{LSO}$= 28 – 40), while higher ratios are shown by the LSS samples, averaging around 44 ($LREE/HREE_{LSS}$ = 40 – 71).

Based on the Ce/Ce* and Eu/Eu* ratios calculated (fig. 42a), where and , it was possible to determine that both units record similar positive ratios for Ce and Eu (Ce/Ce* and Eu/Eu* > 1.0), especially the Eu/Eu* ratio, with values for the two units ranging from 0.9 to 1.25, while the LSS unit record slightly higher values of the Ce/Ce* ratio, ranging from 1.03 to 1.22, versus 1.03 to 1.15 for LSO unit. Core and rim analysis show that Ce/Ce* and Eu/Eu* ratios increase towards the rim, with core ratios averaging around 1.14 and 1.08, for Ce and Eu respectively, and rim ratios averaging between 1.20 and 1.12, respectively.

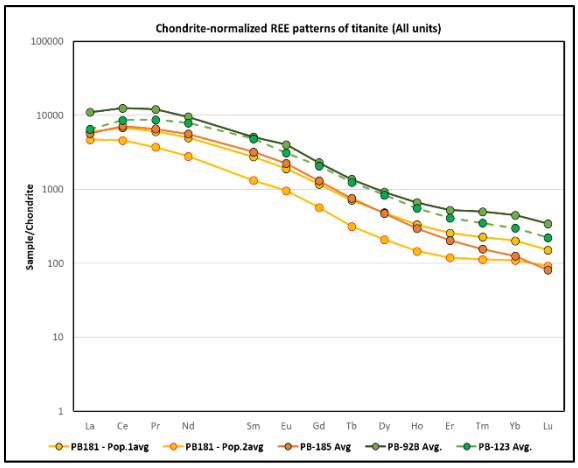

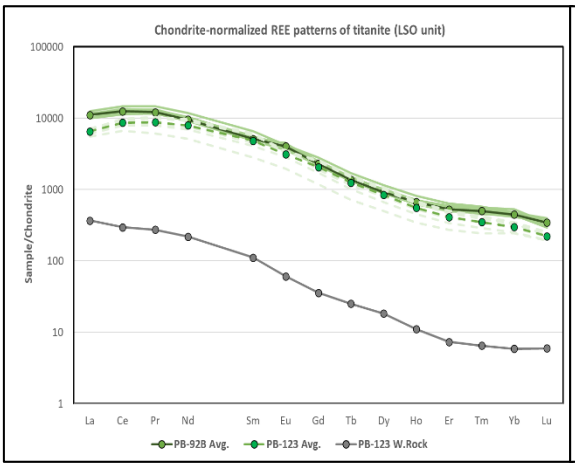

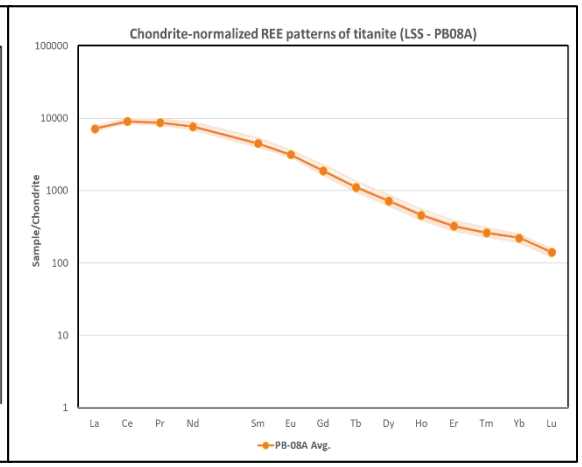

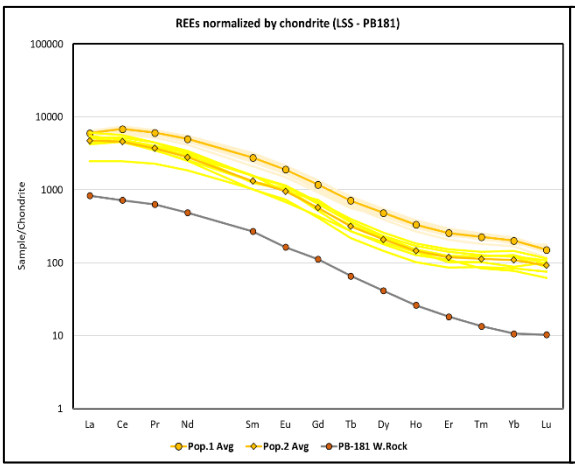

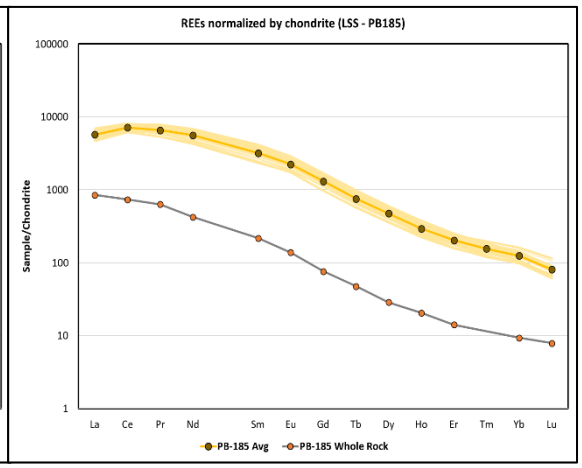

Fig 43: Chondrite-normalized REE patterns for titanite in relation to whole rock. Marked lines represent the sample average

3.1.1.4.3 Zircon

A total of 52 zircon crystals, from five different samples representing the four geological units from Pedra Branca pluton were analyzed, *in situ*, by LA-ICP-MS, except for zircon from the sample PB-123 which were physically separated and concentrated. The samples used were: one from the CSO unit (PB-09), one sample from the ESO unit (PB-22), two samples from the LSO unit (PB-92B and PB-123) and one sample from the LSS unit (PB-181). All data obtained is presented in the form of supplementary data sheets in Appendix I.

In general, zircon occurs as small (< 0.1 mm), subhedral to anhedral crystals, included in different mineral phases, such as K-feldspar, pyroxene, or amphibole and often show diffuse zoning (fig. 44).

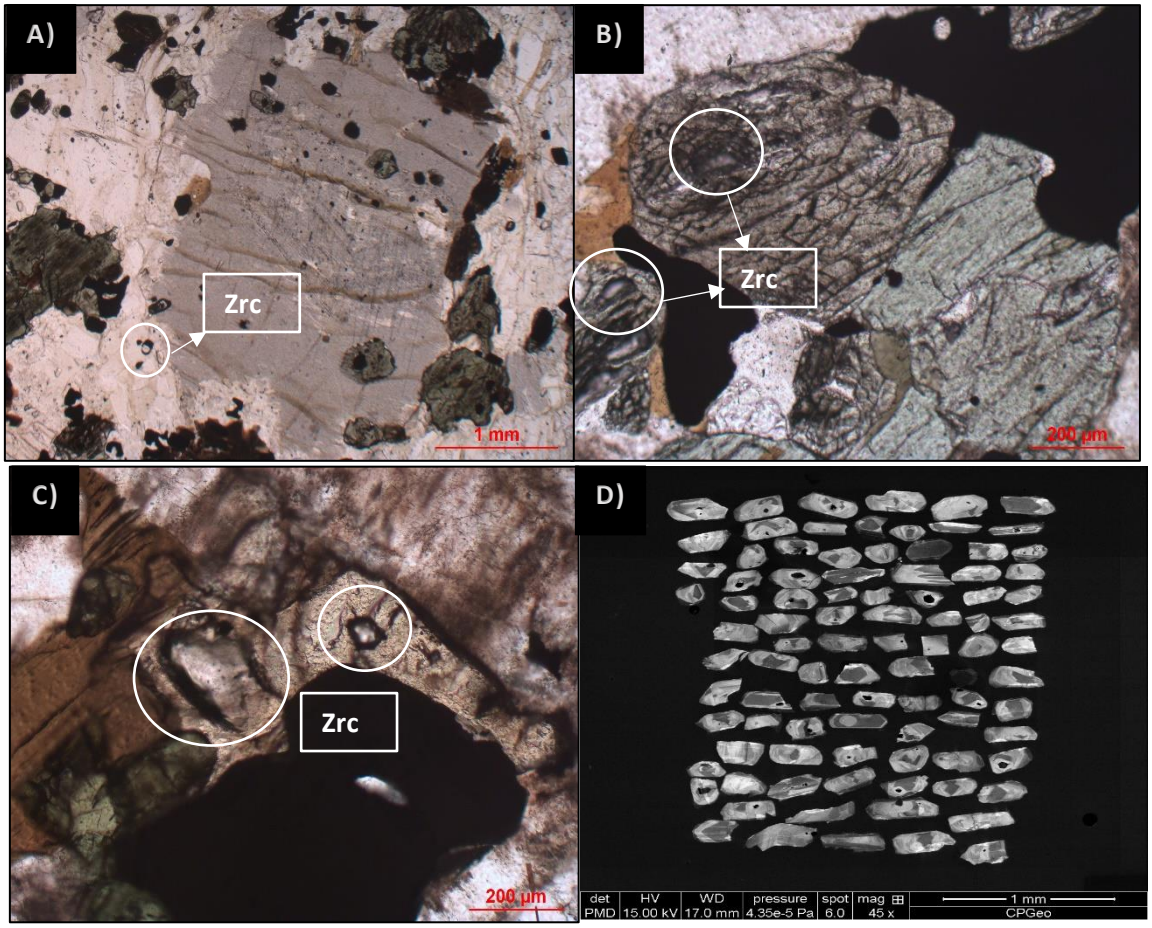

Fig 44: Photomicrographs of zircon on different samples; A) Sample PB-09 (CSO unit); B) Sample PB-92B (LSO unit); C) Sample PB-185 (LSS unit; not analyzed); D) Cathodoluminescence image of the concentrated zircon from sample PB-123 (LSO unit).

All samples analyzed record a steep REE pattern, with $[Lu/Dy]_N$ ranging from 4.0 to 11.6 (~6.8 on average), denoting a strong HREE enrichment in relation to MREEs (fig.45). It is possible to note, based on the REE distribution patterns from figure 45, that zircon from the LSO and LSS units record a wider range of REE content in their composition (gray lines on figure 45), with crystals that are heavily depleted in LREEs, such as Pr, Nd, and Sm, when compared to the population average (colored line in figure 45). Zircon from sample PB-92B record an anomalously high La, with content up to ten times higher than the chondritic value, when compared to the other units, which could be related to micro-inclusions of different accessory phases, such as apatite and titanite, or impurities, such as small fragments of different minerals being analyzed with zircon, due to small zircon crystal size for the used laser beam, since most analysis were made *in situ,* on thin sections (fig.44).

The Ti content in zircon, which can be used as a proxy for crystallization temperature (Ferry & Watson, 2007), amongst the different units are similar, often ranging between 9 and 49 ppm, with the CSO and ESO units averaging the highest values, 36 and 39 ppm respectively, while the LSO and LSS units average the lowest, with 27 and 29 ppm, respectively (fig. 46).

In general, zircon from the Si-oversaturated units record negative Eu anomaly, with [Eu/Eu*] ranging between 0.35 to 0.80, where $Eu* = \sqrt{Sm_N \, x \, Gd_N}$, while the LSS unit does not record any significant Eu anomaly, with [Eu/Eu*] span from 0.9 to 1.3 (fig. 46).

Zircons from the Si-oversaturated units (CSO, ESO and LSO) record higher Hf content, between 8000 and 11000 ppm, and, consequently, lower Zr/Hf ratios, ranging between 45 and 61, when compared to the LSS unit with Hf ranging from 6100 to 7200 ppm, and Zr/Hf ratio span from 69 to 104. Hf in zircon tends to increase from core to rim.

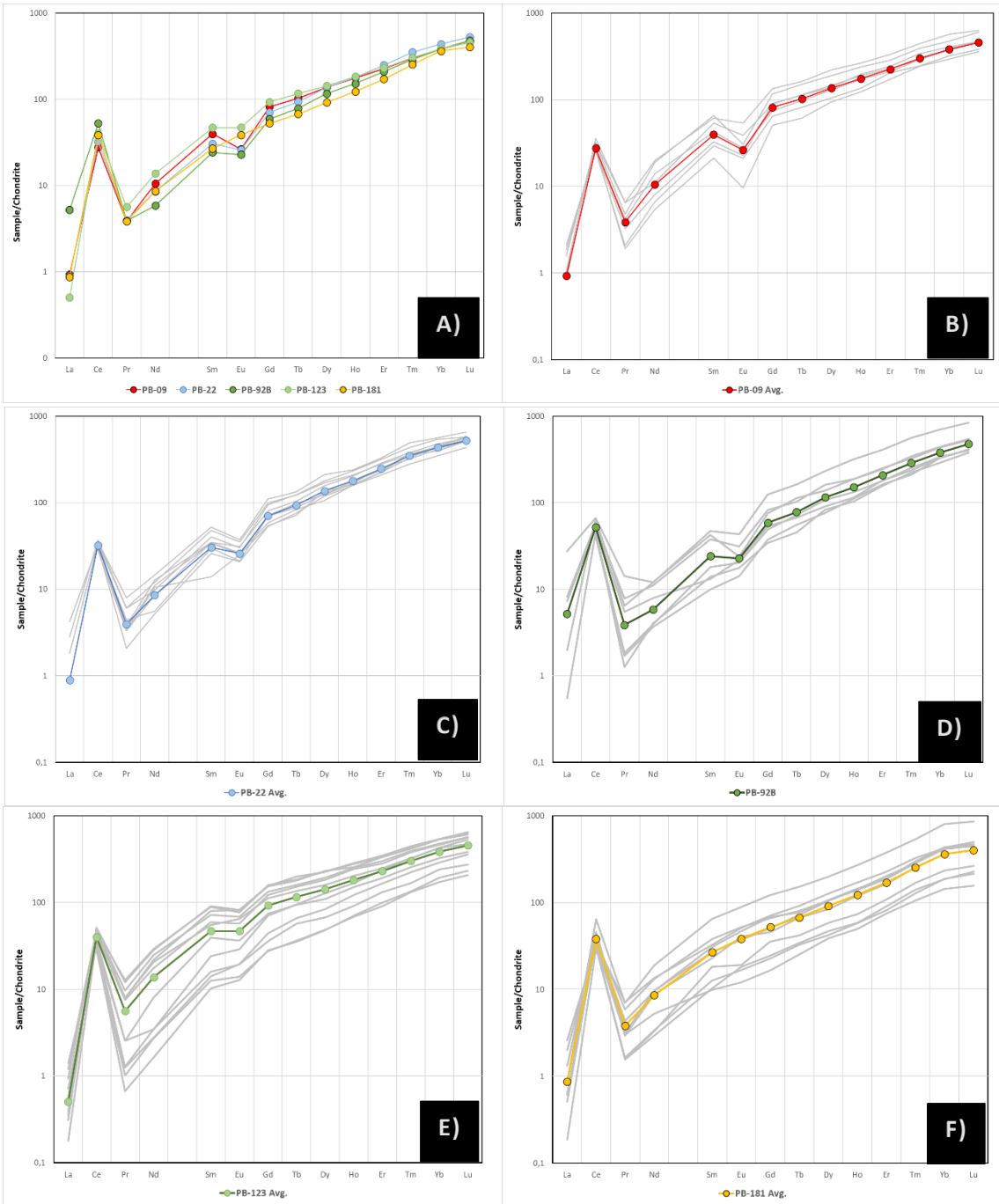

Fig 45: Chondrite-normalized REE patterns for zircon. A) Comparison between the normalized REE distribution patterns between the different units. B) Sample PB-09 (CSO unit); C) Sample PB-22 (ESO unit); D) Sample PB-92B (LSO unit); E) Sample PB-123 (LSO unit); Sample PB-181 (LSS unit). Colored lines represent sample averages and gray lines represent the entire population of crystals analyzed.

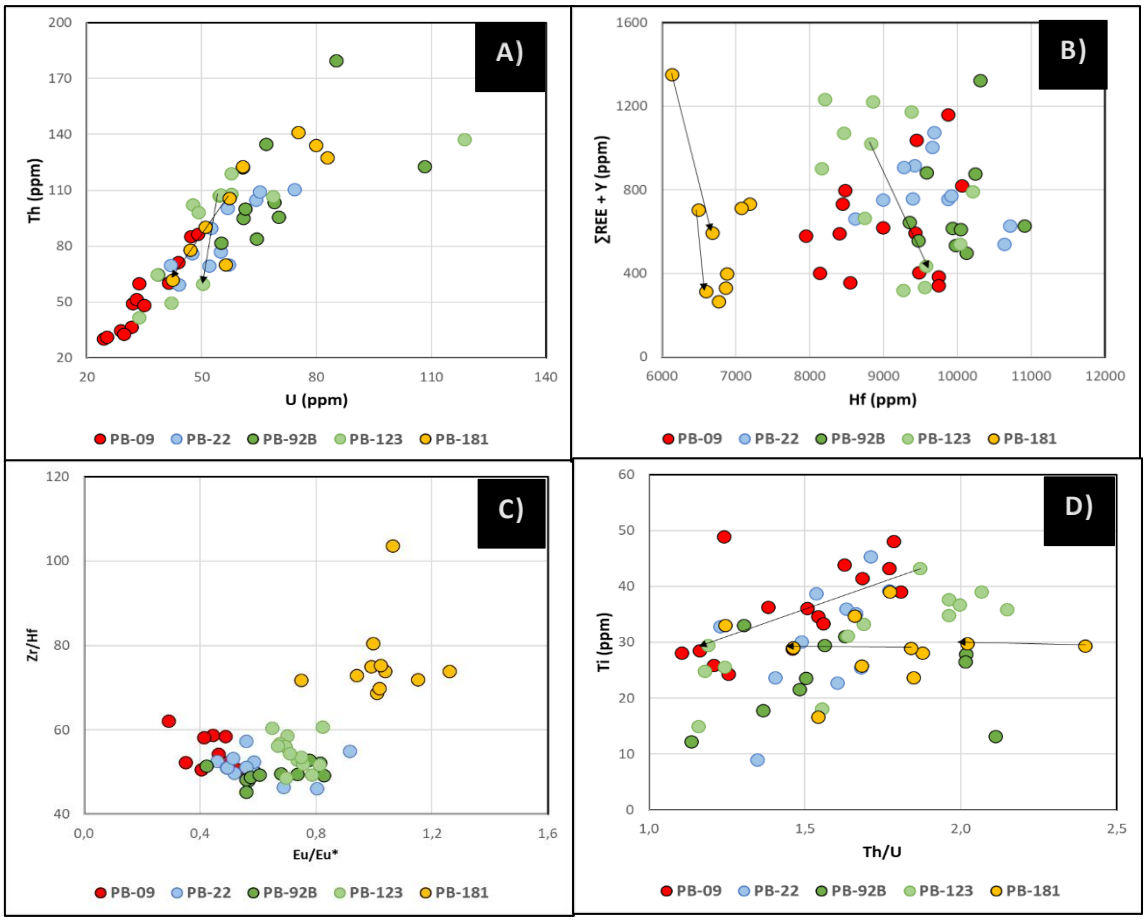

Fig 46: Correlation diagrams for zircon; arrow indicate core and rim analysis (core → rim); A) Th x U (ppm); B) ∑REE+Y x Hf (ppm); C) Zr/Hf x Eu/Eu*; D) Ti x Th/U

3.1.2 Thermometry

Based on EPMA and LA-ICP-MS analyses, crystallization temperature calculated using the following geothermometers formulations; Ti in zircon (Ferry & Watson, 2007); Zr in titanite (Hayden *et al,* 2008); Ti in biotite (Henry *et al,* 2005) and Ti in amphibole (Ridolfi et al, 2012). All data collected and the temperature calculations are provided as data sheets in Appendix III.

3.1.2.1 Temperature estimates from zircon

3.1.2.1.1 Ti in Zircon thermometry

The Ti-in-zircon thermometer proposed by Watson *et al* (2006) and later revised by Ferry & Watson (2007) indicates that the incorporation of Ti by zircon is controlled, mostly, by temperature, TiO_2 activity (αTiO_2) and, to a lesser extent, by SiO_2 activity (αSiO_2), and therefore the Ti content in magmatic zircon can be used as a proxy for its

crystallization temperature. The authors propose the following equation to calculate such crystallization temperature.

$$(1) \quad \log([\mathrm{Ti}]) + \log(\alpha\mathrm{SiO2}) - \log(\alpha\mathrm{TiO2}) = (5.711 \pm 0.072) - \left(\frac{4800 \pm 86}{T(K)}\right)$$

where [Ti] is the zircon titanium concentration, in ppm, αSiO_2 and αTiO_2 are the SiO_2 and TiO_2 activity of the magma during the zircon crystallization.

To apply this geothermometer to the Pedra Branca syenites, the SiO_2 and TiO_2 activity were estimated, qualitatively, based on values adopeted in literature and on petrographic evidence for each unit, such as mineral assemblages and mineral textures.

The SiO_2 activity was estimated based on the occurrence and texture of quartz, while the TiO_2 activity was estimated based on titanite (sphene). The absence of rutile and absence or occurrence of late phase of quartz, in the Pedra Branca syenites rules out Si and Ti saturation during zircon crystallization, and therefore αSiO_2 and αTiO_2 are assumed as $<$ 1.0 for all samples.

For units with the presence of large euhedral titanite (LSO and LSS), higher values of TiO_2 activity were adopted ($\alpha TiO_2 = 0.8$) compared to units where titanite occurs exclusively as thin reaction borders in ilmenite and magnetite (CSO; $\alpha TiO_2 = 0.5$). For the Si-oversaturated units, where quartz occurs as late as interstitial phase ($\alpha SiO_2 = 0.8$), in relation to the Si-undersaturated unit, with the presence of late-stage quartz ($\alpha SiO_2 = 0.5$). The αSiO_2 and αTiO_2 values for every sample are summarized in Table 9:

	αSiO_2	**αTiO_2**
CSO	0.8	0.5
LSO	0.8	0.7
ESO	0.8	0.7
LSS	0.5	0.8

Table 9: Values for SiO_2 and TiO_2 activity assumed for calculation of Ti-in-zircon geothermometry for the different units of the Pedra Branca Syenite.

The assumptions required for estimating the values of SiO_2 and TiO_2 activity add some uncertainty to the results of geothermometry, which are unavoidable at the current stage of research.

Zircon from CSO syenites occurs often as small, interstitial, anhedral crystals (0.1 to 0.4mm) or included in different mineral phases, mostly K-feldspar or pyroxene. It shows the highest Ti concentrations among all units (25-48 ppm), yielding temperatures of 890-985ºC, with average of 942ºC (Fig. 47).

Zircon is more abundant in the ESO unit and occurs mostly as small subhedral to anhedral crystals (0.1 to 0.6 mm), often interstitial but sometimes included in K-feldspar rims. It is noteworthy that it does not occur included exclusively in K-feldspar. It records a wide range of Ti concentration (9-45 ppm), yielding temperatures between 750 and 907 ºC, with an average of 822ºC).

The LSO unit has abundant zircon, occurring often as small subhedral crystals (0.2-0.6mm), usually interstitial but sometimes included, mostly, in pyroxene. Zircon also records a range of Ti (12-43 ppm), resulting in temperatures between 794 and 942ºC, with an average temperature of 879ºC.

The occurrence of zircon in the LSS unit is much different from the other units. It is much less abundant but occurs as large anhedral crystals (0.5-2.0 mm) and is not included in other mineral phases. Their Ti contents are within the same range of the other units (16-40 ppm). Temperatures between 750 and 837 ºC; the lower values compared to the other units, are due to the activity values adopted, more specifically the Si-activity ($\alpha SiO_2 = 0.5$), which is a much lower, when compared to the value adopted for the other units ($\alpha SiO_2 = 0.8$).

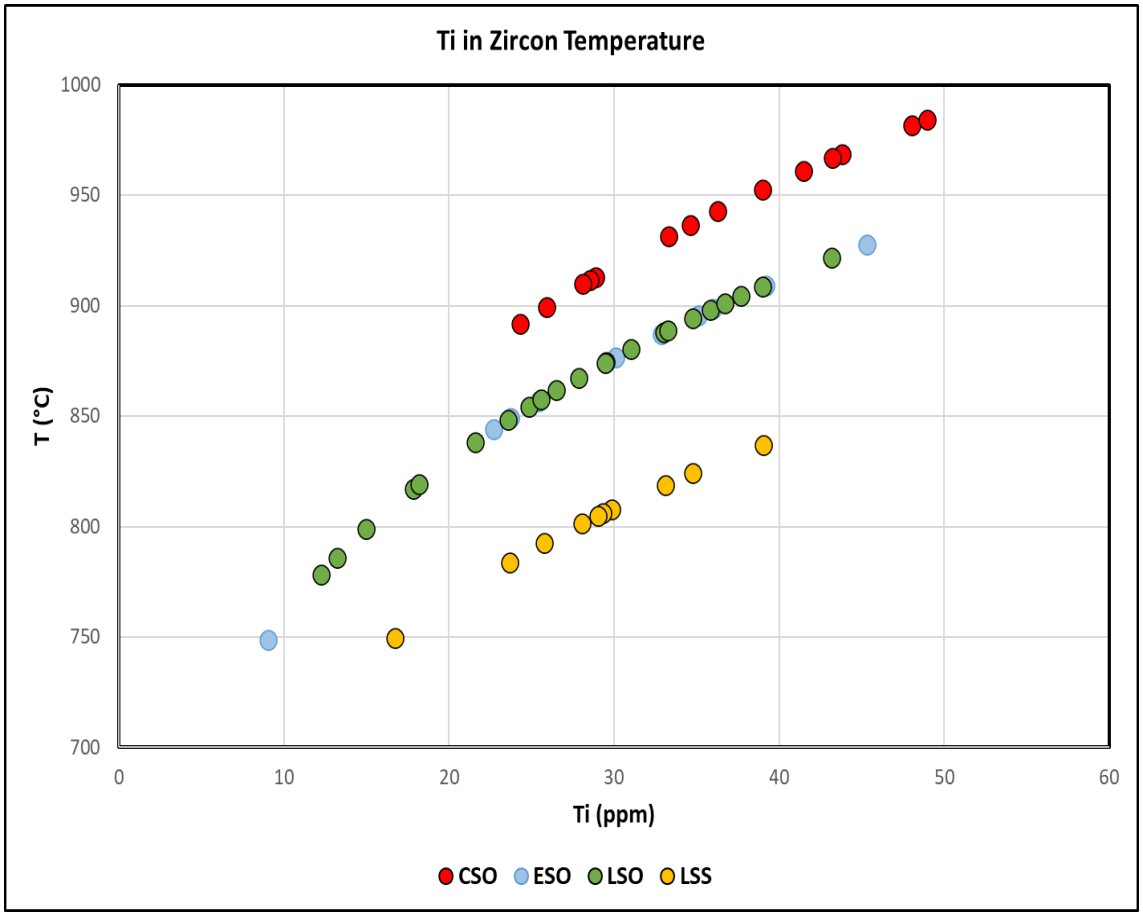

Fig 47: Ti-in-zircon crystallization temperatures for the Pedra Branca syenites

3.1.2.1.2 Zircon saturation temperature (T_{zirsat})

The zircon saturation thermometer is widely used in the literature of felsic magmatic rocks since its original propositon by Watson & Harrison (1983), based on experiments evaluating the effects of temperature and pressure on zircon crystallization. These authors showed that zircon saturation is a function of zirconium concentration, temperature, and magma composition, described by the parameter **M** ((Na+K+2Ca)/(Al*Si)), which as regarded as the most influential factor by Siegel et al (2018); as such, T can be estimated by the formulation.

$$(2)\ T_{sat}(^{\circ}C) = \frac{12900}{\ln\frac{497600}{[Zr, ppm]} + 3.8 + 0.85(M-1)} - 273$$

which was calibrated for pressures up to 25 kbar and compositions ranging from 0.9< M < 1.9.

After nearly three decades in use, the Watson & Harrison calibration was subject of a revision by the original team using additional experiments, with the new formulation shown in Eq. 2 (Boehnke et al., 2013):

$$(3)\ T_{sat}(^{\circ}C) = \frac{10108}{\ln\frac{497600}{[Zr, ppm]} + 1.48 + 1.16(M-1)} - 273$$

Gervasoni et al (2016) proposed a new formulation (eq. 3) intended to expand the geothermometer to a wider set of compositions, including alkaline melts:

$$(4)\ T_{sat}(^{\circ}C) = \frac{\ln[Zr](ppm) - 4.29 + 1.35 lnG}{0.0056}$$

where G is a new compositional parameter which incorporateds the effect of the additional framework-modification elements Mg and Fe ($3Al_2O_3+SiO_2$)/($Na_2O+K_2O+CaO+MgO+FeO$).

3.1.2.1.3 Application of $T_{zircsat}$ in the Pedra Branca units

The Pedra Branca syenites have high M values (3.4-4.8; Table 10) well above the maximum value (1.9) recommended by Watson & Harrison (1983), which renders their calibration (and Boehnke et al.'s recalibration) inappropriate.

Unit	**M** ((Na+K+2Ca)/(Al*Si))
CSO	4.22
ESO	3.43
LSO	4.17
LSS	4.88

Table 10: Summarized values for the parameter M.

The calibration by Gervasoni et al. (2016) is intended to be applied in magmas of higher alkalinity, or M>2.

The compositional parameter G was determined for every unit, yielding values ranging between 3.37 and 3.67. Based on the G values, the whole-rock data obtained and applying eq. 3, the zircon saturation temperatures obtained range between 568 and 583 ºC (table 11), which are much lower temperatures when compared to the crystallization temperatures obtained with the Ti-in-zircon thermometer (fig.48).

Unit	**M**	**G**	**T**
CSO	4.22	3.67	583
ESO	3.43	3.43	584
LSO	4.17	3.37	596
LSS	4.88	3.46	568

Table 11: Compositional parameters (M and G) and estimated temperatures of zircon saturation (in degrees C) based on calibrationns by Gervasoni et al. (2016).

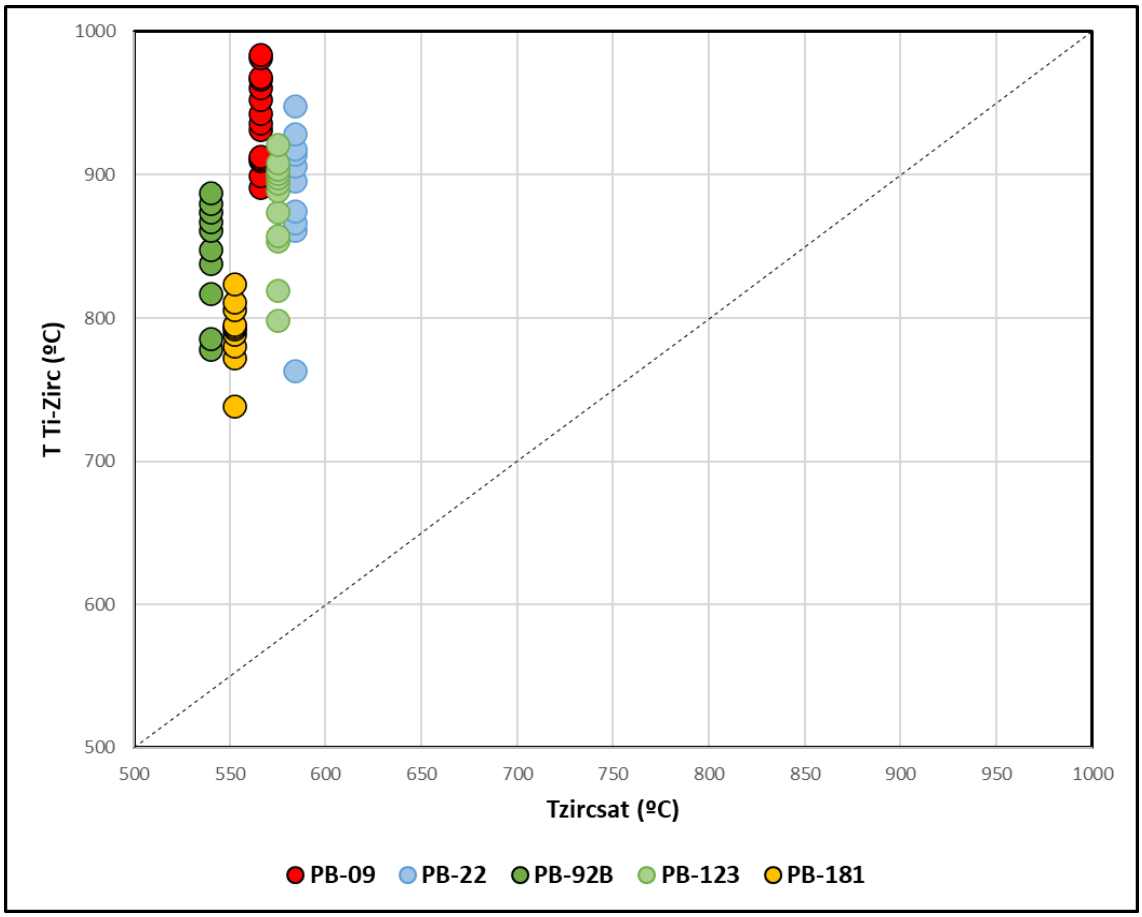

Fig 48: Tzircsat x Ti-in-zircon temperature

3.1.2.2 Temperature estimates from titanite

The Zr-in-titanite thermometer was proposed by Hayden et al (2007) who demonstrated that the incorporation of Zr into the structure of titanite, replacing Ti, is heavily sensitive to temperature and pressure, therefore, the Zr content in titanite could be used as a proxy for estimating the crystallization temperature. The following equation was proposed to estimate T:

$$(5)\ T_{tnt}(^{\circ}C) = \frac{(7708 + 960P)}{(10.52 - (\log \alpha TiO2) - (\log \alpha SiO2) - \log[Zr, ppm]} - 273$$

Where P is the crystallization pressure in GPa, [Zr] is the zirconium content in ppm, and αSiO_2 and αTiO_2 are the melt activity values for Si and Ti respectively.

The titanite crystallization temperature was calculated for all units studied using this model, adopting the same activity values presented in table 1.
A pressure value of 0.38 GPa was used, based on the estimate by Carvalho et al (2012).

3.1.2.2.1 LSO

Titanite from the LSO unit (samples 92B and 123) occurs as late stage, anhedral crystals, most often associated with ilmeno-hematite, in the form of reaction halos, or other mafic phases such as pyroxene or amphibole. Zr contents range between 435 to 1470 ppm, which yield crystallization temperatures from 720 to 790ºC (fig. 49).

3.1.2.2.2 LSS

Titanite is very abundant in LSS (samples 08A, 181 and 185), occurring both as large euhedral crystals (up to 3mm) and as small late-stage interstitial crystals, often associated with other mineral phases, such as ilmeno-hematite and pyroxene. The Zr content varies substantially depending on the size and textural context of the titanite, ranging from 970 ppm in the interstitial crystals up to 6370 ppm in the larger euhedral crystals. It also seems to decrease from the crystal center towards the rim, with center analysis averaging around 3890 ppm and rim analysis averaging around 3400 ppm. As a result of this variation, temperatures also span a wide range, from 750 to 870ºC (fig. 49).

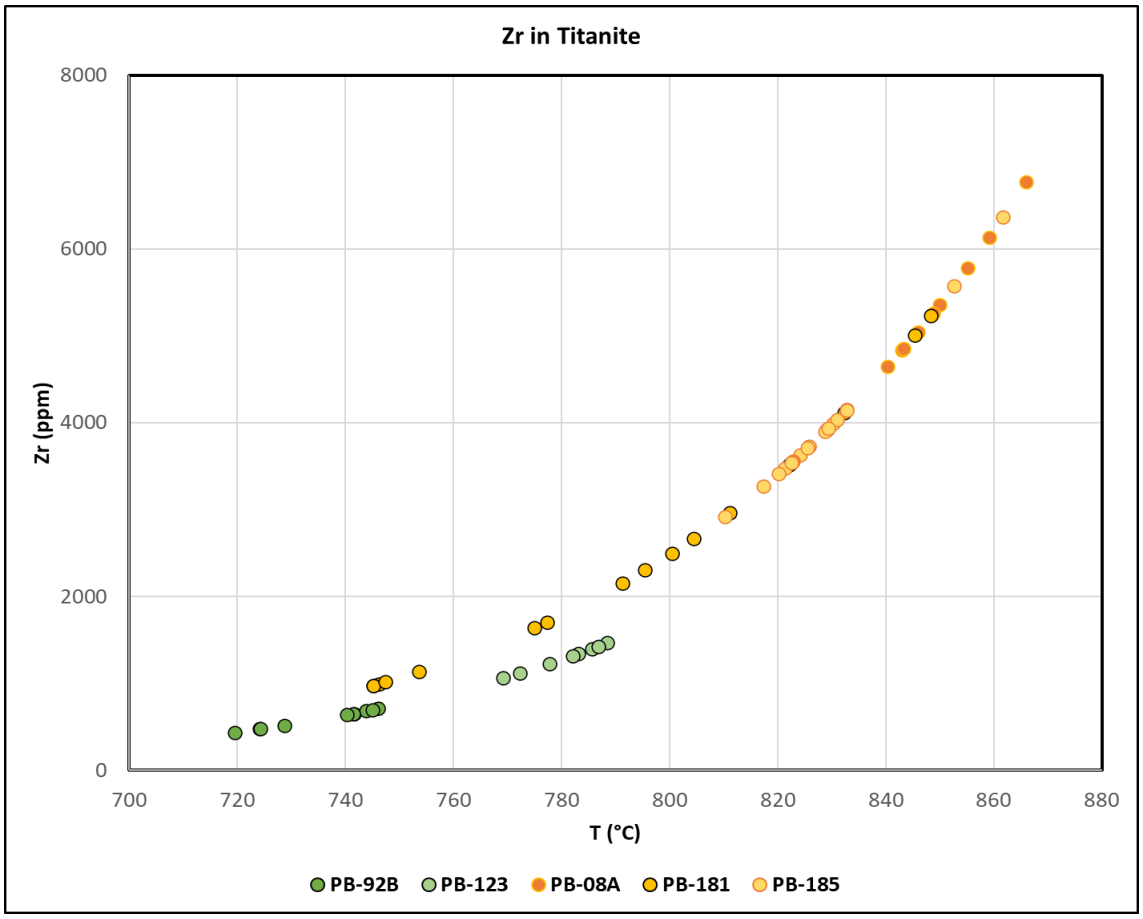

Fig 49: Zr-in-titanite temperatures calculated for the LSO (green) and LSS (yellow) units.

Despite the two different “generations” of titanite described in the LSS unit, all calculations were made adopting the same parameters for pressure and activity, for sake of simplicity. To acquire more accurate results, the temperature calculations for the late-stage crystals should have been made using a distinct set of parameters, since the two generations of titanite present in the LSS unit did not crystallize under the same conditions.

3.1.2.3 Ti in Amphibole and Biotite Thermometers

The crystallization temperatures of amphibole and biotite were calculated using the Ti-based thermometers proposed by Ridolfi et al (2012) and Henry et al (2005), respectively, adopting a pressure value of 0.38 GPa, when required.

Ridolfi et al (2012) propose the following equation (eq. 6) for the calculation of amphibole crystallization temperature:

$$(6)\ T_{tnt}(^{\circ}C) = 17.098 - 1332.3Si - 1035.1Ti - 1208.2Al - 1230.4Fe - 15152.9Mg - 130.4Ca + 200.54Na + 29.408K - 24.41\ln P$$

Where P is the crystallization pressure, the independent variables are given in total a.p.f.u of elements based on 13-CNK (Ridolfi et al, 2012). This geothermometer was calibrated for a wide range of temperature-pressure conditions, from 800-1130 ºC and 130 to 2200MPa, respectively

The Ti-in-biotite thermometer proposed by Henry et al (2005) is calibrated for a more specific set of pressure-temperature conditions and compositions, such as: peraluminous biotite equilibrated at 4 to 6 kbar and temperature ranging between 480 to 800 ºC. Henry et al (2005) proposes the following equation to calculate the crystallization temperature of biotite:

$$(7)\ T_{tnt}(^{\circ}C) = \frac{\left[\ln Ti - a - c(X_{Mg})^3\right]}{b}$$

Where T is temperature in ºC, Ti is the a.p.f.u normalized to 22 Oxygens, X_{Mg} is the Mg# for biotite.

Amphibole from the ESO unit record lower Ti content, when compared to the CSO unit, with values ranging from 1.46 to 1.99 wt% TiO_2 (or 0.16 to 0.22 apfu), which when applying Ridolfi’s thermometer, yield temperatures between 816 and 850ºC (fig. 50).

The LSS unit records the widest range of Ti content in amphibole amongst all units, with values between 0.04 and 1.50 wt% TiO_2 (or 0,004 to 0.163 apfu), yielding temperatures from 702 to 850 ºC. Amphiboles from the sample PB-185 record distinctively lower crystallization temperatures, ranging from 702 to 735ºC, when compared to amphiboles from sample PB-181, from the same unit, that ranges from 776 to 850ºC, which are values much more like the ones obtained in amphiboles from other units (815-857ºC; fig. 50a).

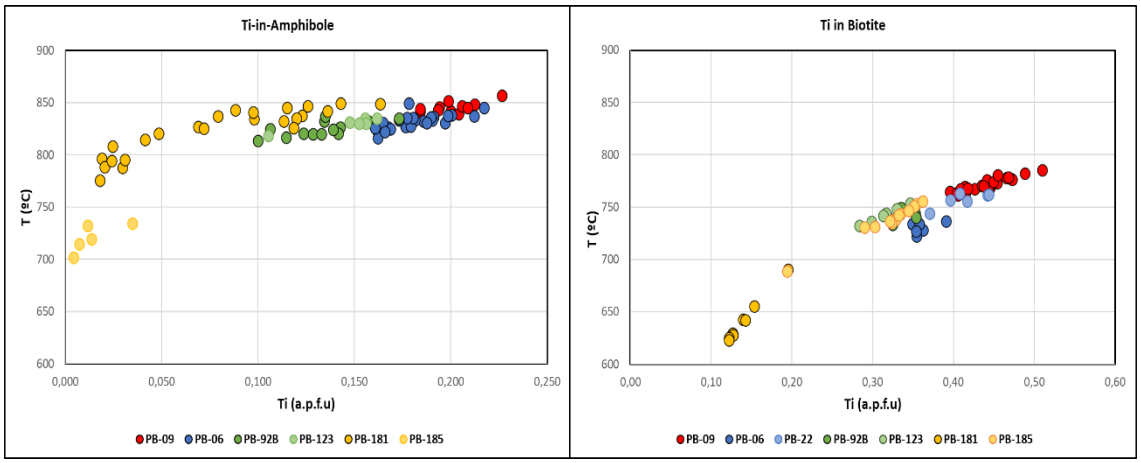

Fig 50: Ti in Amphibole and Ti in Biotite temperatures obtained for all units

Figure 50 shows all the calculated temperatures obtained, for zircon, titanite, biotite and amphibole, for all Pedra Branca units. Biotite records the lowest crystallization temperatures in each unit, ranging from 620ºC in LSS to 790ºC in CSO, whereas zircon records the highest temperatures, with values up to 980ºC in CSO.

It is noticeable that, in the oversaturated units, the temperature ranges obtained for the different minerals studied do not show large overlaps, hence, every mineral phase records the crystallization history during a unique range of temperature, with, zircon recording the highest temperatures, followed by titanite at a lower temperature, then amphibole and lastly biotite at the lowest recorded temperatures (fig.51). This is not observed in the LSS unit, where multiple mineral phases record the same temperature range, for instance, zircon, titanite and amphibole, in sample PB-181, all record the temperature range between 750 and 850ºC.

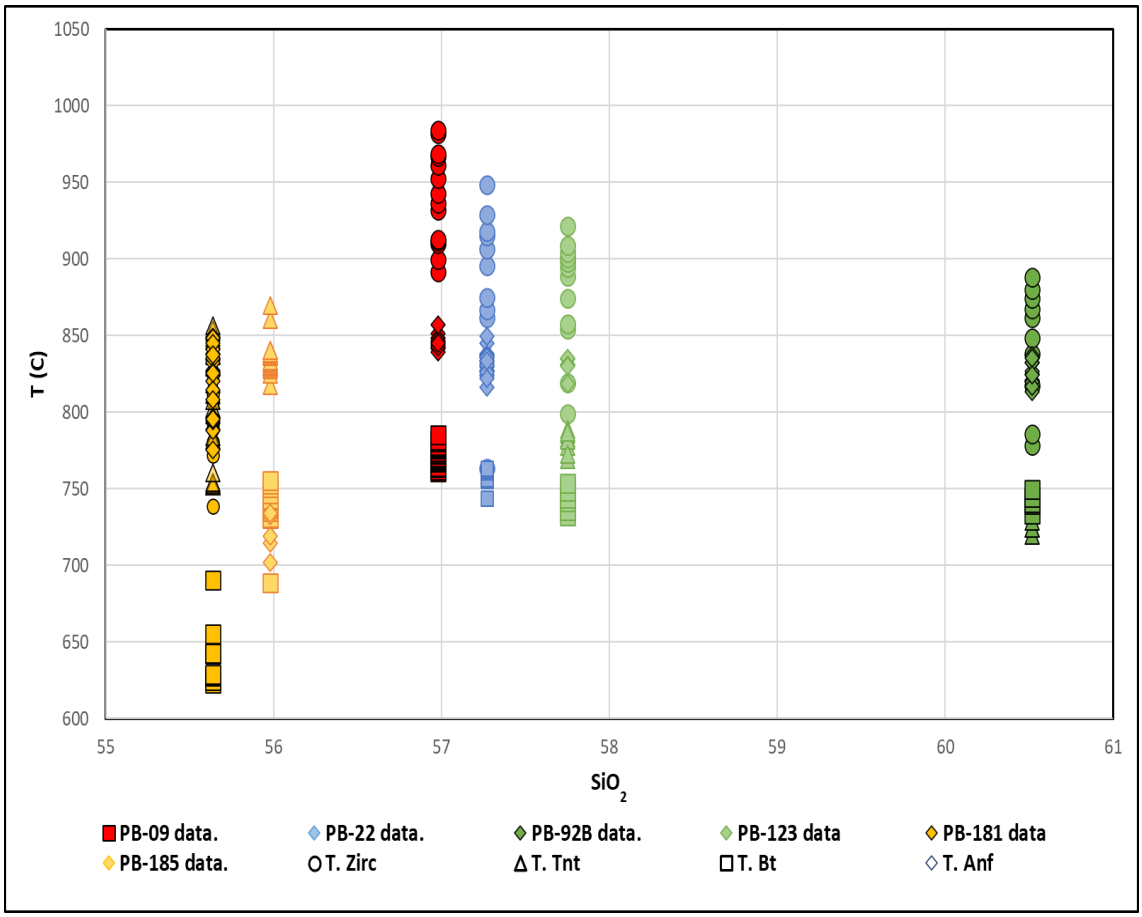

Fig 51: Combination of obtained crystallization temperatures for all units, including zircon, titanite, amphibole and biotite temperatures.

3.1.3 Oxygen Fugacity (*f*O2)

Oxygen fugacity (fO_2) defines the potential for a multivalent element to occur in an oxidized or reduced state (e.g Fe^{2+}/Fe^{3+}; Ce^{3+}/Ce^{4+}; Eu^{2+}/Eu^{3+}; etc) within a given system. For magmas, the methods to determine the oxygen fugacity are plentiful and are based on different multivalent elements, such as Fe-, Mn-, S- or REE-based oxybarometers.

For the purpose to determine the oxygen fugacity for the Pedra Branca plúton, two different approaches were used; a qualitative estimate, based on Ce/Ce* and Eu/Eu* ratios on apatite and a quantitative approach, based on the Ce^{3+}/Ce^{4+} ratio on zircon, an oxybarometer proposed by Smith and Brenan (2016).

3.1.3.1 Apatite

Apatite incorporates a large amount of REE's in its composition, specially LREE's^{3+} (La, Ce, Pr, Eu); Ce and Eu are multivalent elements which are incorporated in their 3+ valency, replacing Ca^{2+} in the apatite structure, through a series of coupled substitutions, but are incompatible in their 4+ and 2+ valences, respectively.

The Ce/Ce* and Eu/Eu* ratios can be used to have an initial understanding of the redox state of the magma that the apatite crystallized from, as it is a measure of the magnitude of the Ce and Eu anomalies, in relation to the adjacent REE's, recorded in the mineral. The Ce/Ce* and Eu/Eu* ratios can be estimated in two different ways; one is based on the composition of chondrite-normalized apatite, where Ce* and Eu*, which are theorical values calculated, that assume all Ce and Eu content in apatite is valency 3+, and are determined by the following equations:

$$(8)\ Eu* = \sqrt{[La]\ x\ [Pr]}$$

$$(9)\ Ce* = \sqrt{[Sm]\ x\ [Gd]}$$

Where [La], [Pr], [Sm] and [Gd] are the chondritic-normalized values for the respective elements in apatite.

Ce* and Eu* can also be determined using the partition coeficients between apatite and melt, which can be calculated with the following equations:

$$(10)\ Eu* = \sqrt{D_{La}^{\frac{Ap}{Melt}} x D_{Pr}^{\frac{Ap}{Melt}}}$$

$$(11)\ Ce* = \sqrt{D_{Sm}^{\frac{Ap}{Melt}}\ x\ D_{Gd}^{\frac{Ap}{Melt}}}$$

Where, $D_{La}^{\frac{Ap}{Melt}}$, $D_{Pr}^{\frac{Ap}{Melt}}$, $D_{Sm}^{\frac{Ap}{Melt}}$ and $D_{Gd}^{\frac{Ap}{Melt}}$ are the partition coefficients of each respective element between apatite and melt.

The Ce/Ce* and Eu/Eu* ratios yield a qualitative estimate of the redox conditions in which apatite crystallized, but no current calibrations are available at the moment to obtaine quantitative values of oxygen fugacity (fO_2).

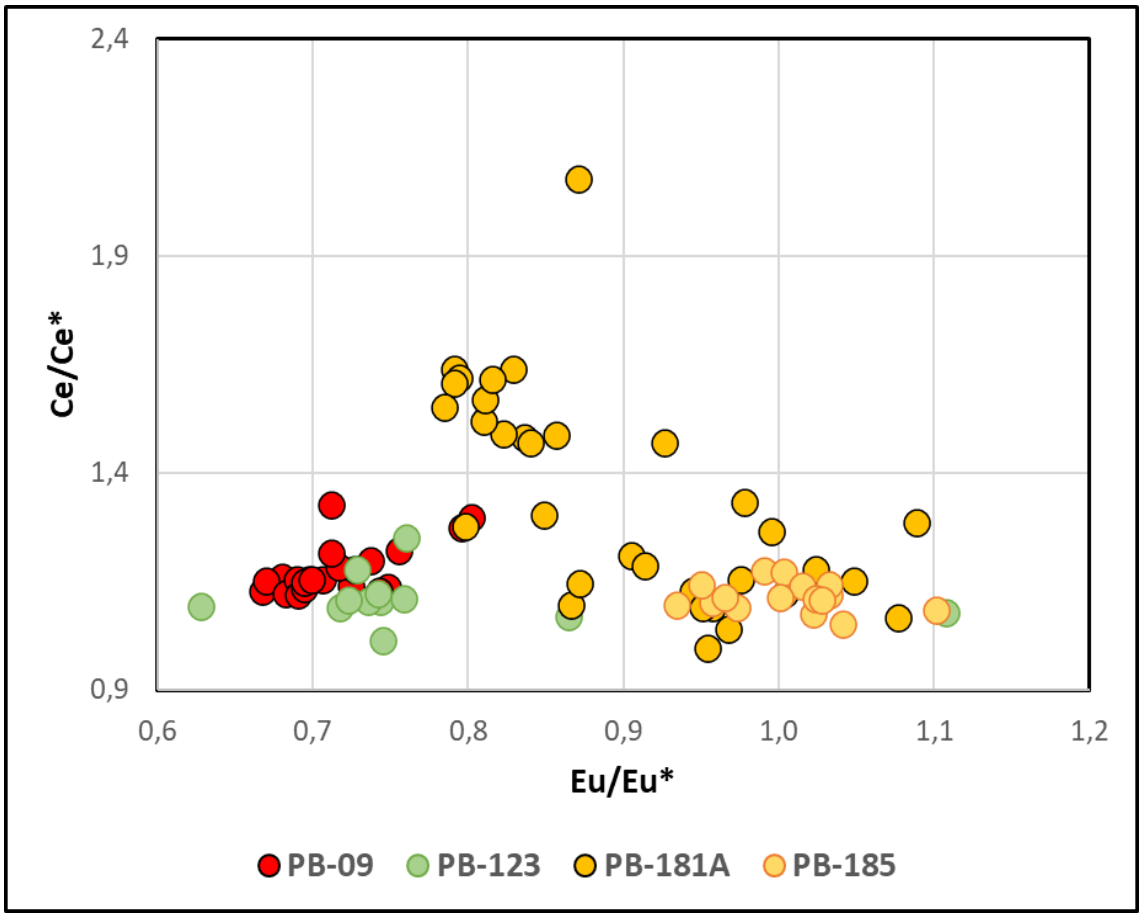

Fig 52: Ce/Ce* x Eu/Eu* diagram for apatite

Apatite from the silica oversaturated units (samples PB-09 and PB-123) records lower Eu/Eu* ratios, ranging from 0.65 to 0.8, in relation to the silica saturated unit (samples PB-181 and PB-185), with values between 0.8 to 1.1. These results indicate that the LSS unit (samples PB-181 and PB-185) records more oxidizing conditions when compared to the other units, due to lower Eu/Eu* ratios, which indicates the predominant presence of Eu^{3+} in relation to its lower valency (Fig. 52).

It is important to mention that other processes can affect the apatite composition during crystallization, especially the magma composition and the co-crystallization of other REE-rich mineral phases. In particular, the co-crystallization of other REE-rich minerals such as allanite, zircon, titanite, or a mineral that incorporates a significative amount of a specific REE, such as the feldspars with Eu, will certainly influence the REE patterns of the apatite. However, in the Pedra Branca syenites, the apatite compositions were shown to be relatively homogeneous in each sample, and the mineralogy and order of crystallization of the mineral phases is similar in the different samples.

3.1.3.2 Zircon

Zircon can incorporate a variety of REE's in its structure, most notably HREE's. Ce and Eu in zircon have been recently used as proxies of oxygen fugacity, due to their multi valent nature, which makes the degree of their incorporation into the zircon structure sensitive to the redox condition of the melt during crystallization. A typical characteristic of zircon is the anomalously high Ce content, in relation to its neighboring REEs (La and Pr), which is the result of favored partitioning of Ce^{4+} in relation to Ce^{3+} in the zircon structure, due to similar ionic radius and being isovalent with Zr^{4+}, which is the element that Ce^{4+} replaces. Such partitioning is sensitive to the redox condition of the melt in which zircon crystallizes (Smythe & Brenan, 2016).

3.1.3.2.1 A brief introduction to the Lattice Strain Model

Most zircon-based oxybarometers used today have as its core the Lattice Strain Model, proposed by Blundy and Wood (1994), which aims to determine the partition coefficient of different elements between a given mineral and melt. According to this model, the partition coefficient of any given element is dependent only on the difference between the ionic radius of such element in relation to the element which it is going to replace in the mineral structure, and should obey equation 12, assuming fixed P-T conditions. For REE's, specifically, the partition coefficient between zircon and melt is dependent on the difference between its ionic radius and that of the Zr^{4+}.

$$(12)\ D_i = D_0\, exp\left[-\frac{4\pi E N_A}{RT}\left(\frac{r_0}{2}(r_0 - r_i)^2 - \frac{1}{3}(r_0 - r_i)^3\right)\right]$$

Where D_i is the zircon-melt partition coefficient, D_0 is the hypothetical strain-free partition coefficient (when assuming no substitution into the crystalline structure), r_0 and r_i is the difference between the ionic radius of the cation which is entering the zircon structure (r_i) in relation to the optimal site radius, or optimal cation radius (r_0) for a given site, E is the Young's module for the crystalline site, N_A is the Avogadro's number, R is the gas constant and T is the temperature, in Kelvin.

Applying the logarithmic function to eq.12 yields a linear relation between mineral-melt partition coefficient ($\log_{10} D_i$) and a lattice-strain term involving their ionic radii (Ballard, 2002), resulting in eq. 13.

$$(13)\ \log_{10} D_i = \log_{10} D_0 - \left[\frac{4\pi E N_A}{RT}\left(\frac{(\frac{r_i}{3} + \frac{r_0}{6})(r_i - r_0)^2)}{2.302}\right)\right]$$

This equation was plotted for the trivalent (REE's^{3+}) and tetravalent elements (Zr^{4+}, Th^{4+}, U^{4+} and Hf^{4+}) in the structure of zircon, assuming a value of 0.94 as the optimal site radius (r_0), which will later be discussed.

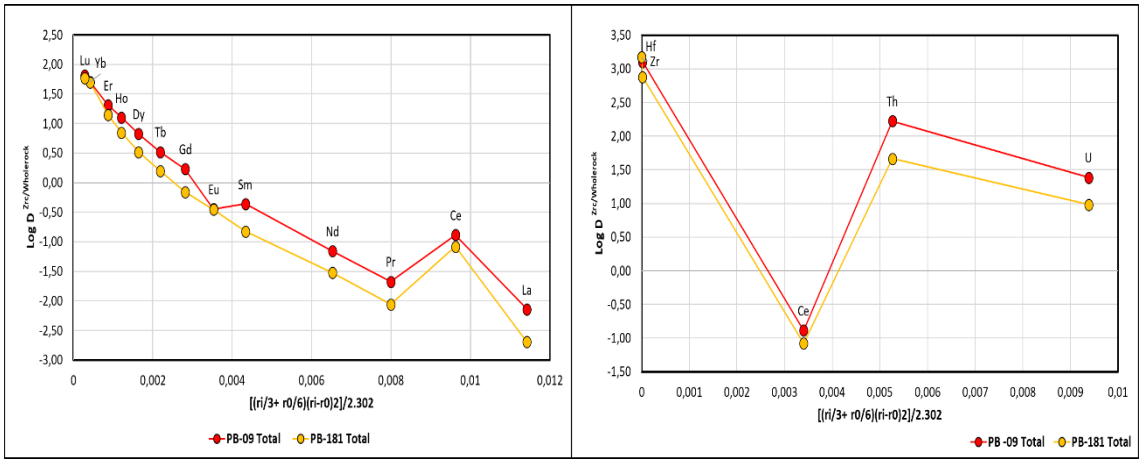

Fig 53: Logarithm of zircon-melt partition coefficients plotted versus the lattice-strain term for trivalent (A) and tetravalent cations (B)

Figure 53 shows the behavior of REE's in zircon when applied the lattice strain model, where most REE's obey the linear function given by eq. y, apart from Eu, Ce and, to a lesser degree, La. The Eu and Ce anomalies are a result of the multivalent nature of these elements; since in terrestrial magmas, Ce and Eu, occur as 3+ and 4+ and 2+ and 3+, respectively, the zircon-melt partition coefficient of Ce and Eu will reflect the Ce^{4+}/Ce^{3+} and Eu^{3+}/Eu^{2+} ratios. Ce^{4+} has a much higher partition coefficient in zircon, due to being isovalent and having similar ionic radii to Zr^{4+}, therefore it increases the partition coefficient of Ce, in relation to the neighboring REEs, resulting in the positive anomaly recorded, whereas for Eu, Eu^{2+} has a lower partition coefficient, in zircon, due to much different ionic radius and valency in relation to Zr^{4+}, which decreases the overall Eu partition coefficient in zircon, resulting in the negative anomaly recorded. The excess La observed, especially in sample PB-09, is often related to zircon contamination by other LREE-rich phases, such as apatite and titanite which are common accessory minerals found with zircon in the samples studied.

3.1.3.2.2 Estimating the value of r_0.

According to the lattice strain model, r_0 represents the optimal site radius which hosts a given element. For the trivalent and tetravalent series, the value for r_0 was estimated by least-squares regression, where the natural logarithm of partition

coefficients (Ln D_i) of each element was plotted in function of its respective effective radius, in Ångström (Shannon, 1976).

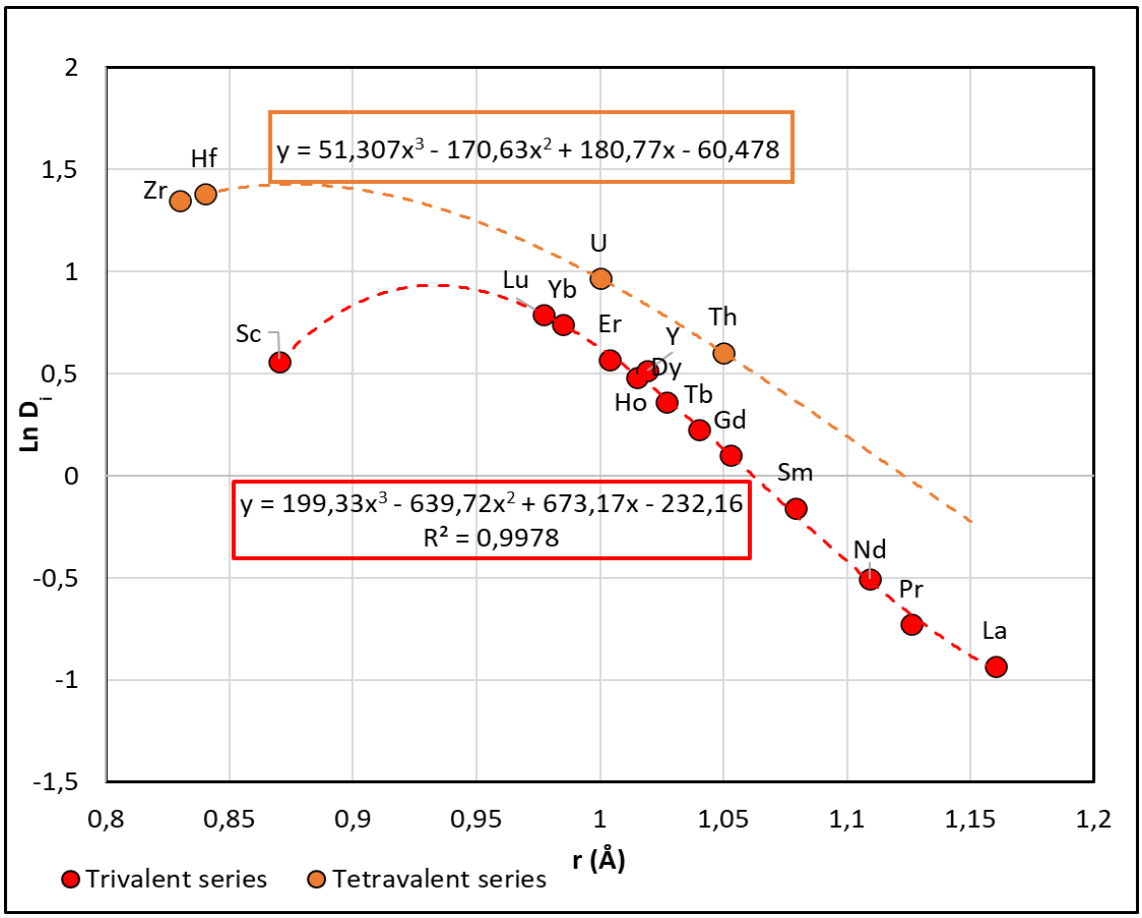

Fig 54: Natural logarithm of the distribution coefficients plotted versus the effective radius of trivalent and tetravalent elements

The roots of the first derivative of the third-degree polynomial given by the regression equates to the inflection points of the curve, which the maximum point, or highest value of Ln D_i, corresponds to the optimal size of the crystal site witch the cations substitute, and its curvature corresponds to the elasticity of the surrounding lattice (Ballard et al, 2002).

Figure 53 shows the regression curves given by two isovalent series of elements which r_0 was estimated for; a trivalent series composed of most $REEs^{3+}$, except for Ce and Eu, and a tetravalent series composed of Zr^{4+}, Hf^{4+}, U^{4+} and Th^{4+}. The value of r_0 for REE^{3+} in zircon obtained, for the different units studied, range between 0.92 to 0.94 Å, whereas the value of r_0 for the tetravalent elements range between 0.88 to 0.91 Å.

3.1.3.2.3 Estimating D_{Ce}^{3+} and D_{Ce}^{4+} in zircon from the lattice strain model

Ballard et al (2002) demonstrate that it is possible to determine the amount of Ce^{3+} and Ce^{4+} in zircon, given the total concentration of Ce in zircon and melt as well as the distribution coefficients for Ce^{3+} and Ce^{4+}, proposing the following equations.

$$(14)\ Ce_{Zrc}^{3+} = Ce_{Zrc} - \frac{Ce_{melt} - \frac{1}{D_{Ce^{3+}}^{zrc/melt}} Ce_{zrc}}{\frac{1}{D_{Ce^{4+}}^{zrc/melt}} - \frac{1}{D_{Ce^{3+}}^{zrc/melt}}}$$

$$(15)\ Ce_{Zrc}^{4+} = \frac{Ce_{melt} - \frac{1}{D_{Ce^{3+}}^{zrc/melt}} Ce_{zrc}}{\frac{1}{D_{Ce^{4+}}^{zrc/melt}} - \frac{1}{D_{Ce^{3+}}^{zrc/melt}}}$$

Where Ce_{melt} and Ce_{zrc} are the total concentration of Ce in the whole-rock and in zircon respectively, assuming the whole-rock composition is equivalent to the melt in which the zircon crystallized, Ce_{zrc}^{3+} and Ce_{zrc}^{4+}, are the calculated concentrations of Ce^{3+} and Ce^{4+} in zircon, and $D_{Ce^{3+}}^{zrc/melt}$, $D_{Ce^{4+}}^{zrc/melt}$ are the distribution coefficient of Ce^{3+} and Ce^{4+} respectively, between zircon and melt.

The total Ce concentrations in zircon and in the whole rock are obtained through direct measurement, whereas the distribution coefficients for Ce^{3+} and Ce^{4+} in zircon are obtained using the lattice strain model.

Based on the linear relationship between the zircon-melt distribution coefficients of REE's^{3+} (Log D_{REE}^{3+}), and the radius term (Fig. 51a), from the lattice strain model, given by:

$$(16)\ \left(\frac{(\frac{r_i}{3} + \frac{r_0}{6})(r_i - r_0)^2)}{2.302} \right)$$

where r_i, refers to the atomic radius of a given REE, and r_0 is the optimal site radius calculated (a value of r_0=0.94 was used)), a line of best fit is obtained by linear regression, excluding Eu and Ce. Interpolating the radius of Ce^{3+} in such line, the value of $Log\ D_{Ce^{3+}}^{zrc/melt}$ is obtained. It is important to mention that depending on the set of REEs chosen to perform the linear regression, different lines could be obtained for the same data set, as shown in figure 54. Often the Nd-Lu or Gd-Lu lines are used to interpolate the value of Log D Ce^{3+}, since both exclude the LREEs (La and Pr) from the linear regression. LREEs occur in very low concentrations in zircon, and their contents are

susceptible to contamination by other LREE-rich phases eventually present as micro-inclusions. The presence of LREEs in the regression, in general, results in overestimation of the $Log\ D_{Ce^{3+}}^{zrc/melt}$ value. Eu is also excluded from the regressions since it occurs in multiple oxidation states. The values or r_0 used for the 3+ and 4+ cation site was 0.94 Å, determined by regression, and 0.84 Å (value of eight-fold coordinated Zr^{4+}) respectively.

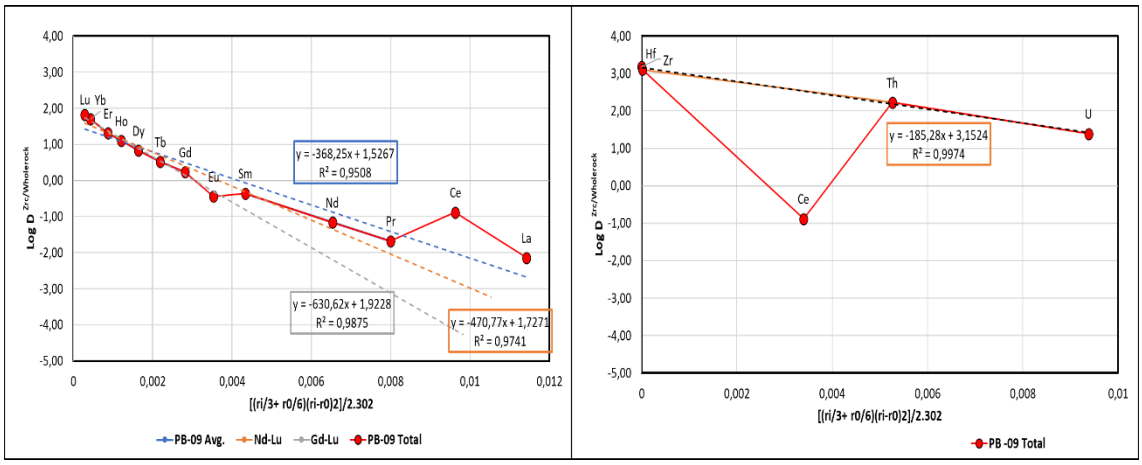

Fig 55: REE^{3+} distribution coefficients plotted in relation to the lattice-strain term, showing the possible different lines for $Log\ D_{Ce^{3+}}^{zrc/melt}$ interpolation; blue line represents the linear regression including all REEs, except Eu and Ce; the orange line represents the linear regression made using the REEs from Nd to Lu, excluding Eu, Pr, Ce and La; and gray line represents the linear regression made using only HREEs, from Gd to Lu. B) Distribution coefficients of tetravalent elements plotted versus the lattice strain term, showing the line used for $Log\ D_{Ce^{4+}}^{zrc/melt}$ interpolation.

The distribution coefficient of Ce^{4+} (D_{Ce}^{4+}) can be obtained by the same method as described previously for Ce^{3+}, changing only the set of elements used in the lattice strain model, from the $REEs^{3+}$ to a tetravalent set, composed of Zr^{4+}, Hf^{4+}, Ce^{4+}, Th^{4+} and U^{4+} (Fig. 54). A linear regression is performed, excluding Ce, obtaining a line with all its parameters, and the value of the radius of Ce^{4+} is interpolated into this line, obtaining the value of $Log\ D_{Ce^{4+}}^{zrc/melt}$. The ionic radii for the elements used (REEs, Th, U, Zr, Hf) were obtained from Shannon (1976), and are presented in Table 12.

Cátions	M^{3+}	M^{4+}
Zr		0.84
Hf		0.83
Ti		0.74
Th		1.05
U		1.00
Sc	0.87	
La	1.16	
Ce	1.143	
Pr	1.126	
Nd	1.109	
Sm	1.079	
Gd	1.053	
Dy	1.027	
Ho	1.015	
Er	1.004	
Yb	0.985	
Lu	0.977	

Table 12: Effective ionic radius (Å) of cations, in octahedral coordination with oxygen, which can replace Zr in zircon (Shannon, 1976).

3.1.3.2.4 Calculating fO_2 based on the Ce^{4+}/Ce^{3+} ratio in zircon

Smythe & Brenan (2016) calibrated a method to estimate the redox conditions during zircon crystallization, based on the Ce^{4+}/Ce^{3+} ratio in zircon, introducing the following equation.

$$(17)\ ln\left[\frac{X_{Ce^{4+}}^{melt}}{X_{Ce^{3+}}^{melt}}\right] = \frac{1}{4}lnfO_2 + \frac{13136\ (\pm591)}{T} - 2.064(\pm0.011)\frac{NBO}{T} - 8.878(\pm0.112).xH_20 - 8.955(\pm0.091)$$

Where T is the zircon crystallization temperature, in Kelvin and $\frac{NBO}{T}$ is the proportion of non-bridging oxygens to tetrahedrally coordinated cations, calculated assuming anhydrous basis and all ferrous iron (FeO). xH_2O is the mole fraction of water dissolved in the melt. $X_{Ce^{4+}}^{melt}$ and $X_{Ce^{3+}}^{melt}$ are the more fractions of Ce^{4+} and Ce^{3+} in the melt, which are related to the values of the zircon-melt distribution coefficients of Ce^{4+} and Ce^{3+} ($D_{Ce^{4+}}^{zrc/melt}$ and $D_{Ce^{3+}}^{zrc/melt}$), based on the equation 18, deduced from the approximation made by Ballard et al (2002).

$$(18)\ \left[\frac{X_{Ce^{4+}}^{melt}}{X_{Ce^{3+}}^{melt}}\right] = \left[\frac{\sum Ce_{zircon} - (\sum Ce_{melt} * D_{Ce^{3+}}^{\frac{zircon}{whole\ rock}}}{(\sum Ce_{melt} * D_{Ce^{4+}}^{\frac{zircon}{whole\ rock}}) - \sum Ce_{zircon}}\right] * 1.0487$$

Where ∑Ce is the total Ce concentration in zircon or melt, $D_{Ce^{4+}}^{zrc/melt}$ and $D_{Ce^{3+}}^{zrc/melt}$ are the zircon-melt distribution coefficients of Ce^{4+} and Ce^{3+}, respectively, and the constant 1.0487 is the mole to wt% conversion factor.

3.1.3.2.5 Estimating *f*O_2 for the Pedra Branca units

When applying the Ce-in-zircon oxygen barometer (Smythe and Brenan 2016) to zircon crystals from the Pedra Branca pluton, some parameters had to be calculated or estimated, such as $\frac{NBO}{T}$, xH_2O, $D_{Ce^{4+}}^{zrc/melt}$ and $D_{Ce^{3+}}^{zrc/melt}$, in order to obtain the values of oxygen fugacity (*f*O_2). The zircon crystallization temperatures were calculated using the Ti-in-zircon thermometer (Ferry and Watson, 2007) and the zircon-melt distribution coefficients were determined using the lattice strain model, as described previously (Blundy and Wood, 1994; Ballard et al, 2002). The proportion of water dissolved in the melt (xH_2O) was the only parameter, which was not quantified, a proportion of 5% H_2O was adopted for all calculations.

Figure 55 shows the oxygen fugacity results obtained for the Pedra Branca units. The results from samples PB-181 (LSS) and PB092b (LSO) are more oxidized than the NNO buffer (up to NNO+ 2 log units), whereas zircon fro sample PB-09 (CSO) yields values close to NNO, mostly at higher crystallization temperatures (890 - 990 ºC).

The quantitative estimates of fO_2 obtained from zircon agree with the quantitative values obtained with apatite, both sets indicating that the LSS unit records more oxidized crystallization conditions.

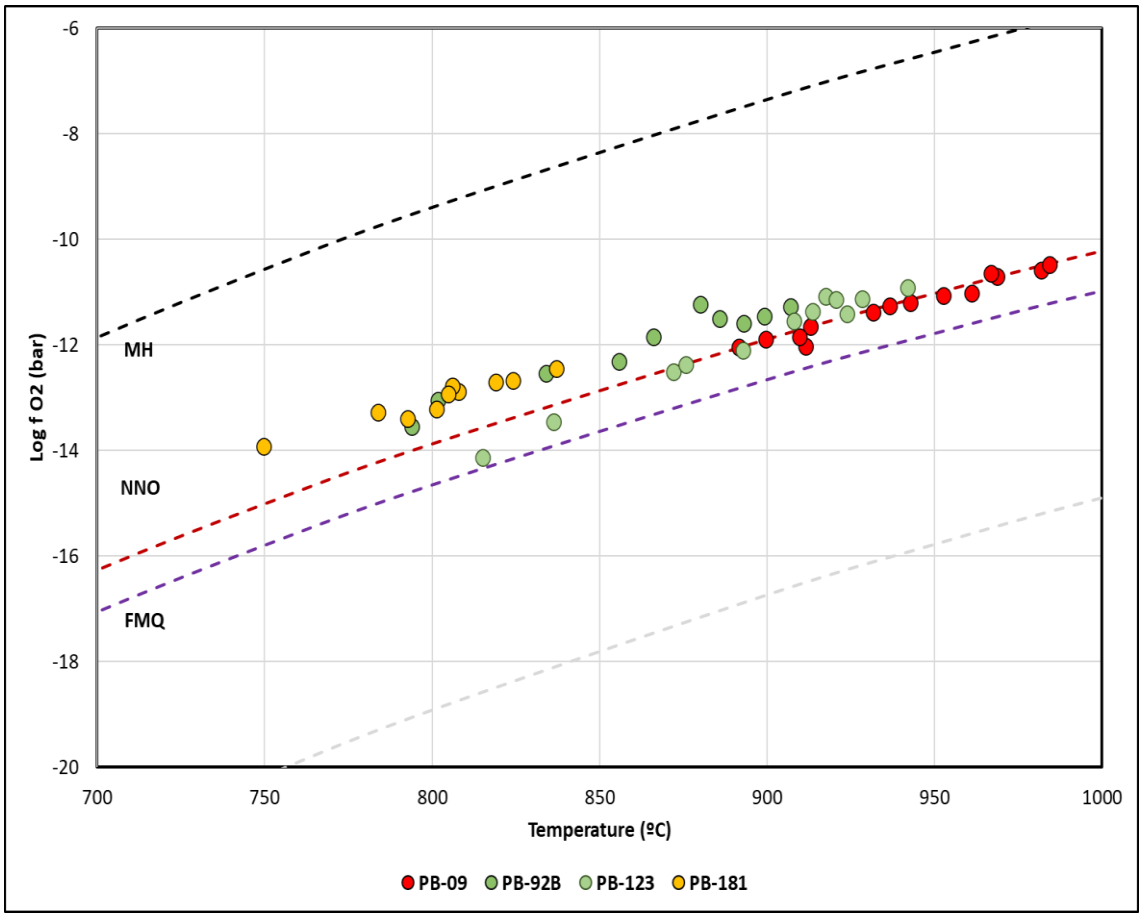

Fig 56: Compiled fO2 results for every unit, in relation to zircon-crystallization temperature

Chapter IV

4.1 Discussion

4.1.1 Factors controlling zircon crystallization in the LSS unit

As one of the main accessory phases studied, the occurrence of zircon among the Pedra Branca units is quite distinct. Zircon is more abundant in the supersaturated units (ESO, LSO and CSO), and record higher crystallization temperatures (800-950ºC) in relation to the saturated unit (LSS; 750-820ºC). Such contrasting differences in the form of occurrence, abundance and composition must be related to the compositional differences observed between the units studied.

Naturally, zircon crystallization occurs after the magma saturation in Zr, which is a process highly influenced by the magma's peralkalinity (Watson & Harrison, 1983; Siegel et al, 2018), represented by the factor M ((Na+K+Ca)/(Al*Si)), where more peralkaline compositions record higher Zr solubility.

Carvalho et al (2012) predict the absence of zircon in the LSS unit, and attribute the Zr enrichment, recorded in mineral phases such as pyroxene and titanite, to the more peralkaline composition (M=3.6), in relation to the supersaturated units (M=2.7). Due to the higher peralkalinity, and consequently, higher solubility of Zr, the crystallization of zircon was interpreted to be initially inhibited, in the LSS unit, causing other mineral phases to incorporate the available Zr, resulting in the mentioned enrichment.

The results obtained in the present work agree with the results published by Carvalho et al (2012), and show, as predicted, the LSS unit being characteristically poor in zircon, occurring in a single sample (PB-181), as well as showing the Zr residing mainly in mafic phases such as pyroxene, amphibole and titanite.

The low crystallization temperatures obtained from the few zircon crystals identified in the LSS unit (sample PB-181), together with the textural characteristics of zircon, pyroxene and amphibole observed (fig. 56), suggest that zircon, in the LSS unit, initially, did not directly crystallize from the melt, but occurred as a product of the destabilization of pyroxene. Pyroxene, by not being stable with the residual melt, or due to the interaction with other fluids, re-equilibrated, producing late-stage hydrous phases (amphibole and biotite), suggested by the abundant presence of relic pyroxene cores included in amphibole crystals, such mineral phases do not incorporate Zr in the same degree as pyroxene does, thus the excess Zr crystallized into zircon in a more evolved

residual melt.

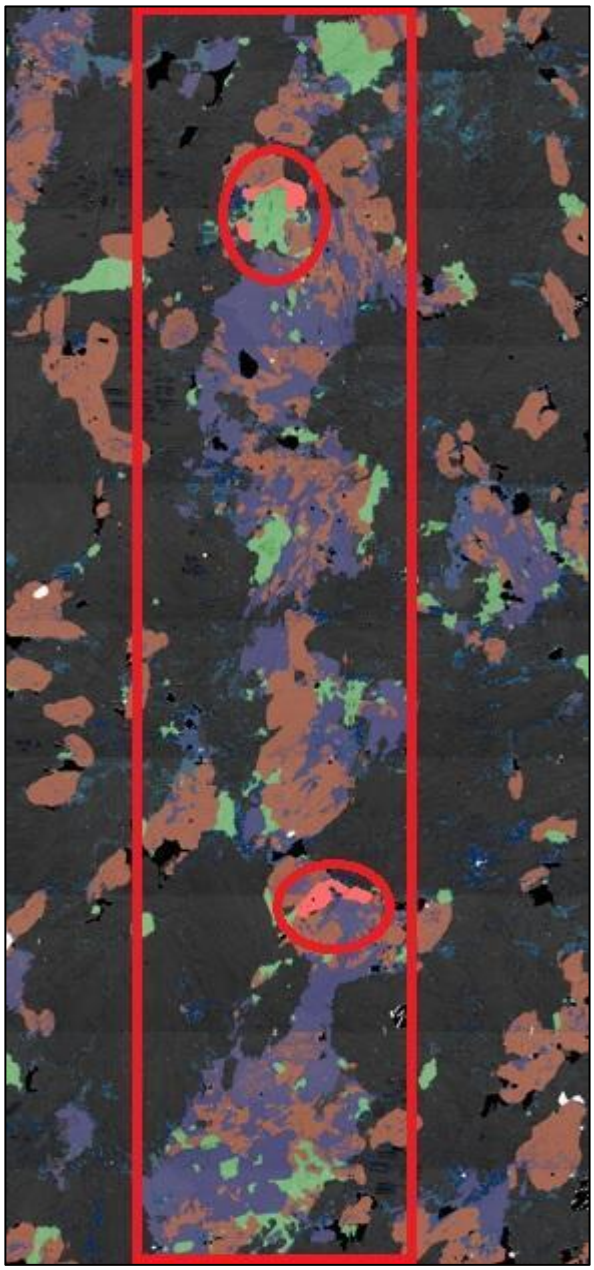

Fig 57: SEM image of a full thin-section of sample PB-181, superimposed with a mineral map, where it is highlighted with a red rectangle the presence of a mafic “strip”; composed of apatite (green), amphibole+biotite (purple), pyroxene (orange) and zircon(red), whrere the only crystals of zircon described in the LSS unit, highlighted in red circles, were identified.

4.1.2 Apatite Homogeneity

Apatite is characteristically the most abundant accessory phase in all the Pedra Branca units, it is the earliest crystallizing mineral studied, recording the highest saturation temperatures (1060 – 1090ºC; Carvalho et al 2012). However, when studying the compositional characteristics of apatite, their homogeneity was noticed; they record the main compositional differences between the units, however they are typically

homogeneous within the same unit, not recording any significant compositional variation, regardless of the textural relationship or size.

The results of CSD in apatite show a possible cause of the homogeneity observed; a majority proportion of the apatite crystals (~90%) are associated with the main mineral phases (K-feldspar, pyroxene, amphibole), where 80% of these crystals are fully included in one of the mentioned phases, as very small crystals (up to 0.175mm), therefore, despite being an early phase mineral, apatite, which was expected to record a large compositional variance, reflecting the magmatic evolution during crystallization, does not show much variance since it gets quickly included into another mineral phase, isolating it from the evolving residual melt.

The inclusion of apatite in other mineral phases possibly functioned as an important mechanism responsible for the homogeneity of the smaller crystals, but it does not justify the homogenization of the large crystals, which are not included and developed in contact with the melt. The exceptionally large crystals studied (1.0 – 3.0mm) do not record significant composition variation, between core and rim, within the same crystal, or in relation to crystals under different textural contexts.

The reason for the observed homogeneity is not yet clear, but some factors were considered, such as: the continuous re-equilibration of apatite with the melt, although we could not identify any textural evidence indicative of such process (any form of zoning or corrosion). Another factor considered was a sampling bias; where, despite the CSD, SEM imagery and petrography results showing apatite crystals under different textural contexts, most of the chemical analyzes were conducted before obtaining this data. It is a possibility that the crystal population chosen for the analyzes were not truly representative of the total population of apatite, representing only a specific set of crystals (e.g a biased result towards large or small crystals, for example), which would give the false impression of a homogeneous result.

4.1.3 Proposed crystallization sequence based on mineral crystallization temperatures

Crystallization temperatures of the main mineral phases (pyroxene, amphibole, and biotite), and accessory minerals (titanite and zircon), which make up the different units of the Pedra Branca pluton were obtained, except for feldspar and apatite, and by compiling these temperatures with apatite saturation results from the literature (Carvalho et al, 2012), a simple crystallization sequence is proposed for the different units (Fig. 58).

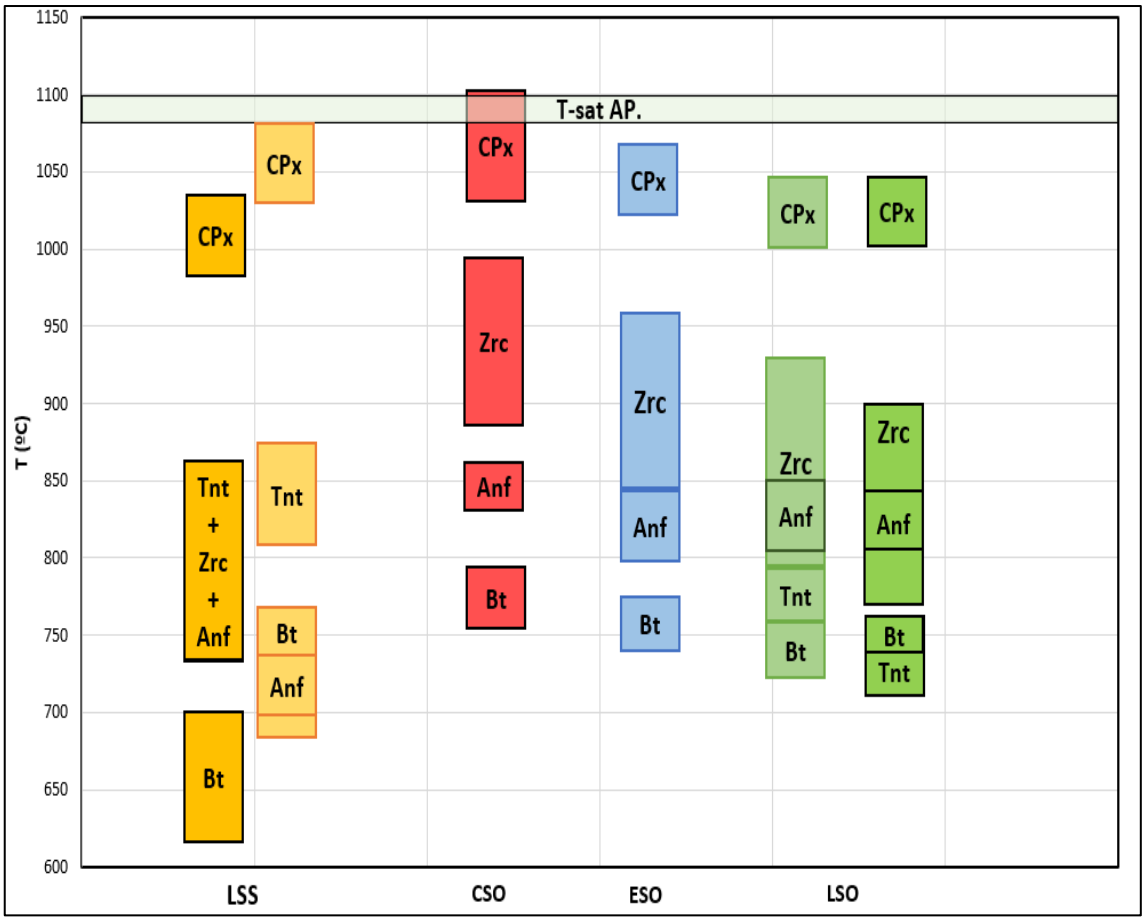

Fig 58: Diagram illustrating the proposed crystallization sequence; the rectangles represent the range of crystallization temperatures obtained for each mineral phase

The crystallization sequences for the three oversaturated units (CSO, LSO and ESO) are similar, with apatite and pyroxene composing the early crystallization phases, alongside alkali feldspar, recording temperatures ranging from 970 to 1100ºC. Although temperatures for alkali-feldspar were not obtained, it is admitted as an early mineral phase based on its abundance (~50-60% in volume) and textural relations. Zircon is an important mineral phase in the oversaturated units since it records the widest range in temperatures, although it's noted that the temperatures get increasingly lower from the CSO towards the LSO unit, from up to 1000ºC in the CSO down to 780ºC in the LSO unit. Amphibole records intermediate crystallization temperatures, with similar values amongst all units, ranging between 800 and 860ºC. Titanite and biotite represent the late-stage phases of crystallization, recording temperatures ranging from 720 up to 800ºC. In general, the proposed crystallization sequence, based on temperature, is quite consistent with the one proposed based on mineral petrography, with the main difference being the earlier crystallization of zircon, especially in the CSO unit.

The crystallization sequence of the LSS unit is, in some ways, like that of the oversaturated units, with apatite, pyroxene and feldspar composing the early crystallization phases, however a significant difference is the lower crystallization temperature of zircon, ranging between 750 to 850ºC, which overlaps with the amphibole and titanite temperatures. Titanite occurs at a much higher temperature, in relation to the oversaturated units, with values up to 875ºC, also recording a wider range of temperatures (750-875ºC). The wide range of temperature recorded represents the two different populations of titanite described, mostly in sample PB-181, where the elevated temperatures are from the large, euhedral, crystals, described as “Pop.1”, whereas the lower temperatures are from titanite associated with Fe-Ti oxides, described as “Pop.2”. Similarly, to the oversaturated units, biotite in the LSS unit also represents a late-stage phase, with the lowest recorded temperatures, ranging between 620 to 750ºC.

4.1.4 Conclusion

The initial qualitative results, based on mineral petrography and the ratios of Ce and Eu in apatite, suggested gradually more oxidizing conditions, from the central unit (CSO) towards the saturated unit (LSS). Using zircon chemistry, it was possible to evaluate the veracity of these results. Based on the Ce-in zircon geobarometer and the use of the lattice strain model, it was possible to quantify the oxygen fugacity of the four units of the Pedra Branca pluton, revealing that the supersaturated crystallized under less oxidizing conditions, with values of fO2 around the NNO buffer, while the saturated unit registers more oxidizing conditions, between NNO+1 and NNO+2.

The results obtained based on zircon confirm the initial qualitative results, suggesting that part of the mineralogical variety, among the units, characteristic of the Pedra Branca pluton, must be attributed to variations in the crystallization conditions and not only to compositional differences between the different units.

Some of the key results from the present work can be summarized as:

- The oversaturated units (CSO, LSO, ESO) record, overall, higher crystallization temperatures, recorded by all the different mineral phases studied, with the most notable difference being the difference in zircon crystallization temperature, where the oversaturated units record temperatures up to 980ºC, whereas the LSS unit record temperatures up to 850ºC
- The results obtained from the application of CSD in apatite suggests the occurrence of magma mixing during the crystallization of the different units

- The oversaturated units record less oxidizing conditions, in relation to the LSS unit, which likely acted as an important factor controlling the mineralogical variation that is, characteristic of the Pedra Branca Syenite.

The characterization of the crystallization conditions of the different units of the Pedra Branca Syenite, presented in the present work, highlights the potential of using *in situ* methods of analysis in accessory minerals to obtain essential information about crystallization processes and magmatic evolution.

Future work may aim to determine what caused the variations in crystallization condition during the evolution of the Pedra Branca pluton, further testing the proposition of Carvalho et al (2014) that occurrence of magma mixing would be the process responsible for the variations contrast between the LSS and the oversaturated units.

References

Ballard J.R.; Palin J.M. & Campbell, I.H. (2002) Relative oxidation states of magmas inferred from Ce(IV)/Ce(III) in zircon: application to porphyry copper deposits of northern Chile. Contributions to Mineralogy Petrology, 144(3), 347–364.

Basei, M. A. S. et al. 1995. A metodologia urânio chumbo na Universidade de São Paulo: princípios metodológicos, aplicações e resultados obtidos. Anais da Academia brasileira de Ciências, 67 (2), p. 221-237,

Blundy, J.D. & Wood, B.J. (1994). Prediction of crystal-melt partition coefficients from elastic moduli. Nature, 372, 452-454.

Boehnke, P., Watson E. B., Trail D., Harrison T. M., Scmitt A. K. (2013). Zircon saturation re-revisited. Chemical Geology, 351, 324-334.

Campos Neto, M.C; Basei, M.A.S.; Vlach, S.R.F.; Caby, R., Szabó, G.A.J; Vasconcelos, P. 2004. Migração de orógenos e superposição de orogêneses: um esboço da colagem brasiliana no sul do Cráton do São Francisco, SE – Brasil. Revista do Instituto de Geociências – USP, São Paulo, 4 (1): 13-40.

Campos Neto, M. C; Caby, R. 1999. Neoproterozoic high-pressure metamorphism and tectonic constraint from nappe system south of the São Francisco craton, southeast Brazil. Precambrian Research, 97: 3-26.

Campos Neto, M. C; Caby, R. 2000. Terrane accretion and upward extrusion of high-pressure granulites in the Neoproterozoic nappes of southeast Brazil: Petrologic and structural constraints. Tectonics, 19 (4): 669-687.

Cashman K.V. & Marsh B.D. 1988: Crystal size distribution (CSD)in rocks and the kinetics and dynamics of crystallization. II.Makaopuhi lava lake. Contr. Mineral. Petrology 99, 3, 292—305.

Carvalho, B.B, 2011. A origem da diversidade geoquímica do Sienito Pedra Branca (MG) a partir da evolução textural e da química de minerais. Dissertação de mestrado, IGc-USP

Carvalho, B.B; Janasi V.A; 2012. Crystallization conditions and controls on trace element residence in the main minerals from the Pedra Branca Syenite, Brazil: An electron microprobe and LA-ICPMS study. Lithos, 153: 208-223.

Carvalho, B.B; Janasi, V.A; Henrique-Pinto, R; 2014. Geochemical and Sr-Nd-Pb isotope constraints on the petrogenesis of the K-rich Pedra Branca Syenite: Implications for the Neoproterozoic post-collisional magmatism in SE Brazil. Lithos, 205: 39-59.

Ebert, H. D.; Hasui, Y.; Costa, J. B. S. O caráter transpressivo do cinturão transcorrente Rio Paraíba do Sul. In: SIMPÓSIO NACIONAL DE ESTUDOS TECTÔNICOS, 3, 1991, Rio Claro. Boletim de Resumos Expandidos... Rio Claro: SBG, 1991. p. 139 –141.

Ferry, J.M; Watson, E.B, 2007. New thermodynamic models and revised calibrations for the Ti-inzircon and Zr-in-rutile thermomethers, 154: 429-437.

Hayden, L.A; Wark, D.A; Watson, E.B, 2007. A thermobarometer for sphene (titanite). Contributions to Mineralogy and Petrology, 155: 529–540.

Heilbron, M; Pedrosa-Soares, AC; Campos Neto, M.C; Silva, L.C; Janasi, V.A; 2004. A Província Mantiqueira. Geologia do Continente Sul-Americano: Evolução da obra de Fernando Flávio Marques de Almeida, São Paulo, Beca, pág. 203-234.

Henry, D., Guidotti, C., Thomson, J., 2005. The Ti-Saturation Surface for Low-to-Medium Pressure Metapelitic Biotites: Implications for Geothermometry and Ti-Substitution Mechanism. American Mineralogist, 90: 316–328

Higgins M.D. 1996: Crystal size distributions and other quantitative textural measurements in lavas and tuff from Egmont volcano (Mt. Taranaki), New Zealand. Bull. Volcanol. 58, 2—3, 194—204.

Higgins M.D. 2000: Measurement of crystal size distributions.Amer. Mineralogist 85, 1105—1116.

Janasi, V. A. . 1992 Sienitos potássicos neoproterozóicos da região de Caldas (MG): aspectos petrológicos e tectônicos. In: XXXVII Congresso Brasileiro de Geologia, 1992, São Paulo. Boletim de Resumos Expandidos. São Paulo: Sociedade Brasileira de Geologia, p. 390-391.

Janasi, V. A. . 1992 Geologia do maciço sienítico Neoproterozóico Capituva, SW de Minas Gerais. In: XXXVII Congresso Brasileiro de Geologia, 1992, São Paulo. Boletim de Resumos Expandidos. São Paulo: Sociedade Brasileira de Geologia, p. 393-394.

Janasi, V.A., 1993. Petrogenesis and tectonic setting of the Neoproterozoic Capituva K-syenitic massif, SW Minas Gerais, Brazil. Revista Brasileira de Geociências, 23(2): 129-138

Janasi, V. A.. 1997. Crustal anatexis and granite genesis in the Socorro-Guaxupé Thrust Nappe, Southeastern Brazil: some geochemical constraints. Revista Brasileira de Geociências, v. 27, n.1, p. 139-150

Gervasoni, F. & Klemme, S.& Rocha-Júnior, E. & Berndt,. J. 2016. Zircon saturation in silicate melts: a new and improved model for aluminous and alkaline melts. Contributions to Mineralogy and Petrology. 171. 21.10.1007/s00410016- 1227-y.

Gonzaga, V.B.C., 2018. Caracterização das condições de cristalização de um magma com base no estudo de seus minerais acessórios. Exemplo do Sienito Pedra Branca, MG. Trabalho de formatura, TF – 18/39, IGc – USP.

Leak, B.E., Woolley, A.R., Arps, C.E.S., Birch, W.D., Gilbert,M.C., Grice, J.D., Hawthorne,F.C., Kato, A., Kisch, H.J., Krivovichev, V.G., Linthout, K., Laird, J. Mandarino, J.A., Maresch, W.V., Nickel, E.H., Rock, N.M.S., Schumacher, J.C., Smith, D.C., Stephenson, N.C.N., Ungaretti, L., Whittaker, E.J.W., Youzhi, G. (1997).Nomenclature of Amphiboles: Report of the sub-committee on amphiboles of the international mineralogical association. Commission on new minerals and mineral names. Amer. Mineral., 82, 1019-1037.

.Morgan D.J. & Jerram D.A. 2006: On estimating crystal shape for crystal size distribution analysis. J. Volcanol. Geotherm. Res. 154, 1—2, 1—7.

Morimoto, N.J, Fabries, J., Fergunson, A.K., Ginzburg, I.V., Ross, M., Seifert, F.A., Aoki, J.Z.K. & Gottardi, G. 1988. Nomenclature of pyroxenes. American Mineralogist, 73: 9-10.

Ridolfi, Filippo, Renzulli, Alberto (2012) Calcic amphiboles in calc-alkaline and alkaline magmas: thermobarometric and chemometric empirical equations valid up to 1,130°C and 2.2 GPa. Contributions to Mineralogy and Petrology, 163 (5). 877-895

Pan, Y. and Fleet, M.E. (2002) Compositions of the Apatite-Group Minerals: Subtitution Mechanisms and Controlling Factors. Reviews in Mineralogy and Geochemistry,48,13-49.

Siégel, C; Bryan, S.E; Allen, C.M; Gust, D.A; 2018. Use and abuse of zircon based thermometers: A critical review and a recommended approach to identify antecrystic zircons. Earth Science Reviews, 176, p.87-116.

Shannon, R.D. (1976). Revised effective ionic radii and systematic studies of interatomic distances in halides and chalcogenides. Acta Crystallographica, A32, 751-767.

Smythe, D. J. & Brenan, J. M. (2016). Magmatic oxygen fugacity estimated using zircon-melt partitioning of cerium. Earth and Planetary Science Letters, 453, 260–266.

Topfner, C. 1996. Brasiliano-granitoide in den Bundesstaaten São Paulo und Minas Gerais, Brasilien – eiene Vergleichende studie. Munchner Geol. Hefte A17.

Vinet N. & Higgins M.D. 2010: Magma solidification processes beneath Kilauea volcano, Hawaii: a quantitative textural and geochemical study of the 1969—1974 Mauna Ulu lavas. J. Petrology 51, 6, 1297—1332.

Watson, B. E. & Harrison, M.T 1983. Zircon saturation revisited: temperature and composition effects in a variety of crustal magma types. Earth and Planetary Science Letters, 64, (2), Pg 295-304,

Wernick, E.B. & Penalva, F. 1980. Contribuição à geologia do Grupo Pinhal (SP e MG). Revista Brasileira de Geociências, 10 (1): 43-62.

Winters, A.M.M 1981. A Geologia do Maciço Sienítico da Pedra Branca, Caldas – MG. Dissertação de Mestrado – Instituto de Geociências, Universidade de S ão Paulo, São Paulo, 92pp.

Appendix I - LA-ICP-MS Results

Pyroxene

PB-09 CPx - LA-ICP-MS																
LA-ICP-MS - Concentração de Elementos Traço (Ppm) - PB-09 (SSI)									LA-ICP-MS - Elementos Traço normalizado por Condrito - PB-09 (SSI)							
Elemento	CPX-1b	CPX-1c	CPX-2b	CPX-2c	CPX-3b	CPX-3c	CPX-4b	CPX-4c	CPX-1b	CPX-1c	CPX-2b	CPX-2c	CPX-3b	CPX-3c	CPX-4b	CPX-4c
Li	42,77	47,99	41,55	48,50	43,54	48,46	45,08	53,04	17,82	19,99	17,31	20,21	18,14	20,19	18,79	22,10
Be	7,85	9,02	7,42	9,61	6,57	8,39	8,01	10,11	196,33	225,40	185,50	240,37	164,13	209,66	200,37	252,63
B	4,20	4,22	3,96	7,60	4,22	5,80	4,99	5,49	2,21	2,22	2,09	4,00	2,22	3,05	2,63	2,89
Mg	57053	60412	61338	59731	60732	66713	67420	71658	0,40	0,42	0,43	0,42	0,42	0,47	0,47	0,50
Si	226389	232808	223683	228009	224563	221005	239475	239162	1,41	1,46	1,40	1,43	1,40	1,38	1,50	1,49
P	<18.26	20,67	<20.24	<18.01	25,29	<20.09	27,29	17,87	0,00	0,01	0,00	0,00	0,01	0,00	0,01	0,01
Ca	148586	148586	148586	148586	148586	148586	148586	148586	11,01	11,01	11,01	11,01	11,01	11,01	11,01	11,01
Sc	57,71	65,57	57,20	58,62	76,87	65,86	60,86	60,16	6,68	7,59	6,62	6,78	8,90	7,62	7,04	6,96
Ti	2005,71	2526,03	1738,53	2108,03	1733,71	1695,88	1557,95	2572,50	3,07	3,86	2,66	3,22	2,65	2,59	2,38	3,93
V	136,78	161,46	133,61	139,70	148,72	142,46	127,22	142,30	1,61	1,90	1,57	1,64	1,75	1,68	1,50	1,67
Cr	69,31	157,91	52,42	53,48	139,06	114,34	131,65	248,33	0,02	0,04	0,01	0,01	0,04	0,03	0,03	0,06
Mn	2517,88	2809,99	2550,33	2571,54	2432,27	2620,04	2383,95	2528,02	0,86	0,96	0,87	0,88	0,83	0,89	0,81	0,86
Co	45,93	50,12	45,33	46,67	41,93	43,07	45,63	46,26	0,06	0,07	0,06	0,06	0,05	0,06	0,06	0,06
Ni	66,29	76,06	72,55	74,68	64,01	66,05	69,61	72,29	0,00	0,00	0,00	0,00	0,00	0,00	0,00	0,00
Cu	1,36	0,83	2,15	5,09	2,07	5,06	4,78	2,70	0,01	0,01	0,01	0,03	0,01	0,03	0,03	0,02
Zn	211,65	233,85	215,52	209,30	175,43	192,24	205,04	216,53	0,46	0,51	0,47	0,45	0,38	0,42	0,44	0,47
Ga	10,30	11,36	9,05	10,32	8,63	8,68	9,54	10,96	0,68	0,75	0,60	0,68	0,57	0,57	0,63	0,72
Rb	<0.186	<0.205	0,21	0,26	0,83	<0.248	0,43	0,24	0,00	0,00	0,06	0,08	0,24	0,00	0,13	0,07
Sr	80,46	77,63	76,54	83,47	73,41	79,54	80,07	86,04	6,76	6,52	6,43	7,01	6,17	6,68	6,73	7,23
Y	41,95	46,03	35,86	45,40	36,43	41,67	41,03	51,55	18,64	20,46	15,94	20,18	16,19	18,52	18,23	22,91
Zr	115,21	130,57	102,70	132,92	105,66	113,44	104,39	142,18	20,80	23,57	18,54	23,99	19,07	20,48	18,84	25,66
Nb	<0.088	<0.107	0,32	<0.093	<0.089	<0.092	0,12	0,13	0,00	0,00	0,86	0,00	0,00	0,00	0,31	0,36
Mo	<0.45	<0.78	<0.70	<0.38	<0.50	<0.56	<0.53	<0.61	0,00	0,00	0,00	0,00	0,00	0,00	0,00	0,00
Sn	1,87	2,46	2,28	2,28	2,75	2,53	2,26	2,05	0,74	0,97	0,90	0,91	1,09	1,01	0,90	0,81
Sb	<0.47	<0.59	<0.46	<0.45	<0.44	<0.45	<0.44	<0.52	0,00	0,00	0,00	0,00	0,00	0,00	0,00	0,00
Cs	<0.113	<0.129	<0.086	<0.124	<0.106	<0.102	<0.108	<0.146	0,00	0,00	0,00	0,00	0,00	0,00	0,00	0,00
Ba	<0.82	<0.65	1,25	1,37	2,51	<0.97	1,35	0,69	0,00	0,00	0,37	0,40	0,74	0,00	0,39	0,20
La	25,05	27,03	22,54	24,70	21,73	22,69	24,18	32,94	68,26	73,64	61,42	67,30	59,21	61,84	65,89	89,77
Ce	96,81	109,91	86,53	100,99	88,47	87,34	96,12	120,52	101,16	114,85	90,41	105,53	92,44	91,26	100,44	125,94
Pr	17,42	20,40	15,58	18,38	15,72	16,64	17,69	21,09	127,15	148,89	113,72	134,19	114,78	121,48	129,14	153,91
Nd	94,51	117,99	87,09	98,98	89,43	83,84	97,09	107,54	132,93	165,94	122,50	139,21	125,78	117,92	136,55	151,26
Sm	24,67	28,73	22,20	26,26	24,50	21,51	25,88	29,48	106,81	124,36	96,11	113,68	106,05	93,13	112,05	127,64
Eu	3,95	5,31	4,31	4,09	3,53	4,60	4,54	4,67	45,39	61,00	49,56	47,01	40,53	52,88	52,14	53,72
Gd	15,84	20,40	13,76	17,48	14,23	15,98	17,44	19,57	51,76	66,66	44,96	57,12	46,50	52,21	57,00	63,97
Tb	2,05	2,73	2,35	2,50	2,03	2,01	2,08	2,96	35,33	47,00	40,47	43,17	34,98	34,74	35,86	51,05
Dy	9,85	12,87	10,23	11,84	10,09	10,12	10,48	14,42	25,86	33,77	26,86	31,08	26,48	26,57	27,50	37,84
Ho	1,76	1,96	1,54	1,89	1,52	1,59	1,84	2,33	20,66	22,98	18,10	22,18	17,88	18,64	21,59	27,42
Er	3,73	4,94	3,80	4,39	4,47	4,10	4,04	5,26	14,97	19,84	15,26	17,62	17,95	16,45	16,24	21,12
Tm	0,62	0,76	0,43	0,73	0,55	0,47	0,63	0,71	17,27	21,32	11,97	20,50	15,37	13,17	17,60	20,06
Yb	3,03	4,80	2,96	4,13	3,82	3,91	3,77	4,85	12,23	19,37	11,92	16,66	15,38	15,78	15,21	19,57
Lu	0,43	0,51	0,33	0,54	0,46	0,58	0,53	0,66	11,27	13,27	8,68	14,04	12,14	15,32	14,00	17,32
Hf	4,58	5,05	4,04	5,98	4,79	4,79	4,89	5,79	25,57	28,23	22,56	33,42	26,74	26,74	27,34	32,35
Ta	<0.200	<0.134	<0.083	<0.139	<0.110	<0.131	<0.107	0,14	0,00	0,00	0,00	0,00	0,00	0,00	0,00	5,52
Pb	0,91	0,67	0,69	2,27	<0.64	<0.66	0,91	1,43	0,25	0,18	0,19	0,62	0,00	0,00	0,25	0,39
Pb	1,11	0,84	0,93	2,28	0,77	1,15	1,07	1,19	0,30	0,23	0,26	0,62	0,21	0,31	0,29	0,33
Pb	1,06	0,74	0,86	2,07	0,79	1,07	1,05	0,93	0,29	0,20	0,24	0,57	0,22	0,29	0,29	0,26
Th	0,14	0,17	0,10	0,15	0,18	0,30	0,22	0,39	3,35	3,90	2,40	3,54	4,18	7,01	5,15	9,14
U	0,02	0,03	0,03	0,02	<0.00	0,01	0,02	0,04	1,33	2,63	2,71	1,26	0,00	0,66	1,34	3,28

LA-ICP-MS results obtained for clinopyroxene – Sample PB-09

LA-ICP-MS - Concentração de Elementos Traço (Ppm) - PB-09 (SSI)							LA-ICP-MS - Elementos Traço normalizado por Condrito					
Elemento	OPX-1	OPX-2	OPX-3	OPX-4	OPX-5	OPX-6	OPX-1	OPX-2	OPX-3	OPX-4	OPX-5	OPX-6
Li	19,08	16,46	14,98	11,26	13,47	12,59	7,95	6,86	6,24	4,69	5,61	5,25
Be	<0.53	0,65	0,49	0,44	<0.49	0,66	0,00	16,32	12,29	10,89	0,00	16,59
B	11,04	14,10	6,80	2,32	3,77	5,67	5,81	7,42	3,58	1,22	1,99	2,98
Mg	128756	128756	128756	128756	128756	128756	0,90	0,90	0,90	0,90	0,90	0,90
Si	334760	263661	303902	291650	286887	283805	2,09	1,65	1,90	1,82	1,79	1,77
P	49,31	<24.91	<15.70	<24.92	<33.86	60,61	0,02	0,00	0,00	0,00	0,00	0,03
Ca	6391	5648	5150	5549	4501	5264	0,47	0,42	0,38	0,41	0,33	0,39
Sc	21,28	12,34	17,01	11,43	16,28	18,90	2,46	1,43	1,97	1,32	1,88	2,19
Ti	12834,94	759,98	779,15	586,18	635,19	673,29	19,63	1,16	1,19	0,90	0,97	1,03
V	180,86	40,87	40,01	35,18	44,36	50,45	2,13	0,48	0,47	0,41	0,52	0,59
Cr	79,23	41,53	34,13	28,85	33,02	33,53	0,02	0,01	0,01	0,01	0,01	0,01
Mn	6465,13	7266,49	6455,85	6482,56	6300,39	6865,90	2,20	2,47	2,20	2,21	2,14	2,34
Co	133,67	119,96	115,20	118,90	115,12	117,96	0,18	0,16	0,15	0,16	0,15	0,15
Ni	156,93	122,21	104,20	106,35	103,35	107,35	0,01	0,01	0,01	0,01	0,01	0,01
Cu	4,29	1,71	2,23	<0.73	6,16	<0.75	0,03	0,01	0,01	0,00	0,04	0,00
Zn	1162,40	1020,25	1163,30	1085,54	1069,82	1153,83	2,52	2,21	2,52	2,35	2,32	2,50
Ga	14,10	9,47	8,14	6,75	10,22	10,73	0,93	0,62	0,54	0,44	0,67	0,71
Rb	28,84	3,42	1,11	<0.26	1,04	<0.30	8,36	0,99	0,32	0,00	0,30	0,00
Sr	28,01	38,06	3,97	<0.135	5,94	0,66	2,35	3,20	0,33	0,00	0,50	0,06
Y	3,61	3,01	3,19	2,27	2,93	3,14	1,61	1,34	1,42	1,01	1,30	1,39
Zr	13,59	3,27	3,24	1,67	4,68	4,39	2,45	0,59	0,59	0,30	0,84	0,79
Nb	16,14	0,27	<0.085	<0.110	<0.153	<0.105	43,04	0,73	0,00	0,00	0,00	0,00
Mo	<1.00	<0.49	<0.41	<0.82	<0.89	<0.87	0,00	0,00	0,00	0,00	0,00	0,00
Sn	4,74	<0.98	1,23	<1.02	<1.27	1,22	1,88	0,00	0,49	0,00	0,00	0,48
Sb	<1.13	<0.83	<0.46	<0.72	<0.92	<0.97	0,00	0,00	0,00	0,00	0,00	0,00
Cs	0,91	0,56	0,15	<0.163	<0.207	<0.222	3,26	2,00	0,54	0,00	0,00	0,00
Ba	132,50	5,93	2,10	<1.36	4,10	<1.63	38,85	1,74	0,62	0,00	1,20	0,00
La	0,95	0,55	0,14	0,18	<0.187	0,44	2,60	1,50	0,38	0,48	0,00	1,21
Ce	2,53	1,23	0,27	0,33	<0.30	0,85	2,64	1,29	0,28	0,34	0,00	0,89
Pr	<0.26	0,33	<0.109	<0.166	<0.251	<0.192	0,00	2,39	0,00	0,00	0,00	0,00
Nd	<2.03	<1.41	1,39	<1.94	<2.14	<1.88	0,00	0,00	1,95	0,00	0,00	0,00
Sm	1,75	<1.11	<0.86	<1.10	<1.49	<1.26	7,58	0,00	0,00	0,00	0,00	0,00
Eu	0,33	<0.36	<0.22	<0.31	<0.42	<0.39	3,83	0,00	0,00	0,00	0,00	0,00
Gd	<1.50	<1.04	<0.59	<1.07	<1.54	<0.97	0,00	0,00	0,00	0,00	0,00	0,00
Tb	0,18	<0.244	<0.116	<0.259	<0.245	<0.168	3,13	0,00	0,00	0,00	0,00	0,00
Dy	<1.51	1,05	0,75	<0.99	<1.33	0,99	0,00	2,75	1,97	0,00	0,00	2,59
Ho	<0.28	<0.217	0,12	<0.136	0,28	<0.187	0,00	0,00	1,43	0,00	3,31	0,00
Er	<0.67	<0.40	0,45	<0.39	<0.67	0,52	0,00	0,00	1,81	0,00	0,00	2,10
Tm	<0.251	0,12	<0.100	0,19	<0.167	<0.214	0,00	3,26	0,00	5,20	0,00	0,00
Yb	<1.40	0,82	1,01	<0.85	<0.94	<1.00	0,00	3,33	4,07	0,00	0,00	0,00
Lu	<0.33	<0.25	<0.131	<0.174	<0.29	<0.221	0,00	0,00	0,00	0,00	0,00	0,00
Hf	<2.11	<1.08	<1.05	<1.65	<1.43	1,07	0,00	0,00	0,00	0,00	0,00	5,99
Ta	0,87	<0.177	<0.111	<0.193	<0.220	<0.187	33,60	0,00	0,00	0,00	0,00	0,00
Pb	<1.01	<1.05	<0.56	<0.97	<1.33	<0.80	0,00	0,00	0,00	0,00	0,00	0,00
Pb	<1.57	0,87	<0.56	<1.05	<0.71	<1.21	0,00	0,24	0,00	0,00	0,00	0,00
Pb	0,4	0,88	<0.25	<0.44	<0.52	<0.28	0,11	0,24	0,00	0,00	0,00	0,00
Th	0,112	0,225	0,054	0,016	<0.00	0,017	2,65	5,30	1,27	0,38	0,00	0,40
U	0,069	<0.00	0,027	0,016	<0.160	0,017	5,66	0,00	2,23	1,32	0,00	1,38

LA-ICP-MS results obtained for orthopyroxene – Sample PB-09

LA-ICP-MS - Concentração de Elementos Traço (Ppm) - PB-22 (SSE)									
Elemento	CPX-1c	CPX-1b	CPX-2	CPX-3	CPX-4c	CPX-4b	CPX-5	CPX-7	CPX-8
Li	39,79	41,82	39,89	35,41	39,15	42,62	38,81	27,76	35,25
Be	6,85	6,51	6,84	7,18	7,41	7,23	6,95	8,07	5,92
B	<1.53	2,69	1,55	1,58	2,16	1,82	3,32	1,95	1,77
Mg	78250	71799	76105	71900	77338	73784	75527	93252	71978
Si	248229	237704	246824	230170	243935	230531	239010	265274	221776
P	<16.86	<14.64	280,00	244,71	18,09	<13.91	17,86	141,95	<14.85
Ca	146275	146275	146275	146275	146275	146275	146275	146275	146275
Sc	55,36	55,60	54,88	59,78	56,76	54,50	55,91	59,66	58,77
Ti	1885,01	960,33	1885,26	1298,62	1677,17	1523,70	2369,32	3665,36	827,31
V	136,20	118,19	133,29	126,75	121,89	123,43	137,38	165,79	112,08
Cr	234,45	63,99	434,94	37,51	58,84	78,08	51,67	326,73	47,30
Mn	3000,71	2867,89	2994,79	2774,28	2783,92	3045,40	3171,57	2941,79	2813,81
Co	41,65	36,06	40,01	35,01	42,97	40,11	41,30	50,37	35,97
Ni	69,29	55,51	61,99	50,93	75,93	65,57	68,70	81,08	49,29
Cu	6,18	2,90	0,81	1,06	4,71	4,78	5,85	1,57	1,67
Zn	252,40	210,61	237,70	215,11	261,90	257,60	266,10	305,93	211,20
Ga	11,21	8,70	10,38	9,69	9,66	9,77	10,30	14,62	7,59
Rb	9,03	0,18	4,22	0,32	0,98	0,56	2,89	2,25	<0.175
Sr	85,43	73,77	88,56	80,53	101,23	104,25	96,49	119,19	70,92
Y	48,89	42,89	50,75	43,25	48,94	44,01	48,12	59,57	37,94
Zr	42,93	38,93	46,58	36,21	104,13	42,48	69,58	39,43	25,30
Nb	1,39	<0.059	1,04	0,91	0,67	0,75	1,82	7,15	<0.098
Mo	<0.40	0,34	0,33	0,28	<0.43	<0.52	<0.56	<0.47	<0.54
Sn	1,87	1,58	1,98	1,93	2,03	1,82	1,87	3,22	2,13
Sb	<0.43	<0.47	<0.47	<0.48	<0.41	<0.47	<0.32	<0.46	<0.51
Cs	0,19	<0.101	0,11	<0.082	<0.077	<0.093	<0.100	<0.112	<0.090
Ba	86,78	<0.97	72,36	3,63	3,89	224,53	13,37	31,51	1,56
La	28,87	22,86	30,76	29,65	29,35	22,92	26,74	39,71	19,94
Ce	118,27	94,21	119,99	109,70	118,19	100,04	109,65	159,54	87,97
Pr	20,79	17,15	20,77	19,42	20,36	18,28	19,34	27,87	15,19
Nd	108,99	89,92	106,90	101,56	109,77	92,79	97,39	139,97	82,11
Sm	26,72	22,50	26,25	26,59	27,36	24,68	25,57	36,08	21,53
Eu	4,83	4,33	4,85	4,43	5,13	3,87	4,77	6,60	4,09
Gd	18,78	14,85	18,55	16,90	18,02	13,98	16,81	23,36	14,06
Tb	2,48	2,08	2,63	2,17	2,51	2,06	2,35	3,24	1,76
Dy	13,29	10,88	13,33	11,27	11,63	10,21	11,02	13,69	9,09
Ho	2,22	1,86	2,28	1,82	2,15	1,83	2,02	2,43	1,62
Er	4,67	3,82	5,71	4,95	4,49	4,51	4,68	6,05	3,84
Tm	0,63	0,66	0,77	0,53	0,57	0,56	0,69	0,81	0,46
Yb	4,71	4,68	5,34	3,86	4,52	4,43	4,30	6,06	3,18
Lu	0,47	0,62	0,78	0,45	0,55	0,47	0,75	0,63	0,58
Hf	3,68	3,24	3,44	2,42	4,88	3,06	3,73	2,18	2,17
Ta	<0.109	<0.101	0,09	0,08	<0.106	0,11	<0.126	0,25	<0.091
Pb	1,27	0,70	1,08	1,36	0,96	1,06	1,73	1,65	1,13
Pb	0,98	1,42	0,77	1,28	1,36	1,61	1,62	1,39	0,89
Pb	0,90	1,02	1,23	1,03	1,57	1,20	1,58	1,59	0,74
Th	0,12	0,05	0,20	0,19	0,78	0,09	0,12	0,11	0,05
U	<0.00	<0.00	0,04	0,05	0,11	0,02	0,02	0,09	0,01

LA-ICP-MS - Elementos Traço normalizado por Condrito - PB-22 (SSE)									
Elemento	CPX-1c	CPX-1b	CPX-2	CPX-3	CPX-4c	CPX-4b	CPX-5	CPX-7	CPX-8
Li	16,58	17,43	16,62	14,75	16,31	17,76	16,17	11,57	14,69
Be	171,23	162,68	171,01	179,46	185,32	180,85	173,65	201,72	148,03
B	0,00	1,42	0,81	0,83	1,14	0,96	1,75	1,02	0,93
Mg	0,55	0,50	0,53	0,50	0,54	0,52	0,53	0,65	0,50
Si	1,55	1,49	1,54	1,44	1,52	1,44	1,49	1,66	1,39
P	0,00	0,00	0,12	0,11	0,01	0,00	0,01	0,06	0,00
Ca	10,84	10,84	10,84	10,84	10,84	10,84	10,84	10,84	10,84
Sc	6,41	6,44	6,35	6,92	6,57	6,31	6,47	6,90	6,80
Ti	2,88	1,47	2,88	1,99	2,56	2,33	3,62	5,60	1,27
V	1,60	1,39	1,57	1,49	1,43	1,45	1,62	1,95	1,32
Cr	0,06	0,02	0,11	0,01	0,01	0,02	0,01	0,08	0,01
Mn	1,02	0,98	1,02	0,94	0,95	1,04	1,08	1,00	0,96
Co	0,05	0,05	0,05	0,05	0,06	0,05	0,05	0,07	0,05
Ni	0,00	0,00	0,00	0,00	0,00	0,00	0,00	0,00	0,00
Cu	0,04	0,02	0,00	0,01	0,03	0,03	0,03	0,01	0,01
Zn	0,55	0,46	0,51	0,47	0,57	0,56	0,58	0,66	0,46
Ga	0,74	0,57	0,68	0,64	0,64	0,64	0,68	0,96	0,50
Rb	2,62	0,05	1,22	0,09	0,28	0,16	0,84	0,65	0,00
Sr	7,18	6,20	7,44	6,77	8,51	8,76	8,11	10,02	5,96
Y	21,73	19,06	22,55	19,22	21,75	19,56	21,39	26,47	16,86
Zr	7,75	7,03	8,41	6,54	18,80	7,67	12,56	7,12	4,57
Nb	3,71	0,00	2,76	2,42	1,80	2,00	4,84	19,07	0,00
Mo	0,00	0,25	0,24	0,20	0,00	0,00	0,00	0,00	0,00
Sn	0,74	0,63	0,79	0,77	0,80	0,72	0,74	1,28	0,85
Sb	0,00	0,00	0,00	0,00	0,00	0,00	0,00	0,00	0,00
Cs	0,69	0,00	0,38	0,00	0,00	0,00	0,00	0,00	0,00
Ba	25,45	0,00	21,22	1,07	1,14	65,84	3,92	9,24	0,46
La	78,66	62,28	83,81	80,80	79,97	62,45	72,86	108,21	54,34
Ce	123,59	98,45	125,38	114,63	123,50	104,54	114,58	166,71	91,92
Pr	151,74	125,16	151,61	141,73	148,64	133,44	141,16	203,43	110,90
Nd	153,29	126,46	150,35	142,84	154,39	130,50	136,98	196,86	115,48
Sm	115,65	97,40	113,65	115,10	118,46	106,84	110,71	156,17	93,22
Eu	55,56	49,74	55,72	50,87	58,96	44,49	54,80	75,86	47,03
Gd	61,38	48,53	60,63	55,24	58,88	45,67	54,92	76,34	45,95
Tb	42,78	35,89	45,35	37,35	43,22	35,47	40,50	55,86	30,31
Dy	34,89	28,55	34,99	29,59	30,53	26,79	28,91	35,93	23,87
Ho	26,10	21,84	26,79	21,38	25,32	21,48	23,75	28,53	19,04
Er	18,76	15,34	22,95	19,86	18,03	18,11	18,81	24,30	15,42
Tm	17,77	18,55	21,65	14,97	15,90	15,81	19,39	22,81	12,86
Yb	19,00	18,87	21,52	15,55	18,22	17,88	17,33	24,44	12,84
Lu	12,33	16,26	20,43	11,67	14,33	12,33	19,67	16,54	15,29
Hf	20,58	18,09	19,20	13,53	27,27	17,12	20,82	12,16	12,14
Ta	0,00	0,00	3,62	3,17	0,00	4,12	0,00	9,57	0,00
Pb	0,35	0,19	0,30	0,37	0,26	0,29	0,47	0,45	0,31
Pb	0,27	0,39	0,21	0,35	0,37	0,44	0,44	0,38	0,25
Pb	0,25	0,28	0,34	0,28	0,43	0,33	0,43	0,44	0,20
Th	2,72	1,21	4,64	4,44	18,26	2,11	2,84	2,63	1,09
U	0,00	0,00	3,17	4,19	9,08	1,80	1,82	7,07	0,53

LA-ICP-MS results obtained for clinopyroxene – Sample PB-22

	LA-ICP-MS - Concentração de Elementos Traço (Ppm) - PB-92B (SLS)										LA-ICP-MS - Elementos Traço normalizado por Condrito - PB-92B (SLS)									
Elemento	**CPX-1**	**CPX-2c**	**CPX-2b**	**CPX-3c**	**CPX-3b**	**CPX-4**	**CPX-5**	**CPX-6**	**CPX-7**	**CPX-8**	**CPX-1**	**CPX-2c**	**CPX-2b**	**CPX-3c**	**CPX-3b**	**CPX-4**	**CPX-5**	**CPX-6**	**CPX-7**	**CPX-8**
Li	76,42	73,36	73,80	60,78	56,52	73,80	66,24	66,98	70,40	70,09	31,84	30,57	30,75	25,32	23,55	30,75	27,60	27,91	29,33	29,21
Be	14,62	14,56	15,05	13,50	13,69	13,64	13,06	12,58	14,52	10,61	365,51	363,91	376,20	337,39	342,33	340,97	326,39	314,54	363,08	265,16
B	3,69	3,53	<2.02	4,04	3,68	2,95	3,44	2,56	4,48	3,37	1,94	1,86	0,00	2,12	1,94	1,55	1,81	1,35	2,36	1,77
Mg	72184	81233	84824	76101	88720	73723	70023	70596	68541	71173	0,51	0,57	0,59	0,53	0,62	0,52	0,49	0,49	0,48	0,50
Si	220495	252961	261740	232263	263583	236246	220248	227038	224126	231866	1,38	1,58	1,64	1,45	1,65	1,48	1,38	1,42	1,40	1,45
P	<18.65	<19.62	<19.85	<18.16	<22.67	<25.34	2788,51	24,42	<19.89	<21.09	0,00	0,00	0,00	0,00	0,00	0,00	1,21	0,01	0,00	0,00
Ca	151209	151209	151209	151209	151209	151209	151209	151209	151209	151209	11,20	11,20	11,20	11,20	11,20	11,20	11,20	11,20	11,20	11,20
Sc	47,04	49,42	50,07	45,62	51,51	48,39	46,87	46,25	44,64	45,52	5,44	5,72	5,80	5,28	5,96	5,60	5,43	5,35	5,17	5,27
Ti	906,60	1195,43	1703,02	1183,27	2637,65	1436,86	1376,91	912,01	944,48	986,62	1,39	1,83	2,60	1,81	4,03	2,20	2,11	1,39	1,44	1,51
V	110,71	114,80	127,33	108,76	131,22	115,31	103,86	102,81	100,43	104,68	1,30	1,35	1,50	1,28	1,54	1,36	1,22	1,21	1,18	1,23
Cr	54,44	73,38	48,12	100,91	57,28	61,92	16,79	39,40	46,86	46,30	0,01	0,02	0,01	0,03	0,01	0,02	0,00	0,01	0,01	0,01
Mn	2746,20	2835,59	3008,92	2861,10	3071,89	3043,57	2670,83	2855,26	2732,05	2977,87	0,93	0,96	1,02	0,97	1,05	1,04	0,91	0,97	0,93	1,01
Co	40,79	44,85	51,06	45,28	57,37	46,22	44,84	41,27	43,05	43,96	0,05	0,06	0,07	0,06	0,08	0,06	0,06	0,05	0,06	0,06
Ni	81,69	91,59	110,61	88,21	120,63	91,32	91,57	81,14	88,48	89,96	0,00	0,01	0,01	0,01	0,01	0,01	0,01	0,00	0,01	0,01
Cu	3,85	1,83	5,33	2,09	79,92	2,70	55,51	0,75	4,44	3,42	0,02	0,01	0,03	0,01	0,48	0,02	0,33	0,00	0,03	0,02
Zn	275,66	321,26	361,11	297,59	379,90	305,04	308,91	265,81	274,81	284,51	0,60	0,70	0,78	0,64	0,82	0,66	0,67	0,58	0,60	0,62
Ga	7,86	8,76	10,46	8,31	12,25	7,79	10,98	7,56	6,85	7,38	0,52	0,58	0,69	0,55	0,81	0,51	0,72	0,50	0,45	0,49
Rb	<0.25	0,60	1,41	0,75	2,51	<0.41	1,02	<0.223	0,34	0,30	0,00	0,18	0,41	0,22	0,73	0,00	0,30	0,00	0,10	0,09
Sr	104,95	103,33	118,69	101,68	136,32	104,84	155,60	106,87	109,52	114,07	8,82	8,68	9,97	8,54	11,46	8,81	13,08	8,98	9,20	9,59
Y	28,21	29,25	34,19	29,16	41,71	30,71	47,66	28,96	27,35	30,04	12,54	13,00	15,19	12,96	18,54	13,65	21,18	12,87	12,15	13,35
Zr	37,44	39,29	44,75	46,32	57,40	33,27	35,83	37,21	41,69	42,65	6,76	7,09	8,08	8,36	10,36	6,01	6,47	6,72	7,53	7,70
Nb	<0.102	1,74	3,48	1,29	5,84	1,66	2,69	0,12	<0.143	<0.104	0,00	4,64	9,28	3,43	15,58	4,42	7,18	0,32	0,00	0,00
Mo	<0.39	<0.64	<0.56	<0.78	<0.67	<1.09	<0.87	<0.83	<0.65	<0.52	0,00	0,00	0,00	0,00	0,00	0,00	0,00	0,00	0,00	0,00
Sn	1,30	2,66	3,25	1,83	3,43	2,19	2,54	2,91	1,61	<1.04	0,51	1,06	1,29	0,73	1,36	0,87	1,01	1,15	0,64	0,00
Sb	<0.78	<0.77	<0.80	<0.66	<0.93	<0.82	<0.80	0,77	<0.58	0,52	0,00	0,00	0,00	0,00	0,00	0,00	0,00	3,31	0,00	2,21
Cs	<0.134	<0.157	<0.137	<0.128	<0.188	<0.267	<0.185	<0.145	<0.141	<0.122	0,00	0,00	0,00	0,00	0,00	0,00	0,00	0,00	0,00	0,00
Ba	<1.24	3,20	10,03	5,20	17,52	<2.03	7,84	<1.34	1,89	<1.65	0,00	0,94	2,94	1,52	5,14	0,00	2,30	0,00	0,55	0,00
La	24,11	26,41	30,10	26,03	38,17	31,69	123,96	24,31	35,38	25,83	65,71	71,96	82,03	70,94	104,00	86,34	337,76	66,25	96,41	70,39
Ce	90,90	101,61	111,14	92,96	134,40	100,32	310,83	88,55	102,77	93,34	94,99	106,18	116,13	97,14	140,44	104,83	324,79	92,53	107,39	97,53
Pr	14,98	16,28	18,85	16,90	21,77	15,89	43,53	16,04	16,53	15,20	109,38	118,86	137,57	123,34	158,91	116,01	317,75	117,11	120,62	110,92
Nd	75,11	81,67	97,52	80,40	114,47	77,61	176,84	81,17	83,14	78,70	105,65	114,86	137,17	113,08	161,00	109,15	248,72	114,16	116,93	110,69
Sm	18,83	21,35	20,94	18,32	25,05	18,14	33,48	19,43	18,60	17,63	81,52	92,41	90,64	79,33	108,45	78,51	144,95	84,09	80,52	76,32
Eu	4,06	3,54	3,85	3,94	4,67	3,49	6,74	3,57	3,77	3,70	46,63	40,69	44,21	45,26	53,65	40,06	77,51	41,07	43,30	42,51
Gd	12,16	12,37	13,81	11,20	17,23	11,58	17,72	12,01	11,08	11,89	39,73	40,41	45,14	36,60	56,31	37,83	57,92	39,26	36,21	38,84
Tb	1,38	1,44	1,74	1,58	2,13	1,51	2,63	1,49	1,65	1,14	23,81	24,91	30,07	27,21	36,69	26,09	45,39	25,68	28,38	19,59
Dy	6,49	7,57	8,28	6,58	10,91	6,21	11,64	7,19	7,62	6,29	17,04	19,87	21,72	17,27	28,64	16,31	30,56	18,88	20,00	16,52
Ho	1,06	0,96	1,39	1,04	1,75	1,09	1,62	1,19	1,05	1,18	12,51	11,25	16,28	12,25	20,54	12,82	19,04	14,03	12,37	13,85
Er	2,38	2,99	2,37	2,72	3,12	2,60	3,48	2,76	2,48	2,36	9,55	12,00	9,53	10,92	12,51	10,45	13,97	11,10	9,96	9,46
Tm	0,42	0,43	0,37	0,43	0,73	0,44	0,56	0,24	0,42	0,47	11,89	12,11	10,31	11,94	20,64	12,26	15,84	6,65	11,74	13,19
Yb	2,76	2,41	2,46	2,54	3,34	3,41	4,17	3,59	1,96	3,37	11,13	9,73	9,92	10,24	13,48	13,73	16,83	14,46	7,90	13,59
Lu	0,35	0,45	0,46	0,54	0,61	0,35	0,54	0,30	0,42	0,28	9,21	11,82	12,00	14,15	16,04	9,12	14,12	7,83	10,91	7,39
Hf	2,36	2,47	2,66	2,92	4,76	1,65	4,30	4,22	1,62	2,47	13,20	13,81	14,85	16,29	26,62	9,20	24,02	23,57	9,05	13,79
Ta	<0.138	<0.173	<0.200	<0.171	0,36	<0.171	0,20	<0.146	<0.158	<0.157	0,00	0,00	0,00	0,00	14,01	0,00	7,54	0,00	0,00	0,00
Pb	1,63	2,28	2,22	1,81	2,23	2,87	1,57	0,98	1,97	2,07	0,45	0,62	0,61	0,50	0,61	0,79	0,43	0,27	0,54	0,57
Pb	1,65	1,67	1,92	1,37	2,54	3,24	1,18	1,23	1,90	1,97	0,45	0,46	0,53	0,37	0,70	0,89	0,32	0,34	0,52	0,54
Pb	1,59	2,00	1,83	1,42	1,67	3,46	1,18	1,54	1,61	1,40	0,44	0,55	0,50	0,39	0,46	0,95	0,32	0,42	0,44	0,39
Th	<0.082	0,15	0,21	0,21	0,35	0,70	2,80	0,07	0,05	0,09	0,00	3,55	4,91	4,98	8,23	16,38	65,79	1,62	1,24	2,10
U	0,02	<0.00	0,03	0,06	0,03	0,06	0,34	<0.00	0,01	<0.067	1,84	0,00	2,18	4,89	2,50	5,26	28,23	0,00	1,04	0,00

LA-ICP-MS results obtained for clinopyroxene – Sample PB-92B

	LA-ICP-MS - Concentração de Elementos Traço (Ppm) - PB-181A (SLSI)										LA-ICP-MS - Elementos Traço normalizado por Condrito - PB-181A (SLSI)									
Elemento	**PX-1c**	**PX-1b**	**PX-2**	**PX-3**	**PX-4b**	**PX-4c**	**PX-5b**	**PX-5c**	**PX-6c**	**PX-6b**	**PX-1c**	**PX-1b**	**PX-2**	**PX-3**	**PX-4b**	**PX-4c**	**PX-5b**	**PX-5c**	**PX-6c**	**PX-6b**
Li	29,81	33,02	52,98	28,45	29,24	33,91	26,67	25,91	23,64	25,30	12,42	13,76	22,07	11,85	12,18	14,13	11,11	10,80	9,85	10,54
Be	28,36	25,66	28,39	26,33	26,23	26,47	23,91	25,39	22,07	26,20	709,09	641,52	709,70	658,23	655,80	661,63	597,63	634,65	551,68	654,97
B	6,53	3,75	4,89	4,53	5,19	6,66	5,96	4,88	4,06	3,92	3,43	1,97	2,57	2,39	2,73	3,51	3,13	2,57	2,14	2,06
Mg	63505	56617	51168	55669	55035	68941	56015	58948	61174	55919	0,44	0,40	0,36	0,39	0,39	0,48	0,39	0,41	0,43	0,39
Si	245311	231349	200607	221260	223996	244537	226999	225628	228825	216811	1,53	1,45	1,25	1,38	1,40	1,53	1,42	1,41	1,43	1,36
P	23,92	14,52	<11.98	<13.53	<15.87	<17.65	<16.84	<14.80	<15.91	<14.06	0,01	0,01	0,00	0,00	0,00	0,00	0,00	0,00	0,00	0,00
Ca	132355	132355	132355	132355	132355	132355	132355	132355	132355	132355	9,80	9,80	9,80	9,80	9,80	9,80	9,80	9,80	9,80	9,80
Sc	50,45	56,43	48,88	45,17	48,91	49,75	50,50	48,75	46,45	51,08	5,84	6,53	5,66	5,23	5,66	5,76	5,84	5,64	5,38	5,91
Ti	3281,07	1149,62	2820,15	3547,34	2071,56	3540,81	1665,27	2432,56	3389,62	2657,04	5,02	1,76	4,31	5,42	3,17	5,41	2,55	3,72	5,18	4,06
V	297,30	269,79	276,31	285,75	253,24	257,00	243,48	236,17	213,79	244,93	3,50	3,17	3,25	3,36	2,98	3,02	2,86	2,78	2,52	2,88
Cr	216,66	133,16	120,76	97,12	97,09	95,58	142,84	121,45	109,97	104,50	0,05	0,03	0,03	0,02	0,02	0,02	0,04	0,03	0,03	0,03
Mn	2776,51	2944,28	2779,23	2684,67	2712,02	2990,04	2758,18	2825,87	2711,60	2767,29	0,94	1,00	0,95	0,91	0,92	1,02	0,94	0,96	0,92	0,94
Co	55,32	53,48	50,96	50,49	48,64	61,09	49,01	52,27	52,45	51,05	0,07	0,07	0,07	0,07	0,06	0,08	0,06	0,07	0,07	0,07
Ni	107,58	102,87	99,77	98,92	97,77	124,74	97,77	102,95	111,26	106,47	0,01	0,01	0,01	0,01	0,01	0,01	0,01	0,01	0,01	0,01
Cu	3,54	4,34	39,42	5,59	2,68	2,70	4,42	0,75	1,20	2,03	0,02	0,03	0,24	0,03	0,02	0,02	0,03	0,00	0,01	0,01
Zn	394,17	359,63	377,48	358,61	339,24	440,12	338,90	353,09	386,90	358,82	0,85	0,78	0,82	0,78	0,73	0,95	0,73	0,76	0,84	0,78
Ga	9,58	9,30	9,68	9,89	8,30	11,59	9,42	9,30	9,02	9,08	0,63	0,61	0,64	0,65	0,55	0,76	0,62	0,61	0,59	0,60
Rb	2,11	3,15	7,74	<0.154	0,89	9,13	2,70	0,73	0,96	<0.166	0,61	0,91	2,24	0,00	0,26	2,65	0,78	0,21	0,28	0,00
Sr	1491,41	784,00	1545,55	885,25	574,93	646,13	628,09	578,33	636,79	639,85	125,33	65,88	129,88	74,39	48,31	54,30	52,78	48,60	53,51	53,77
Y	9,34	6,94	19,94	14,34	10,98	12,53	11,20	12,06	17,35	15,90	4,15	3,08	8,86	6,37	4,88	5,57	4,98	5,36	7,71	7,07
Zr	418,11	241,09	358,77	418,22	343,24	383,42	345,56	392,63	375,35	501,71	75,47	43,52	64,76	75,49	61,96	69,21	62,37	70,87	67,75	90,56
Nb	0,52	0,08	0,21	0,12	<0.073	0,79	<0.072	0,21	0,75	0,09	1,37	0,22	0,56	0,33	0,00	2,11	0,00	0,56	2,00	0,24
Mo	<0.38	0,98	<0.46	<0.34	<0.50	0,26	<0.31	<0.49	<0.44	<0.59	0,00	0,71	0,00	0,00	0,00	0,19	0,00	0,00	0,00	0,00
Sn	3,45	2,69	3,29	3,64	2,86	2,06	3,24	2,44	2,49	2,74	1,37	1,07	1,30	1,44	1,14	0,82	1,29	0,97	0,99	1,09
Sb	<0.44	<0.41	<0.36	<0.40	<0.47	<0.48	<0.41	<0.49	<0.32	<0.38	0,00	0,00	0,00	0,00	0,00	0,00	0,00	0,00	0,00	0,00
Cs	<0.087	0,11	0,24	<0.073	<0.118	<0.130	<0.103	<0.078	<0.116	<0.091	0,00	0,39	0,84	0,00	0,00	0,00	0,00	0,00	0,00	0,00
Ba	4076,97	208,93	16,91	2940,89	1,41	66,47	63,81	21,31	10,66	0,90	1195,59	61,27	4,96	862,43	0,41	19,49	18,71	6,25	3,13	0,26
La	15,00	14,38	27,47	18,13	16,17	16,84	15,80	15,27	23,59	19,55	40,86	39,18	74,84	49,39	44,07	45,88	43,06	41,61	64,28	53,26
Ce	43,27	36,94	74,06	60,38	51,10	52,49	49,78	46,55	68,60	59,66	45,21	38,60	77,38	63,09	53,39	54,85	52,02	48,64	71,68	62,34
Pr	6,06	4,87	10,79	9,57	7,62	7,81	7,12	6,99	10,86	9,42	44,23	35,55	78,76	69,84	55,65	56,97	51,96	51,02	79,25	68,78
Nd	27,86	21,55	53,92	47,11	36,31	35,95	35,64	35,28	49,26	43,63	39,19	30,31	75,84	66,27	51,07	50,57	50,13	49,62	69,29	61,36
Sm	5,13	4,23	10,75	10,65	7,55	7,65	7,22	6,58	11,16	9,31	22,22	18,31	46,52	46,11	32,67	33,11	31,26	28,49	48,32	40,28
Eu	1,78	1,18	3,21	2,59	2,12	2,36	1,71	1,63	2,55	2,29	20,50	13,53	36,92	29,72	24,37	27,11	19,63	18,73	29,26	26,32
Gd	3,63	2,80	7,50	5,60	4,08	5,04	4,62	4,88	7,25	5,67	11,85	9,16	24,53	18,31	13,32	16,47	15,09	15,95	23,71	18,53
Tb	0,39	0,36	0,81	0,70	0,46	0,64	0,53	0,55	0,91	0,68	6,64	6,24	14,02	12,11	8,00	10,97	9,17	9,51	15,61	11,74
Dy	2,26	1,80	3,61	3,13	2,60	2,57	2,44	2,86	4,13	3,06	5,93	4,72	9,47	8,22	6,82	6,75	6,41	7,51	10,85	8,04
Ho	0,33	0,20	0,55	0,48	0,51	0,51	0,40	0,49	0,56	0,71	3,86	2,38	6,48	5,67	5,98	5,99	4,69	5,78	6,63	8,38
Er	0,84	0,70	1,77	1,24	0,96	1,15	0,98	0,86	1,39	1,24	3,39	2,82	7,09	5,00	3,84	4,63	3,94	3,44	5,57	4,96
Tm	0,20	0,18	0,26	0,19	0,21	<0.160	<0.145	0,18	<0.131	0,19	5,58	5,02	7,24	5,29	5,76	0,00	0,00	5,10	0,00	5,40
Yb	1,52	0,76	1,76	1,23	1,53	1,43	1,33	1,59	2,45	2,25	6,12	3,08	7,12	4,97	6,15	5,75	5,37	6,41	9,88	9,09
Lu	0,31	0,24	0,40	0,24	0,33	0,39	0,34	0,29	0,31	0,37	8,20	6,37	10,55	6,20	8,56	10,19	8,97	7,56	8,15	9,78
Hf	11,56	10,79	9,31	12,92	13,03	9,99	12,68	12,14	10,25	14,44	64,58	60,26	52,01	72,17	72,82	55,79	70,83	67,82	57,26	80,67
Ta	<0.096	<0.111	<0.064	<0.083	<0.091	<0.085	<0.121	<0.114	<0.082	<0.078	0,00	0,00	0,00	0,00	0,00	0,00	0,00	0,00	0,00	0,00
Pb	29,32	14,26	36,00	12,32	7,38	9,73	7,29	5,07	8,17	7,28	8,03	3,91	9,86	3,37	2,02	2,67	2,00	1,39	2,24	1,99
Pb	29,39	13,22	33,76	11,75	7,63	9,54	6,49	5,31	7,16	5,74	8,05	3,62	9,25	3,22	2,09	2,61	1,78	1,45	1,96	1,57
Pb	28,65	13,72	33,94	12,40	7,94	10,03	7,12	5,09	8,29	6,66	7,85	3,76	9,30	3,40	2,18	2,75	1,95	1,39	2,27	1,82
Th	0,29	0,36	0,18	0,13	0,18	0,09	0,16	0,06	0,55	0,08	6,80	8,53	4,21	2,95	4,27	2,22	3,81	1,37	12,85	1,93
U	0,08	0,01	0,02	0,04	0,03	<0.06	<0.059	<0.059	0,10	0,01	6,59	1,01	1,34	3,27	2,37	0,00	0,00	0,00	8,38	0,50

LA-ICP-MS results obtained for clinopyroxene – Sample PB-181

Amphibole

LA-ICP-MS results obtained for amphibole – Sample PB-09

	LA-ICP-MS - Concentração de Elementos Traço (Ppm) - PB-09 (CSO)										LA-ICP-MS - Elementos Traço normalizado por Condrito - PB-09 (CSO)									
Element	anf69	anf70	anf71	anf72	anf78	anf79	anf80	anf81	Média	Mediana	anf69	anf70	anf71	anf72	anf78	anf79	anf80	anf81	Média	Mediana
Li	8,08	6,95	7,17	6,75	7,14	6,98	7,17	7,65	7,24	7,16	3,37	2,9	2,99	2,81	2,98	2,91	2,99	3,19	3,02	2,99
B	16,55	<15,74	<15,10	21,26	17,65	<15,10	<15,24	16,36	17,96	17,10	8,71	0	0	11,19	9,29	0	0	8,61	4,73	4,31
Na	12284	12731	13058	13055	13702	14257	13816	13876	13347	13380	1,7	1,76	1,8	1,8	1,89	1,97	1,91	1,92	1,84	1,85
Mg	74746	79825	77691	80488	77030	78316	75993	76407	77562	77360	0,523	0,558	0,543	0,563	0,539	0,548	0,531	0,534	0,54	0,54
Al	43913	45900	44788	45677	44478	44371	43774	44880	44723	44633	3,4	3,56	3,47	3,54	3,45	3,44	3,39	3,48	3,47	3,46
Si	191710	195578	191984	200626	203357	204358	203522	203865	199375	201991	1,198	1,222	1,2	1,254	1,27	1,28	1,27	1,27	1,25	1,26
P	57,3	70,31	64,3	69,3	57,45	87,26	94,63	86,73	73,41	69,81	0,0249	0,0306	0,028	0,0301	0,025	0,038	0,041	0,038	0,03	0,03
K	9429	11272	11572	11118	13220	12459	11571	11723	11545	11572	11,04	13,2	13,55	13,02	15,48	14,59	13,55	13,73	13,52	14
Ca	79046	79046	79046	79046	79046	79046	79046	79046	79046	79046	5,86	5,86	5,86	5,86	5,86	5,86	5,86	5,86	5,86	5,86
Sc	53,88	58,67	57,19	57,13	59,47	57,67	56,74	57,73	57,31	57,43	6,24	6,79	6,62	6,61	6,88	6,67	6,57	6,68	6,63	6,65
Ti	7070	6209	7663	7480	7913	7672	7334	7452	7349	7466	10,81	9,49	11,72	11,44	12,1	11,73	11,21	11,39	11,24	11,42
V	225,6	279,9	247,3	250,1	274,8	266,6	246,3	243,1	254,2	248,7	2,65	3,29	2,91	2,94	3,23	3,14	2,9	2,86	2,99	2,93
Cr	89,89	136,0	95,0	122,7	143,0	145,4	130,8	110,3	121,6	126,8	0,023	0,034	0,024	0,031	0,036	0,037	0,033	0,028	0,031	0,032
Mn	1230	1275	1324	1422	1430	1449	1373	1348	1356	1361	0,418	0,434	0,45	0,484	0,486	0,493	0,467	0,458	0,46	0,46
Fe	36870	39107	40157	41231	44937	44127	42035	42968	41429	41633	0,133	0,141	0,144	0,148	0,162	0,159	0,151	0,155	0,15	0,15
Co	55,12	56,76	58,46	55,44	63,5	63,36	59,86	63,71	59,53	59,16	0,072	0,074	0,077	0,073	0,083	0,083	0,078	0,083	0,078	0,077
Ni	103,9	109,1	110,8	104,6	121,2	117,3	113,6	119,5	112,5	112,2	0,006	0,007	0,007	0,006	0,007	0,007	0,007	0,007	0,007	0,007
Cu	1,22	1,04	0,99	1,39	1,57	1,42	1,21	1,69	1,32	1,31	0,007	0,006	0,006	0,008	0,009	0,008	0,007	0,010	0,008	0,008
Zn	249,1	257,6	262,7	261,8	258,3	249,9	243,6	264,1	255,9	257,9	0,539	0,558	0,569	0,567	0,559	0,541	0,527	0,572	0,554	0,559
Ga	25,26	25,27	27,55	25,85	26,41	26,28	24,81	27,6	26,13	26,07	1,66	1,66	1,81	1,7	1,74	1,73	1,63	1,82	1,72	1,72
Ge	19,42	20,41	21,43	20,56	19,41	22,63	20,43	21,17	20,68	20,50	0,402	0,423	0,444	0,426	0,402	0,469	0,423	0,438	0,43	0,42
As	<0,81	1,24	1,43	1,78	1,58	1,77	1,1	1,82	1,53	1,58	0	0,430	0,500	0,620	0,550	0,620	0,380	0,640	0,47	0,53
Rb	8,34	10,1	11,74	11,32	13,9	12,18	10,58	11,84	11,25	11,53	2,42	2,93	3,4	3,28	4,03	3,53	3,07	3,43	3,26	3,34
Sr	277,3	294,8	328,5	299,2	326,0	319,0	264,0	280,5	298,7	297,0	23,3	24,78	27,6	25,14	27,39	26,81	22,19	23,57	25,1	25,0
Y	63,22	75,11	73,59	73,22	73,15	71,41	68,26	68,52	70,81	72,28	28,1	33,38	32,71	32,54	32,51	31,74	30,34	30,45	31,47	32,13
Zr	136,0	196,5	160,9	174,1	170,1	163,3	170,9	173,5	168,2	170,5	24,56	35,47	29,04	31,42	30,7	29,48	30,85	31,32	30,4	30,8
Nb	16,7	18,51	18,44	19,03	19,92	18,66	19,04	19,05	18,67	18,85	44,52	49,35	49,18	50,75	53,11	49,77	50,76	50,81	49,78	50,26
Mo	<0,34	<0,29	<0,25	<0,32	<0,36	<0,45	<0,40	<0,40	-	-	0	0	0	0	0	0	0	0	-	-
Sn	4,73	4,61	3,62	4,32	13,01	18,51	30,18	20,59	12,45	8,87	1,88	1,83	1,43	1,72	5,16	7,34	11,98	8,17	4,94	3,52
Ba	206,7	249,5	256,7	242,9	265,1	251,4	236,8	243,1	244,0	246,3	60,62	73,18	75,28	71,23	77,73	73,71	69,44	71,27	71,6	72,2
La	72,76	76,02	75	75,39	76,56	76,38	72,15	78,01	75,28	75,71	198,3	207,1	204,4	205,4	208,6	208,1	196,6	212,6	205,1	206,3
Ce	238,1	256,2	257,2	252,4	258,7	256,0	241,2	256,1	252,0	256,1	248,8	267,7	268,7	263,7	270,3	267,5	252,1	267,6	263,3	267,6
Pr	37,72	41,98	42,35	40,62	42,1	41,99	38,88	40,83	40,81	41,41	275,3	306,4	309,1	296,5	307,3	306,5	283,8	298,0	297,9	302,2
Nd	187,7	222,4	223,6	205,4	213,0	212,0	193,5	201,5	207,4	208,7	264,0	312,8	314,5	288,9	299,6	298,1	272,1	283,4	291,7	293,5
Sm	43,3	50,14	48,04	47,55	47,11	46,52	42,21	44,96	46,23	46,82	187,5	217,1	208,0	205,9	204,0	201,4	182,7	194,7	200,1	202,7
Eu	8,94	7,95	7,21	8,1	6,63	7,10	8,18	7,82	7,74	7,89	102,8	91,41	82,85	93,12	76,17	81,66	93,99	89,87	88,98	90,64
Gd	29,10	32,53	33,39	31,99	33,35	31	30,71	31,18	31,66	31,59	95,1	106,3	109,1	104,6	109,0	101,3	100,3	101,9	103,5	103,2
Tb	3,39	3,94	4,1	3,86	3,9	3,74	3,61	3,76	3,79	3,81	58,42	67,87	70,68	66,48	67,23	64,51	62,26	64,88	65,29	65,68
Dy	15,99	18,53	17,32	17,88	17,38	17,82	16,48	16,99	17,30	17,35	41,97	48,63	45,45	46,93	45,62	46,77	43,25	44,59	45,40	45,54
Ho	2,60	3,00	2,92	3,07	2,86	2,81	2,83	2,87	2,87	2,87	30,5	35,21	34,36	36,09	33,55	32,99	33,28	33,73	33,71	33,64
Er	5,68	6,57	6,73	6,72	6,6	6,47	6,74	5,99	6,44	6,59	22,8	26,4	27,04	26,98	26,49	25,96	27,08	24,07	25,85	26,45
Tm	0,672	0,722	0,778	0,903	0,801	0,709	0,774	0,775	0,77	0,77	18,87	20,29	21,85	25,36	22,51	19,92	21,74	21,76	21,54	21,75
Yb	4,48	5,86	5,09	5,16	5,51	4,37	4,91	5,06	5,06	5,08	18,05	23,65	20,52	20,82	22,2	17,63	19,81	20,4	20,39	20,46
Lu	0,534	0,686	0,66	0,696	0,57	0,616	0,667	0,572	0,63	0,64	14,02	18	17,31	18,27	14,96	16,16	17,5	15,01	16,40	16,74
Hf	6,1	8,06	6,63	7	6,25	6,93	6,92	6,87	6,85	6,90	34,09	45,03	37,02	39,1	34,92	38,71	38,67	38,36	38,24	38,52
Ta	0,526	0,586	0,645	0,619	0,647	0,597	0,689	0,626	0,62	0,62	20,23	22,55	24,82	23,79	24,87	22,97	26,5	24,07	23,73	23,93
Pb	3,21	3,31	3,21	3	3,01	3,14	2,62	2,81	3,04	3,08	0,879	0,906	0,879	0,823	0,823	0,859	0,718	0,771	0,83	0,84
Th	0,289	0,405	0,553	0,408	0,509	0,503	0,345	0,38	0,42	0,41	6,81	9,52	13,01	9,59	11,97	11,83	8,11	8,94	9,97	9,56
U	0,047	0,053	0,044	0,04	0,052	0,034	0,047	0,047	0,05	0,05	3,84	4,35	3,64	3,24	4,29	2,8	3,82	3,84	3,73	3,83
Th	<-NaN	<-NaN	<-NaN	<-NaN	<-NaN	<-NaN	<-NaN	<-NaN	-	-	<-1,00	<-1,00	<-1,00	<-1,00	<-1,00	<-1,00	<-1,00	<-1,00	-	-

LA-ICP-MS - Concentração de Elementos Traço (Ppm) - PB-92B (LSO)							LA-ICP-MS - Elementos Traço normalizado por Condrito - PB-92B (L					
Element	**ANF-5c**	**ANF-5b**	**ANF-6c**	**ANF-6b**	**ANF-7c**	**ANF-7b**	**ANF-5c**	**ANF-5b**	**ANF-6c**	**ANF-6b**	**ANF-7c**	**ANF-7b**
Li	22,13	19,91	22,59	23,1	21,48	24,99	9,22	8,3	9,41	9,63	8,95	10,41
Be	11,65	13,27	9,97	11,19	10,31	10,8	291,17	331,69	249,13	279,76	257,8	270,08
B	3,66	3,32	4,1	5,05	4,88	2,82	1,93	1,75	2,16	2,66	2,57	1,48
Mg	81172,69	84209,74	77546,09	79423,06	82257,06	83253,8	0,57	0,59	0,54	0,56	0,58	0,58
Si	199586,84	216523,02	201235,94	208035,17	212019,92	208504,81	1,25	1,35	1,26	1,3	1,33	1,3
Si	192128,42	200377,64	186631,47	192865,58	198200,09	197113,28	1,2	1,25	1,17	1,21	1,24	1,23
P	<24.64	<23.27	36,22	41,77	<22.77	<25.21	0	0	0,016	0,018	0	0
Ca	79260,33	79260,33	79260,33	79260,34	79260,33	79260,33	5,87	5,87	5,87	5,87	5,87	5,87
Sc	32,84	36,71	34,8	33,68	34,88	39,41	3,8	4,25	4,03	3,9	4,04	4,56
Ti	6800,38	6738,51	6652,3	6530,09	6149,78	7162,51	10,4	10,3	10,17	9,98	9,4	10,95
V	151,06	170,93	154,32	149,46	180,76	202,22	1,78	2,01	1,82	1,76	2,13	2,38
Cr	76,7	83,57	87,76	81,45	69,67	128,5	0,0193	0,021	0,0221	0,0205	0,0175	0,0323
Mn	1950,65	1945,9	2027,47	2038,5	2059,57	2057,93	0,663	0,662	0,69	0,693	0,701	0,7
Co	64,74	64,01	63,14	65,53	69,35	66,54	0,0847	0,0838	0,0826	0,0858	0,0908	0,0871
Ni	156,53	152,18	147,81	160,04	156,82	161,54	0,00949	0,00922	0,00896	0,0097	0,0095	0,00979
Cu	2,13	0,91	1,92	3,75	2,48	3,64	0,0127	0,0054	0,0114	0,0223	0,0147	0,0217
Zn	434,26	439,99	409,05	477,23	437,89	481,68	0,94	0,952	0,885	1,033	0,948	1,043
Ga	19,06	19,69	18,56	21,08	21,49	22,19	1,254	1,295	1,221	1,39	1,41	1,46
Rb	8,48	9,8	8,97	9,23	9,43	9,86	2,46	2,84	2,6	2,68	2,73	2,86
Sr	155,47	161,72	151,12	156,88	147,68	159,32	13,06	13,59	12,7	13,18	12,41	13,39
Y	48,74	43,36	41,29	44,96	33,05	36,16	21,66	19,27	18,35	19,98	14,69	16,07
Zr	55,83	53,79	50,99	50,41	52,93	51,6	10,08	9,71	9,2	9,1	9,55	9,31
Nb	20,81	20,26	18,42	20,95	16,75	17,17	55,49	54,02	49,13	55,85	44,67	45,78
Mo	<0.62	<0.57	<0.58	<0.65	<0.83	<0.56	0	0	0	0	0	0
Sn	5,21	4,88	4,98	4,66	4,49	5,38	2,07	1,94	1,98	1,85	1,78	2,14
Sb	<0.64	<0.67	<0.53	<0.55	<0.58	<0.74	0	0	0	0	0	0
Cs	<0.140	<0.126	<0.144	<0.161	<0.128	<0.117	0	0	0	0	0	0
Ba	58,45	64,22	61,38	66,6	62,93	67,68	17,14	18,83	18	19,53	18,46	19,85
La	59,11	61,21	56,02	60,91	52,73	58,1	161,07	166,77	152,64	165,97	143,67	158,31
Ce	193,47	183,99	173,72	193,1	151,68	166,11	202,17	192,26	181,53	201,78	158,49	173,57
Pr	30,83	29,28	28,04	30,12	22,87	25,2	225,01	213,7	204,69	219,88	166,9	183,92
Nd	155,02	134,81	139,83	150,34	113,71	113,81	218,02	189,6	196,67	211,45	159,93	160,07
Sm	33,86	31,29	30,65	31,03	21,36	23,28	146,56	135,44	132,67	134,32	92,46	100,76
Eu	7,06	6,98	6,2	5,82	5,06	5,41	81,19	80,22	71,27	66,86	58,15	62,24
Gd	21,23	18,68	18,85	22,72	12,74	16	69,38	61,03	61,61	74,25	41,63	52,29
Tb	2,66	2,28	2,31	2,38	1,82	1,6	45,78	39,22	39,76	41,06	31,39	27,5
Dy	13,75	10,61	11,26	12,94	9,08	10,05	36,09	27,84	29,56	33,96	23,84	26,38
Ho	1,86	1,76	1,8	2,07	1,57	1,31	21,85	20,71	21,12	24,32	18,42	15,42
Er	4,18	3,94	3,84	4,83	3,15	3,39	16,8	15,81	15,41	19,41	12,67	13,61
Tm	0,55	0,373	0,71	0,65	0,55	0,39	15,54	10,49	20,07	18,18	15,51	10,96
Yb	4,06	3,38	3,62	4,03	3,03	3,3	16,35	13,61	14,59	16,25	12,21	13,31
Lu	0,44	0,422	0,59	0,7	0,49	0,48	11,61	11,08	15,56	18,35	12,74	12,59
Hf	3,45	3,52	4,08	5,16	3,17	3,31	19,29	19,64	22,77	28,8	17,7	18,51
Ta	0,52	0,47	0,551	0,63	0,49	0,56	20,04	18,08	21,19	24,27	18,88	21,53
Pb	1,87	2,16	2,36	2,04	1,72	2,16	0,51	0,59	0,65	0,56	0,47	0,59
Pb	1,92	2,22	1,95	2,74	2,57	1,58	0,52	0,61	0,53	0,75	0,7	0,43
Pb	2,22	1,81	2,53	2,07	2,26	2,54	0,61	0,496	0,69	0,57	0,62	0,7
Th	0,141	0,166	0,142	0,137	0,218	0,134	3,32	3,9	3,35	3,23	5,12	3,16
U	<0.073	<0.00	<0.00	0,053	0,06	0,013	0	0	0	4,36	4,95	1,07

LA-ICP-MS results obtained for amphibole – Sample PB-92B

LA-ICP-MS - Concentração de Elementos Traço (Ppm) - PB-181 (LSS).																	
Element	**ANF-1-px1**	**ANF-1b-px**	**ANF-2-px2**	**ANF-2b-px**	**ANF-3-px3**	**ANF-3b-px**	**ANF-4-px4**	**ANF-4b-px**	**anf69**	**anf70**	**anf71**	**anf72**	**anf73**	**anf74**	**anf75**	**Média**	**Mediana**
Li	17,05	14,11	16,02	13,33	17,5	17,46	15,74	12,38	19,20	21,54	15,27	20,75	15,86	15,36	14,03	16,37	15,86
Be	12,09	15,56	17,68	16,29	15,68	14,54	13,57	14,25	-	-	-	-	-	-	-	14,96	15,05
B	10,38	12,28	9,56	9,1	8,89	10,35	9,72	12,41	16,90	15,12	13,25	14,61	13,82	15,80	12,32	12,30	12,32
Na	-	-	-	-	-	-	-	-	25684	26511	25212	27140	26892	25573	24228	25891	25684
Mg	84413	86711	80828	79406	79828	86815	84149	84303	87600	92053	87567	92838	92418	86550	87220	86180	86711
Al	-	-	-	-	-	-	-	-	29887	31416	30502	29321	32691	29817	30359	30570	30359
Si	212886	220250	210572	205760	203004	227233	216558	219095	205085	219006	212443	220877	222716	205764	201488	213516	212886
Si	220287	221165	207628	209320	204447	223738	212977	222129	-	-	-	-	-	-	-	215211	216632
P	21,25	<14.82	29,98	23,93	<15.25	20,69	28,62	<14.16	43,1	<25,43	37,88	32,75	54,49	41,72	41,3	34,16	32,75
K	-	-	-	-	-	-	-	-	11312	12257	12099	11620	12204	12078	11781	11907	12078
Ca	66937	66937	66937	66937	66937	66937	66937	66937	64395	64395	64395	64395	64395	64395	64395	65750	66937
Sc	24,56	24,71	23,65	22,68	22,53	22,95	22,52	25,44	30,39	31,15	29,02	31,74	30,72	29,81	30,67	26,84	25,44
Ti	4684	4140	7936	7505	8019	6590	5229	3849	3087	3528	3284	2456	3574	4616	4783	4885	4616
V	161,5	165,6	173,8	171,1	170,3	148,7	157,9	164,5	153,9	142,15	152,32	171,89	151,67	151,27	153,61	159,4	157,9
Cr	78,54	70,57	83,09	80,18	81,21	77,98	81,35	94,92	71,35	77,29	79,58	76,99	81,19	76,85	86,4	79,83	79,58
Mn	2491	2516	2531	2545	2495	2655	2497	2746	2430	2409	2334	2627	2541	2321	2369	2501	2497
Fe	-	-	-	-	-	-	-	-	43650	43464	42411	46323	46972	40511	40184	43359	43464
Co	69,59	71,17	71,86	70,76	68,54	72,79	68,21	68,82	66,82	70,64	65,55	69,27	69,9	68,16	67,18	69,28	69,27
Ni	145,2	148,8	145,8	152,2	141,4	153,5	137,4	137,7	139,9	142,5	131,3	136,6	139,3	137,8	142,4	142,1	141,4
Cu	2,58	8,57	1,38	2,56	1,95	1,65	1,48	2,14	1,33	6,05	1,38	3,41	9,72	9,05	1,1	3,62	2,14
Zn	566,8	548,7	546,5	597,1	534,6	606,8	564,5	547,5	510,7	536,5	495,8	552,7	571,9	548,7	557,4	552,4	548,7
Ga	16	16,29	16,65	17,01	15,31	17,87	16,82	14,2	19,33	19,57	19,24	18,11	21,53	18,7	21,2	17,86	17,87
Ge	-	-	-	-	-	-	-	-	13,5	12,73	12,61	13,98	14,02	13,04	13,97	13,41	13,5
As	-	-	-	-	-	-	-	-	<1.07	<1.16	<0.86	0,96	<1.15	<0.62	<0.72	0,96	0,96
Rb	13,99	13,7	14,57	15,29	13,44	14,91	15,41	11,44	14,28	13,84	14,22	14,23	15,86	14,8	14,53	14,30	14,28
Sr	650,1	641,3	771,9	795,4	739,1	743,0	766,2	571,1	569,0	590,2	690,8	611,2	666,2	696,8	698,4	680,0	690,8
Y	4,68	3,49	6,92	6,96	6,37	7,76	7,77	4,75	5,01	6,02	7,19	4,51	6,45	10,64	9,83	6,56	6,45
Zr	216,1	139,3	276,9	287,9	276,0	347,3	307,8	141,3	342,5	343,3	340,9	309,9	358,6	299,2	344,0	288,7	307,8
Nb	4,92	4,92	9,46	10,16	8,15	6,76	7,59	2,42	5,42	7,82	7,41	3,76	6,78	7,81	6,87	6,68	6,87
Mo	<0.57	<0.45	0,381	<0.65	<0.47	<0.46	<0.55	<0.48	<0.47	<0.40	<0.34	<0.25	<0.35	<0.33	0,202	0,292	0,292
Sn	2,37	2,68	2,89	2,48	3,15	2,75	2,27	2,19	2,34	2,56	2	2,19	2,22	1,96	2,51	2,44	2,37
Sb	<0.41	<0.49	<0.40	<0.41	<0.47	<0.54	<0.46	<0.39	-	-	-	-	-	-	-	-	-
Cs	<0.089	<0.102	<0.075	<0.087	<0.098	<0.107	<0.065	<0.066	-	-	-	-	-	-	-	-	-
Ba	159,4	170,8	214,2	220,8	216,1	173,9	186,2	125,1	184,8	168,8	167,6	153,7	194,1	169,5	175,3	178,7	173,9
La	15,33	16,09	20,85	20,27	19,92	19,35	20,66	15,24	16,15	15,64	18,57	15,2	16,75	21,99	18,88	18,06	18,57
Ce	38,13	38,95	55	56,62	55,24	54,69	51,9	37,41	39,27	41,08	48,01	38,62	41,43	57,99	58,3	47,51	48,01
Pr	4,79	5,02	7,84	8,00	7,22	7,56	7,20	5,33	5,02	5,6	6,31	4,71	5,98	8,24	8,36	6,48	6,31
Nd	20,38	21,85	39,26	37,16	34,38	32,43	32,23	22,34	20,14	23,19	29,45	19,89	27,29	37,06	39,52	29,10	29,45
Sm	3,85	3,03	6,08	7,78	5,54	7,15	6,32	4,77	3,29	4,45	6,41	3,53	4,42	7,97	7,67	5,48	5,54
Eu	0,730	0,870	1,40	1,81	1,41	1,23	1,61	1,04	0,84	1,02	1,25	0,97	1,06	1,88	1,92	1,27	1,23
Gd	2,43	1,38	4,25	4,51	4,1	4,25	3,54	2,16	2,59	2,94	3,5	2,16	3,59	4,98	4,88	3,42	3,54
Tb	0,205	0,237	0,398	0,391	0,414	0,539	0,343	0,396	0,265	0,299	0,421	0,255	0,386	0,572	0,613	0,38	0,391
Dy	1,10	0,97	1,69	1,61	1,41	<1.13	1,28	1,07	1,33	1,63	1,72	0,88	1,36	2,36	2,4	1,49	1,385
Ho	0,141	<0.146	0,243	0,233	0,199	<0.165	0,338	0,215	0,24	0,227	0,257	0,173	0,315	0,389	0,329	0,25	0,24
Er	0,390	0,520	0,740	0,54	0,56	<0.46	0,91	0,29	0,264	0,528	0,722	0,476	0,646	0,825	0,77	0,58	0,55
Tm	<0.103	<0.130	0,114	0,131	0,125	<0.185	0,14	<0.142	0,055	0,058	0,076	0,056	0,076	0,149	0,112	0,10	0,112
Yb	<0.52	0,56	1,08	0,63	0,64	1,46	<0.61	<0.57	0,51	0,65	0,6	0,55	0,9	1,08	1,21	0,82	0,645
Lu	<0.156	<0.113	0,15	<0.112	<0.117	0,199	<0.135	0,179	0,115	0,114	0,179	0,102	0,169	0,24	0,168	0,16	0,1685
Hf	7,08	6,85	8,73	8,38	7,31	9,62	9,02	4,56	9,36	9,65	9,95	10,38	10,84	7,6	10,14	8,63	9,02
Ta	<0.125	<0.098	0,42	0,306	0,149	0,17	0,205	<0.092	0,194	0,265	0,183	0,073	0,16	0,238	0,129	0,21	0,1885
Pb	3,81	6,08	6,02	6,73	7,33	5,03	6,01	5,24	8,13	7,76	6,25	5,95	7,81	10,82	8,23	6,75	6,25
Pb	4,61	6,87	5,85	5,84	7,31	5,35	4,97	5,28	-	-	-	-	-	-	-	5,76	5,595
Pb	4,20	6,71	6,64	6,83	7,60	5,56	5,75	4,70	-	-	-	-	-	-	-	6,00	6,195
Th	<0.00	0,0066	0,034	0,0117	0,0125	0,035	<0.060	0,014	0,007	<0.0156	0,019	0,027	0,025	0,104	0,008	0,025	0,016
U	<0.00	<0.00	<0.00	0,0056	0,006	0,0084	0,060	<0.051	0,003	<0,00	<0,00	0,003	<0,00	0,005	<0,00	0,013	0,006

LA-ICP-MS results obtained for amphibole – Sample PB-181

LA-ICP-MS - Elementos Traço normalizado por Condrito - PB-181 (LSS)																	
Element	ANF-1-px1	ANF-1b-px	ANF-2-px2	ANF-2b-px	ANF-3-px3	ANF-3b-px	ANF-4-px4	ANF-4b-px	anf69	anf70	anf71	anf72	anf73	anf74	anf75	Média	Mediana
Li	7,11	5,88	6,67	5,55	7,29	7,28	6,56	5,16	8,90	7,96	6,97	7,69	7,27	8,31	6,48	7,01	7,11
Be	302,22	388,96	442,08	407,34	391,92	363,38	339,3	356,36	-	-	-	-	-	-	-	373,9	376,2
B	5,46	6,47	5,03	4,79	4,68	5,45	5,12	6,53	3,54	3,66	3,48	3,75	3,71	3,53	3,34	4,57	4,68
Na		-	-	-	-	-	-	-	0,61	0,64	0,61	0,65	0,65	0,61	0,61	0,626	0,613
Mg	0,59	0,606	0,565	0,555	0,558	0,607	0,588	0,59	2,32	2,44	2,36	2,27	2,53	2,31	2,35	1,42	0,61
Al		-	-	-	-	-	-	-	1,28	1,37	1,33	1,38	1,39	1,29	1,26	1,33	1,33
Si	1,33	1,38	1,32	1,29	1,27	1,42	1,35	1,37	0,02	0,00	0,02	0,01	0,02	0,02	0,02	0,723	1,27
Si	1,38	1,38	1,3	1,31	1,28	1,4	1,33	1,39	-	-	-	-	-	-	-	1,35	1,36
P	0,0092	0	0,013	0,0104	0	0,009	0,0124	0	13,25	14,35	14,17	13,61	14,29	14,14	13,79	6,51	0,013
K		-	-	-	-	-	-	-	4,77	4,77	4,77	4,77	4,77	4,77	4,77	4,77	4,77
Ca	4,96	4,96	4,96	4,96	4,96	4,96	4,96	4,96	3,52	3,60	3,36	3,67	3,56	3,45	3,55	4,29	4,96
Sc	2,84	2,86	2,74	2,62	2,61	2,66	2,61	2,94	4,72	5,39	5,02	3,76	5,46	7,06	7,31	4,04	2,94
Ti	7,16	6,33	12,13	11,48	12,26	10,08	8	5,89	1,81	1,67	1,79	2,02	1,78	1,78	1,81	5,73	5,89
V	1,9	1,95	2,05	2,01	2	1,75	1,86	1,94	0,02	0,02	0,02	0,02	0,02	0,02	0,02	1,04	1,75
Cr	0,0198	0,0178	0,0209	0,0202	0,0204	0,0196	0,0205	0,0239	0,83	0,82	0,79	0,89	0,86	0,79	0,81	0,40	0,0239
Mn	0,847	0,856	0,861	0,866	0,849	0,903	0,849	0,934	0,16	0,16	0,15	0,17	0,17	0,15	0,14	0,537	0,847
Fe		-	-	-	-	-	-	-	0,09	0,09	0,09	0,09	0,09	0,09	0,09	0,089	0,089
Co	0,0911	0,0932	0,0941	0,0926	0,0897	0,0953	0,0893	0,0901	0,01	0,01	0,01	0,01	0,01	0,01	0,01	0,05	0,0893
Ni	0,0088	0,00902	0,00883	0,00923	0,00857	0,0093	0,00833	0,00834	0,01	0,04	0,01	0,02	0,06	0,05	0,01	0,017	0,009
Cu	0,0153	0,051	0,0082	0,0152	0,0116	0,0098	0,0088	0,0127	1,11	1,16	1,07	1,20	1,24	1,19	1,21	0,55	0,051
Zn	1,227	1,188	1,183	1,292	1,157	1,313	1,222	1,185	1,27	1,29	1,27	1,19	1,42	1,23	1,40	1,3	1,2
Ga	1,052	1,072	1,096	1,119	1,007	1,18	1,107	0,934	0,28	0,26	0,26	0,29	0,29	0,27	0,29	0,70	0,934
Ge		-	-	-	-	-	-	-	0,00	0,00	0,00	0,34	0,00	0,00	0,00	0,049	0,000
As		-	-	-	-	-	-	-	4,14	4,01	4,12	4,13	4,60	4,29	4,21	4,21	4,14
Rb	4,05	3,97	4,22	4,43	3,89	4,32	4,47	3,31	47,81	49,60	58,05	51,36	55,98	58,55	58,69	27,51	4,47
Sr	54,63	53,89	64,86	66,84	62,11	62,44	64,39	47,99	2,23	2,68	3,20	2,00	2,87	4,73	4,37	33,3	47,99
Y	2,08	1,553	3,08	3,09	2,83	3,45	3,46	2,11	61,82	61,96	61,53	55,94	64,74	54,00	62,08	29,58	3,46
Zr	39,01	25,15	49,98	51,97	49,82	62,7	55,56	25,51	14,45	20,86	19,75	10,03	18,08	20,81	18,31	32,1	25,2
Nb	13,13	13,12	25,23	27,1	21,72	18,01	20,25	6,45	0,00	0,00	0,00	0,00	0,00	0,00	0,15	9,68	6,45
Mo	0	0	0,276	0	0	0	0	0	0,93	1,02	0,79	0,87	0,88	0,78	1,00	0,437	0,28
Sn	0,94	1,06	1,14	0,99	1,25	1,09	0,9	0,87	54,20	49,49	49,14	45,07	56,92	49,70	51,41	24,28	1,25
Sb	0	0	0	0	0	0	0	0	-	-	-	-	-	-	-	-	-
Cs	0	0	0	0	0	0	0	0	-	-	-	-	-	-	-	-	-
Ba	46,74	50,07	62,8	64,74	63,37	50,99	54,59	36,69	54.20	49.49	49.14	45.07	56.92	49.70	51.41	53,75	52,79
La	**41,78**	**43,83**	**56,81**	**55,22**	**54,28**	**52,74**	**56,28**	**41,53**	**44**	**42,6**	**50,6**	**41,41**	**45,64**	**59,91**	**51,45**	**49,21**	**50,6**
Ce	**39,84**	**40,7**	**57,47**	**59,16**	**57,72**	**57,14**	**54,24**	**39,09**	**41,04**	**42,92**	**50,17**	**40,36**	**43,29**	**60,59**	**60,92**	**49,64**	**50,17**
Pr	**34,97**	**36,66**	**57,26**	**58,43**	**52,69**	**55,16**	**52,54**	**38,91**	**36,65**	**40,86**	**46,04**	**34,36**	**43,69**	**60,18**	**60,99**	**47,29**	**46,04**
Nd	**28,66**	**30,73**	**55,21**	**52,27**	**48,35**	**45,61**	**45,32**	**31,42**	**28,32**	**32,62**	**41,43**	**27,97**	**38,38**	**52,12**	**55,58**	**40,93**	**41,43**
Sm	**16,68**	**13,1**	**26,32**	**33,67**	**23,99**	**30,93**	**27,34**	**20,66**	**14,25**	**19,28**	**27,76**	**15,3**	**19,15**	**34,49**	**33,19**	**23,74**	**23,99**
Eu	**8,39**	**10,03**	**16,07**	**20,86**	**16,25**	**14,17**	**18,49**	**11,92**	**9,61**	**11,72**	**14,39**	**11,17**	**12,24**	**21,55**	**22,08**	**14,60**	**14,17**
Gd	**7,94**	**4,5**	**13,89**	**14,74**	**13,41**	**13,89**	**11,58**	**7,05**	**8,46**	**9,62**	**11,45**	**7,05**	**11,72**	**16,29**	**15,95**	**11,17**	**11,58**
Tb	**3,53**	**4,08**	**6,86**	**6,75**	**7,14**	**9,3**	**5,91**	**6,82**	**4,57**	**5,16**	**7,26**	**4,4**	**6,66**	**9,86**	**10,58**	**6,59**	**6,75**
Dy	**2,88**	**2,55**	**4,43**	**4,23**	**3,69**	0	**3,36**	**2,81**	**3,48**	**4,28**	**4,52**	**2,3**	**3,56**	**6,19**	**6,3**	**3,64**	**3,56**
Ho	**1,65**	0	**2,86**	**2,74**	**2,34**	0	**3,97**	**2,53**	**2,82**	**2,67**	**3,02**	**2,03**	**3,7**	**4,57**	**3,87**	**2,58**	**2,74**
Er	**1,57**	**2,11**	**2,96**	**2,15**	**2,23**	0	**3,67**	**1,16**	**1,06**	**2,12**	**2,9**	**1,91**	**2,59**	**3,31**	**3,09**	**2,19**	**2,15**
Tm	0	0	**3,2**	**3,69**	**3,52**	0	**3,94**	0	**1,55**	**1,63**	**2,12**	**1,57**	**2,12**	**4,19**	**3,14**	**2,04**	**2,12**
Yb	0	**2,26**	**4,34**	**2,54**	**2,6**	**5,87**	0	0	**2,06**	**2,61**	**2,42**	**2,21**	**3,64**	**4,37**	**4,89**	**2,65**	**2,54**
Lu	0	0	**3,93**	0	0	**5,22**	0	**4,7**	**3,01**	**3,00**	**4,69**	**2,67**	**4,44**	**6,29**	**4,4**	**2,82**	**3,01**
Hf	39,57	38,27	48,75	46,82	40,85	53,73	50,39	25,49	52.31	53.91	55.60	57.99	60.55	42.48	56.67	42,98	43,84
Ta	0	0	16,15	11,78	5,72	6,54	7,9	0	7.46	10.20	7.05	2.81	6.14	9.15	4.96	6,01	6,13
Pb	1,04	1,67	1,65	1,84	2,01	1,38	1,65	1,44	2.23	2.13	1.71	1.63	2.14	2.96	2.25	1,59	1,65
Pb	1,26	1,88	1,6	1,6	2	1,47	1,36	1,45	-	-	-	-	-	-	-	1,58	1,54
Pb	1,15	1,84	1,82	1,87	2,08	1,52	1,58	1,29	-	-	-	-	-	-	-	1,64	1,70
Th	0	0,16	0,8	0,28	0,29	0,83	0	0,32	0,16	0,00	0,45	0,63	0,60	2,45	0,19	0,477	0,290
U	0	0	0	0,46	0,49	0,69	4,89	0	0,28	0,00	0,00	0,27	0,00	0,44	0,00	0,501	0,000
Th		-	-	-	-	-	-	-	<-1.00	<-1.00	<-1.00	<-1.00	<-1.00	<-1.00	<-1.00	-	-

LA-ICP-MS results obtained for amphibole – Sample PB-181 - Continuation

Apatite

LA-ICP-MS - Concentração de Elementos Traço (Ppm) - PB-09 (CSI).

Element	AP01a	AP01b	AP01c	AP01d	AP02a_spot	AP02b_spot	AP03a	AP03b	AP03c	AP04a	AP04b	AP04c	AP04d	AP05a	AP05b	AP05c	AP05d	AP06a	AP06b	AP06c	AP07a	AP07b	AP07c
Li	-	-	-	-	-	-	-	-	-	-	-	-	-	-	-	-	-	-	-	-	-	-	-
B	0,97	1,03	1,17	0,63	0,94	1,79	1,24	1,60	1,85	1,73	0,74	2,56	1,48	1,83	1,06	1,89	1,64	1,04	1,05	0,84	1,62	1,43	2,16
Na	-	-	-	-	-	-	-	-	-	-	-	-	-	-	-	-	-	-	-	-	-	-	-
Mg	146,9	178,8	204,1	123,0	218,3	1195	418,9	969,9	348,7	321,4	227,0	509,0	263,8	648,6	467,4	1018	1161	286,2	477,6	465,8	874,6	576,3	868,5
Al	-	-	-	-	-	-	-	-	-	-	-	-	-	-	-	-	-	-	-	-	-	-	-
Si	2397	2449	2465	2433	2166	3997	3561	4396	3222	2296	2088	2970	2156	3811	3489	4615	5507	2248	2763	2891	4123	3507	4418
P	213195	211882	207145	214019	264977	238877	217617	205827	227518	241106	227716	235374	227146	205698	201251	202856	211024	243726	251644	232885	223251	200404	214515
K	-	-	-	-	-	-	-	-	-	-	-	-	-	-	-	-	-	-	-	-	-	-	-
Ca	393085	393085	393086	393086	393086	393086	393086	393086	393086	393086	393086	393086	393086	393086	393086	393086	393086	393086	393086	393086	393086	393086	393086
Cs	0,22	0,21	0,22	0,19	0,12	0,16	0,16	0,16	0,21	0,21	0,18	0,19	0,22	0,20	0,16	0,16	0,24	0,13	0,12	0,20	0,25	0,25	0,29
Sc	-	-	-	-	-	-	-	-	-	-	-	-	-	-	-	-	-	-	-	-	-	-	-
Ti	813,1	807,6	808,2	794,3	882,1	857,5	783,4	747,7	812,8	812,8	795,6	816,4	809,5	787,2	794,4	770,6	782,9	779,0	789,0	791,8	793,8	776,7	785,4
V	18,53	18,00	16,37	17,08	14,23	17,94	17,30	17,30	16,17	19,05	17,90	21,39	18,19	17,43	18,99	19,47	14,64	11,67	10,94	9,84	17,30	17,30	17,02
Cr	-	-	-	-	-	-	-	-	-	-	-	-	-	-	-	-	-	-	-	-	-	-	-
Mn	421,9	406,6	433,8	406,4	341,4	368,3	323,6	291,4	321,7	430,2	404,5	439,2	421,2	407	411,53	388	418,84	393,6	388,4	384,6	415,4	412,4	420,2
Fe	633,1	666,6	726,2	566,5	690,1	1852	886,8	1464	678,5	1004,0	665,3	1070	737,0	1117,3	1081	1584	1881	729,5	984,4	1045	1283	1085	1439
Co	-	-	-	-	-	-	-	-	-	-	-	-	-	-	-	-	-	-	-	-	-	-	-
Ni	-	-	-	-	-	-	-	-	-	-	-	-	-	-	-	-	-	-	-	-	-	-	-
Cu	-	-	-	-	-	-	-	-	-	-	-	-	-	-	-	-	-	-	-	-	-	-	-
Zn	-	-	-	-	-	-	-	-	-	-	-	-	-	-	-	-	-	-	-	-	-	-	-
Ga	0,25	0,28	0,24	0,24	0,20	0,47	0,33	0,43	0,29	0,22	0,21	0,32	0,22	0,31	0,33	0,43	0,67	0,31	0,30	0,34	0,37	0,41	0,46
Ge	324,4	344,5	330,3	340,7	271,9	281,7	376,7	373,9	373,4	286,1	280,7	346,1	278,3	378,1	366,1	380,7	391,6	369,0	363,5	365,0	402,0	375,9	388,5
As	18,48	17,65	17,80	17,05	16,48	15,17	20,06	20,07	19,08	14,83	15,32	18,58	15,63	20,21	19,91	20,49	20,47	15,50	15,04	15,77	20,07	18,90	19,55
Rb	<0,023	0,03	0,04	<0,024	0,04	0,19	0,07	0,15	0,06	0,03	<0,025	0,03	<0,030	0,07	0,05	0,12	0,29	0,06	0,11	0,09	0,05	0,10	0,09
Sr	1697	1729	1618	1666	1834	1599	1292	1321	1422	1604	1525	1634	1614	1562	1517	1498	1384	1488	1516	1485	1611	1438	1461
Y	396,0	428,1	404,6	405,6	329,8	325,0	440,0	446,1	437,7	310,7	324,6	370	316,95	479,9	452,0	466,0	505,7	309,2	327,1	365,7	486,5	447,3	476,6
Zr	2,74	3,36	3,39	2,83	3,36	3,12	6,56	6,34	5,80	2,54	2,93	3,91	2,82	8,21	7,18	7,72	8,87	4,94	5,28	5,96	4,09	3,78	3,45
Nb	<0,0095	0,01	0,01	0,01	0,01	0,02	0,02	0,02	0,02	0,01	0,01	0,02	0,01	<0,0107	0,03	0,02	0,02	0,02	0,02	0,01	0,02	0,02	0,02
Mo	-	-	-	-	-	-	-	-	-	-	-	-	-	-	-	-	-	-	-	-	-	-	-
Sn	-	-	-	-	-	-	-	-	-	-	-	-	-	-	-	-	-	-	-	-	-	-	-
Ba	0,30	0,41	0,34	0,36	0,29	0,50	0,24	0,43	0,42	0,30	0,42	0,28	0,38	0,35	0,45	0,64	2,17	0,17	0,40	0,34	0,57	0,43	0,64
La	2374	2514	2380	2449	3287	2628	2786	2826	2705	1953	2030	2294	1976	2803	2751	2758	2892	2254	2292	2474	2937	2687	2848
Ce	5831	6328	6013	6058	7689	6385	6714	6638	6463	4820	5076	5897	5055	6660	6745	6597	7041	6506	6525	6592	7232	7000	7015
Pr	675,4	713,2	690,1	676,7	613,3	650,8	752,5	753,3	728,6	550,6	573,3	657,4	554,7	754,2	744,6	757,6	802,1	670,7	687,4	708,8	813,0	743,3	779,3
Nd	2636	2763	2625	2640	2186	2170	2856	2992	2900	2098	2246	2599	2125	3104	3028	3057	3325	2380	2483	2656	3224	2940	3111
Sm	397,5	416,8	398,1	398,6	329,0	315,7	427,9	448,7	434,5	321,8	337,7	394,1	320,7	482,9	460,1	467,7	499,2	348,1	361,3	395,4	498,9	451,1	480,9
Eu	65,61	70,11	65,74	68,21	56,18	55,71	78,58	81,22	77,94	56,72	58,84	69,23	55,98	81,03	78,05	79,39	85,33	66,97	69,07	71,53	83,53	78,18	81,50
Gd	239,7	251,7	238,6	236,8	193,7	182,9	255,1	265,2	251,0	188,4	202,8	227,5	188,7	287,1	274,2	278,1	297,6	200,4	208,5	226,2	286,5	264,3	278,7
Gd ©	**227,0**	**238,00**	**226**	**224,0**	**177,0**	**169,0**	**241,0**	**251,0**	**237,0**	**178,0**	**192,0**	**215,0**	**178,0**	**273,0**	**260,0**	**264,0**	**283,0**	**187,0**	**195,0**	**212,0**	**271,0**	**250,0**	**264,0**
Tb	23,90	24,82	23,70	24,01	19,53	18,69	24,75	27,02	25,00	18,44	19,68	22,36	18,85	28,43	27,36	27,78	29,88	19,30	20,51	22,57	28,53	26,61	27,89
Tb ©	**23,90**	**24,80**	**23,70**	**24,00**	**19,50**	**18,70**	**24,80**	**27,00**	**25,00**	**18,40**	**19,70**	**22,40**	**18,90**	**28,40**	**27,40**	**27,80**	**29,90**	**19,30**	**20,50**	**22,60**	**28,50**	**26,60**	**27,90**
Dy	96,50	102,24	97,12	98,01	81,43	76,33	103,05	108,75	101,36	74,80	79,42	91,02	77,67	114,39	110,61	114,84	122,86	78,26	82,75	92,33	118,74	110,56	113,79
Ho	15,06	15,79	15,29	15,42	12,31	11,58	16,19	17,08	15,80	11,90	12,16	14,39	11,99	18,25	17,45	17,66	19,30	12,23	13,11	14,39	18,10	17,28	17,79
Er	33,56	35,52	33,77	34,25	27,13	25,47	35,25	37,68	34,45	25,40	26,82	30,74	26,10	39,96	37,53	38,58	41,10	25,82	27,05	30,96	39,24	36,60	38,79
Tm	3,83	4,08	3,84	3,80	3,08	2,87	4,02	4,18	4,06	2,83	3,02	3,32	2,91	4,42	4,36	4,48	4,65	2,91	2,92	3,38	4,61	4,09	4,44
Yb	22,08	23,57	22,66	22,26	17,88	16,46	24,37	25,34	23,83	15,77	16,97	20,46	16,32	25,57	24,67	25,61	27,22	17,64	18,04	20,49	26,99	23,48	25,49
Lu	2,97	3,01	2,85	2,89	2,17	2,12	3,19	3,34	3,04	2,11	2,15	2,54	2,08	3,19	3,10	3,21	3,53	2,17	2,38	2,56	3,32	3,07	3,11
Hf	0,39	0,35	0,25	0,34	0,28	0,27	0,35	0,33	0,38	0,13	0,25	0,24	0,24	0,51	0,32	0,35	0,41	0,22	0,16	0,29	0,38	0,33	0,42
Ta	0,03	0,03	0,02	0,03	0,01	0,02	0,02	0,02	0,02	0,02	0,01	0,02	0,02	0,04	0,02	0,02	0,03	0,02	0,02	0,02	0,03	0,01	0,03
Pb	5,98	6,27	5,56	5,89	5,47	4,45	6,22	6,22	6,12	5,78	4,99	6,14	5,39	7,59	7,13	7,60	6,85	6,67	6,53	6,30	7,48	6,06	6,47
Th	35,11	39,41	36,34	35,07	36,76	31,10	64,43	69,86	58,19	26,45	28,94	39,64	26,63	65,27	61,23	67,18	73,40	34,94	38,88	43,56	53,49	47,81	52,08
U	5,22	5,97	5,65	5,19	4,99	4,67	9,56	9,76	8,34	4,29	4,63	5,80	4,35	8,35	8,27	8,80	9,30	5,59	6,01	6,56	7,96	7,03	7,96
Th	34,23	44,22	36,38	40,27	36,77	38,70	71,09	69,46	54,86	23,94	28,48	36,25	27,29	67,07	57,40	68,41	74,09	33,47	40,09	42,10	57,48	49,77	62,08
U	4,89	6,14	5,34	5,20	3,99	4,47	9,70	8,59	8,17	3,17	4,56	7,50	4,76	8,22	8,98	10,75	11,33	4,72	9,31	8,18	5,58	6,78	8,06
∑REE	12405	13253	12597	12715	14500	12529	14067	14213	13753	10130	10674	12310	10421	14391	14292	14212	15176	12571	12780	13297	15299	14372	14811

Element	ap51	ap52	ap53	ap54	ap55	ap59	ap60	ap61	ap62	ap63	ap64	ap65	ap66	ap67	ap68
Li	2,63	4,21	3,68	4,41	2,31	4,43	6,24	3,55	3,15	4,07	4,25	<2,52	3,46	2,78	4,94
B	<28,91	<30,05	<42,62	<45,42	<44,62	<28,77	<28,26	<24,26	<30,66	<38,27	<34,12	<54,31	<49,01	<44,85	<50,64
Na	946,5	1290	1138	1118	1147	1356	1321	1132	1061	1146	1344	1151	1074	842,2	1960
Mg	145,6	138,3	261,6	273,9	294,1	207,8	1358	157,3	685,7	169,5	211,5	261,0	180,6	219,6	1407
Al	6,14	<4,64	<6,79	<7,12	200,5	32,91	559,7	13,43	210,5	<6,10	5,62	<8,94	<7,37	12,68	595,0
Si	1858	2918	<2463,87	2777	<2443,08	2465	3824	<1419,27	6007	2721	2232	3453	<2750,95	2555	8427
P	124046	131887	128092	135125	136805	126390	123492	130639	131923	128828	129445	131322	125434	131844	127957
K	<28,79	<28,63	<42,72	<43,72	<42,05	<28,03	<28,45	<24,49	51,28	<38,11	<34,15	<53,52	<47,19	<43,77	102,76
Ca	383580	383580	383580	383580	383580	383580	383580	383580	383580	383580	383580	383580	383580	383580	383580
Cs	-	-	-	-	-	-	-	-	-	-	-	-	-	-	-
Sc	1,14	1,44	1,87	<1,55	1,89	1,28	<1,01	<0,88	<1,01	<1,35	<1,17	<1,89	<1,69	<1,53	<1,72
Ti	697,7	759,5	716,1	752,1	730,8	701,4	723,9	711,1	718,2	729,0	724,9	727,3	735,0	734,4	727,4
V	16,51	24,07	15,41	19,70	12,44	23,95	18,20	18,91	18,55	21,85	17,56	18,15	20,43	14,14	29,38
Cr	<2,99	<3,02	<4,49	<4,45	<4,31	<2,90	3,26	<2,44	<3,02	<3,72	<3,42	<5,38	<4,76	<4,30	<5,09
Mn	376,8	383,4	417,4	421,4	431,0	303,7	381,6	330,5	327,6	328,5	474,9	411,5	371,2	379,8	292,0
Fe	1337	1394	1525	1494	2148	1370	2132	1292	1616	1329	1488	1483	1295	1250	1974
Co	0,63	0,81	<0,44	0,95	5,97	0,89	1,92	0,71	1,75	0,81	0,64	<0,56	<0,44	0,73	2,97
Ni	5,29	4,49	3,95	5,85	14,77	4,64	8,27	4,53	4,96	4,84	5,44	3,48	3,59	3,84	9,31
Cu	<1,09	<1,08	<1,62	<1,84	55,42	2,11	0,98	<0,91	<1,15	<1,42	<1,29	<2,02	<1,81	1,95	1,92
Zn	5,84	<2,70	11,11	13,49	<4,84	11,22	6,29	<2,84	<3,35	<3,26	2,79	5,02	5,71	<3,84	5,50
Ga	<0,45	<0,43	<0,71	<0,71	<0,67	0,48	0,49	0,59	<0,49	<0,65	<0,57	<0,74	<0,83	<0,65	<0,82
Ge	251,2	226,5	256,3	229,7	265,4	218,7	328,6	306,5	299,7	270,0	253,7	310,9	293,1	301,1	269,9
As	16,21	11,76	16,16	13,58	16,74	21,01	21,00	18,26	18,37	19,58	18,88	23,85	20,91	17,85	21,04
Rb	<0,47	<0,49	<0,66	<0,77	<0,77	<0,51	0,66	<0,41	<0,50	<0,58	<0,62	<1,09	0,92	<0,75	<0,88
Sr	1608	1708	1628	1637	1878	1309	1260	1464	1409	1437	1949	1530	1526	1556	1434
Y	475,6	380,7	436,1	400,5	461,4	404,6	547,3	522,0	511,3	420,4	410,2	555,0	544,9	508,3	499,9
Zr	6,33	3,46	4,98	4,12	6,06	4,08	10,43	5,32	5,85	9,31	5,17	11,40	13,14	10,81	5,75
Nb	<0,097	<0,103	0,09	<0,154	<0,133	<0,075	<0,085	<0,074	<0,096	0,06	<0,060	<0,177	<0,084	<0,106	<0,155
Mo	<0,90	<0,89	<1,05	<1,63	1,50	<0,98	<0,95	<0,75	0,68	<1,10	<0,86	<1,47	<1,40	<1,65	<1,66
Sn	<0,52	<0,37	<0,81	<0,58	<0,82	<0,43	<0,62	<0,32	<0,48	<0,66	0,33	<0,77	<0,83	1,11	57,24
Ba	0,67	1,15	<0,97	1,34	2,02	<0,70	0,60	<0,69	<0,82	0,84	1,88	<0,96	<0,80	<0,71	4,11
La	2567	2189	2547	2305	2594	2344	3529	3001	2965	2864	2713	3208	2984	2960	2800
Ce	5518,3	4682	5472	5161	6296	4788	7184	6448	6408	5848	5600	7062	6490	6500	5937
Pr	662,9	574,0	642,7	607,1	687,87	533,1	825,6	784,5	752,3	674,2	644,9	819,6	751,9	784,6	711,4
Nd	2831	2390	2792	2543	2950	2302	3463	3307	3200	2767	2669	3564	3246	3287	3012
Sm	450,0	374,6	430,9	383,2	449,1	356,5	525,8	513,7	499,8	428,5	415,0	562,7	486,6	516,9	474,2
Eu	70,64	59,71	70,03	64,99	61,72	54,42	88,36	77,96	73,98	76,44	64,07	91,75	80,69	83,24	79,01
Gd	290,8	236,8	268,8	249,7	279,5	226,2	329,8	317,00	308,9	264,8	254,9	348,2	304,2	323,6	302,6
Gd ©	-	-	-	-	-	-	-	-	-	-	-	-	-	-	-
Tb	28,91	23,06	26,39	24,79	28,28	22,75	33,55	32,20	31,15	27,16	24,23	36,23	31,82	32,08	30,67
Tb ©	-	-	-	-	-	-	-	-	-	-	-	-	-	-	-
Dy	117,1	93,1	100,3	93,6	110,0	88,4	128,4	126,2	122,0	103,0	95,0	139,0	116,1	121,9	116,2
Ho	17,70	14,75	15,57	14,95	16,80	13,95	23,63	19,56	18,90	15,41	14,91	21,20	19,20	20,18	18,05
Er	40,92	32,40	37,02	33,05	37,23	29,19	46,22	45,28	44,22	33,99	33,93	43,57	40,98	44,10	38,84
Tm	4,58	3,69	4,38	3,28	3,82	3,18	5,77	4,83	4,89	3,50	3,23	5,08	4,86	5,16	4,49
Yb	23,64	19,55	23,71	18,83	21,74	18,48	34,26	29,89	29,77	19,90	21,11	29,52	22,67	28,56	25,86
Lu	3,58	2,49	3,02	2,70	2,78	2,32	3,77	3,44	3,39	2,93	2,70	3,40	3,11	3,07	3,38
Hf	<0,47	<0,38	<0,70	0,66	<0,63	<0,44	0,88	0,94	1,06	<0,58	0,52	0,46	0,63	0,81	<0,84
Ta	<0,066	0,06	0,08	0,04	0,10	0,06	0,06	0,04	0,10	<0,043	<0,081	<0,106	<0,072	<0,101	<0,076
Pb	6,02	5,02	5,30	5,18	5,94	4,06	5,73	4,31	5,08	5,08	7,71	8,21	4,22	6,83	5,25
Th	44,75	29,16	39,40	34,66	45,99	25,97	76,82	53,86	55,44	63,77	60,35	69,40	60,91	62,74	53,15
U	5,86	4,15	4,30	4,41	4,90	3,90	9,40	7,39	7,21	9,69	8,73	7,20	6,99	6,38	6,45
Th	<-NaN	<-NaN	<-NaN	<-NaN	<-NaN	<-NaN	<-NaN	<-NaN	<-NaN	<-NaN	<-NaN	<-NaN	<-NaN	<-NaN	<-NaN
U	-	-	-	-	-	-	-	-	-	-	-	-	-	-	-
∑REE	12627	10696	12434	11505	13539	10781	16222	14711	14462	13129	12557	15933	14582	14710	13554

LA-ICP-MS results obtained for apatite – Sample PB-09

LA-ICP-MS results obtained for apatite – Sample PB-09 – Continuation

LA-ICP-MS - Elementos Traço normalizado por Condrito - PB-09 (CSO)

Element	AP01a	AP01b	AP01c	AP01d	AP02a_spc	AP02b_spc	AP03a	AP03b	AP03c	AP04a	AP04b	AP04c	AP04d	AP05a	AP05b	AP05c	AP05d	AP06a	AP06b	AP06c	AP07a	AP07b	AP07c
Li	-	-	-	-	-	-	-	-	-	-	-	-	-	-	-	-	-	-	-	-	-	-	-
B	0,51	0,54	0,62	0,33	0,50	0,94	0,65	0,84	0,97	0,91	0,39	1,35	0,78	0,96	0,56	0,99	0,86	0,55	0,56	0,44	0,85	0,75	1,14
Na	-	-	-	-	-	-	-	-	-	-	-	-	-	-	-	-	-	-	-	-	-	-	-
Mg	0,00	0,00	0,00	0,00	0,00	0,01	0,00	0,01	0,00	0,00	0,00	0,00	0,00	0,00	0,00	0,01	0,01	0,00	0,00	0,00	0,01	0,00	0,01
Al	-	-	-	-	-	-	-	-	-	-	-	-	-	-	-	-	-	-	-	-	-	-	-
Si	0,02	0,02	0,02	0,02	0,01	0,03	0,02	0,03	0,02	0,01	0,01	0,02	0,01	0,02	0,02	0,03	0,03	0,01	0,02	0,02	0,03	0,02	0,03
P	92,69	92,12	90,06	93,05	115,21	103,86	94,62	89,49	98,92	104,83	99,01	102,34	98,76	89,43	87,50	88,20	91,75	105,97	109,41	101,25	97,07	87,13	93,27
K	-	-	-	-	-	-	-	-	-	-	-	-	-	-	-	-	-	-	-	-	-	-	-
Ca	29,12	29,12	29,12	29,12	29,12	29,12	29,12	29,12	29,12	29,12	29,12	29,12	29,12	29,12	29,12	29,12	29,12	29,12	29,12	29,12	29,12	29,12	29,12
Cs	0,03	0,02	0,03	0,02	0,01	0,02	0,02	0,02	0,02	0,02	0,02	0,02	0,03	0,02	0,02	0,02	0,03	0,02	0,01	0,02	0,03	0,03	0,03
Sc	-	-	-	-	-	-	-	-	-	-	-	-	-	-	-	-	-	-	-	-	-	-	-
Ti	1243,00	1235,00	1236,00	1215,00	1349,00	1311,00	1198,00	1143,00	1243,00	1243,00	1216,00	1248,00	1238,00	1204,00	1215,00	1178,00	1197,00	1191,00	1206,00	1211,00	1214,00	1188,00	1201,00
V	0,22	0,21	0,19	0,20	0,17	0,21	0,20	0,20	0,19	0,22	0,21	0,25	0,21	0,21	0,22	0,23	0,17	0,14	0,13	0,12	0,20	0,20	0,20
Cr	-	-	-	-	-	-	-	-	-	-	-	-	-	-	-	-	-	-	-	-	-	-	-
Mn	0,14	0,14	0,15	0,14	0,12	0,13	0,11	0,10	0,11	0,15	0,14	0,15	0,14	0,14	0,14	0,13	0,14	0,13	0,13	0,13	0,14	0,14	0,14
Fe	0,00	0,00	0,00	0,00	0,00	0,01	0,00	0,01	0,00	0,00	0,00	0,00	0,00	0,00	0,00	0,01	0,01	0,00	0,00	0,00	0,00	0,00	0,01
Co	-	-	-	-	-	-	-	-	-	-	-	-	-	-	-	-	-	-	-	-	-	-	-
Ni	-	-	-	-	-	-	-	-	-	-	-	-	-	-	-	-	-	-	-	-	-	-	-
Cu	-	-	-	-	-	-	-	-	-	-	-	-	-	-	-	-	-	-	-	-	-	-	-
Zn	-	-	-	-	-	-	-	-	-	-	-	-	-	-	-	-	-	-	-	-	-	-	-
Ga	0,02	0,02	0,02	0,02	0,01	0,03	0,02	0,03	0,02	0,01	0,01	0,02	0,01	0,02	0,02	0,03	0,04	0,02	0,02	0,02	0,02	0,03	0,03
Ge	6,72	7,13	6,84	7,05	5,63	5,83	7,80	7,74	7,73	5,92	5,81	7,17	5,76	7,83	7,58	7,88	8,11	7,64	7,53	7,56	8,32	7,78	8,04
As	6,44	6,15	6,20	5,94	5,74	5,28	6,99	6,99	6,65	5,17	5,34	6,48	5,45	7,04	6,94	7,14	7,13	5,40	5,24	5,49	6,99	6,59	6,81
Rb	-	0,01	0,01	-	0,01	0,05	0,02	0,04	0,02	0,01	-	0,01	-	0,02	0,01	0,03	0,08	0,02	0,03	0,03	0,01	0,03	0,03
Sr	142,58	145,31	135,95	140,00	154,14	134,34	108,59	110,99	119,53	134,75	128,16	137,27	135,66	131,23	127,45	125,90	116,28	125,02	127,39	124,81	135,34	120,87	122,78
Y	175,99	190,25	179,80	180,28	146,56	144,45	195,53	198,28	194,54	138,11	144,27	164,23	140,87	213,30	200,87	207,11	224,74	137,42	145,35	162,52	216,20	198,78	211,81
Zr	0,50	0,61	0,61	0,51	0,61	0,56	1185,00	1144,00	1048,00	0,46	0,53	0,71	0,51	1,48	1297,00	1393,00	1,60	0,89	0,95	1075,00	0,74	0,68	0,62
Nb	-	0,03	0,02	0,03	0,03	0,05	0,05	0,06	0,04	0,03	0,03	0,05	0,03	-	0,07	0,06	0,05	0,05	0,05	0,04	0,05	0,06	0,06
Mo	-	-	-	-	-	-	-	-	-	-	-	-	-	-	-	-	-	-	-	-	-	-	-
Sn	-	-	-	-	-	-	-	-	-	-	-	-	-	-	-	-	-	-	-	-	-	-	-
Ba	0,09	0,12	0,10	0,11	0,08	0,15	0,07	0,13	0,12	0,09	0,12	0,08	0,11	0,10	0,13	0,19	0,64	0,05	0,12	0,10	0,17	0,13	0,19
La	10018	10607	10043	10333	13869	11090	11755	11924	11413	8242	8565	9679	8338	11826	11608	11635	12202	9509	9670	10440	12393	11338	12018
Ce	9527	10341	9825	9898	12563	10434	10970	10847	10560	7876	8294	9635	8260	10882	11021	10779	11505	10631	10662	10772	11817	11438	11462
Pr	7110	7508	7264	7123	6456	6851	7921	7929	7670	5796	6035	6919	5839	7938	7838	7975	8443	7060	7236	7461	8558	7824	8203
Nd	5645	5917	5621	5653	4681	4647	6116	6406	6209	4492	4810	5565	4550	6646	6485	6545	7120	5096	5318	5686	6904	6296	6662
Sm	2598	2724	2602	2605	2150	2063	2797	2933	2840	2103	2207	2576	2096	3156	3007	3057	3263	2275	2362	2584	3261	2948	3143
Eu	1131	1209	1133	1176	968,6	960,5	1355	1400	1344	977,9	1014	1194	965,2	1397	1346	1369	1471	1155	1191	1233	1440	1348	1405
Gd	1105	1158	1100	1090	861,0	822,0	1173	1221	1153	866,0	934,0	1046	866,0	1328	1265	1285	1377	910,0	949,0	1032	1319	1217	1285
Tb	632,2	656,2	626,7	634,9	513,4	492,5	654,1	714,9	661,1	487,6	520,4	591,2	498,3	752,6	723,9	735,3	791,0	508,7	541,0	596,0	754,6	703,5	737,7
Dy	379,9	402,5	382,4	385,9	320,6	300,5	405,7	428,1	399,1	294,5	312,7	358,3	305,8	450,4	435,5	452,1	483,7	308,1	325,8	363,5	467,5	435,3	448,0
Ho	266,1	279,0	270,1	272,4	217,5	204,6	286,0	301,8	279,2	210,2	214,8	254,2	211,8	322,4	308,3	312,0	341,0	216,1	231,6	254,2	319,8	305,3	314,3
Er	202,8	214,6	204,0	206,9	163,9	153,9	213,0	227,7	208,2	153,5	162,1	185,7	157,7	241,5	226,8	233,1	248,3	156,0	163,4	187,1	237,1	221,1	234,4
Tm	150,2	160,0	150,6	149,0	120,8	112,5	157,6	163,9	159,2	111,0	118,4	130,2	114,1	173,3	171,0	175,7	182,4	114,1	114,5	132,5	180,8	160,4	174,1
Yb	129,9	138,6	133,3	130,9	105,2	96,82	143,4	149,1	140,2	92,76	99,82	120,4	96,00	150,4	145,1	150,6	160,1	103,8	106,1	120,5	158,8	138,1	149,9
Lu	116,93	118,50	112,20	113,78	85,55	83,58	125,59	131,50	119,69	83,23	84,69	100,00	82,05	125,59	122,05	126,38	138,98	85,43	93,70	100,79	130,71	120,87	122,44
Hf	2,17	1,97	1,41	1,92	1,54	1,50	1,93	1,82	2,10	0,74	1,39	1,32	1,32	2,84	1,80	1,97	2,27	1,25	0,92	1,64	2,14	1,83	2,36
Ta	0,97	0,97	0,62	1,07	0,52	0,58	0,81	0,69	0,69	0,83	0,52	0,79	0,80	1,55	0,92	0,68	1,16	0,70	0,65	0,79	1,14	0,53	1,05
Pb	1637,00	1717,00	1523,00	1613,00	1500,00	1219,00	1703,00	1703,00	1676,00	1582,00	1367,00	1681,00	1476,00	2,08	1,95	2,08	1,88	1,83	1,79	1,73	2,05	1,66	1,77
Th	826,04	927,20	854,97	825,16	864,85	731,81	1516,03	1643,86	1369,23	622,37	680,96	932,72	626,57	1535,67	1440,68	1580,73	1727,17	822,14	914,88	1024,99	1258,64	1124,95	1225,51
U	428,04	489,42	462,94	425,43	409,20	382,49	783,87	800,08	683,72	351,53	379,70	475,25	356,75	684,56	677,61	721,32	762,57	458,50	492,74	537,45	652,43	576,07	652,39
Th	805,32	1040,50	856,03	947,61	865,22	910,63	1672,81	1634,44	1290,84	563,22	670,08	852,96	642,16	1578,17	1350,48	1609,75	1743,25	787,42	943,23	990,48	1352,41	1170,99	1460,64
U	400,60	503,62	437,56	426,45	326,70	366,35	794,90	703,75	669,77	259,86	373,76	614,73	390,25	673,99	736,05	881,15	928,99	387,05	763,27	670,45	457,11	556,10	660,77

Element	ap51	ap52	ap53	ap54	ap55	ap59	ap60	ap61	ap62	ap63	ap64	ap65	ap66	ap67	ap68
Li	1,09	1,75	1,53	1,84	0,96	1,85	2,6	1,48	1,31	1,7	1,77		1,44	1,16	2,06
B															
Na	0,1306	0,178	0,157	0,1543	0,1583	0,187	0,182	0,1563	0,1464	0,158	0,185	0,159	0,148	0,1163	0,271
Mg	0,00102	0,00097	0,00183	0,00192	0,00206	0,00145	0,0095	0,0011	0,00479	0,00119	0,00148	0,00182	0,00126	0,00154	0,00984
Al	0,00048	-	-	-	0,01554	0,00255	0,0434	0,00104	0,01632	-	0,00044	-	-	0,00098	0,0461
Si	0,0116	0,0182	-	0,0174	-	0,0154	0,0239	-	0,0375	0,017	0,014	0,0216	-	0,016	0,0527
P	53,93	57,34	55,69	58,75	59,48	54,95	53,69	56,8	57,36	56,01	56,28	57,1	54,54	57,32	55,63
K	-	-	-	-	-	-	-	-	0,06	-	-	-	-	-	0,12
Ca	28,41	28,41	28,41	28,41	28,41	28,41	28,41	28,41	28,41	28,41	28,41	28,41	28,41	28,41	28,41
Cs															
Sc	0,132	0,167	0,216		0,218	0,148									
Ti	1,067	1,161	1,095	1,15	1,117	1,072	1,107	1,087	1,098	1,115	1,108	1,112	1,124	1,123	1,112
V	0,1942	0,283	0,181	0,232	0,1463	0,282	0,214	0,222	0,218	0,257	0,207	0,214	0,24	0,166	0,346
Cr	-	-	-	-	-	-	0,00082	-	-	-	-	-	-	-	-
Mn	0,1282	0,1304	0,142	0,1433	0,1466	0,1033	0,1298	0,1124	0,1114	0,1117	0,1615	0,14	0,1262	0,1292	0,0993
Fe	0,00481	0,00501	0,00548	0,00538	0,00773	0,00493	0,00767	0,00465	0,00581	0,00478	0,00535	0,00533	0,00466	0,0045	0,0071
Co	0,00083	0,00106	-	0,00124	0,00782	0,00117	0,00252	0,00093	0,00229	0,00106	0,00084	-	-	0,00096	0,00389
Ni	0,00032	0,00027	0,00024	0,00035	0,0009	0,00028	0,0005	0,00027	0,0003	0,00029	0,00033	0,00021	0,00022	0,00023	0,00056
Cu	-	-	-	-	0,33	0,0125	0,0058	-	-	-	-	-	-	0,0116	0,0115
Zn	0,0126	-	0,024	0,0292	-	0,0243	0,0136		-	-	0,006	0,0109	0,0124		0,0119
Ga		-				0,032	0,032	0,039							
Ge	5,2	4,69	5,31	4,76	5,49	4,53	6,8	6,34	6,2	5,59	5,25	6,44	6,07	6,23	5,59
As	5,65	4,1	5,63	4,73	5,83	7,32	7,32	6,36	6,4	6,82	6,58	8,31	7,28	6,22	7,33
Rb	-	-	-	-	-	-	0,192						0,27		
Sr	135,16	143,56	136,83	137,55	157,81	110,04	105,89	123,04	118,37	120,79	163,82	128,61	128,26	130,78	120,53
Y	211,37	169,18	193,84	178,01	205,07	179,81	243,26	232,01	227,23	186,86	182,33	246,68	242,19	225,93	222,16
Zr	1.142	0,624	0,898	0,744	1,094	0,736	1,88	0,96	1,055	1,68	0,934	2,06	2,37	1,95	1,038
Nb	-	-	0,24	-	-	-	-	-	-	0,164		-	-	-	-
Mo	-	-	-	-	1,09	-	-	-	0,49	-	-	-	-	-	-
Sn	-	-	-	-	-	-	-	-	-	-	0,13	-	-	0,44	22,71
Ba	0,198	0,338	-	0,39	0,59	-	0,18	-	-	0,25	0,55	-	-	-	1,2
La	6994	5966	6939	6282	7068	6386	9617	8176	8080	7805	7393	8740	8130	8064	7630
Ce	5766	4892,6	5718	5392	6579	5003	7507	6738	6696	6111	5852	7379	6782	6792	6204
Pr	4838	4190	4691	4432	5021	3891	6026	5726	5491	4921	4707	5982	5488	5727	5192
Nd	3982	3362	3927	3576	4149	3237	4870	4652	4501	3891	3754	5012	4565	4624	4236
Sm	1948	1622	1865	1659	1944	1543	2276	2224	2164	1855	1797	2436	2107	2238	2053
Eu	812,0	686,4	804,9	747,0	709,4	625,5	1016	896,1	850,4	878,6	736,5	1055	927,5	956,8	908,2
Gd	950,4	773,8	878,5	816,0	913,3	739,2	1078	1036	1009	865,5	832,9	1138	994,0	1057	988,9
Tb	498,4	397,6	454,9	427,4	487,5	392,3	578,5	555,1	537,1	468,2	417,8	624,6	548,7	553,2	528,9
Dy	307,2	244,2	263,1	245,6	288,7	232,0	337,0	331,2	320,3	270,4	249,3	364,9	304,7	319,9	305,1
Ho	208,0	173,3	183,0	175,7	197,4	164,0	277,6	229,8	222,0	181,1	175,2	249,1	225,6	237,1	212,1
Er	164,3	130,1	148,7	132,8	149,5	117,2	185,6	181,9	177,6	136,5	136,3	175,0	164,6	177,1	156,0
Tm	128,8	103,7	122,9	92,27	107,3	89,19	162,0	135,7	137,4	98,38	90,73	142,6	136,5	144,9	126,2
Yb	95,34	78,83	95,62	75,94	87,66	74,52	138,1	120,5	120,0	80,24	85,13	119,0	91,4	115,2	104,3
Lu	94	65,32	79,33	70,75	73,09	60,99	98,83	90,36	89,03	76,81	70,97	89,36	81,56	80,68	88,65
Hf				3,67			4,93	5,27	5,9		2,91	2,54	3,49	4,52	
Ta	-	2,12	2,9	1,71	3,72	2,34	2,45	1,34	3,88						
Pb	1,65	1,38	1,45	1,42	1,63	1,11	1,57	1,18	1,39	1,39	2,11	2,25	1,16	1,87	1,44
Th	1052,83	686,21	927,12	815,62	1082,19	611,15	1807,49	1267,3	1304,44	1500,56	1420,09	1633	1433,22	1476,32	1520,67
U	479,98	340,27	352,24	361,42	401,61	319,53	770,63	605,49	590,69	793,96	715,94	590,43	572,6	523,3	528,86
Th	-	-													
U															

	LA-ICP-MS - Concentração de Elementos Traço (Ppm) - PB-123 (CSI).											LA-ICP-MS - Elementos Traço normalizado por Condrito - PB-123 (CSO)								
Element	**AP-01**	**AP-02**	**AP-0340um**	**AP-05**	**AP-04c**	**AP-04b**	**AP-06**	**AP-07c**	**AP-07b**	**AP-09**	**AP-01**	**AP-02**	**AP-0340um**	**AP-05**	**AP-04c**	**AP-04b**	**AP-06**	**AP-07c**	**AP-07b**	**AP-09**
B	2,58	1,24	2,67	1,84	1,95	2,45	1,74	2,42	1,91	1,49	1,36	0,65	1,41	0,97	1,03	1,29	0,91	1,27	1,01	0,79
Mg	49,66	58,46	52,22	31,80	33,00	84,45	72,38	19,58	43,70	52,59	0,00035	0,00041	0,00037	0,00022	0,00023	0,00059	0,00051	0,00014	0,00031	0,00037
Si	3988,41	2762,79	2955,54	3284,96	3493,50	3933,64	2607,97	2378,15	3240,87	2446,73	0,0249	0,0173	0,0185	0,0205	0,0218	0,0246	0,0163	0,0149	0,0203	0,0153
P	239856,09	247229,66	203264,86	237952,11	242610,63	246599,61	260022,66	260282,38	253218,91	246978,14	104,29	107,49	88,38	103,46	105,48	107,22	113,05	113,17	110,1	107,38
Ca	393085,56	393085,53	393085,53	393085,53	393085,53	393085,53	393085,53	393085,53	393085,53	393085,53	29,12	29,12	29,12	29,12	29,12	29,12	29,12	29,12	29,12	29,12
Cs	0,09	0,11	<0,136	0,12	0,15	0,14	0,10	0,08	0,08	0,12	0,0101	0,0129	0	0,0137	0,0172	0,0157	0,0112	0,0097	0,0095	0,0134
Ti	831,94	855,44	835,05	834,69	816,74	818,49	843,44	826,17	889,67	845,63	1,272	1,308	1,277	1,276	1,249	1,252	1,29	1,263	1,36	1,293
V	12,09	11,60	24,46	12,87	11,89	15,24	11,34	10,40	10,11	9,49	0,1423	0,1364	0,2878	0,1514	0,1399	0,1793	0,1335	0,1223	0,1189	0,1116
Mn	501,72	405,89	264,71	344,95	253,25	276,65	258,39	224,05	297,27	224,36	0,1707	0,1381	0,09	0,1173	0,0861	0,0941	0,0879	0,0762	0,1011	0,0763
Fe	373,74	330,06	383,45	308,59	270,36	391,66	361,27	231,43	329,48	354,26	0,00134	0,00119	0,00138	0,00111	0,00097	0,00141	0,0013	0,00083	0,00119	0,00127
Ga	0,35	0,25	0,24	0,30	0,31	0,37	0,29	0,33	0,27	0,26	0,0227	0,0163	0,0155	0,0197	0,0205	0,0241	0,0188	0,022	0,0178	0,017
Ge	472,32	337,90	300,88	413,81	436,73	467,35	331,95	471,06	407,34	299,22	9,78	7	6,23	8,57	9,04	9,68	6,87	9,75	8,43	6,19
As	23,13	16,12	15,19	20,20	21,25	23,32	17,33	21,42	20,64	15,37	8,06	5,62	5,29	7,04	7,4	8,12	6,04	7,46	7,19	5,36
Rb	<0,020	<0,0221	<0,105	<0,023	<0,027	0,04	<0,028	<0,030	<0,035	<0,040	0	0	0	0	0	0,0129	0	0	0	0
Sr	2129,02	2109,83	2281,93	2207,91	2074,09	2145,42	2157,53	2059,48	2357,15	2275,21	178,91	177,3	191,76	185,54	174,29	180,29	181,31	173,07	198,08	191,19
Y	522,92	284,35	356,17	459,06	500,14	519,53	367,30	473,36	473,46	275,25	232,41	126,38	158,3	204,03	222,28	230,9	163,24	210,38	210,43	122,33
Zr	3,97	1,95	2,87	1,75	2,45	2,86	0,76	1,69	1,06	1,39	0,717	0,352	0,519	0,316	0,442	0,516	0,1373	0,305	0,191	0,251
Nb	0,03	0,02	0,02	0,02	0,03	0,03	0,03	0,02	0,04	0,01	0,09	0,0445	0,057	0,058	0,068	0,078	0,089	0,058	0,096	0,0245
Ba	0,48	0,72	1,27	0,80	0,60	1,41	1,05	0,71	0,59	1,54	0,141	0,21	0,372	0,236	0,175	0,413	0,307	0,209	0,174	0,453
La	3897,31	3168,31	2844,97	3101,85	3469,49	3582,55	2464,37	3155,08	2491,50	2622,31	10619,37	8633,01	7751,95	8451,9	9453,64	9761,72	6714,91	8596,96	6788,83	7145,25
Ce	9496,27	6836,81	5613,07	7949,28	8490,10	8947,75	6460,56	8827,59	7963,49	5869,11	9922,96	7144	5865,27	8306,46	8871,58	9349,79	6750,85	9224,23	8321,31	6132,83
Pr	1060,91	696,65	590,42	914,91	958,48	1006,63	739,00	977,48	894,39	629,80	7743,9	5085,03	4309,62	6678,2	6996,24	7347,69	5394,14	7134,89	6528,4	4597,07
Nd	3878,78	2401,02	2380,78	3334,41	3505,04	3740,26	2759,16	3421,54	3289,75	2259,49	5455,39	3376,96	3348,49	4689,74	4929,73	5260,56	3880,68	4812,29	4626,93	3177,9
Sm	576,29	319,57	349,71	499,80	528,11	568,50	401,67	527,35	518,46	311,80	2494,75	1383,42	1513,89	2163,64	2286,18	2461,04	1738,82	2282,89	2244,43	1349,77
Eu	90,33	88,28	66,54	92,76	94,65	103,75	73,82	94,41	98,14	67,21	1038,3	1014,66	764,85	1066,21	1087,94	1192,5	848,48	1085,16	1128,09	772,48
Gd	335,13	185,74	213,08	291,07	307,48	326,59	230,04	297,62	300,09	180,93	1095,2	607	696,34	951,21	1004,85	1067,27	751,76	972,62	980,69	591,28
Tb	32,30	16,70	20,80	27,94	29,30	31,58	22,24	28,58	28,67	16,54	556,85	287,98	358,67	481,73	505,25	544,55	383,37	492,76	494,28	285,21
Dy	125,98	63,30	81,17	110,53	114,96	120,77	87,00	112,24	110,59	62,54	330,67	166,13	213,04	290,1	301,73	316,97	228,34	294,59	290,25	164,15
Ho	19,01	9,72	12,37	16,95	17,55	18,19	13,42	16,75	17,00	9,64	223,36	114,27	145,37	199,18	206,27	213,75	157,75	196,88	199,74	113,27
Er	40,57	21,40	26,98	35,64	36,51	38,94	27,86	35,93	35,94	20,63	162,93	85,93	108,35	143,14	146,65	156,41	111,87	144,31	144,34	82,87
Tm	4,35	2,34	2,96	3,93	4,00	4,22	3,08	3,89	3,84	2,25	122,19	65,81	83,12	110,4	112,35	118,64	86,62	109,31	107,93	63,17
Yb	25,67	13,83	18,53	22,22	22,77	23,86	16,80	21,96	22,60	12,82	103,53	55,76	74,72	89,61	91,83	96,21	67,72	88,55	91,14	51,69
Lu	3,11	1,89	2,41	2,66	2,71	2,90	2,05	2,58	2,76	1,72	81,56	49,49	63,22	69,86	71,01	76,04	53,87	67,83	72,35	45,11
Hf	0,34	0,18	0,33	0,36	0,39	0,40	0,25	0,37	0,38	0,21	1,91	1	1,84	2,03	2,18	2,21	1,38	2,08	2,14	1,15
Ta	0,02	0,02	0,03	0,03	0,03	0,03	0,02	0,03	0,02	0,01	0,92	0,586	1,03	1,03	0,96	1,08	0,69	0,98	0,93	0,53
Pb	9,64	6,01	5,73	7,71	7,11	8,15	5,20	7,11	8,81	5,44	2,64	1,646	1,569	2,11	1,95	2,23	1,425	1,95	2,41	1,489
Th	130,31	69,73	49,90	89,27	93,13	104,82	52,01	91,71	85,65	47,49	3066,17	1640,74	1174,15	2100,37	2191,26	2466,28	1223,86	2157,96	2015,21	1117,49
U	13,20	7,35	5,51	8,73	8,53	9,90	5,45	8,86	8,18	4,64	1082,17	602,25	451,37	715,73	699,35	811,13	446,59	726,31	670,44	380,23
Th	<-NaN	<-NaN	<-NaN	<-NaN	<-NaN	<-NaN	<-NaN	<-NaN	<-NaN	<-NaN	<-1,00	<-1,00	<-1,00	<-1,00	<-1,00	<-1,00	<-1,00	<-1,00	<-1,00	<-1,00
U	15,68	7,70	7,74	8,39	9,27	10,33	5,50	8,53	8,55	5,10	1284,94	631,02	634,41	687,69	760,09	846,36	450,49	699,58	701,03	418,22

LA-ICP-MS results obtained for apatite – Sample PB-123

LA-ICP-MS results obtained for apatite – Sample PB-181

LA-ICP-MS - Concentração de Elementos Traço (Ppm) - PB-181 (LSS).																																		
	AP01.a	AP01b	AP02a	AP02b	AP03a	AP03b	AP04a	AP04b	AP05a_spo	AP06a_spo	AP07a	AP07b	AP08a_spo	AP09a	AP09b	AP10a_spo	AP11a_spo	AP11b_spo	ap52	ap53	ap54	ap55	ap56	ap57	ap58	ap59	ap61	ap62	ap63	ap64	ap65	ap66	ap67	ap68
Li	-	-	-	-	-	-	-	-	-	-	-	-	-	-	-	-	-	-	n.d.	2,76	1,32	1,38	1,37	n.d.	n.d.	n.d.	2,12	n.d.	n.d.	n.d.	n.d.	n.d.	n.d.	1,58
B	n.d.	1,21	1,09	1,62	0,88	1,04	1,67	n.d.	1,08	n.d.	0,92	0,90	n.d.	1,43	0,46	n.d.	2,92	1,05														44,12	n.d.	
Na	-	-	-	-	-	-	-	-	-	-	-	-	-	-	-	-	-	-	1766	2394	2002	2398	2566	2481	2439	2308	2367	2543	1936	2683	2236	2323,55	2918,72	2371,6
Mg	155,11	19,64	27,69	15,82	15,51	13,77	26,03	269,27	15,07	18,70	17,28	38,65	18,44	28,78	26,49	55,63	157,84	51,59	37,69	60,97	33,96	17,88	17,18	15,56	18,85	11,92	109,49	14,18	33,46	40,13	15,91	23,28	26,24	29,38
Al	-	-	-	-	-	-	-	-	-	-	-	-	-	-	-	-	-	-	1030	245,9	8,48	n.d.	n.d.	46,02	52,12	n.d.	82,97	n.d.	15,06	13,47	n.d.	n.d.	n.d.	7,9
Si	3359,44	3296,47	3228,81	3100,49	3657,65	3353,55	3891,60	3255,40	3593,37	2698,98	3708,27	3486,64	2906,80	4145,36	3246,45	2873,39	3316,03	5024,44	55,44	47,66	2641	3268	3672	n.d.	2473	6495	5414	2991	n.d.	4643	n.d.	n.d.	5730,48	3561,78
P	254164,33	247580,98	245258,73	236228,55	232312,78	230100,64	203487,20	213590,45	240405,50	208892,61	232043,30	237328,08	234198,50	241833,70	236182,28	214664,75	211842,75	203892,19	128777	128925	121655	130769	131931	123425	129398	132875	128485	131204	125551	128404	126760	127064,3	129583,49	126923,91
K																			73,99	52,88	n.d.	n.d.	48,35	41,53	n.d.	58,48	87,63	n.d.	n.d.	n.d.	n.d.	n.d.	65,17	n.d.
Ca	393085,53	393085,53	393085,53	393085,53	393085,53	393085,56	393085,53	393085,53	393085,50	393085,47	393085,50	393085,47	393085,50	393085,47	393085,47	393085,47	393085,50	393085,50	381078	381079	381078	381079	381078	381079	381078	381078	381078	381078	381079	381079	381079	381078,47	381078,5	381078,5
Cs	0,08	0,07	n.d.	n.d.	n.d.	0,08	0,08						n.d.			0,06	0,09		-	-	-	-	-	-	-	-	-	-	-	-	-	-	-	-
Sc	-	-	-	-	-	-	-	-	-	-	-	-	-	-	-	-	-	-	1,35	n.d.	0,95	n.d.	n.d.	n.d.	n.d.	n.d.	1,43	n.d.	n.d.	n.d.	n.d.	n.d.	n.d.	n.d.
Ti	827,47	804,64	813,47	793,03	801,44	760,20	782,13	786,18	797,05	790,35	803,53	803,99	776,47	786,42	767,31	791,94	800,25	794,44	726,98	727,03	692,70	719,69	719,62	694,79	695,93	745,26	704,41	735,71	711,21	727,93	692,16	712,31	705,79	694,84
V	105,53	102,17	122,02	90,56	140,40	93,46	125,13	92,49	118,79	69,37	132,08	80,56	123,92	103,12	125,82	97,32	107,36	101,09	120,70	68,96	69,12	85,27	115,62	79,86	133,87	132,00	114,03	117,78	105,66	47,18	126,65	91,79	102,45	74,8
Cr	-	-	-	-	-	-	-	-	-	-	-	-	-	-	-	-	-	-	n.d.	4,18	n.d.	n.d.	n.d.	n.d.	n.d.	n.d.	n.d.	n.d.	n.d.	n.d.	n.d.	n.d.	n.d.	n.d.
Mn	355,49	331,62	283,00	246,33	279,87	268,34	297,02	308,32	275,20	272,06	276,71	272,51	296,93	277,91	285,25	333,78	291,54	251,70	286,8	230,6	235,7	234,3	334,2	313,7	330,6	416,4	256,9	226,2	155,0	280,2	241,3	239,18	275,11	309,95
Fe	264,97	223,82	397,98	170,55	186,70	150,70	197,04	359,16	179,32	189,98	183,74	223,36	168,85	170,36	173,77	229,45	727,28	300,40	1156	1309	1096	1112	1091	1093	1156	1117	1113	1095	1067	1148	1112	1080,99	1141,96	1108,4
Co	-	-	-	-	-	-	-	-	-	-	-	-	-	-	-	-	-	-	0,76	0,64	0,40	0,54	0,59	0,36	0,57	0,46	n.d.	0,69	0,38	0,80	n.d.	0,56	0,77	0,88
Ni	-	-	-	-	-	-	-	-	-	-	-	-	-	-	-	-	-	-	4,89	2,70	2,99	4,85	4,36	5,00	2,88	6,34	6,65	4,69	2,14	n.d.	3,80	5,05	2,08	4,09
Cu	-	-	-	-	-	-	-	-	-	-	-	-	-	-	-	-	-	-	n.d.	9,76	n.d.	n.d.	n.d.	n.d.	n.d.	n.d.	3,77	n.d.	n.d.	n.d.	n.d.	n.d.	n.d.	n.d.
Zn	-	-	-	-	-	-	-	-	-	-	-	-	-	-	-	-	-	-	3,03	6,78	5,21	2,10	n.d.	2,71	n.d.	3,33	3,92	n.d.	n.d.	n.d.	n.d.	n.d.	n.d.	4,02
Ga	0,47	0,39	0,41	0,35	0,44	0,35	0,36	0,82	0,43	0,30	0,41	0,40	0,41	0,71	0,43	0,39	0,65	1020,00	0,47		0,57				0,69					0,98				
Ge	427,16	433,54	458,47	419,12	443,43	414,64	437,11	341,55	402,52	349,93	441,83	405,04	375,55	448,27	412,13	373,55	314,97	362,34	159,7	317,0	243,0	322,2	354,3	310,2	371,3	342,8	311,2	313,2	270,5	250,3	315,5	264,29	391,05	303,77
As	47,21	41,98	42,72	43,64	44,47	34,99	39,19	38,37	38,39	36,31	33,05	42,81	40,60	46,23	42,50	26,93	27,65	35,30	29,86	41,80	36,50	35,24	38,71	44,12	39,60	37,34	35,15	35,32	34,27	34,67	32,48	32,26	48,06	33,5
Rb	1020,00	0,03	0,05	0,02	n.d.	0,04	0,06	1,89	n.d.	0,02	0,03	0,07	0,04	0,30	0,10	n.d.	1112,00	0,20	0,55	n.d.	0,73	n.d.	n.d.	n.d.	n.d.	n.d.	n.d.	n.d.	n.d.	n.d.	7,36	n.d.	n.d.	n.d.
Sr	15285,96	14126,87	10271,11	9938,20	12112,82	11843,68	13428,49	13524,82	14520,33	10799,49	10582,65	10173,73	13032,34	16814,16	15477,22	13613,13	12777,04	13073,68	11492	11694	11166	11660	15999	15527	15307	16240	12040	11110	13980	12440	10832	11114,21	13259,35	12487,49
Y	294,59	283,70	224,07	230,52	253,97	225,12	363,04	273,86	260,88	208,05	245,63	212,79	307,46	374,11	325,83	348,17	223,22	261,50	100,6	276,7	217,0	295,0	405,6	381,9	409,3	420,4	369,9	350,5	422,1	210,5	299,0	241,16	415,93	313,96
Zr	17,36	5,66	1129,00	1,90	4,71	3,52	6,73	4,09	6,39	3,26	5,08	3,95	4,25	3,94	3,97	4,44	5,07	5,75	9,30	3,45	2,75	3,39	6,22	6,33	6,84	4,87	7,84	5,81	5,58	2,91	5,64	4,54	1,7	8,22
Nb	0,03	0,02	0,01	0,01	0,03	0,01	0,02	0,01	0,02	0,01	0,02	0,02	0,03	0,03	0,02	0,03	0,01	0,02	n.d.	n.d.	0,40	n.d.	n.d.	0,09	n.d.	n.d.	n.d.	n.d.	n.d.	0,16	n.d.	n.d.	n.d.	0,101
Mo	-	-	-	-	-	-	-	-	-	-	-	-	-	-	-	-	-	-	n.d.	n.d.	n.d.	n.d.	n.d.	n.d.	n.d.	n.d.	n.d.	n.d.	n.d.	n.d.	n.d.	0,83	n.d.	1,36
Sn	-	-	-	-	-	-	-	-	-	-	-	-	-	-	-	-	-	-	n.d.	n.d.	n.d.	n.d.	0,36	n.d.	n.d.	n.d.	n.d.	n.d.	n.d.	n.d.	n.d.	n.d.	n.d.	n.d.
Ba	8,16	5,63	4,21	2,45	3,22	3,51	5,43	6,28	3,38	3,53	3,22	6,21	4,25	14,25	7,14	7,56	15,32	83,11	8,84	6,00	4,39	2,90	4,00	3,29	5,82	4,53	9,55	3,01	4,60	3,81	3,53	2,31	1,31	4,68
La	3564,63	3741,66	3725,37	3964,53	4131,06	4990,97	4310,47	3419,14	3474,21	3356,12	4087,29	3690,38	3023,81	3070,31	3105,30	3474,63	3214,73	3723,24	2989	4299	3306	4487	4555	4193	4486	4379	4245	3986	2903	3260	4663	3629	3982	4073
Ce	7717,91	7761,55	7783,92	7409,56	7492,12	7024,90	7800,44	6149,74	7078,81	5899,87	7620,37	6791,64	6636,43	7846,92	7173,30	6464,16	5502,13	6213,71	3419	6869	5271	7080	7778	7149	8081	7561	7291	6662	5744	5227	7105	5615	8014	6563
Pr	686,65	685,93	609,44	625,34	641,40	598,09	714,76	560,75	652,89	519,01	651,12	596,37	632,65	761,93	700,39	646,23	496,83	576,36	258,8	596,2	470,8	647,5	773,3	707,4	776,0	758,1	713,9	644,1	639,3	494,6	646,7	518,5	913,1	632,0
Nd	2360,77	2307,23	1926,39	1999,42	2147,33	1955,27	2498,57	1951,68	2273,39	1720,47	2147,19	1859,55	2255,35	2613,17	2389,75	2326,86	1693,05	1973,43	833,2	2086	1713	2236	2863	2558	2807	2757	2561	2337	2500	1767	2322	1878	3656	2226
Sm	291,32	290,28	222,85	231,50	250,30	223,38	313,54	244,36	292,50	200,32	247,08	211,98	314,61	365,85	332,36	312,64	209,01	238,66	91,9	248,0	199,2	276,3	378,6	348,8	382,0	365,7	335,9	310,1	365,5	207,6	266,0	216,7	527,5	279,1
Eu	64,69	63,16	53,24	53,84	57,61	51,09	72,47	55,84	67,36	46,79	57,22	49,00	70,80	93,70	81,23	71,57	50,68	57,03	22,66	53,30	42,67	56,86	83,42	75,42	82,33	87,42	72,52	66,78	80,29	45,28	59,08	48,2	106,01	59,57
Gd	185,03	175,37	141,73	143,76	159,99	140,19	193,06	149,74	183,13	122,11	154,86	131,25	188,86	216,63	196,31	189,45	129,50	149,62	68,87	171,1	135,4	174,8	245,4	207,4	234,6	227,6	216,1	204,6	228,6	140,3	178,5	150,6	312,46	192,87
Gd ©	**164,00**	**154,00**	**120,00**	**123,00**	**139,00**	**120,00**	**171,00**	**132,00**	**132,00**	**136,00**	**163,00**	**105,00**	**142,00**	**133,00**	**112,00**	**101,00**	**99,00**	**136,00**	-	-	-	-	-	-	-	-	-	-	-	-	-	-	-	-
Tb	16,27	15,16	11,79	12,06	13,12	11,61	17,62	13,66	15,98	10,51	12,44	10,77	17,33	20,59	18,04	18,11	11,28	12,82	5,11	14,58	11,33	14,94	22,31	19,97	21,41	23,08	19,99	18,61	20,92	11,13	15,16	12,16	29,14	16,35
Tb ©	**15,80**	**14,70**	**11,30**	**11,60**	**12,70**	**11,20**	**17,10**	**13,30**	**12,40**	**13,10**	**15,50**	**10,20**	**13,90**	**12,00**	**10,40**	**9,80**	**9,40**	**14,30**	-	-	-	-	-	-	-	-	-	-	-	-	-	-	-	-
Dy	62,46	58,67	44,81	45,93	50,46	41,45	72,30	52,86	59,72	40,64	47,82	40,27	68,49	83,23	72,32	74,45	43,74	49,41	19,87	52,24	42,73	59,16	82,04	74,74	83,20	83,25	74,11	67,70	84,87	46,70	54,20	44,38	94,94	60,6
Ho	9,63	9,46	7,23	7,31	8,12	7,04	11,49	8,72	9,16	6,53	7,61	6,62	10,75	12,55	11,40	11,42	6,86	8,17	3,47	9,64	6,69	9,36	13,45	12,33	13,75	13,93	12,47	11,10	14,07	6,94	8,84	7,58	14,23	10,59
Er	20,66	20,69	16,30	16,66	18,25	16,14	26,84	19,89	19,86	14,41	17,40	15,57	23,34	27,64	25,32	25,29	17,01	18,30	7,97	21,79	15,34	22,44	32,02	29,90	30,51	29,68	28,12	28,43	33,65	17,45	21,46	17,07	29,85	25,06
Tm	2,37	2,22	1,95	1,97	2,06	1,78	3,12	2,41	2,08	1,72	2,03	1,71	2,71	3,27	2,95	2,95	1,93	2,20	0,92	2,51	2,03	2,44	3,78	3,48	3,52	3,16	3,46	3,00	3,57	1,66	2,43	1,8	3,07	2,65
Yb	14,41	14,13	12,41	12,70	12,88	11,48	20,98	15,85	12,76	10,39	12,60	11,23	15,14	19,73	17,30	17,72	13,07	14,61	6,57	15,62	11,32	16,48	22,30	19,07	22,92	21,83	21,49	17,38	19,93	12,62	15,49	11,78	17,21	20,06
Lu	2,05	1,82	1,77	1,84	1,85	1,62	2,71	2,06	1,69	1,41	1,83	1,59	1,85	2,34	2,11	2,20	1,84	2,17	1,26	2,15	1,92	2,35	2,96	2,55	2,82	2,60	2,87	2,20	2,44	1,91	2,39	1,83	2	2,75
Hf	0,26	0,17	0,16	0,08	0,21	0,11	0,21	0,21	0,25	0,14	0,19	0,17	0,26	0,23	0,23	0,18	0,11	0,14	n.d.	0,71	n.d.	n.d.	n.d.	1,00	n.d.	1,23	0,45	n.d.	0,93	0,30	n.d.	n.d.	0,79	1,35
Ta	0,01	0,02	0,02	0,01	0,01	0,01	0,01	n.d.	0,01	0,01	0,01	0,02	0,01	0,02	0,02	0,02	0,01	0,01	n.d.	n.d.	n.d.	0,10	n.d.	n.d.	n.d.	0,13	0,07	n.d.	0,06	n.d.	n.d.	0,019	n.d.	n.d.
Pb	34,26	34,89	38,58	35,29	34,23	36,77	33,49	31,48	31,63	27,02	36,99	35,09	42,53	30,63	31,93	43,07	46,85	32,41	26,43	35,92	20,15	26,53	27,57	27,68	29,84	26,52	30,15	27,41	23,55	20,08	23,48	19,35	15,74	20,47
Th	95,92	125,40	122,25	129,50	144,42	129,29	169,35	100,72	111,28	75,91	140,85	126,03	82,35	128,17	97,62	88,52	105,82	119,58	110,2	144,7	85,88	156,6	177,9	149,0	173,9	148,6	138,1	119,0	119,9	63,43	149,8	98,66	84,82	124,62
U	5,44	4,75	8,05	7,60	8,64	6,43	8,64	5,63	6,66	5,63	9,42	6,97	5,03	8,71	6,74	4,87	5,03	6,41	6,13	7,57	4,55	7,70	7,61	7,59	7,69	7,00	6,43	5,11	4,83	2,41	6,93	4,6	0,338	6,91
Th	102,88	103,94	125,91	263,39	150,84	140,61	155,72	94,87	116,99	74,81	154,20	127,53	79,10	130,54	96,80	84,74	74,60	109,09	n.d.	n.d.	n.d.	n.d.	n.d.	n.d.	n.d.	n.d.	n.d.	n.d.	n.d.	n.d.	n.d.	n.d.	n.d.	n.d.
U	5,56	3,74	7,74	9,03	7,81	8,86	9,02	4,93	6,67	6,12	9,62	7,57	4,84	8,38	7,49	5,00	4,29	4,90	-	-	-	-	-	-	-	-	-	-	-	-	-	-	-	-

LA-ICP-MS results obtained for apatite – Sample PB-181 - Continuation

LA-ICP-MS - Elementos Traço normalizado por Condrito - PB-181 (LSS)

	AP01a	AP01b	AP02a	AP02b	AP03a	AP03b	AP04a	AP04b	AP05a_spo	AP06a_spo	AP07a	AP07b	AP08a_spo	AP09a	AP09b	AP10a_spo	AP11a_spo	AP11b_spo
Li	-	-	-	-	-	-	-	-	-	-	-	-	-	-	-	-	-	-
B	-	0,64	0,57	0,85	0,46	0,55	0,88	-	0,57	-	0,48	0,48	-	0,75	0,24	-	1,54	0,55
Na	-	-	-	-	-	-	-	-	-	-	-	-	-	-	-	-	-	-
Mg	0,00	0,00	0,00	0,00	0,00	0,00	0,00	0,00	0,00	0,00	0,00	0,00	0,00	0,00	0,00	0,00	0,00	0,00
Al	-	-	-	-	-	-	-	-	-	-	-	-	-	-	-	-	-	-
Si	0,02	0,02	0,02	0,02	0,02	0,02	0,02	0,02	0,02	0,02	0,02	0,02	0,02	0,03	0,02	0,02	0,02	0,03
P	110,51	107,64	106,63	102,71	101,01	100,04	88,47	92,87	104,52	90,82	100,89	103,19	101,83	105,15	102,69	93,33	92,11	88,65
K	-	-	-	-	-	-	-	-	-	-	-	-	-	-	-	-	-	-
Ca	29,12	29,12	29,12	29,12	29,12	29,12	29,12	29,12	29,12	29,12	29,12	29,12	29,12	29,12	29,12	29,12	29,12	29,12
Cs	0,01	0,01	<LQ	<LQ	<LQ	0,01	0,01	<LQ	<LQ	<LQ	<LQ	<LQ	<LQ	<LQ	<LQ	0,01	0,01	<LQ
Sc	-	-	-	-	-	-	-	-	-	-	-	-	-	-	-	-	-	-
Ti	1265,00	1230,00	1244,00	1213,00	1225,00	1162,00	1196,00	1202,00	1219,00	1208,00	1229,00	1229,00	1187,00	1202,00	1173,00	1211,00	1224,00	1215,00
V	1241,00	1202,00	1436,00	1065,00	1652,00	1100,00	1472,00	1088,00	1398,00	0,82	1554,00	0,95	1458,00	1213,00	1480,00	1145,00	1263,00	1189,00
Cr	-	-	-	-	-	-	-	-	-	-	-	-	-	-	-	-	-	-
Mn	0,12	0,11	0,10	0,08	0,10	0,09	0,10	0,10	0,09	0,09	0,09	0,09	0,10	0,09	0,10	0,11	0,10	0,09
Fe	0,00	0,00	0,00	0,00	0,00	0,00	0,00	0,00	0,00	0,00	0,00	0,00	0,00	0,00	0,00	0,00	0,00	0,00
Co	-	-	-	-	-	-	-	-	-	-	-	-	-	-	-	-	-	-
Ni	-	-	-	-	-	-	-	-	-	-	-	-	-	-	-	-	-	-
Cu	-	-	-	-	-	-	-	-	-	-	-	-	-	-	-	-	-	-
Zn	-	-	-	-	-	-	-	-	-	-	-	-	-	-	-	-	-	-
Ga	0,03	0,03	0,03	0,02	0,03	0,02	0,02	0,05	0,03	0,02	0,03	0,03	0,03	0,05	0,03	0,03	0,04	0,07
Ge	8,84	8,98	9,49	8,68	9,18	8,58	9,05	7,07	8,33	7,24	9,15	8,39	7,78	9,28	8,53	7,73	6,52	7,50
As	16,45	14,63	14,88	15,21	15,49	12,19	13,65	13,37	13,38	12,65	11,52	14,92	14,15	16,11	14,81	9,38	9,64	12,30
Rb	0,30	0,01	0,02	0,01	<LQ	0,01	0,02	0,55	<LQ	0,01	0,01	0,02	0,01	0,09	0,03	<LQ	0,32	0,06
Sr	1284,53	1187,13	863,12	835,14	1017,88	995,27	1128,44	1136,54	1220,20	907,52	889,30	854,94	1095,15	1412,95	1300,61	1143,96	1073,70	1098,63
Y	130,93	126,09	99,59	102,45	112,88	100,05	161,35	121,72	115,95	92,47	109,17	94,57	136,65	166,27	144,81	154,74	99,21	116,22
Zr	3,13	1021,00	0,20	0,34	0,85	0,64	1214,00	0,74	1154,00	0,59	0,92	0,71	0,77	0,71	0,72	0,80	0,92	1037,00
Nb	0,09	0,06	0,04	0,02	0,07	0,03	0,06	0,03	0,06	0,03	0,06	0,04	0,09	0,07	0,05	0,08	0,04	0,05
Mo	-	-	-	-	-	-	-	-	-	-	-	-	-	-	-	-	-	-
Sn	-	-	-	-	-	-	-	-	-	-	-	-	-	-	-	-	-	-
Ba	2,39	1650,00	1233,00	0,72	0,95	1030,00	1593,00	1,84	0,99	1037,00	0,95	1,82	1245,00	4,18	2,09	2,22	4,49	24,37
La	15040,63	15787,59	15718,86	16727,97	17430,63	21058,95	18187,64	14426,75	14659,11	14160,84	17245,95	15571,22	12758,69	12954,89	13102,53	14660,89	13564,26	15709,87
Ce	12610,96	12682,27	12718,82	12107,12	12242,03	11478,59	12745,82	10048,59	11566,68	9640,31	12451,58	11097,45	10843,84	12821,76	11721,08	10562,35	8990,41	10153,12
Pr	7227,89	7220,32	6415,16	6582,53	6751,58	6295,68	7523,79	5902,63	6872,53	5463,26	6853,89	6277,58	6659,47	8020,32	7372,53	6802,42	5229,79	6066,95
Nd	5055,18	4940,54	4125,03	4281,41	4598,14	4186,87	5350,26	4179,19	4868,07	3684,09	4597,84	3981,91	4829,44	5595,65	5117,24	4982,57	3625,37	4225,76
Sm	1904,05	1897,25	1456,54	1513,07	1635,95	1460,00	2049,28	1597,12	1911,76	1309,28	1614,90	1385,49	2056,27	2391,18	2172,29	2043,40	1366,08	1559,87
Eu	1115,34	1088,97	917,93	928,28	993,28	880,86	1249,48	962,76	1161,38	806,72	986,55	844,83	1220,69	1615,52	1400,52	1233,97	873,79	983,28
Gd	798,00	749,00	584,00	599,00	676,00	584,00	832,00	642,00	642,00	662,00	793,00	511,00	691,00	647,00	545,00	491,00	482,00	662,00
Tb	422,00	393,00	302,00	310,00	340,00	299,00	457,00	356,00	332,00	350,00	414,00	273,00	372,00	321,00	278,00	262,00	251,00	369,00
Dy	245,91	230,98	176,42	180,83	198,66	163,19	284,65	208,11	235,12	160,00	188,27	158,54	269,65	327,68	284,72	293,11	172,20	194,53
Ho	170,14	167,14	127,74	129,15	143,46	124,38	203,00	154,06	161,84	115,37	134,45	116,96	189,93	221,73	201,41	201,77	121,20	144,35
Er	124,83	125,02	98,49	100,66	110,27	97,52	162,18	120,18	120,00	87,07	105,14	94,08	141,03	167,01	152,99	152,81	102,78	110,57
Tm	92,94	87,22	76,47	77,10	80,63	69,61	122,35	94,51	81,57	67,57	79,73	67,14	106,27	128,24	115,69	115,69	75,65	86,27
Yb	84,76	83,12	73,00	74,71	75,76	67,53	123,41	93,24	75,06	61,12	74,12	66,06	89,06	116,06	101,76	104,24	76,88	85,94
Lu	80,71	71,77	69,49	72,56	72,76	63,94	106,69	80,94	66,69	55,43	71,93	62,40	72,68	92,13	82,99	86,61	72,36	85,43
Hf	1,44	0,93	0,88	0,45	1,18	0,63	1,20	1,16	1,38	0,79	1,03	0,97	1,46	1,29	1,29	0,98	0,59	0,75
Ta	0,48	0,69	0,67	0,34	0,34	0,26	0,48	<LQ	0,55	0,42	0,44	0,61	0,56	0,91	0,71	0,84	0,53	0,31
Pb	9,39	9,56	10,57	9,67	9,38	10,07	9,18	8,62	8,66	7,40	10,13	9,61	11,65	8,39	8,75	11,80	12,84	8,88
Th	2257,04	2950,52	2876,40	3047,13	3398,18	3042,01	3984,79	2369,79	2618,41	1786,23	3314,10	2965,36	1937,64	3015,73	2297,00	2082,93	2489,81	2813,60
U	446,27	389,46	659,87	623,13	708,55	527,06	708,35	461,62	546,12	461,70	772,24	570,92	412,30	714,08	552,58	398,86	412,02	525,76
Th	2420,80	2445,65	2962,64	6197,40	3549,28	3308,36	3664,10	2232,27	2752,74	1760,35	3628,18	3000,59	1861,10	3071,52	2277,60	1993,84	1755,28	2566,78
U	455,81	306,72	634,12	739,97	640,27	726,50	739,64	404,18	547,03	501,80	788,34	620,60	396,51	687,07	613,60	409,49	351,60	401,41

	ap52	ap53	ap54	ap55	ap56	ap57	ap58	ap59	ap61	ap62	ap63	ap64	ap65	ap66	ap67	ap68
Li	-	1,15	0,55	0,57	0,57	-	-	-	0,88	-	-	-	-	-	-	0,66
B	-	-	-	-	-	-	-	-	-	-	-	-	-	23,22	-	-
Na	0,24	0,33	0,28	0,33	0,35	0,34	0,34	0,32	0,33	0,35	0,27	0,37	0,31	0,32	0,40	0,33
Mg	0,00	0,00	0,00	0,00	0,00	0,00	0,00	0,00	0,00	0,00	0,00	0,00	0,00	0,00	0,00	0,00
Al	0,08	0,02	0,00	-	-	0,00	0,00	-	0,01	-	0,00	0,00	-	-	-	0,00
Si	0,03	0,03	0,02	0,02	0,02	-	0,02	0,04	0,03	0,02	-	0,03	-	-	0,04	0,02
P	55,99	56,05	52,89	56,86	57,36	53,66	56,26	57,77	55,86	57,05	54,59	55,83	55,11	55,25	54,78	55,18
K	0,09	0,06	-	-	0,06	0,05	-	0,07	0,10	-	-	-	-	-	0,08	-
Ca	28,23	28,23	28,23	28,23	28,23	28,23	28,23	28,23	28,23	28,23	28,23	28,23	28,23	28,23	28,23	28,23
Cs	-	-	-	-	-	-	-	-	-	-	-	-	-	-	-	-
Sc	0,16	<LQ	0,11	<LQ	<LQ	<LQ	<LQ	<LQ	0,17	<LQ	<LQ	<LQ	<LQ	<LQ	<LQ	<LQ
Ti	1,11	1,11	1,06	1,10	1,10	1,06	1,06	1,14	1,08	1,13	1,09	1,11	1,06	1,09	1,08	1,06
V	1,42	0,81	0,81	1,00	1,36	0,94	1,58	1,55	1,34	1,39	1,24	0,56	1,49	1,08	1,21	0,88
Cr	<LQ	0,00	<LQ	<LQ	<LQ	<LQ	<LQ	<LQ	<LQ	<LQ	<LQ	<LQ	<LQ	<LQ	<LQ	<LQ
Mn	0,10	0,08	0,08	0,08	0,11	0,11	0,11	0,14	0,09	0,08	0,05	0,10	0,08	0,08	0,09	0,11
Fe	0,00	0,00	0,00	0,00	0,00	0,00	0,00	0,00	0,00	0,00	0,00	0,00	0,00	0,00	0,00	0,00
Co	0,00	0,00	0,00	0,00	0,00	0,00	0,00	0,00	<LQ	0,00	0,00	0,00	<LQ	0,00	0,00	0,00
Ni	0,00	0,00	0,00	0,00	0,00	0,00	0,00	0,00	0,00	0,00	0,00	-	0,00	0,00	0,00	0,00
Cu	<LQ	0,06	<LQ	<LQ	<LQ	<LQ	<LQ	<LQ	0,02	<LQ	<LQ	<LQ	<LQ	<LQ	<LQ	<LQ
Zn	0,01	0,01	0,01	0,00	<LQ	0,01	<LQ	0,01	0,01	<LQ	<LQ	-	<LQ	<LQ	<LQ	0,01
Ga	0,03	<LQ	0,04	<LQ	<LQ	<LQ	0,05	<LQ	<LQ	<LQ	<LQ	0,07	<LQ	<LQ	<LQ	<LQ
Ge	3,31	6,56	5,03	6,67	7,33	6,42	7,69	7,10	6,44	6,49	5,60	5,18	6,53	5,47	8,10	6,29
As	10,40	14,56	12,72	12,28	13,49	15,37	13,80	13,01	12,25	12,31	11,94	12,08	11,32	11,24	16,75	11,67
Rb	0,16	<LQ	0,21	<LQ	<LQ	<LQ	<LQ	<LQ	<LQ	<LQ	<LQ	<LQ	2,13	<LQ	<LQ	<LQ
Sr	965,70	982,67	938,36	979,81	1344,49	1304,82	1286,27	1364,70	1011,73	933,57	1174,80	1045,34	910,26	933,97	1114,23	1049,37
Y	44,71	122,97	96,46	131,09	180,25	169,74	181,90	186,83	164,41	155,76	187,59	93,54	132,87	107,18	184,86	139,54
Zr	1,68	0,62	0,50	0,61	1,12	1,14	1,24	0,88	1,42	1,05	1,01	0,53	1,02	0,82	0,31	1,48
Nb	<LQ	<LQ	1,07	<LQ	<LQ	0,23	<LQ	<LQ	<LQ	<LQ	<LQ	0,43	<LQ	<LQ	<LQ	0,27
Mo	<LQ	<LQ	<LQ	<LQ	<LQ	<LQ	<LQ	<LQ	<LQ	<LQ	<LQ	<LQ	<LQ	0,60	<LQ	0,99
Sn	<LQ	<LQ	<LQ	<LQ	0,14	<LQ	<LQ	<LQ	<LQ	<LQ	<LQ	<LQ	<LQ	<LQ	<LQ	<LQ
Ba	2,59	1,76	1,29	0,85	1,17	0,96	1,71	1,33	2,80	0,88	1,35	1,12	1,04	0,68	0,39	1,37
La	8144	11715	9009	12227	12410	11426	12224	11932	11566	10861	7911	8884	12707	9887	10849	11098
Ce	3573	7177	5507,4	7398	8127	7470	8444	7901	7619	6961	6002	5462	7424	5867	8374	6858
Pr	1889	4352	3436	4726	5644	5163	5664	5533	5211	4702	4666	3610	4721	3785	6665	4613
Nd	1172	2934	2409	3145	4027	3598	3948	3877	3601	3287	3516	2485	3266	2641	5142	3130
Sm	397,7	1074	862,5	1196	1639	1510	1654	1583	1454	1343	1582	898,5	1151	938,2	2284	1208
Eu	260,5	612,7	490,5	653,6	958,8	866,8	946,3	1005	833,6	767,6	922,9	520,5	679,0	554,0	1219	684,7
Gd	225,1	559,25	442,62	571,07	801,90	677,64	766,71	743,89	706,06	668,74	746,94	458,60	583,25	492,15	1021,10	630,31
Tb	88,11	251,3	195,4	257,7	384,6	344,3	369,2	397,9	344,6	320,9	360,6	191,9	261,4	209,6	502,5	281,9
Dy	52,15	137,1	112,2	155,3	215,3	196,2	218,4	218,5	194,5	177,7	222,8	122,6	142,3	116,5	249,2	159,1
Ho	40,79	113,3	78,64	110,0	158,1	144,9	161,6	163,7	146,5	130,5	165,3	81,58	103,9	89,07	167,2	124,5
Er	31,99	87,50	61,62	90,11	128,6	120,10	122,54	119,2	112,9	114,2	135,1	70,10	86,19	68,55	119,9	100,6
Tm	25,81	70,51	57,12	68,45	106,1	97,87	98,74	88,88	97,30	84,18	100,26	46,57	68,14	50,64	86,35	74,54
Yb	26,50	62,99	45,63	66,46	89,93	76,89	92,43	88,02	86,67	70,07	80,36	50,88	62,46	47,50	69,41	80,87
Lu	33,00	56,36	50,27	61,78	77,80	66,83	74,09	68,33	75,42	57,83	64,04	50,14	62,63	47,96	52,37	72,22
Hf	<LQ	3,97	<LQ	<LQ	<LQ	5,58	<LQ	6,87	2,52	<LQ	5,19	1,68	<LQ	<LQ	4,42	7,56
Ta	<LQ	<LQ	<LQ	3,84	<LQ	<LQ	<LQ	4,99	2,58	<LQ	2,35	<LQ	<LQ	0,73	<LQ	<LQ
Pb	7,24	9,84	5,52	7,27	7,55	7,58	8,18	7,27	8,26	7,51	6,45	5,50	6,43	5,30	4,31	5,61
Th	2593,13	3405,44	2020,72	3684,73	4186,60	3505,98	4091,92	3497,20	3248,37	2799,90	2822,19	1492,46	3523,73	2321,49	1995,65	2932,29
U	502,76	620,21	373,05	631,20	623,82	622,05	629,93	573,55	527,14	419,02	395,70	197,29	567,88	377,36	27,68	566,54
Th	<LQ	<LQ	<LQ	<LQ	<LQ	<LQ	<LQ	<LQ	<LQ	<LQ	<LQ	<LQ	<LQ	<LQ	<LQ	<LQ
U	<LQ	<LQ	<LQ	<LQ	<LQ	<LQ	<LQ	<LQ	<LQ	<LQ	<LQ	<LQ	<LQ	<LQ	<LQ	<LQ

LA-ICP-MS results obtained for apatite – Sample PB-185

	LA-ICP-MS - Concentração de Elementos Traço (Ppm) - PB-185 (LSS).													
Element	AP01a_spot	AP01b_spot	AP02a_spot	AP02b_spot	AP03a	AP03b	AP04a	AP04b	AP05a	AP05b	AP06a_spot	AP06b_spot	AP07a	AP07b
B	3,40	6,45	1,31	1,11	3,01	2,62	1,77	1,39	4,04	2,33	2,96	1,35	1,01	2,09
Mg	190,99	1041,05	160,98	127,00	645,85	610,33	44,17	44,98	42,91	66,28	608,10	70,84	45,07	589,68
Si	5007,62	7182,00	2468,32	3648,87	6451,59	5771,17	3259,98	3319,92	3811,26	4355,81	4823,03	3505,26	3206,32	4849,36
P	217718,69	223280,59	223184,45	234193,20	234115,52	232024,45	224306,41	234046,72	229917,06	230504,05	220281,88	276598,66	239049,09	227931,38
Ca	393085,59	393085,59	393085,59	393085,56	393085,56	393085,56	393085,56	393085,56	393085,53	393085,53	393085,53	393085,53	393085,53	393085,53
Cs	0,14	0,51	0,10	0,08	0,34	0,28	0,08	<0,053	<0,057	<0,055	0,18	0,11	0,09	0,24
Ti	760,58	776,78	771,06	787,53	782,75	775,54	754,99	793,43	769,80	785,95	775,06	813,62	798,88	757,15
V	61,29	64,57	15,32	19,31	32,53	31,23	35,38	35,13	30,51	25,13	34,51	48,62	17,87	22,06
Mn	536,57	545,75	506,74	529,73	470,57	461,56	503,50	490,36	523,72	511,77	566,01	578,96	550,69	542,12
Fe	598,92	1126,20	260,58	331,51	781,77	721,86	311,36	314,80	317,52	346,04	1634,78	349,49	287,42	719,89
Ga	13,18	1,05	0,29	0,36	0,82	0,73	0,36	0,35	0,74	0,58	0,54	0,71	0,58	0,82
Ge	570,76	535,83	269,37	382,60	603,98	566,33	409,68	433,44	477,54	507,85	395,61	424,29	408,73	446,60
As	41,38	35,35	19,24	29,21	41,57	38,47	36,95	37,42	37,69	41,95	36,55	39,76	35,62	36,14
Rb	0,21	0,36	0,08	0,02	0,15	0,18	<0,0229	<0,028	<0,029	<0,027	<0,036	0,11	0,04	0,12
Sr	26870,45	25385,34	21475,39	21082,54	23753,42	22814,94	22586,23	23001,04	22428,27	23449,46	25220,40	26869,87	23475,18	23130,48
Y	333,67	284,22	146,75	215,36	384,40	328,29	267,45	279,30	294,75	326,22	198,09	198,01	215,35	234,50
Zr	5,70	4,62	2,98	3,68	3,16	2,40	5,27	4,90	5,59	6,35	3,29	3,70	1,88	2,28
Nb	0,04	0,02	0,02	0,01	0,03	0,03	0,01	0,01	0,03	0,02	0,01	0,02	0,01	0,02
Ba	879,62	7,73	5,17	6,63	6,84	6,02	4,21	6,78	24,87	13,37	7,56	29,13	21,07	15,82
La	5348,72	5543,14	4871,81	4677,28	4949,95	4434,03	3893,71	4040,56	4369,63	4746,69	3824,46	3868,22	3777,55	4032,89
Ce	10416,08	9494,62	9046,19	8525,56	10608,63	9483,30	7298,78	7667,46	8631,39	8946,56	6902,41	7152,65	7025,20	7286,98
Pr	974,46	847,08	860,05	842,17	991,38	889,67	692,05	719,79	783,09	842,43	577,20	607,53	636,78	646,65
Nd	3152,93	2719,83	1406,42	1993,74	3428,82	3036,27	2366,30	2486,91	2700,62	2893,60	1921,27	1988,27	2028,59	2165,53
Sm	380,39	318,94	164,29	245,66	441,22	388,83	299,04	313,08	331,21	361,61	218,03	226,55	236,22	258,50
Eu	94,07	78,77	40,78	59,69	103,65	91,72	69,65	71,38	75,45	81,56	52,35	55,93	56,85	63,05
Gd	233,61	200,80	103,21	149,27	261,26	227,55	180,45	187,64	202,45	222,46	133,82	141,23	141,43	156,70
Gd ©	**204,00**	**174,00**	**78,00**	**125,00**	**232,00**	**201,00**	**160,00**	**166,00**	**178,00**	**197,00**	**114,00**	**121,00**	**122,00**	**136,00**
Tb	19,29	16,60	8,41	12,16	22,67	19,65	15,46	16,07	17,22	19,04	11,03	11,53	12,14	13,28
Tb ©	**18,70**	**16,00**	**7,90**	**11,60**	**22,00**	**19,10**	**15,00**	**15,60**	**16,70**	**18,50**	**10,60**	**11,10**	**11,70**	**12,80**
Dy	71,47	62,11	30,92	44,35	85,72	73,62	57,24	59,97	62,48	71,15	40,08	39,74	45,28	48,90
Ho	10,90	9,22	4,71	6,99	12,82	11,07	8,81	9,05	9,71	11,06	5,95	6,31	6,84	7,45
Er	24,27	19,92	10,34	14,72	27,23	23,61	18,82	19,92	20,85	23,57	13,12	13,48	15,05	16,58
Tm	2,56	2,07	1,08	1,66	2,83	2,59	1,90	2,00	2,12	2,44	1,39	1,36	1,62	1,72
Yb	15,34	12,04	6,64	9,77	16,50	14,40	12,22	12,59	12,48	14,54	8,12	8,52	9,64	10,79
Lu	2,11	1,82	0,88	1,33	2,05	1,80	1,60	1,68	1,76	1,96	1,24	1,27	1,41	1,58
Hf	0,27	0,23	0,09	0,17	0,19	0,17	0,18	0,12	0,20	0,22	0,10	0,09	0,19	0,19
Ta	0,01	0,02	0,01	0,01	0,03	0,01	0,01	0,01	0,01	0,02	<0,0056	0,01	0,01	0,01
Pb	69,34	58,47	31,02	44,30	56,60	52,33	45,16	47,64	50,43	52,64	53,58	56,42	46,39	46,67
Th	362,57	191,70	117,56	168,26	264,43	199,93	125,29	143,77	192,84	226,49	138,41	136,04	140,42	171,03
U	27,31	18,35	9,44	13,09	23,69	19,34	10,39	11,40	14,14	15,48	11,12	12,14	11,14	13,02
Th	371,69	189,60	121,42	174,91	275,25	207,94	127,60	129,75	196,66	218,16	141,33	130,91	144,65	174,92
U	26,56	17,49	10,22	13,15	22,75	21,62	8,45	8,95	15,00	16,68	10,10	13,99	11,31	12,22

	LA-ICP-MS - Elementos Traço normalizado por Condrito - PB-181 (LSS)													
Element	AP01a_spot	AP01b_spot	AP02a_spot	AP02b_spot	AP03a	AP03b	AP04a	AP04b	AP05a	AP05b	AP06a_spot	AP06b_spot	AP07a	AP07b
B	1,79	3,40	0,69	0,58	1,58	1,38	0,93	0,73	2,13	1,23	1,56	0,71	0,53	1,10
Mg	0,00	0,01	0,00	0,00	0,00	0,00	0,00	0,00	0,00	0,00	0,00	0,00	0,00	0,00
Si	0,03	0,04	0,02	0,02	0,04	0,04	0,02	0,02	0,02	0,03	0,03	0,02	0,02	0,03
P	94,66	97,08	97,04	101,82	101,79	100,88	97,52	101,76	99,96	100,22	95,77	120,26	103,93	99,10
Ca	29,12	29,12	29,12	29,12	29,12	29,12	29,12	29,12	29,12	29,12	29,12	29,12	29,12	29,12
Cs	0,02	0,06	0,01	0,01	0,04	0,03	0,01	0,00	0,00	0,00	0,02	0,01	0,01	0,03
Ti	1163,00	1188,00	1179,00	1204,00	1197,00	1186,00	1154,00	1213,00	1177,00	1202,00	1185,00	1244,00	1222,00	1158,00
V	0,72	0,76	0,18	0,23	0,38	0,37	0,42	0,41	0,36	0,30	0,41	0,57	0,21	0,26
Mn	0,18	0,19	0,17	0,18	0,16	0,16	0,17	0,17	0,18	0,17	0,19	0,20	0,19	0,18
Fe	0,00	0,00	0,00	0,00	0,00	0,00	0,00	0,00	0,00	0,00	0,01	0,00	0,00	0,00
Ga	0,87	0,07	0,02	0,02	0,05	0,05	0,02	0,02	0,05	0,04	0,04	0,05	0,04	0,05
Ge	11,82	11,09	5,58	7,92	12,50	11,73	8,48	8,97	9,89	10,51	8,19	8,78	8,46	9,25
As	14,42	12,32	6,70	10,18	14,48	13,40	12,87	13,04	13,13	14,62	12,74	13,85	12,41	12,59
Rb	0,06	0,10	0,02	0,01	0,04	0,05	0,00	0,00	0,00	0,00	0,00	0,03	0,01	0,03
Sr	2258,02	2133,22	1804,65	1771,64	1996,09	1917,22	1898,00	1932,86	1884,73	1970,54	2119,36	2257,97	1972,70	1943,74
Y	148,30	126,32	65,22	95,72	170,84	145,90	118,87	124,14	131,00	144,99	88,04	88,00	95,71	104,22
Zr	1029,00	0,83	0,54	0,66	0,57	0,43	0,95	0,88	1009,00	1147,00	0,59	0,67	0,34	0,41
Nb	0,10	0,07	0,04	0,03	0,08	0,07	0,03	0,04	0,07	0,05	0,03	0,06	0,03	0,04
Ba	257,95	2,27	1517,00	1943,00	2,00	1766,00	1236,00	1,99	7,29	3,92	2,22	8,54	6,18	4,64
La	22568,44	23388,78	20556,16	19735,36	20885,86	18708,99	16429,16	17048,78	18437,26	20028,23	16136,96	16321,60	15939,08	17016,41
Ce	17019,74	15514,08	14781,36	13930,65	17334,36	15495,59	11926,11	12528,53	14103,58	14618,56	11278,45	11687,34	11479,08	11906,83
Pr	10257,47	8916,63	9053,16	8864,95	10435,58	9364,95	7284,74	7576,74	8243,05	8867,68	6075,79	6395,05	6702,95	6806,84
Nd	6751,46	5824,05	3011,61	4269,25	7342,23	6501,65	5067,02	5325,29	5782,91	6196,15	4114,07	4257,54	4343,88	4637,11
Sm	2486,21	2084,58	1073,79	1605,62	2883,79	2541,37	1954,51	2046,27	2164,77	2363,46	1425,03	1480,72	1543,92	1689,54
Eu	1621,90	1358,10	703,10	1029,14	1787,07	1581,38	1200,86	1230,69	1300,86	1406,21	902,59	964,31	980,17	1087,07
Gd	992,70073	846,7153	379,562	608,2725	1128,954	978,1022	778,5888	807,7859	866,18	958,6375	554,7445	588,8078	593,674	661,8005
Gd ©	-	-	-	-	-	-	-	-	-	-	-	-	-	-
Tb	500	427,8075	211,2299	310,1604	588,2353	510,6952	401,0695	417,1123	446,5241	494,6524	283,4225	296,7914	312,8342	342,246
Tb ©	-	-	-	-	-	-	-	-	-	-	-	-	-	-
Dy	281,38	244,53	121,73	174,61	337,48	289,84	225,35	236,10	245,98	280,12	157,80	156,46	178,27	192,52
Ho	192,58	162,90	83,22	123,50	226,50	195,58	155,65	159,89	171,55	195,41	105,12	111,48	120,85	131,63
Er	146,65	120,36	62,48	88,94	164,53	142,66	113,72	120,36	125,98	142,42	79,27	81,45	90,94	100,18
Tm	100,39	81,06	42,43	65,02	110,98	101,57	74,63	78,27	83,22	95,69	54,39	53,37	63,61	67,25
Yb	90,24	70,82	39,06	57,47	97,06	84,71	71,88	74,06	73,41	85,53	47,76	50,12	56,71	63,47
Lu	82,87	71,61	34,45	52,48	80,71	70,71	63,15	65,94	69,13	77,17	48,86	49,80	55,55	62,24
Hf	1,52	1,27	0,48	0,92	1,08	0,95	1,01	0,66	1,09	1,20	0,58	0,48	1,09	1,06
Ta	0,54	0,87	0,28	0,43	1,32	0,50	0,45	0,37	0,35	0,71	0,00	0,35	0,26	0,51
Pb	19,00	16,02	8,50	12,14	15,51	14,34	12,37	13,05	13,82	14,42	14,68	15,46	12,71	12,79
Th	8530,98	4510,65	2766,03	3959,00	6221,97	4704,27	2947,97	3382,74	4537,44	5329,17	3256,76	3200,87	3303,99	4024,27
U	2238,75	1503,99	773,86	1073,10	1941,76	1585,13	852,00	934,17	1158,67	1269,18	911,68	994,69	913,17	1067,03
Th	8745,69	4461,14	2856,86	4115,50	6476,49	4892,70	3002,40	3052,98	4627,31	5133,24	3325,50	3080,31	3403,42	4115,76
U	2177,27	1433,70	838,00	1077,85	1864,71	1771,99	692,96	733,92	1229,19	1367,24	827,95	1146,98	926,79	1001,34

Titanite

LA-ICP-MS results obtained for titanite – Sample PB-123

LA-ICP-MS - Concentração de Elementos Traço (Ppm) - PB-123 (LSO).								
Element	**Tit_1**	**Tit_2**	**Tit_3**	**Tit_4**	**Tit_5**	**Tit_6**	**Tit_7**	**Tit_8**
Li	0,37	43,9	0,54	0,402	<0.197	0,22	0,69	0,3
Mg	890,41	22275,81	730,56	948,51	955,77	913,55	660,98	881,01
Al	10749,65	24301,2	10620,42	10656,71	10805,68	10155,9	10728,01	10957,08
Si	147446,56	185454,84	138795,13	140021,14	143806,28	142085,36	137363,19	143092,8
P	501,7	232,23	387,16	485,53	517,39	472,86	479,1	374,95
Ca42	202730,02	198684,14	197674,59	194162,72	199523,53	196155,67	194316,81	201039,23
Ca44	200116,28	200116,28	200116,28	200116,27	200116,27	200116,27	200116,25	200116,25
Sc	10,21	8,76	8,83	11,5	10,77	11,39	10,88	9,78
Ti46	186566,2	182324,44	180727,86	176004,44	179915,58	178666,67	174716,95	177340,7
Ti49	208861,77	204676,64	205177,09	199436,5	200139,63	201074,83	196444,8	204741,89
V	695,21	717,48	689,9	675,01	671,09	667,16	659,26	664,08
Cr	125,93	127,56	122,6	124,97	112,84	93,95	128,07	114,97
Mn	779,09	846,76	802,23	812,98	820,26	813,96	747,6	794,93
Fe	18826,5	29482,62	16985,14	18840,13	18794,49	19638,29	17927,81	18177,28
Co	0,257	13,81	0,213	0,195	0,199	0,356	0,529	0,179
Sr	299,04	255,04	273,84	300,75	296,02	322,65	277,35	288,2
Y	1358,65	1084,66	1146,6	983,97	1076,07	1367,94	726,08	1263,62
Zr	1400,9	1062,61	1229,86	1343,29	1319,6	1468,12	1427,03	1120,34
Nb	713,37	514,38	600,05	593,64	643,58	789,75	599,45	665,64
Sn	85,67	66,45	83,19	73,67	81,02	90,08	82,37	80,42
Sb	<0.47	<0.76	<0.49	<0.42	<0.46	<0.47	<0.47	<0.49
Ba	0,42	831,05	0,7	0,21	0,48	0,25	1,52	0,31
La	2631,2	2534,46	2404,86	2211,08	2342,52	2563,25	2016,86	2548,14
Ce	9163,2	8343,04	8281,88	7583,46	8034,58	9340,86	6371,26	9046,5
Pr	1354,25	1243,6	1190,99	1075,35	1149,92	1414,54	839,93	1358,79
Nd	6658,12	5425,58	5445,56	4935,77	5389,78	6888,49	3630,64	6470,19
Sm	1363,8	1079,66	1047,03	939,39	1076,03	1403,78	644,53	1329,07
Eu	305,2	312,42	308,81	245,95	275,61	286,27	171,03	303,25
Gd	767,17	579,23	623,18	522,86	608,92	801,26	359,12	750,37
Tb	87,92	66,75	71,99	58,84	69,64	91,88	41,41	84,9
Dy	392,19	305,67	313,81	252,88	303,21	408,13	190,77	374,69
Ho	57,3	44,91	46,68	38,55	44,62	58,32	29,25	54,16
Er	125,13	100,36	100,43	84,36	98,63	123,18	68,05	115,47
Tm	14,9	12,19	12,53	10,3	12,34	14,55	8,61	13,89
Yb	86,47	76,68	75,94	62	71,62	81,7	59,8	80,79
Lu	9,67	8,35	8,44	7,46	8,4	8,87	7,36	8,89
Hf	60,07	39,38	46,33	51,21	56,35	64,93	62,49	48,51
Ta	38,96	16,23	23,51	28,01	38,45	60,43	31,42	34,58
Pb	21,9	21,76	21,29	17,21	18,39	19,55	23,54	20,6
Pb	4,67	9,4	4,55	3,91	4,1	4,53	4,28	4,09
Pb	21,74	24	18,64	14,78	17,58	18,99	18,18	21,04
Th	333,31	278,75	280,62	209,67	252,11	296,58	265,21	305,68
U	50,51	43,7	45,65	41,47	44,55	44,89	55,39	46,43

LA-ICP-MS results obtained for titanite – Sample PB-123 - Continuation

LA-ICP-MS - Elementos Traço normalizado por Condrito - PB-123 (LSO)								
Element	Tit_1	Tit_2	Tit_3	Tit_4	Tit_5	Tit_6	Tit_7	Tit_8
La	7169,47	6905,9	6552,75	6024,75	6382,9	6984,34	5495,53	6943,15
Ce	9574,92	8717,91	8654	7924,2	8395,59	9760,57	6657,53	9452,98
Pr	9885,01	9077,4	8693,34	7849,25	8393,54	10325,1	6130,87	9918,16
Nd	9364,45	7630,91	7659,01	6942,01	7580,56	9688,45	5106,39	9100,13
Sm	5903,91	4673,86	4532,61	4066,6	4658,14	6076,96	2790,18	5753,54
Eu	3508,03	3591,08	3549,58	2827,04	3167,95	3290,44	1965,9	3485,69
Gd	2507,1	1892,91	2036,52	1708,68	1989,95	2618,49	1173,59	2452,18
Tb	1515,9	1150,78	1241,25	1014,42	1200,76	1584,08	713,97	1463,75
Dy	1029,38	802,28	823,65	663,72	795,83	1071,21	500,71	983,43
Ho	673,27	527,75	548,52	453,03	524,28	685,29	343,77	636,46
Er	502,53	403,04	403,32	338,79	396,1	494,7	273,3	463,73
Tm	418,42	342,52	352,09	289,32	346,77	408,57	241,9	390,25
Yb	348,69	309,17	306,19	250,01	288,79	329,42	241,13	325,75
Lu	253,87	219,19	221,65	195,84	220,39	232,76	193,24	233,45

LA-ICP-MS results obtained for titanite – Sample PB-92B

LA-ICP-MS - Elementos Traço normalizado por Condrito - PB-92B (LSO)										
Element	Tit-1	Tit-4	Tit-5	Tit-6	Tit-7	Tit-8	Tit-10	Tit-11	Tit-12	Tit-13
La	10287,49	11455,82	11614,5	11060,06	12581,83	10591,86	11525,26	9911,47	11190,18	11149,89
Ce	12046,79	13451,01	13080,76	12070,76	14585,46	11005,93	13223,96	11272,34	12680,74	12074,88
Pr	11397,13	12922,14	12126,08	11465,08	14562,03	10348,63	13232,97	11723,48	12634,19	12215,54
Nd	9669,23	10418,37	9391,27	8862,93	11799,39	7566,56	10026,22	9058,49	10119,03	10081,13
Sm	5136,26	5468,32	4982,97	4997,85	6569,03	3767,38	5615,94	4873,87	5611,93	5182,28
Eu	3914,61	4351,81	4520,91	3984,1	4189,92	3683,92	3780,91	3573,34	3646,69	3651,72
Gd	2417,2	2490,89	2169,74	2373,18	2788,35	1642,81	2407,45	2202,64	2402,39	2299,71
Tb	1440,12	1492,36	1300,37	1365,01	1698,84	933,27	1438,55	1329,4	1499,61	1432,92
Dy	921,69	958,62	887,18	944,75	1141,22	655,4	989,94	906,42	984,83	1004,18
Ho	673,53	717,34	620,77	669,7	816,59	491,45	665,6	661,31	710,78	701,48
Er	547	562,76	499,11	554,12	636,74	372,98	522,32	493,38	538,15	590,22
Tm	499,32	550,68	466,03	519,8	574,54	400,31	448,43	483,7	517,05	561,91
Yb	455,76	472,78	414,28	471	479,7	391,1	439,05	442,66	428,99	528,53
Lu	323,99	394,01	349,45	372,1	360,25	295,12	294,41	312,92	303,33	344,9

LA-ICP-MS - Concentração de Elementos Traço (Ppm) - PB-92B (LSO).										
Element	**Tit-1**	**Tit-4**	**Tit-5**	**Tit-6**	**Tit-7**	**Tit-8**	**Tit-10**	**Tit-11**	**Tit-12**	**Tit-13**
Li	0,81	0,95	0,91	1,25	1,06	1,05	<0.29	0,58	<0.47	6,23
Mg	506,3	641,26	653,51	458,75	617,01	448,26	460,4	571,44	526,23	931,37
Al	9468,51	8677,63	8340,71	13618,32	8493,09	16731,79	10557,36	11096,96	8135,08	9372,12
Si	157625,9	154313,9	141660,91	155370,55	131719,16	167081,36	140138,27	139297,72	132658,83	139378,11
P	254,52	280,55	256,61	136,81	220,81	194,05	199,8	191,32	233,93	218,47
Ca42	174067,2	180730,6	175505,14	175458,06	177591,08	172901,22	185229,67	185531,2	178651,94	184974,61
Ca44	185750,8	185750,8	185750,83	185750,81	185750,81	185750,83	185750,81	185750,8	185750,81	185750,8
Sc	5,25	6,03	5,38	4,98	6,08	6,01	6,52	5,2	5,8	7,92
Ti46	155543,3	162640,3	167717,89	170801,13	175727,92	164266,3	177093,39	166881,83	176991,47	212771,89
Ti49	171855,6	186108,6	187919,81	187999,28	206607,36	181551,55	190868,98	186501,55	197244,7	236431,97
V	624,74	720,58	800,8	775,33	1016,94	667,76	760,56	701,49	729,47	898,25
Cr	94,91	129,79	145,81	194,53	349,78	102,23	123,5	122,03	112,32	222,48
Mn	708,61	753,8	680,15	618,76	895,75	681,18	745,02	687,21	766,73	1286,72
Fe	15348,67	16199,53	19543,54	14066,38	61003,62	16758,44	16092,18	15207,18	16628,69	115554,6
Co	<0.164	<0.157	0,94	0,27	3,51	<0.27	<0.17	0,31	0,135	21,46
Sr	165,76	182,36	174,29	274,03	199,6	456,34	235,8	215,67	193,95	182,03
Y	1497,45	1526,08	1458,99	1396,36	2034,62	1050,08	1662,35	1400,34	1666,21	1420,54
Zr	435,03	708,29	653,29	474,88	681,2	475,9	694,77	516,73	652,72	639,31
Nb	813,84	1003,3	901,14	717,95	1080,08	858,96	1062,57	844,49	1022,15	1018,58
Sn	115,1	131,93	118,92	90,27	126,14	96,9	115,17	97,03	110,41	98,31
Sb	<1.32	<1.24	<1.38	<0.94	<2.12	<1.91	<1.74	<1.67	<1.81	<1.27
Ba	<2.48	<1.63	<2.42	10,3	<3.46	528,71	<2.10	131,02	<2.84	<2.29
La	3775,51	4204,29	4262,52	4059,04	4617,53	3887,21	4229,77	3637,51	4106,8	4092,01
Ce	11528,78	12872,62	12518,28	11551,71	13958,28	10532,67	12655,33	10787,63	12135,47	11555,66
Pr	1561,41	1770,33	1661,27	1570,72	1995	1417,76	1812,92	1606,12	1730,88	1673,53
Nd	6874,82	7407,46	6677,19	6301,55	8389,37	5379,83	7128,64	6440,59	7194,63	7167,68
Sm	1186,47	1263,18	1151,07	1154,5	1517,45	870,26	1297,28	1125,86	1296,35	1197,11
Eu	340,57	378,61	393,32	346,62	364,52	320,5	328,94	310,88	317,26	317,7
Gd	739,66	762,21	663,94	726,19	853,23	502,7	736,68	674,01	735,13	703,71
Tb	83,53	86,56	75,42	79,17	98,53	54,13	83,44	77,11	86,98	83,11
Dy	351,16	365,23	338,02	359,95	434,81	249,71	377,17	345,35	375,22	382,59
Ho	57,32	61,05	52,83	56,99	69,49	41,82	56,64	56,28	60,49	59,7
Er	136,2	140,13	124,28	137,97	158,55	92,87	130,06	122,85	134	146,97
Tm	17,78	19,6	16,59	18,51	20,45	14,25	15,96	17,22	18,41	20
Yb	113,03	117,25	102,74	116,81	118,96	96,99	108,88	109,78	106,39	131,07
Lu	12,34	15,01	13,31	14,18	13,73	11,24	11,22	11,92	11,56	13,14
Hf	24,16	34,37	29,33	25,09	26,73	23,69	29,47	27,54	29,28	39,56
Ta	40,82	45,58	40,52	23,02	29,55	37,13	35,74	27,82	37,42	50,82
Pb	29,84	33,86	28,24	29,06	26,21	29,95	25,85	19,27	25,46	31,96
Pb	<2.82	8,37	5,18	10,15	5,14	8,7	5,26	3,36	4,68	5,14
Pb	34,07	41,92	41,36	37,78	37,13	34,96	28,6	26,05	28,78	28,35
Th	537,98	699,14	659,79	508,77	570,94	459,12	466,16	469,6	504,19	570,2
U	64,93	78,73	72,27	66,12	61,88	56,12	56,16	54,37	55,9	62,67

LA-ICP-MS results obtained for titanite – Sample PB-92B - Continuation

LA-ICP-MS results obtained for titanite – Sample PB-08A

LA-ICP-MS - Concentração de Elementos Traço (Ppm) - PB-08A (LSS).									
Element	**Tit_1**	**Tit_2**	**Tit_3**	**Tit_4**	**Tit_5n**	**Tit_5b**	**Tit_6**	**Tit_7**	**Tit_8**
Li	<0.194	0,227	0,32	0,334	0,396	0,23	0,238	<0.181	0,187
Mg	694,71	790,45	916,92	694,93	1417,92	1197,02	697,75	708,62	1021,47
Al	6316,02	6945,53	6921,64	7070,23	6589,22	6418,41	6608,59	6720,73	6194,23
Si	146883	148080,6	149878,6	143288,2	143213,6	140119,6	141628,1	141846,3	138760,7
P	490,89	356,64	565,3	274,19	561,53	518,39	456,18	492,91	575,58
Ca42	195613,6	201198,4	198123,5	198281,5	201158,6	199529,8	197784,5	197703,3	197949,2
Ca44	200116,2	200116,2	200116,2	200116,2	200116,2	200116,2	200116,3	200116,2	200116,2
Sc	6,93	5,85	5,82	6,25	8,19	8,18	7,45	7,69	7,84
Ti46	176015,9	177255,3	174052,8	172829,5	178771,7	174176,6	169592	168730,3	168014,6
Ti49	197290,9	194592	199487,8	190102,7	199729,1	191588,3	187342	184978,6	186240,9
V	726,3	703,17	693,84	686,38	687,13	659,27	703,15	698,74	670,46
Cr	87,45	82,66	83,62	69,83	80,74	84,56	95,98	90,36	85,73
Mn	772,18	778,37	715,47	728,07	798,52	763,05	770,48	737,37	805,8
Fe	26496,85	24608,45	25882,91	22921,78	26761,94	25528,82	25631,36	25477,69	25562,27
Co	0,172	0,243	0,72	0,171	0,326	0,245	0,187	0,202	0,235
Sr	1323,01	1367,23	1195,53	1114,03	1521,05	1439,71	1338,54	1347,94	1479,54
Y	837,05	798,2	811,35	861	1073,87	1012,61	898,35	954,64	957,72
Zr	5360,45	4837,89	5047,04	4648,04	5262,62	4850,48	6768,51	6132,5	5780,81
Nb	728,44	554,99	761,67	348,4	803,87	743,54	694,59	745,76	801,98
Sn	81,49	69,64	75,82	53,14	83,99	81,63	72,88	76,4	81,61
Sb	<0.53	0,55	<0.57	<0.52	<0.53	<0.52	<0.51	<0.56	<0.56
Ba	0,53	0,281	11,68	<0.203	0,392	0,469	0,77	0,274	0,59
La	2533,33	2454,8	2517,28	2807,08	2818,55	2721,37	2577,58	2592,05	2741,03
Ce	8669,83	8387,44	8443,6	8735,58	9288,25	9069,65	8185,56	8215,82	8925,77
Pr	1148,15	1112,1	1147,87	1167,19	1318,86	1279,82	1108,03	1162,8	1236,11
Nd	5272,36	5013,39	5142,08	5213,39	6198,86	6056,58	5107,1	5316,78	5641,45
Sm	991,99	930,26	952,4	944,44	1231,9	1207,49	973,56	1023,01	1093,64
Eu	266,24	257,2	254,82	258,17	310,81	307,24	251,9	264,76	279,87
Gd	546,11	502,25	510,39	519,31	685,37	675,46	543,36	569,31	602,73
Tb	60,29	56,14	56,75	58,61	78,06	77,58	60,37	65,28	68,42
Dy	254,72	238,2	238,03	249,49	329,24	323,73	256,39	276,7	291,78
Ho	35,49	33,51	33,76	36,36	46,33	46,39	37,73	39,83	41,5
Er	71,96	69,29	70,1	77,25	94,8	95,08	78,79	82,1	87,04
Tm	8,21	8,08	8,41	8,82	10,72	10,84	9,29	9,81	9,84
Yb	47,72	49,79	48,96	55,02	60,33	61,27	56,96	57,54	56,08
Lu	4,6	4,67	4,97	5,61	5,89	5,83	5,47	5,63	5,54
Hf	157,97	123,33	145,38	110,44	162,52	159,67	200,21	189,37	175,4
Ta	44,44	22,73	49,43	7,73	64,46	64,97	34,7	47,83	56,35
Pb	22,9	28,38	26,82	24,11	17,51	17,62	33,02	22,58	23,19
Pb	13,26	15	15,43	11,58	11,98	11,72	18,08	12,49	15,89
Pb	25,94	29,29	28,7	26,92	23,49	22,29	33,61	26,61	30,38
Th	231,88	239,53	229,98	312,99	231,6	228,08	296,86	278,43	270,79
U	32,01	45,21	37,15	41,32	18,63	18,27	43,34	31,43	23,7

LA-ICP-MS results obtained for titanite – Sample PB-08A - Continuation

LA-ICP-MS - Elementos Traço normalizado por Condrito - PB-08A (LSS)									
Element	**Tit_1**	**Tit_2**	**Tit_3**	**Tit_4**	**Tit_5n**	**Tit_5b**	**Tit_6**	**Tit_7**	**Tit_8**
La	6902,81	6688,83	6859,08	7648,72	7679,98	7415,19	7023,37	7062,81	7468,76
Ce	9059,38	8764,3	8822,99	9128,09	9705,6	9477,17	8553,36	8584,97	9326,82
Pr	8380,65	8117,51	8378,62	8519,63	9626,72	9341,78	8087,82	8487,57	9022,71
Nd	7415,42	7051,18	7232,19	7332,47	8718,51	8518,4	7182,98	7477,88	7934,53
Sm	4294,32	4027,09	4122,96	4088,49	5332,89	5227,22	4214,54	4428,63	4734,36
Eu	3060,24	2956,33	2929	2967,44	3572,53	3531,51	2895,39	3043,16	3216,91
Gd	1784,69	1641,33	1667,95	1697,08	2239,78	2207,4	1775,69	1860,5	1969,72
Tb	1039,54	967,9	978,52	1010,52	1345,92	1337,63	1040,87	1125,6	1179,73
Dy	668,57	625,18	624,76	654,83	864,15	849,69	672,93	726,25	765,83
Ho	417,04	393,72	396,71	427,25	544,42	545,12	443,37	468,01	487,62
Er	288,99	278,29	281,54	310,23	380,71	381,87	316,43	329,74	349,54
Tm	230,75	227,01	236,14	247,83	301,21	304,55	260,9	275,52	276,51
Yb	192,43	200,77	197,41	221,87	243,26	247,05	229,67	232,01	226,15
Lu	120,71	122,55	130,33	147,15	154,56	153,01	143,44	147,74	145,28

LA-ICP-MS results obtained for titanite – Sample PB-181A

LA-ICP-MS - Concentração de Elementos Traço (Ppm) - PB-181 (LSS).																		
Element	**Tit-1**	**Tit-2**	**Tit-3**	**Tit-4**	**Tit-5**	**Tit-6-px**	**Tit-7**	**Tit-8**	**Tit-9**	**Tit_01_TF**	**Tit_03_TF**	**Tit_04_TF**	**Tit_05_TF**	**Tit_09_TF**	**Tit_11_TF**	**Tit_15_TF**	**Tit_16_TF**	**Tit_2c_TF**
Li	0,198	2,46	3,23	<0.219	<0.46	24,1	2,92	1,6	<0.37	0,296	0,214	0,457	0,32	0,19	0,357	0,51	0,922	0,218
Mg	759,94	892,53	1045,14	506,43	760,81	42156,6	1396,07	854,93	458,39	667,29	798,74	2009,73	624,22	869,49	779	1151,56	929,77	885,21
Al	6215,23	6770,01	7749,27	6225,17	6362,63	7287,41	6207,89	5837,47	6983,17	5899,44	6127,39	6378,24	6370,68	6265,61	6166,67	6388,16	7097,91	6348,47
Si	127672,6	130854,5	120092,5	125918,7	142044,2	215668,3	131135,8	119354,9	125042,7	143036,4	143036,4	143036,4	143036,4	143036,4	143036,4	143036,4	143036,4	143036,5
P	236,94	71,16	187,04	137,37	219,82	107,63	277,6	95,23	101,95	263,5	319,43	299,97	263,07	358,44	296,64	488,03	566,57	345,02
Ca42	190873	190873	190873	190873	190873	190873	190873	190873	190873	201319,7	199774,5	192246,8	200394,1	204939,1	208515,8	209553,2	203065,7	212607,6
Ca44	185479,1	185171,8	184917,3	188153,8	191273,4	187608	191398,5	181979,6	183006,8	211971,8	206183,8	196607,1	208137,7	205862,5	204079,8	214323,8	212072,4	214407,8
Sc	6,94	5,54	7,98	5,31	6,6	52,21	10,93	7,95	5,9	6,5	5,68	5,72	4,01	6,63	5,53	9,58	8,55	6,56
Ti46	177013,9	169751,7	169322	178573,5	177380	82302,87	186883,7	172815,4	174978	197897,5	190974,5	179234,1	186852,6	185721,8	183920,8	198999,6	198218,5	200497
Ti49	198096,6	186670	189941,6	197938,1	197851,3	86207,66	200078,2	187748,8	186934,1	219072,2	212886,1	202611,9	208128,9	206565,4	205822,3	215474,6	217694,5	218295,9
V	848,52	999,46	813,44	808,63	900,72	547,57	983,12	987,61	938,95	881,68	988,99	913,77	1023,88	996,4	943,87	1036,19	1060,37	977,57
Cr	138,58	361,1	129,23	159,23	158,58	161,42	222,02	561,23	281	154,2	154,88	130,76	149,45	144,24	106,95	195,58	193,72	136,73
Mn	802,4	786,6	801,22	742,94	863,65	2510,5	853,21	745,82	626,18	903,83	863,44	864,38	741,25	883,89	838,45	883,03	834,61	870,31
Fe	21843,67	24198,74	21678,85	19982,37	22217,26	71756,48	25197,77	21796,64	19391,08	23892,49	25814,7	26598,25	25434,51	26322,8	24907,12	29434,06	27302,09	26772,4
Co	<0.216	1,63	1,64	0,299	0,31	36,87	0,81	0,69	0,197	0,341	0,165	1,142	0,228	0,284	0,342	0,358	0,47	0,262
Sr	1329,99	1677,14	1870,62	1144,67	1291,19	1661,98	1383,55	1542,8	980,25	1342,93	1357,83	1325,01	1135,79	1340,68	1302,05	1386,71	1621,02	1372,57
Y	697	381,8	159,76	369,88	650,31	294,08	681,88	275,24	415,36	426,87	765,98	745,44	766,64	578,45	358,86	801,91	695,6	794,38
Zr	1705,51	995,42	2665,43	976,87	1639,87	975,69	4115,47	1016,82	1134,73	3533,64	2302,02	2964,84	2151,86	3514,48	2499,48	5235	5008,97	3924,43
Nb	566,85	85,64	456,05	373,37	527,87	268,95	518,71	70,45	197,81	630,37	553,31	440,96	365,49	677,04	361,67	926,68	967,99	682,24
Sn	40,78	33	76,31	47,41	55,68	21,4	41,68	24,8	26,31	52,07	54,18	51,69	49,53	54,06	49,14	60,03	64,16	58,19
Sb	<1.47	<2.43	<1.54	<1.35	<2.08	<1.33	<1.31	<0.95	<1.36	0,249	<0.190	0,183	0,244	0,19	0,197	<0.104	0,146	0,171
Ba	<2.24	1296,61	10,59	<1.97	<5.06	22,86	<3.12	1656,73	<2.45	0,69	0,99	184,73	2,21	1,12	0,81	1,72	292,3	0,281
La	2117,95	2012,27	858,19	2243,95	2084,58	907,17	2089,39	1915,95	1919,6	1598,47	2171,7	2247,82	2204,64	2073,33	1547,97	2276,04	2362,6	2333,03
Ce	5882,44	4650,96	999,09	5417,58	5535,63	2346,48	5765,89	4334,72	4996,52	4636,9	6660,27	6898,48	7012,77	6353,38	4395,1	6994,75	7029,75	7116,09
Pr	770,33	549,88	114	607,1	718,04	314,3	767,3	482,16	610,86	529,29	866,91	882,55	894	779,73	475,47	893,06	850,83	904,46
Nd	3298,34	2295,43	531,42	2211,75	2975,94	1322,98	3242,16	1767,21	2429,32	2120,03	3741,52	3909,47	3806,09	3275,53	1813,87	3871,9	3534,75	3856,27
Sm	579,6	363,03	102,57	286,47	486,71	236,21	583,52	233,94	354,98	359,34	695,59	742,44	719,6	555,54	298,49	708,29	607,58	696,19
Eu	145,02	82,13	26,45	88,04	131,03	59,39	148,94	64,44	98,36	100,06	181,47	186,5	188,39	145,15	91,74	185,12	162,64	179,92
Gd	335,37	222,39	64,66	158,76	281,37	134,66	328,88	127,79	194,72	210,07	403,12	411,12	394,85	303,63	169,27	397,86	347,69	402,76
Tb	37,07	21,29	8,17	15,52	32,45	15,74	36,92	12,73	20,76	23,04	46,2	45,4	46,1	34,58	19,02	46,91	40,2	46,26
Dy	169,92	88,96	42,85	72,65	166,35	68,22	164,17	55,5	88,97	98,62	203,25	199,47	201,98	149,34	85,62	209,23	174,36	207,98
Ho	26,13	12,09	6,3	11,85	27,16	10,89	25,85	8,65	14,5	15,65	30,83	29,95	29,69	22,8	13,07	32,51	26,89	31,76
Er	60,23	25,34	16,36	29,82	61,29	27,34	58,06	21,38	35,17	37,97	68,48	66,55	66,41	51,32	31,1	73,55	61,86	70,52
Tm	7,94	3,64	2,71	4,49	8,51	3	7,83	3,08	4,53	5,02	8,53	8,15	8,31	6,44	4,37	8,92	7,38	8,62
Yb	47,2	21,94	16,81	30,26	44,51	19,28	45,23	20,78	30,04	36,12	54,9	52,54	55,39	41,45	31,45	55,11	47,96	55,28
Lu	5,65	3,84	3,26	4,11	6,72	2,36	6,2	2,89	3,31	4,35	5,87	5,61	6,02	4,47	3,68	5,71	5,26	5,87
Hf	55,09	38,31	93,09	46,91	52,14	33,12	103,75	26,32	33,48	97,22	75,64	89,12	69,08	98,47	61,44	176,06	163,89	116,44
Ta	9,4	1,25	4,49	3,57	7,95	8,21	8,45	0,7	5,34	11,94	12,3	8,32	4,54	14,77	4,67	42,59	33,11	19,29
Pb	23,05	39,53	89,3	22,48	34,61	99,13	40,65	71,28	12,53	29,33	34,55	39,01	26,11	31,49	27,03	35,24	49,94	32,39
Pb	15,08	37,4	85,5	18,49	22,32	104,75	32,62	65,01	8,58	22,14	21,12	28,14	17,29	21,08	19,92	22,1	34,94	18,73
Pb	28,45	41,04	84,99	20,96	33,62	109,28	38,1	70,18	14,6	28,48	37,51	43,23	29,78	31,87	25,4	41,26	56,84	33,98
Th	262,85	73,11	7,68	165,5	294,99	105,49	172,65	79,99	139,99	120,86	287,24	269,29	206,05	210,47	104,1	346,5	385,24	295,32
U	29,18	4,59	13,78	17,05	29,82	11,02	30,63	7,14	12,05	18,44	36,75	33,6	20,38	33,61	23,75	37,69	38,35	39,1

LA-ICP-MS results obtained for titanite – Sample PB-181A - Continuation

LA-ICP-MS - Elementos Traço normalizado por Condrito - PB-181 (LSS)																		
Element	Tit-1	Tit-2	Tit-3	Tit-4	Tit-5	Tit-6-px	Tit-7	Tit-8	Tit-9	Tit_01_TF	Tit_03_TF	Tit_04_TF	Tit_05_TF	Tit_09_TF	Tit_11_TF	Tit_15_TF	Tit_16_TF	Tit_2c_TF
Li	0,082	1,02	1,35	0	0	10,04	1,22	0,667	0	0,123	0,089	0,19	0,133	0,079	0,149	0,213	0,384	0,091
Mg	0,00531	0,00624	0,00731	0,00354	0,00532	0,295	0,00976	0,00598	0,00321	0,00467	0,00559	0,01405	0,00437	0,00608	0,00545	0,00805	0,0065	0,00619
Al	0,482	0,525	0,601	0,483	0,493	0,565	0,481	0,453	0,541	0,457	0,475	0,494	0,494	0,486	0,478	0,495	0,55	0,492
Si	0,798	0,818	0,751	0,787	0,89	1,35	0,82	0,746	0,782	0,894	0,894	0,894	0,894	0,894	0,894	0,894	0,894	0,894
P	0,103	0,031	0,081	0,06	0,096	0,047	0,121	0,041	0,044	0,115	0,139	0,13	0,114	0,156	0,129	0,212	0,246	0,15
Ca42	14,14	14,14	14,14	14,14	14,14	14,14	14,14	14,14	14,14	14,91	14,8	14,24	14,84	15,18	15,45	15,52	15,04	15,75
Ca44	13,74	13,72	13,7	13,94	14,17	13,9	14,18	13,48	13,56	15,7	15,27	14,56	15,42	15,25	15,12	15,88	15,71	15,88
Sc	0,803	0,641	0,923	0,615	0,764	6,04	1,265	0,92	0,683	0,752	0,658	0,662	0,464	0,767	0,64	1,109	0,99	0,76
Ti46	270,66	259,56	258,9	273,05	271,22	125,85	285,75	264,24	267,55	302,6	292,01	274,06	285,71	283,98	281,22	304,28	303,09	306,57
Ti49	302,9	285,43	290,43	302,66	302,52	131,82	305,93	287,08	285,83	334,97	325,51	309,8	318,24	315,85	314,71	329,47	332,87	333,79
V	9,98	11,76	9,57	9,51	10,6	6,44	11,57	11,62	11,05	10,37	11,64	10,75	12,05	11,72	11,1	12,19	12,47	11,5
Cr	0,0349	0,0908	0,0325	0,0401	0,0399	0,0406	0,0559	0,1412	0,0707	0,0388	0,039	0,0329	0,0376	0,0363	0,0269	0,0492	0,0487	0,0344
Mn	0,273	0,268	0,273	0,253	0,294	0,854	0,29	0,254	0,213	0,307	0,294	0,294	0,2521	0,301	0,285	0,3	0,284	0,296
Fe	0,0786	0,087	0,078	0,0719	0,0799	0,258	0,0906	0,0784	0,0698	0,0859	0,0929	0,0957	0,0915	0,0947	0,0896	0,1059	0,0982	0,0963
Co	0	0,00213	0,00214	0,00039	0,00041	0,0483	0,00106	0,0009	0,00026	0,00045	0,00022	0,00149	0,0003	0,00037	0,00045	0,00047	0,00062	0,00034
Sr	111,76	140,94	157,2	96,19	108,5	139,66	116,26	129,65	82,37	112,85	114,1	111,35	95,44	112,66	109,42	116,53	136,22	115,34
Y	309,78	169,69	71	164,39	289,03	130,7	303,06	122,33	184,6	189,72	340,44	331,31	340,73	257,09	159,49	356,4	309,15	353,06
Zr	307,85	179,68	481,12	176,33	296,01	176,12	742,87	183,54	204,82	637,84	415,53	535,17	388,42	634,38	451,17	944,95	904,15	708,38
Nb	1511,61	228,36	1216,14	995,65	1407,65	717,2	1383,24	187,86	527,49	1680,99	1475,5	1175,88	974,63	1805,44	964,44	2471,14	2581,3	1819,31
Sn	16,18	13,09	30,28	18,82	22,09	8,49	16,54	9,84	10,44	20,66	21,5	20,51	19,66	21,45	19,5	23,82	25,46	23,09
Sb	0	0	0	0	0	0	0	0	0	1,07	0	0,78	1,05	0,81	0,85	0	0,63	0,74
Ba	0	380,24	3,11	0	0	6,7	0	485,84	0	0,204	0,289	54,17	0,649	0,328	0,239	0,505	85,72	0,082
La	5770,98	5483,02	2338,39	6114,31	5680,04	2471,86	5693,17	5220,58	5230,51	4355,51	5917,44	6124,84	6007,18	5649,39	4217,9	6201,75	6437,59	6357,04
Ce	6146,75	4859,93	1043,98	5661	5784,36	2451,91	6024,96	4529,49	5221,03	4845,24	6959,53	7208,44	7327,87	6638,85	4592,58	7309,04	7345,61	7435,83
Pr	5622,82	4013,73	832,13	4431,41	5241,14	2294,17	5600,75	3519,38	4458,84	3863,4	6327,84	6441,97	6525,56	5691,45	3470,6	6518,72	6210,41	6601,91
Nd	4639,02	3228,45	747,43	3110,75	4185,57	1860,73	4560	2485,53	3416,77	2981,76	5262,34	5498,55	5353,14	4606,93	2551,16	5445,71	4971,52	5423,73
Sm	2509,09	1571,55	444,01	1240,13	2106,99	1022,57	2526,04	1012,75	1536,71	1555,6	3011,2	3214,04	3115,17	2404,95	1292,15	3066,19	2630,21	3013,79
Eu	1666,89	943,99	304,02	1011,92	1506,12	682,6	1712	740,7	1130,6	1150,07	2085,88	2143,73	2165,41	1668,4	1054,47	2127,79	1869,45	2068
Gd	1095,98	726,75	211,29	518,82	919,52	440,07	1074,78	417,61	636,34	686,51	1317,38	1343,54	1290,37	992,26	553,18	1300,18	1136,23	1316,2
Tb	639,13	367,1	140,85	267,57	559,48	271,32	636,58	219,49	358,01	397,21	796,47	782,68	794,85	596,28	327,85	808,76	693,18	797,65
Dy	445,99	233,5	112,47	190,67	436,6	179,04	430,89	145,68	233,52	258,84	533,47	523,53	530,13	391,98	224,73	549,16	457,64	545,87
Ho	307,05	142,02	74,02	139,29	319,18	127,96	303,71	101,67	170,43	183,88	362,28	351,99	348,91	267,9	153,62	382,07	315,99	373,24
Er	241,87	101,77	65,7	119,76	246,13	109,79	233,19	85,86	141,24	152,5	275,01	267,28	266,71	206,12	124,91	295,38	248,42	283,23
Tm	223,04	102,33	76,26	126,18	239,05	84,33	219,97	86,61	127,22	140,89	239,55	228,92	233,29	180,76	122,8	250,5	207,28	242,06
Yb	190,31	88,45	67,77	122,02	179,48	77,76	182,39	83,8	121,14	145,64	221,35	211,84	223,34	167,14	126,8	222,23	193,4	222,89
Lu	148,41	100,67	85,61	107,86	176,43	61,99	162,64	75,75	86,95	114,27	153,96	147,29	158,13	117,35	96,63	149,88	137,99	154,05
Hf	307,76	214,01	520,05	262,08	291,29	185,02	579,59	147,05	187,03	543,13	422,55	497,87	385,9	550,13	343,25	983,57	915,6	650,5
Ta	361,5	48,09	172,71	137,22	305,66	315,86	325	26,77	205,22	459,09	472,94	319,83	174,72	568,26	179,52	1638,2	1273,55	741,83
Pb	6,31	10,83	24,47	6,16	9,48	27,16	11,14	19,53	3,43	8,03	9,47	10,69	7,15	8,63	7,41	9,65	13,68	8,87
Pb	4,13	10,25	23,42	5,06	6,12	28,7	8,94	17,81	2,35	6,07	5,79	7,71	4,74	5,78	5,46	6,06	9,57	5,13
Pb	7,79	11,24	23,29	5,74	9,21	29,94	10,44	19,23	4	7,8	10,28	11,84	8,16	8,73	6,96	11,3	15,57	9,31
Th	6184,74	1720,29	180,67	3894,2	6941	2482,23	4062,31	1882,14	3293,88	2843,79	6758,69	6336,33	4848,21	4952,18	2449,4	8152,94	9064,5	6948,65
U	2391,53	376,18	1129,88	1397,14	2444,53	903,02	2510,41	585,63	987,32	1511,3	3012,48	2753,96	1670,35	2754,6	1946,6	3089,09	3143,77	3204,9

LA-ICP-MS results obtained for titanite – Sample PB-185A

LA-ICP-MS - Concentração de Elementos Traço (Ppm) - PB-185 (LSS).																		
Element	**Tit_01**	**Tit_02**	**Tit_04**	**Tit_05c**	**Tit_05b**	**Tit_06**	**Tit_07**	**Tit_14**	**Tit_15_1**	**Tit_15_2**	**Tit_15_3**	**Tit_16**	**Tit_17**	**Tit_18c**	**Tit_18b**	**Tit_19**	**Tit_20c**	**Tit_20b**
Li	0,232	0,177	0,204	0,297	0,114	0,16	0,32	0,461	0,174	0,17	0,24	0,856	0,367	0,295	0,285	0,467	0,261	0,177
Mg	673,96	498,5	767,53	593,33	465,12	517,97	703,91	1006,08	462,08	502,24	632,77	1174,98	679,67	747,44	649,7	570,53	666,38	674,65
Al	3935,78	4495,17	4090,39	4297,1	4575,87	4598,57	4357,04	4898,34	5233,34	4101,85	4013,48	5667,49	4529,76	4390,53	3885,46	4692,19	4838,18	4288,72
Si	139756,8	142685,3	143560,2	144835,9	146604,8	137805,2	142611,1	149147,3	148072,6	143593,1	137902,2	146026,1	152496,2	140449,8	142916,3	146787,2	140958,7	142849,9
P	322,17	401,71	351,82	499,22	316,38	331,84	326,36	396,64	239,13	269,96	353,6	361,71	334,91	390,88	273,58	338,18	463,33	307,31
Ca42	200116,3	200116,3	200116,3	200116,3	200116,3	200116,3	200116,3	200116,3	200116,3	200116,3	200116,3	200116,3	200116,3	200116,3	200116,3	200116,3	200116,3	200116,3
Ca44	202766,2	199811,3	204698,3	201356,8	198911,6	197354,3	199552,8	205002,3	202422,3	203968,4	194693,7	207415,3	204794,3	200352,9	198214,3	205402,5	201622,5	198297,5
Sc	6,16	6,39	6,95	6,13	5,61	7,03	6,46	6,82	6,92	5,66	5,34	7,02	5,95	7,1	5	6,33	7	6,21
Ti46	199058,8	202044	202066,7	201546,3	196270,4	191180,9	201932,8	211686	205693,8	195946,9	184143,9	206696	191779,9	202047,8	196786,1	198564,1	199211,3	197559,6
Ti49	228310,1	226522,7	225496,4	227439,8	217310,2	212899,4	230577,5	236104,9	224596,1	218506,7	205955,7	225745,1	215187,8	229575,9	218884,8	223968,5	227153,2	224277
V	759,46	574,27	621,56	548,96	684,18	590,71	736,27	586,94	716,84	691,76	597,53	835,12	636,51	598,48	640,27	617,28	503,23	688,28
Cr	14,85	18,96	18,79	22,75	19,48	17,31	19,2	20,67	18,19	17,42	18,53	19,47	17,19	25,04	15,12	19,68	17,54	20,47
Mn	682,86	824,59	741,4	601,67	834,2	775,58	748,19	799,28	856,29	805,44	775,92	829,43	793,34	600,83	661,4	853,04	696,36	794,1
Fe	19342,16	19207,61	19339,71	19085,24	18884,33	17876,92	19130,09	20343,1	19628,51	18911,88	18330,51	21337,31	18893,63	20341,67	18930,76	19679,3	20001,09	19468,44
Co	0,244	0,168	0,33	0,196	0,148	0,234	0,232	0,647	0,13	0,217	0,316	1,009	0,329	0,261	0,202	0,226	0,204	0,353
Sr	3073,58	2570,87	3188,25	2960,21	2272,04	2121,18	2981,64	3101,97	2281,54	2510,32	2768,91	2158,39	2137,61	3039,94	2765,95	2590,73	3041,53	2856,57
Y	548,86	657,05	675,67	683,76	526,08	639,69	535,74	652,32	621,44	449,32	539,12	717,92	558,2	697,16	460,47	616,76	731,09	565,8
Zr	3904,58	3726,27	3897,85	3480,65	3415,99	5571,88	3633,41	3708,04	6363,22	3985,46	2918,52	4148,23	3554,8	4033,14	3268,38	3548,15	4143,1	3540,56
Nb	596,91	447,48	568,15	580,44	511,87	697,16	518,5	505,92	663,53	573,03	486,98	463,17	602,66	507,1	545,86	469,69	493,29	490,55
Sn	51,21	62,34	64,47	66,06	55,6	57,75	56,1	64,75	50,39	50,08	57,01	51,42	57,81	64,26	48,83	58,72	74,17	53,03
Sb	<0.122	<0.116	<0.107	<0.096	0,148	<0.140	<0.096	<0.100	0,122	0,106	<0.078	0,203	<0.104	<0.098	<0.103	0,114	<0.121	<0.115
Ba	0,498	1,78	4,27	0,7	0,366	0,374	1,11	9,03	0,187	0,502	0,69	7,89	0,48	0,457	0,258	19,18	0,61	1,66
La	2047,43	2003,52	2323,19	2288,85	1976,27	2249,75	1928,59	2154,74	2219,76	1782,93	1914,92	2538,86	2160,18	2122,53	1720,42	2064,96	2346,88	1945,13
Ce	6348,86	6566,66	7200,95	7592,52	6469,36	6985,92	6149,86	7167,27	6766,65	5952,01	6557,36	7741,56	7462,06	7027,7	5882,08	7088,22	7643,81	6446,54
Pr	814,02	939,04	959,04	1022,82	800,61	887,48	831,19	997,34	846,77	728,77	903,65	973,62	945,89	981,4	733,17	952,46	1076,88	845,75
Nd	3549,69	4389,16	4368,11	4634,56	3387,7	3849,53	3713,98	4544,49	3597,34	3027,87	3910,23	4178,86	3918,22	4540,04	3154,89	4266,93	4876,76	3774,85
Sm	621,43	856,85	802,95	906,43	625,79	700,39	677,64	852,64	640,45	542,17	727,02	750,64	699,13	866,48	560,69	813,13	962,23	696,74
Eu	161,04	224,6	201,74	231,8	171,31	181,59	181,82	227,61	173,02	153,19	195,73	192,88	193,14	222,17	150,47	215,23	250,7	180,28
Gd	350,6	470,83	438,95	486,39	338,92	376,03	380,03	464,11	357,81	298,93	374,44	413,98	366,31	460,41	296,66	433,48	518,35	370,81
Tb	38,85	50,57	47,87	53,18	37,24	40,83	41,34	51,09	40,4	32,83	39,74	46,41	40,55	51,32	33,29	47,51	56,85	40,73
Dy	158,13	203,98	197,65	216,96	153,43	174,07	171,77	207,18	179,83	136,12	157,89	193,19	162	209,57	139,15	190,85	229,23	166,37
Ho	22,77	27	27,87	29,76	21,36	25,12	23,51	28,41	25,5	19,13	21	27,88	23,22	28,42	19,87	26,3	32,07	22,73
Er	45,31	53,38	54,24	58,65	45,26	51,54	46,52	56,7	52,13	39,19	43,83	59,29	48,24	57,91	40,12	52,12	63,03	48
Tm	4,82	5,7	6	6,07	4,94	5,87	4,95	5,92	6,19	4,38	4,49	7	5,28	6,15	4,23	5,8	6,59	5,32
Yb	26,72	31,29	30,93	33,42	29,66	34,57	27,09	31,16	37,59	25,45	24,48	40,21	30,14	32,85	24,48	32,94	34,94	30,1
Lu	2,5	3,14	3,05	3,15	3	3,45	2,53	3,1	4,06	2,61	2,41	4,39	3,04	3,22	2,34	3,22	3,34	2,93
Hf	116,22	118,2	122,86	111,03	101,63	160,01	116,85	123,25	211,72	118,64	92,36	124,58	114,01	134,55	99,9	114,68	128,75	115,57
Ta	48,01	40,86	49,44	55,7	35,93	41,53	42,76	44,27	35,16	33,74	39,18	22,3	40,13	47,55	36,72	37,67	46,5	35,22
Pb	15	24,51	17,35	16,34	28,84	26,06	16,85	21,47	35,11	26,96	18,32	39,46	20,31	14,76	15,51	25,73	17,76	22,09
Pb	10,9	16,44	12,78	13,17	18,2	16,39	12,52	16,62	18,21	16,94	13,76	21,89	13,33	11,09	11,48	17,33	12,76	15,16
Pb	18,34	23,18	19,1	20,68	25,28	26,93	19,16	23,63	36,39	24,67	19,85	40,75	21,78	18,58	17,46	23,98	22,05	22,57
Th	131,01	122,95	128,92	144,54	138,52	183,77	111,41	131,19	358,92	131,03	97,19	344,21	124,24	136,92	101,51	124,57	148,75	130,01
U	11,73	22,21	11,55	11,82	33,26	26,97	13,36	14,74	55,13	30,55	13,37	47,54	18,95	11,87	11,35	24,9	11,66	19,05

LA-ICP-MS results obtained for titanite – Sample PB-185A - Continuation

LA-ICP-MS - Elementos Traço normalizado por Condrito - PB-185 (LSS)																		
Element	**Tit_01**	**Tit_02**	**Tit_04**	**Tit_05c**	**Tit_05b**	**Tit_06**	**Tit_07**	**Tit_14**	**Tit_15_1**	**Tit_15_2**	**Tit_15_3**	**Tit_16**	**Tit_17**	**Tit_18c**	**Tit_18b**	**Tit_19**	**Tit_20c**	**Tit_20b**
Li	0,097	0,074	0,085	0,124	0,047	0,067	0,133	0,192	0,073	0,071	0,1	0,357	0,153	0,123	0,119	0,195	0,109	0,074
Mg	0,00471	0,00349	0,00537	0,00415	0,00325	0,00362	0,00492	0,00704	0,00323	0,00351	0,00442	0,00822	0,00475	0,00523	0,00454	0,00399	0,00466	0,00472
Al	0,305	0,348	0,317	0,333	0,355	0,356	0,338	0,38	0,406	0,318	0,311	0,439	0,351	0,34	0,301	0,364	0,375	0,332
Si	0,873	0,892	0,897	0,905	0,916	0,861	0,891	0,932	0,925	0,897	0,862	0,913	0,953	0,878	0,893	0,917	0,881	0,893
P	0,14	0,175	0,153	0,217	0,138	0,144	0,142	0,172	0,104	0,117	0,154	0,157	0,146	0,17	0,119	0,147	0,201	0,134
Ca42	14,82	14,82	14,82	14,82	14,82	14,82	14,82	14,82	14,82	14,82	14,82	14,82	14,82	14,82	14,82	14,82	14,82	14,82
Ca44	15,02	14,8	15,16	14,92	14,73	14,62	14,78	15,19	14,99	15,11	14,42	15,36	15,17	14,84	14,68	15,22	14,93	14,69
Sc	0,713	0,74	0,804	0,709	0,65	0,814	0,747	0,789	0,801	0,655	0,618	0,812	0,688	0,821	0,579	0,733	0,81	0,719
Ti46	304,37	308,94	308,97	308,17	300,11	292,33	308,77	323,68	314,52	299,61	281,57	316,05	293,24	308,94	300,9	303,61	304,6	302,08
Ti49	349,1	346,37	344,8	347,77	332,28	325,53	352,57	361,02	343,42	334,11	314,92	345,18	329,03	351,03	334,69	342,46	347,33	342,93
V	8,93	6,76	7,31	6,46	8,05	6,95	8,66	6,91	8,43	8,14	7,03	9,82	7,49	7,04	7,53	7,26	5,92	8,1
Cr	0,00374	0,00477	0,00473	0,00572	0,0049	0,00435	0,00483	0,0052	0,00458	0,00438	0,00466	0,0049	0,00432	0,0063	0,0038	0,00495	0,00441	0,00515
Mn	0,2323	0,28	0,252	0,2047	0,284	0,264	0,254	0,272	0,291	0,274	0,264	0,282	0,27	0,2044	0,225	0,29	0,237	0,27
Fe	0,0696	0,0691	0,0696	0,0687	0,0679	0,0643	0,0688	0,0732	0,0706	0,068	0,0659	0,0768	0,068	0,0732	0,0681	0,0708	0,0719	0,07
Co	0,00032	0,00022	0,00043	0,00026	0,00019	0,00031	0,0003	0,00085	0,00017	0,00028	0,00041	0,00132	0,00043	0,00034	0,00026	0,0003	0,00027	0,00046
Sr	258,28	216,04	267,92	248,76	190,93	178,25	250,56	260,67	191,73	210,95	232,68	181,38	179,63	255,46	232,43	217,71	255,59	240,05
Y	243,94	292,02	300,3	303,89	233,82	284,31	238,11	289,92	276,19	199,7	239,61	319,07	248,09	309,85	204,65	274,11	324,93	251,47
Zr	704,8	672,61	703,58	628,28	616,61	1005,76	655,85	669,32	1148,6	719,4	526,81	748,78	641,66	728	589,96	640,46	747,85	639,09
Nb	1591,77	1193,29	1515,06	1547,84	1364,98	1859,09	1382,66	1349,13	1769,4	1528,08	1298,6	1235,13	1607,1	1352,26	1455,64	1252,5	1315,45	1308,13
Sn	20,32	24,74	25,58	26,22	22,06	22,92	22,26	25,7	19,99	19,87	22,62	20,4	22,94	25,5	19,38	23,3	29,43	21,04
Sb	0	0	0	0	0,64	0	0	0	0,52	0,45	0	0,87	0	0	0	0,49	0	0
Ba	0,146	0,521	1,25	0,205	0,107	0,11	0,326	2,65	0,055	0,147	0,202	2,31	0,141	0,134	0,076	5,63	0,178	0,486
La	5578,84	5459,17	6330,23	6236,64	5384,93	6130,12	5255,02	5871,23	6048,38	4858,13	5217,76	6917,88	5886,04	5783,45	4687,78	5626,58	6394,76	5300,07
Ce	6634,13	6861,71	7524,5	7933,67	6760,04	7299,81	6426,19	7489,31	7070,69	6219,45	6852	8089,41	7797,35	7343,47	6146,37	7406,7	7987,26	6736,2
Pr	5941,76	6854,29	7000,3	7465,81	5843,84	6477,97	6067,07	7279,88	6180,8	5319,46	6596,01	7106,7	6904,32	7163,5	5351,58	6952,23	7860,43	6173,35
Nd	4992,53	6173,23	6143,61	6518,38	4764,69	5414,25	5223,6	6391,69	5059,55	4258,6	5499,62	5877,44	5510,86	6385,43	4437,26	6001,31	6859,02	5309,22
Sm	2690,19	3709,29	3475,96	3923,95	2709,03	3031,98	2933,49	3691,06	2772,53	2347,04	3147,28	3249,51	3026,53	3751,01	2427,23	3520,03	4165,49	3016,18
Eu	1851,06	2581,59	2318,86	2664,35	1969,13	2087,22	2089,86	2616,15	1988,68	1760,85	2249,81	2217	2220,02	2553,67	1729,56	2473,9	2881,63	2072,22
Gd	1145,75	1538,65	1434,47	1589,5	1107,59	1228,86	1241,94	1516,7	1169,32	976,88	1223,67	1352,89	1197,08	1504,61	969,48	1416,6	1693,95	1211,78
Tb	669,87	871,87	825,27	916,89	642,01	703,92	712,83	880,87	696,55	566,08	685,22	800,21	699,12	884,81	573,97	819,14	980,25	702,25
Dy	415,05	535,37	518,77	569,45	402,69	456,89	450,83	543,78	472	357,27	414,41	507,07	425,19	550,06	365,22	500,92	601,65	436,66
Ho	267,53	317,23	327,47	349,72	250,96	295,2	276,22	333,88	299,6	224,79	246,77	327,61	272,8	333,99	233,48	308,99	376,82	267,1
Er	181,97	214,39	217,82	235,56	181,75	207	186,84	227,71	209,36	157,4	176,03	238,12	193,73	232,57	161,13	209,32	253,12	192,75
Tm	135,37	160,17	168,57	170,62	138,82	164,8	139,06	166,23	174	123,15	126,16	196,76	148,32	172,76	118,83	162,99	185,02	149,33
Yb	107,76	126,17	124,73	134,76	119,59	139,4	109,25	125,64	151,56	102,6	98,71	162,14	121,55	132,44	98,72	132,84	140,87	121,36
Lu	65,75	82,39	80	82,8	78,85	90,46	66,53	81,45	106,44	68,44	63,25	115,16	79,91	84,56	61,53	84,57	87,68	76,89
Hf	649,27	660,33	686,36	620,29	567,75	893,9	652,79	688,53	1182,81	662,82	515,96	695,98	636,92	751,69	558,09	640,66	719,26	645,65
Ta	1846,39	1571,42	1901,68	2142,4	1382,01	1597,23	1644,69	1702,64	1352,22	1297,88	1506,74	857,66	1543,38	1828,68	1412,44	1449	1788,28	1354,56
Pb	4,11	6,72	4,75	4,48	7,9	7,14	4,62	5,88	9,62	7,39	5,02	10,81	5,56	4,04	4,25	7,05	4,87	6,05
Pb	2,99	4,5	3,5	3,61	4,99	4,49	3,43	4,55	4,99	4,64	3,77	6	3,65	3,04	3,15	4,75	3,5	4,15
Pb	5,02	6,35	5,23	5,67	6,93	7,38	5,25	6,47	9,97	6,76	5,44	11,16	5,97	5,09	4,78	6,57	6,04	6,18
Th	3082,56	2892,98	3033,45	3400,87	3259,38	4324	2621,4	3086,85	8445,19	3082,95	2286,83	8098,95	2923,29	3221,59	2388,45	2931,08	3499,99	3059,13
U	961,74	1820,5	946,33	969,02	2726,62	2210,97	1094,93	1208,1	4518,56	2504,29	1096,08	3896,91	1553,44	973,06	929,95	2041,08	955,58	1561,37

Zircon

LA-ICP-MS results obtained for zircon– Sample PB-09

	LA-ICP-MS - Elementos Traço normalizado por Condrito - PB-09 (CSO)														
Element	Zr-1	Zr-2	Zr-3	Zr-4	Zr-5	Zr-6	Zr-7	Zr-8	Zr-9	Zr-10	Zr-11	Zr-12	Zr-13	Zr-14	Zr-15
Li	1,01	1,22	0,65	1,52	0,94	0,523	0,72	0,8	0,96	2,14	0,4	0,93	1,72	0,96	0,95
Mg	0,0108	0	0,00012	0,0204	0,00001	0,00179	0,00041	0,00022	0,00001	0,00004	0,0002	0	0,07	0,00054	0,0069
Al	0,01461	0	0,00127	0,0481	0,0398	0,1467	0	0,0225	0,01226	0,0448	0,00375	0,00219	0,642	0,00284	0,0372
Si	1,04	1,054	1,084	1,079	1,037	1,013	1,084	1,123	1,059	1,077	1,076	1,145	1,32	1,065	1,24
P	0,062	0,062	0,039	0,063	0	0,054	0,078	0,042	0,076	0,061	0,077	0,1	0,09	0,08	0,15
Ca	0,244	0	0	0,043	0	0	0	0	0	0,046	0,057	0	0,222	0	0,074
Ca	0,214	0	0	0	0	0	0	0	0	0	0,0237	0	0,244	0	0
Sc	29,5	29,06	29,87	31,51	30,64	30,29	30,18	32,38	31,57	30,98	31,57	30,31	36,19	31,83	33,85
Ti	0,0735	0,0396	0,0529	0,0441	0,0372	0,0634	0,051	0,0554	0,0436	0,0749	0,0596	0,043	0,067	1,32	0,0661
Mn	0,0188	0	0	0,0114	0	0,00043	0	0	0,00026	0,00071	0	0	0,0183	0,00635	0,00105
Fe	0,00659	0	0	0,0123	0	0,00129	0	0,00019	0,00009	0,00032	0,00015	0	0,0413	0,0055	0,00416
Co	0,00238	0	0	0,0102	0	0,00048	0	0,0003	0	0	0	0	0,0287	0	0,00252
Rb	0,13	0	0	0,439	0	0,74	0	0,296	0	0,97	0	0	0,38	0	0,269
Sr	0,194	0,0248	0,035	0,249	0,351	3,22	0,0176	0,95	0,251	0,442	0,078	0	17,36	0,027	0,82
Y	185,55	103,75	148,94	151,21	91,78	205,01	158,46	144,33	98,29	101,52	271,71	88,79	212,63	82,89	296,67
Zr	89131,1	89131,09	89131,1	89131,09	89131,09	89131,08	89131,08	89131,09	89131,08	89131,08	89131,08	89131,09	89131,09	89131,08	89131,08
Nb	2,5	2,4	2,1	2,89	2,47	2,04	2,33	2,06	1,63	2,79	2,05	2,1	1,61	6,33	3,18
Mo	2,3	1,58	1,14	1,78	0	1,18	2,52	1,38	1,83	3,09	1,6	1,92	2,61	2,26	1,93
Sn	0	0	0	0	0	0	0	0	0	0	0	0	0	0,9	0
Sb	0	0	0	0	0	0	0	0	0	0	0	0	0	0	0
Ba	0	0	0	0	0	35,23	0	6,27	0	0	0	0	3,88	0	5,46
La	2,08	0	0	0	0,99	1,86	0	0	0	4,71	0,85	0	1,58	0	1,06
Ce	26,14	21,57	24,61	26,75	20,1	25,41	24,82	25,24	19,42	22,46	30,79	20,92	31,65	20,84	35,56
Pr	4,21	0	0	1,92	0	3,26	3,66	2,08	1,71	0	4,77	0	6,48	2,24	6,55
Nd	14,03	3,7	6,56	5,43	0	8	6,6	6,63	0	0	18,88	0	11,07	5,51	19,86
Sm	42,62	0	29,53	21,36	0	32,84	28,72	29,41	9,64	0	65,89	12,64	53,74	0	61,61
Eu	27,48	14,21	19,25	9,61	11,93	22,64	0	20,99	6,97	14,29	30,68	8,35	39	0	53,57
Gd	74,67	36,79	63,51	50,71	36,14	90,98	72,38	64,22	30,94	33,57	116,58	19,56	88,97	25,47	135,09
Tb	98,1	43,55	82,48	61,17	39,49	113,11	86,52	81,66	41,23	42,16	150,73	38,58	114,93	38,27	162,8
Dy	129,94	65,69	108,33	94,3	62,28	140,39	110,42	104,85	62,75	68,06	190,55	46,33	146,3	58,88	220,39
Ho	172,9	85,57	144,42	123,45	75,57	197,58	145,56	135,78	83,26	88,63	238,85	75,63	189,22	73,47	265,41
Er	210,83	120,07	183,58	173,2	106,07	243,94	187,01	205,73	112,63	126,78	286,83	98,8	229,26	95,27	334,22
Tm	292,92	174,63	230,69	244,42	132,71	338,91	233,34	245,03	157,06	173,48	394,18	151,75	288,32	134,19	446,23
Yb	375,09	209,55	294,44	295,76	184,66	409,17	307,98	321,98	224,38	226,36	474,42	191,82	389,66	185,64	572
Lu	465,17	250,83	385,23	359,12	253,95	472,34	401,47	380,15	282,18	300,37	605,8	239,11	464,74	228,62	635,72
Hf	47155,94	45440,43	46920,13	44384,53	47756,76	47347,93	50242,63	52691,92	54429,5	52940,46	52786,66	54420,48	56204,42	57077,51	55140,47
Ta	16,06	13,08	15,94	6,44	25,34	0	19,64	12,82	21,76	12,16	13,25	0	20,35	27,86	19,56
Pb	3,38	3,12	4,06	4,78	3,16	5,44	5	4,84	3,36	3,56	5,56	3,88	5,05	4,63	6,81
Pb	0	0	0	0,33	0,55	0,74	0,95	0,83	0	0	0	0	0	0	0
Pb	1,06	0,81	0,75	1,06	0,79	1,53	1,11	1,11	0,63	0,88	1,72	0,9	1,5	0,98	1,65
Th	1411,55	819,12	1157,29	1421,31	716,53	1526,25	1209,78	1136,4	865,82	736,85	2005,36	770,32	1677,92	802,64	2037,84
U	2756,01	2361,75	2612,09	3390,65	1989,14	3159,16	2704,1	2865,86	2593,26	2068,44	3865,53	2429,71	3595,56	2686,76	4009,74

	LA-ICP-MS - Concentração de Elementos Traço (Ppm) - PB-185 (CSO).														
Element	Zr-1	Zr-2	Zr-3	Zr-4	Zr-5	Zr-6	Zr-7	Zr-8	Zr-9	Zr-10	Zr-11	Zr-12	Zr-13	Zr-14	Zr-15
Li	2,42	2,93	1,57	3,65	2,27	1,26	1,72	1,92	2,3	5,13	0,96	2,22	4,13	2,31	2,29
Mg	1547,82	<0.90	16,91	2924,02	1,61	255,62	58,22	31,64	1,6	6,03	28,54	<0.91	10017,03	77,03	993,41
Al	188,44	<10.86	16,35	621,06	514,02	1891,8	<11.06	290,58	158,1	578,47	48,35	28,3	8279,81	36,57	479,38
Si	166409,2	168667	173417,7	172575,6	165932,8	162071,8	173378,4	179742,2	169406,5	172374,9	172084,7	183173	211338	170342,5	198308,1
P	142,4	142,25	90,15	145,99	<138.61	123,56	178,93	96,63	174,27	139,76	177,72	218,86	213,34	183,46	342,97
Ca	3296,66	<762.11	<792.05	584,85	<2052.14	<658.87	<736.87	<704.48	<513.21	625,66	767,87	<903.73	2992,07	<888.91	1003,14
Ca	2888,12	<226.62	<241.06	<145.59	<642.16	<201.88	<223.92	<214.09	<158.11	<178.63	320,18	<279.62	3291,98	<266.75	<235.85
Sc	254,85	251,06	258,09	272,22	264,72	261,73	260,77	279,74	272,72	267,71	272,81	261,86	312,68	275,04	292,47
Ti	48,06	25,92	34,61	28,86	24,31	41,48	33,33	36,25	28,53	48,95	39,01	28,12	43,82	865,36	43,25
Mn	55,33	<1.03	<1.10	33,56	<3.29	1,27	<1.02	<0.99	0,75	2,08	<0.92	<1.29	53,79	18,68	3,09
Fe	1831,92	<10.25	<10.75	3423,26	<28.67	358,06	<9.97	51,64	24,08	87,95	42,05	<12.79	11474,94	1534,35	1155,19
Co	1,82	<0.186	<0.219	7,8	<0.96	0,37	<0.116	0,233	<0.140	<0.148	<0.193	<0.198	21,92	<0.26	1,93
Rb	0,45	<0.40	<0.44	1,51	<0.94	2,56	<0.51	1,02	<0.34	3,36	<0.41	<0.70	1,32	<0.74	0,93
Sr	2,31	0,295	0,42	2,96	4,18	38,33	0,21	11,26	2,99	5,25	0,92	<0.24	206,58	0,32	9,74
Y	417,48	233,44	335,11	340,22	206,5	461,28	356,53	324,73	221,14	228,43	611,34	199,78	478,42	186,49	667,5
Zr	493786,3	493786,3	493786,3	493786,3	493786,3	493786,2	493786,2	493786,2	493786,2	493786,2	493786,2	493786,2	493786,2	493786,2	493786,2
Nb	0,94	0,9	0,79	1,08	0,93	0,76	0,87	0,77	0,61	1,05	0,77	0,79	0,6	2,37	1,19
Mo	3,18	2,18	1,57	2,45	<4.47	1,63	3,47	1,91	2,52	4,27	2,21	2,65	3,6	3,12	2,67
Sn	<1.67	<1.91	<2.10	<1.22	<5.94	<1.38	<1.85	<1.80	<1.16	<1.49	<1.52	<1.99	<2.50	2,26	<1.96
Sb	<1.02	<1.16	<1.45	<0.67	<4.16	<1.18	<1.30	<1.36	<0.84	<1.11	<1.38	<1.71	<1.68	<1.64	<1.23
Ba	<1.64	<1.50	<2.23	<1.78	<6.38	120,12	<2.18	21,38	<1.62	<2.10	<2.28	<3.57	13,22	<2.73	18,62
La	0,76	<0.25	<0.36	<0.195	0,362	0,68	<0.29	<0.29	<0.20	1,73	0,31	<0.42	0,58	<0.27	0,39
Ce	25,01	20,64	23,55	25,6	19,23	24,31	23,75	24,16	18,58	21,5	29,46	20,02	30,29	19,94	34,03
Pr	0,58	<0.27	<0.34	0,26	<1.01	0,45	0,5	0,28	0,23	<0.22	0,65	<0.41	0,89	0,31	0,9
Nd	9,97	2,63	4,66	3,86	<6.25	5,68	4,69	4,72	<1.88	<1.95	13,42	<2.48	7,87	3,92	14,12
Sm	9,84	<2.38	6,82	4,93	<5.15	7,59	6,63	6,79	2,23	<1.94	15,22	2,92	12,41	<2.33	14,23
Eu	2,39	1,24	1,67	0,84	1,04	1,97	<0.91	1,83	0,61	1,24	2,67	0,73	3,39	<0.93	4,66
Gd	22,85	11,26	19,43	15,52	11,06	27,84	22,15	19,65	9,47	10,27	35,67	5,99	27,23	7,8	41,34
Tb	5,69	2,53	4,78	3,55	2,29	6,56	5,02	4,74	2,39	2,45	8,74	2,24	6,67	2,22	9,44
Dy	49,51	25,03	41,27	35,93	23,73	53,49	42,07	39,95	23,91	25,93	72,6	17,65	55,74	22,43	83,97
Ho	14,71	7,28	12,29	10,51	6,43	16,81	12,39	11,56	7,09	7,54	20,33	6,44	16,1	6,25	22,59
Er	52,5	29,9	45,71	43,13	26,41	60,74	46,57	51,23	28,05	31,57	71,42	24,6	57,09	23,72	83,22
Tm	10,43	6,22	8,21	8,7	4,72	12,07	8,31	8,72	5,59	6,18	14,03	5,4	10,26	4,78	15,89
Yb	93,02	51,97	73,02	73,35	45,79	101,47	76,38	79,85	55,65	56,14	117,66	47,57	96,64	46,04	141,86
Lu	17,72	9,56	14,68	13,68	9,68	18	15,3	14,48	10,75	11,44	23,08	9,11	17,71	8,71	24,22
Hf	8440,91	8133,84	8398,7	7944,83	8548,46	8475,28	8993,43	9431,85	9742,88	9476,34	9448,81	9741,27	10060,59	10216,87	9870,14
Ta	0,42	0,34	0,41	0,17	0,66	<0.27	0,51	0,33	0,57	0,32	0,34	<0.44	0,53	0,72	0,51
Pb	12,32	11,39	14,84	17,44	11,52	19,85	18,26	17,65	12,28	13	20,31	14,16	18,42	16,88	24,87
Pb	<1.62	<1.28	<1.61	1,21	2,01	2,7	3,47	3,04	<1.45	<1.92	<1.44	<1.83	<2.91	<2.07	<1.76
Pb	3,86	2,94	2,74	3,86	2,87	5,57	4,05	4,05	2,3	3,22	6,27	3,28	5,49	3,59	6,02
Th	59,99	34,81	49,18	60,41	30,45	64,87	51,42	48,3	36,8	31,32	85,23	32,74	71,31	34,11	86,61
U	33,62	28,81	31,87	41,37	24,27	38,54	32,99	34,96	31,64	25,24	47,16	29,64	43,87	32,78	48,92

LA-ICP-MS results obtained for zircon– Sample PB-22

	LA-ICP-MS - Elementos Traço normalizado por Condrito - PB-22 (ESO)																							
Element	**Zr-1**	**Zr-2**	**Zr-3**	**Zr-4**	**Zr-5**	**Zr-6**	**Zr-7**	**Zr-8**	**Zr-9**	**Zr-10**	**Zr-11**	**Zr-12**	**Zr-1**	**Zr-2**	**Zr-3**	**Zr-4**	**Zr-5**	**Zr-6**	**Zr-7**	**Zr-8**	**Zr-9**	**Zr-10**	**Zr-11**	**Zr-12**
Li	1,88	1,12	2,19	1,44	1,31	0,65	2,38	0,54	1,27	0,95	1,77	1,22	4,51	2,68	5,27	3,44	3,14	1,56	5,7	1,3	3,05	2,29	4,26	2,94
Mg	0,00162	0,00089	0,00586	0,00041	0	0,00411	0,00599	0,00012	0,00001	0,00011	0,00134	0,0182	231,53	127,59	837,81	59,32	<0.80	587,75	856,15	17,57	1,53	16,2	192,18	2605,57
Al	0,98	0,00575	0,0111	0,095	0,0103	0,0257	0,156	0,0335	0,00147	0,00118	0,0068	0,0412	12647,16	74,14	142,76	1219,58	132,3	331,11	2015,56	431,78	19	15,26	88,12	531,89
Si	1,42	1,093	1,036	0,994	1,047	0,985	0,926	1,036	0,976	0,922	0,996	1,025	226965,8	174833,5	165785,6	158993,6	167474	157567,1	148162,4	165689	156098,1	147474,6	159329,4	164066
P	0,19	0,11	0,13	0,12	0,16	0,07	0,14	0,12	0,13	0,07	0,13	0,1	438,02	244,97	291,46	271,09	373,11	171,68	330,47	272,39	305,36	160,74	307,21	227,35
Ca	0	0	0,109	0	0	0,054	0	0	0	0	0	0,312	<688.96	<528.30	1478,18	<423.51	<587.97	727,5	<484.88	<456.66	<511.66	<333.73	<512.60	4210,29
Ca	0,063	0	0,121	0,098	0	0,0414	0,0181	0	0	0,0096	0	0,317	854,33	<178.72	1639,32	1327,16	<197.00	558,96	244,11	<150.49	<165.66	129,07	<163.83	4279,74
Sc	33,89	31,23	30,7	32,73	32,36	30,41	29,07	32,68	29,82	30,86	30,19	30,29	292,8	269,86	265,26	282,78	279,56	262,75	251,17	282,35	257,64	266,64	260,86	261,67
Ti	0,193	0,0138	0,05	0,055	0,054	0,06	0,046	0,039	0,0347	0,036	8,56	0,069	126,28	9,03	32,87	35,99	35,13	39,2	30,12	25,44	22,72	23,74	5596,63	45,32
Mn	0	0,00034	0,0097	0,00047	0	0,00381	0,00279	0	0	0	0,0209	0,033	<1.31	0,99	28,57	1,39	<0.87	11,19	8,2	<0.74	<0.79	<0.55	61,31	96,96
Fe	0	0,0007	0,0033	0,00037	0	0,00355	0,0137	0,00011	0	0,00011	0,0509	0,0089	<17.21	194,43	917,34	101,61	<7.99	986,24	3816,61	29,97	<6.59	31,32	14150,72	2465,45
Co	0	0,00029	0,00113	0,00019	0	0,00102	0,00106	0	0	0	0,0039	0,00218	<0.33	0,223	0,86	0,144	<0.179	0,78	0,81	<0.104	<0.117	<0.080	2,98	1,66
Rb	3,78	0,12	0	0	0,151	0,347	0,86	0,47	0	0	0	0,37	13,05	0,41	<0.35	<0.29	0,52	1,2	2,96	1,63	<0.33	<0.22	<0.33	1,27
Sr	27,38	0,055	0,13	1,92	0,046	0,181	4,61	1,42	0	0,042	0,0188	0,323	325,81	0,66	1,55	22,88	0,55	2,15	54,85	16,9	<0.184	0,5	0,223	3,85
Y	189,81	161,04	134,42	234,79	190,51	256,19	190,82	269,76	166,3	194,67	126,06	228,43	427,08	362,35	302,46	528,28	428,64	576,42	429,34	606,96	374,18	438,01	283,63	513,96
Zr	89131,07	89131,06	89131,06	89131,06	89131,07	89131,06	89131,08	89131,08	89131,08	89131,08	89131,08	89131,08	493786,1	493786,1	493786,1	493786,1	493786,1	493786,1	493786,2	493786,2	493786,2	493786,2	493786,2	493786,2
Nb	3,69	2,63	2,46	3,19	2,82	2,04	3,11	2,98	2,59	2,25	20,72	2,54	1,39	0,98	0,92	1,2	1,06	0,77	1,16	1,12	0,97	0,84	7,77	0,95
Mo	2,58	1,91	1,52	1,51	2,43	1,41	1,3	0	1,23	1,3	2,08	1,87	3,56	2,64	2,1	2,08	3,35	1,95	1,8	<1.24	1,7	1,8	2,87	2,59
Sn	0	0	0	0	0	0	0	0	0	0	1,25	0	<1.84	<1.35	<1.57	<1.07	<1.48	<1.42	<1.42	<1.39	<1.38	<0.86	3,15	<1.09
Sb	0	0	0	0	0	0	0	0	0	0	0	0	<1.25	<0.98	<1.21	<0.83	<1.12	<0.83	<0.79	<0.86	<1.13	<0.62	<1.07	<0.92
Ba	165,36	0	0	1,89	0	0	34,98	11,9	0	0	0	0	563,87	<1.84	<2.09	6,44	<2.24	<1.53	119,28	40,57	<1.68	<1.33	<2.10	<1.65
La	4,23	0,93	0	0	0	0	1,83	0	0	0	1,15	2,81	1,55	0,34	<0.27	<0.17	<0.29	<0.22	0,67	<0.22	<0.23	<0.161	0,42	1,03
Ce	32,58	28,9	29,95	34,62	30,22	33,87	33,03	35,53	30,68	28,34	26,71	37	31,18	27,66	28,66	33,13	28,92	32,41	31,61	34,01	29,36	27,13	25,56	35,41
Pr	3,34	0	2,87	3,81	4,43	6,07	3,52	8,01	2,09	3,32	2,27	6,11	0,46	<0.24	0,39	0,52	0,61	0,83	0,48	1,1	0,29	0,46	0,31	0,84
Nd	8,52	3,73	0	12,78	5,59	9,8	11,07	14,64	5,17	10,57	5,56	12,1	6,06	2,65	<2.55	9,09	3,97	6,97	7,87	10,41	3,68	7,52	3,95	8,6
Sm	34,7	11,91	9,3	34,99	29,97	40,48	34,4	52,16	25,97	13,98	0	47,93	8,02	2,75	2,15	8,08	6,92	9,35	7,95	12,05	6	3,23	<2.04	11,07
Eu	26,35	19,12	12,51	31,04	21,21	30,42	25,48	37,44	20,74	25,25	9,54	35,35	2,29	1,66	1,09	2,7	1,85	2,65	2,22	3,26	1,8	2,2	0,83	3,08
Gd	58,73	47,61	35,56	80,48	71,03	94,58	70,4	110,56	53,19	54,45	34,12	99,15	17,97	14,57	10,88	24,63	21,73	28,94	21,54	33,83	16,28	16,66	10,44	30,34
Tb	83,43	69,81	55,89	104,45	98,87	124,21	87,57	134,06	76,25	72,05	51,93	123,29	4,84	4,05	3,24	6,06	5,73	7,2	5,08	7,78	4,42	4,18	3,01	7,15
Dy	106,18	100,65	76,26	158,06	123,65	178,55	125,88	212,73	119,55	137,29	83,93	169,46	40,45	38,35	29,05	60,22	47,11	68,03	47,96	81,05	45,55	52,31	31,98	64,56
Ho	160,47	142,41	117,7	204,83	168,2	232,57	176,53	240,02	158,65	162,12	107,85	209,8	13,66	12,12	10,02	17,43	14,31	19,79	15,02	20,43	13,5	13,8	9,18	17,85
Er	224,45	193,19	171,26	289,16	250,85	315,81	238,67	330,69	210,15	226,31	166,23	279,8	55,89	48,1	42,64	72	62,46	78,64	59,43	82,34	52,33	56,35	41,39	69,67
Tm	330,36	297,75	227,07	379,04	320,51	436,64	365,08	494,09	280,62	367,17	193,74	358,45	11,76	10,6	8,08	13,49	11,41	15,54	13	17,59	9,99	13,07	6,9	12,76
Yb	456,25	347,08	345,91	479,11	417,96	541,48	443,48	564,94	350,34	397,14	297,76	442,54	113,15	86,08	85,78	118,82	103,65	134,29	109,98	140,11	86,88	98,49	73,84	109,75
Lu	555,92	427,93	410,87	556,81	521,05	573,39	531,08	656,74	433,07	514,83	378,4	584,57	21,18	16,3	15,65	21,21	19,85	21,85	20,23	25,02	16,5	19,61	14,42	22,27
Hf	55144,37	59841,24	59402,03	52615,36	52484,7	53978,89	55374,93	54117,48	48107,09	50246,71	50454,1	51808,73	9870,84	10711,58	10632,96	9418,15	9394,76	9662,22	9912,11	9687,03	8611,17	8994,16	9031,28	9273,76
Ta	15,6	19,9	31,57	20,29	11,75	18,47	26,16	26,69	12,17	19,28	17,91	39,98	0,41	0,52	0,82	0,53	0,31	0,48	0,68	0,69	0,32	0,5	0,47	1,04
Pb	7,38	5,74	6,48	8,66	4,93	7,36	7,95	6,57	5,58	5,7	5,91	5,36	26,93	20,97	23,67	31,6	18	26,87	29,03	23,98	20,38	20,82	21,58	19,56
Pb	1,25	0,45	0,64	0,7	0	0,57	0,64	0,41	0	0,6	0	0	4,55	1,65	2,33	2,56	<2.09	2,07	2,33	1,49	<1.47	2,19	<1.36	<1.20
Pb	2,07	1,17	1,28	1,44	1,08	1,82	1,58	2,05	1,08	1,82	0,8	1,61	7,54	4,27	4,66	5,25	3,94	6,65	5,75	7,48	3,95	6,64	2,92	5,86
Th	1637,28	1394,5	1647,78	2462,37	1638,86	2360,72	2597,86	2570,55	1791,66	1813,94	1244,13	2109,69	69,58	59,27	70,03	104,65	69,65	100,33	110,41	109,25	76,15	77,09	52,88	89,66
U	4256,21	3605,45	4674,59	5254,67	3433,44	4644,17	6078,92	5333,02	3890,26	4501,24	3172,98	4297,1	51,93	43,99	57,03	64,11	41,89	56,66	74,16	65,06	47,46	54,92	38,71	52,42

LA-ICP-MS results obtained for zircon– Sample PB-92B

	LA-ICP-MS - Elementos Traço normalizado por Condrito - PB-92B(LSO)												
Element	Zr5	Zr-6	Zr-7	Zr-8	Zr-9	Zr-10	Zr-12	Zr-13	Zr-14	Zr-15	Zr-17	Zr-18	Zr-20
Li	1,53	2,4	2,6	2,95	2,07	2,4	4,88	2,85	2,45	2,21	4,59	3,22	1,77
Mg	0,00005	0	0,00002	0,00056	0,00029	0,00009	0,19	0,00018	0,00002	0,00032	0,00004	0,00003	0,00002
Al	0,0354	0,00158	0,0128	0,00311	0,061	0,00186	0,75	0,00173	0,257	0,00301	0,069	0,093	0,00251
Si	1,12	1,01	1,13	1,02	1	1,06	1,26	0,95	1,12	1,12	1,06	1,08	1,16
P	0,067	0,069	0,85	0,092	0,067	0,223	0,067	0,063	0,083	0,07	0,052	0,046	0,171
Ca	0	0	0,419	0,084	0	0	1,76	0	0	0	0	0	0
Ca	0,0203	0	0,366	0	0,0272	0,0242	1,71	0	0,0285	0	0	0	0,0381
Sc	34,68	35,22	37,67	35,92	34,67	34,43	34,03	31,91	34,29	33,09	33,54	33,13	33,76
Ti	0,0202	0,0451	0,0494	5,76	0,033	0,0361	2,74	0,0272	0,0426	0,0474	0,0505	0,0187	0,0405
Mn	0	0	0,00303	0,0215	0	0,00038	0,243	0	0	0	0,00089	0,0004	0,00055
Fe	0,00012	0	0,0002	0,0235	0,00044	0,00017	0,124	0,00028	0,00029	0,00027	0,00052	0,00019	0
Co	0	0	0	0,00343	0	0	0,0275	0,00019	0	0,00035	0	0	0
Rb	0,178	0	0	0	0	0	0,28	0	3,01	0	1,42	0	0
Sr	0,657	0	4,34	0,104	2,2	0,173	3,69	0,037	8,45	0,029	0,354	2,9	0,49
Y	330,74	152,23	175,5	147,22	128,94	147,08	130,68	140,71	216,55	159,8	124,27	157,66	214,45
Zr	89131,08	89131,08	89131,09	89131,08	89131,08	89131,09	89131,08	89131,09	89131,09	89131,09	89131,09	89131,08	89131,09
Nb	7,51	3,93	5,61	20,76	3,93	4,43	24,46	5,79	5,76	3,43	5,96	5,63	4,27
Mo	5,69	3,77	3,54	4,31	3,26	2,96	2,16	2,9	3,68	1,49	1,66	2,6	2,94
Sn	0,55	0	0	0,64	0	0	0	0,63	0	0	0	0	0
Sb	0	0	0	0	0	0	0	0	0	0	0	0	0
Ba	0	0	0	0	0	0	1,74	0	49,44	0	0,76	0	0
La	1,98	0,55	148,18	2,86	0	7,36	52,4	0	8,21	0	6,31	0	27,7
Ce	64,82	45,59	156,05	49,15	40,96	53,96	118,7	49,12	57,06	46,42	47,14	52,36	66,85
Pr	6,47	1,83	99,96	2,2	1,7	5,5	74,61	1,27	7,86	0	0	0	14,22
Nd	12,02	0	75,75	5,78	3,68	7,9	70,88	4,04	11,04	3,98	3,62	0	12,12
Sm	47,32	18,07	67,03	12,22	9,97	13,21	82,68	13,94	38,05	20,31	27,04	10,92	42,43
Eu	43,31	20,21	33,84	22,4	14,25	21,96	53,11	17,79	31,3	25,98	16,99	12,29	23,94
Gd	124,02	49,12	73,41	41,78	37,67	53,46	53,03	34,27	82,66	55,02	32,28	44,27	75,96
Tb	162,88	72,03	82,31	57,95	55,88	67,14	41,55	45,28	102,46	61,36	42,65	58,5	112,76
Dy	232,41	108,02	120,35	94,13	76,44	90,9	107,54	83,09	161,05	108,12	65,06	93,63	138,01
Ho	318,34	132,91	156,75	122,63	112,21	115,95	120,86	103,76	188,3	140,75	89,15	126,74	188,84
Er	411,18	180,32	206,77	170,37	162,36	180,52	166,36	156,76	252,01	184,97	129,67	186,61	243,78
Tm	560,42	253,73	305,49	252,55	211,75	236,66	224,94	223,57	326,64	249,73	204,1	272,99	345,13
Yb	704,54	337,73	408,92	321,33	329,13	329,42	272,63	289,52	436,31	346,63	252,74	335,46	443,62
Lu	843,82	401,84	458,87	362,78	410,67	412,22	388,62	377,97	528,91	456,2	347,82	476,6	546,25
Hf	57589,01	55507,57	55401,82	51637,74	55734,65	56092,78	49580,19	52910,71	57207,11	52221,3	56536,21	60959,07	53546
Ta	54,87	17,71	27,63	32,16	15,26	25,02	45,17	29,16	27,3	27,6	32,33	35,37	33,2
Pb	9,47	7,44	8,64	7,87	6,71	8,57	6,22	7,26	8,33	8,86	7,06	11,68	7,73
Pb	0,44	0	0,82	0,68	0	0,67	1,69	0,8	1,21	0,56	0,98	0,59	0
Pb	2,69	1,53	1,97	2,05	1,72	2,07	2,01	1,92	3,26	1,7	1,69	1,89	1,97
Th	4226,62	2234,94	2405,37	2280,36	1922,2	2436,56	2446,5	2250,91	3169,51	2353,27	1973,79	2891,48	2873,75
U	6976,91	4985,4	5038,9	5088,19	4513,96	5644,78	6245,07	5739,35	5471,91	5032,12	5271,4	8877,1	4968,15

	LA-ICP-MS - Concentração de Elementos Traço (Ppm) - PB-92B (LSO).												
Element	Zr5	Zr-6	Zr-7	Zr-8	Zr-9	Zr-10	Zr-12	Zr-13	Zr-14	Zr-15	Zr-17	Zr-18	Zr-20
Li	3,66	5,76	6,24	7,09	4,96	5,76	11,7	6,83	5,88	5,31	11,02	7,73	4,26
Mg	7,31	<0.55	3,51	79,52	41,13	13,24	27133,41	25,58	2,5	45,77	6,34	4,82	2,15
Al	457,3	20,43	165,27	40,14	786,77	23,94	9687,17	22,27	3317,08	38,86	888,73	1196,96	32,39
Si	178694,8	161601,3	180748,9	163958	160790,7	169009,1	201619,8	152196,6	179825,5	179286,4	170350,8	172494,9	185466,8
P	153,56	159,78	1962,57	210,61	154,51	512,75	154,98	144,54	190,65	161,57	119,99	106,48	392,24
Ca	<828.60	<749.57	5659,74	1137,03	<632.62	<860.51	23697,43	<652.02	<873.54	<1047.58	<954.25	<731.28	<1007.07
Ca	273,77	<215.77	4942,1	<221.95	367,38	326,29	23092,07	<189.30	384,44	<303.12	<275.95	<203.87	514,05
Sc	299,61	304,3	325,44	310,33	299,52	297,45	294,04	275,67	296,23	285,9	289,81	286,25	291,66
Ti	13,2	29,51	32,33	3768,43	21,6	23,58	1790,33	17,82	27,84	31	33,02	12,24	26,51
Mn	<0.89	<0.91	8,91	63,12	<0.75	1,13	714,29	<0.77	<1.07	<1.35	2,62	1,18	1,61
Fe	32,43	<11.72	55,52	6545,45	121,86	46,94	34393,29	77,24	80,26	74,73	144,75	52,12	<15.92
Co	<0.100	<0.142	<0.169	2,62	<0.148	<0.144	21,04	0,143	<0.225	0,269	<0.135	<0.133	<0.234
Rb	0,61	<0.43	<0.53	<0.43	<0.33	<0.48	0,96	<0.26	10,38	<0.58	4,88	<0.47	<0.60
Sr	7,82	<0.183	51,67	1,23	26,2	2,06	43,91	0,43	100,5	0,35	4,21	34,49	5,84
Y	744,17	342,52	394,88	331,24	290,12	330,93	294,04	316,6	487,25	359,55	279,61	354,73	482,51
Zr	493786,2	493786,2	493786,2	493786,2	493786,2	493786,2	493786,2	493786,2	493786,2	493786,2	493786,2	493786,2	493786,2
Nb	2,82	1,47	2,11	7,79	1,47	1,66	9,17	2,17	2,16	1,29	2,23	2,11	1,6
Mo	7,85	5,21	4,89	5,95	4,5	4,09	2,98	4,01	5,08	2,06	2,29	3,58	4,06
Sn	1,39	<1.39	<1.90	1,61	<1.34	<1.74	<2.33	1,59	<1.61	<1.75	<1.81	<1.61	<2.07
Sb	<1.08	<1.12	<1.13	<1.17	<0.84	<1.19	<1.42	<1.20	<1.21	<1.57	<1.37	<1.09	<1.72
Ba	<1.45	<1.77	<1.88	<1.48	<1.57	<2.08	5,93	<1.60	168,6	<3.10	2,59	<2.02	<2.19
La	0,73	0,203	54,38	1,05	<0.21	2,7	19,23	<0.165	3,01	<0.25	2,32	<0.25	10,17
Ce	62,04	43,63	149,34	47,03	39,2	51,64	113,6	47,01	54,6	44,42	45,12	50,11	63,98
Pr	0,89	0,25	13,69	0,3	0,23	0,75	10,22	0,17	1,08	<0.32	<0.33	<0.178	1,95
Nd	8,55	<2.13	53,86	4,11	2,62	5,61	50,4	2,87	7,85	2,83	2,57	<1.82	8,61
Sm	10,93	4,17	15,48	2,82	2,3	3,05	19,1	3,22	8,79	4,69	6,25	2,52	9,8
Eu	3,77	1,76	2,94	1,95	1,24	1,91	4,62	1,55	2,72	2,26	1,48	1,07	2,08
Gd	37,95	15,03	22,46	12,79	11,53	16,36	16,23	10,49	25,29	16,84	9,88	13,55	23,24
Tb	9,45	4,18	4,77	3,36	3,24	3,89	2,41	2,63	5,94	3,56	2,47	3,39	6,54
Dy	88,55	41,15	45,85	35,86	29,12	34,63	40,97	31,66	61,36	41,19	24,79	35,67	52,58
Ho	27,09	11,31	13,34	10,44	9,55	9,87	10,28	8,83	16,02	11,98	7,59	10,79	16,07
Er	102,38	44,9	51,48	42,42	40,43	44,95	41,42	39,03	62,75	46,06	32,29	46,47	60,7
Tm	19,95	9,03	10,88	8,99	7,54	8,43	8,01	7,96	11,63	8,89	7,27	9,72	12,29
Yb	174,73	83,76	101,41	79,69	81,62	81,7	67,61	71,8	108,2	85,96	62,68	83,19	110,02
Lu	32,15	15,31	17,48	13,82	15,65	15,71	14,81	14,4	20,15	17,38	13,25	18,16	20,81
Hf	10308,43	9935,85	9916,93	9243,16	9976,5	10040,61	8874,85	9471,02	10240,07	9347,61	10119,98	10911,67	9584,73
Ta	1,43	0,46	0,72	0,84	0,4	0,65	1,17	0,76	0,71	0,72	0,84	0,92	0,86
Pb	34,56	27,14	31,52	28,72	24,5	31,3	22,7	26,51	30,39	32,34	25,75	42,64	28,2
Pb	1,61	<1.31	3,01	2,48	<1.33	2,46	6,18	2,92	4,42	2,06	3,59	2,15	<2.38
Pb	9,8	5,6	7,2	7,48	6,26	7,55	7,34	6,99	11,9	6,22	6,19	6,89	7,2
Th	179,63	94,99	102,23	96,92	81,69	103,55	103,98	95,66	134,7	100,01	83,89	122,89	122,13
U	85,12	60,82	61,47	62,08	55,07	68,87	76,19	70,02	66,76	61,39	64,31	108,3	60,61

LA-ICP-MS results obtained for zircon– Sample PB-123

	LA-ICP-MS - Elementos Traço normalizado por Condrito - PB-123(LSO)												LA-ICP-MS - Concentração de Elementos Traço (Ppm) - PB-123 (LSO).											
Element	**ZR-01**	**ZR-02**	**ZR-03**	**ZR-04**	**ZR-05**	**ZR-06**	**ZR-07**	**ZR-08b**	**ZR-08c**	**ZR-09**	**ZR-10**	**ZR-11**	**ZR-01**	**ZR-02**	**ZR-03**	**ZR-04**	**ZR-05**	**ZR-06**	**ZR-07**	**ZR-08b**	**ZR-08c**	**ZR-09**	**ZR-10**	**ZR-11**
Li	0	1,06	1,1	0,51	0	0	1,52	1,89	0,86	1,59	1,02	0,96	<0.72	2,53	2,64	1,23	<0.95	<0.99	3,64	4,54	2,07	3,81	2,45	2,31
Mg	0,00009	0	0	0	0	0	0	0,00022	0,00001	0	0,00001	0	12,95	<0.45	0,59	<0.31	<0.39	<0.40	<0.39	30,82	0,73	0,51	1,04	0,5
Al	0,0171	0,00022	0,00115	0,00033	0,0002	0,00012	0,00098	0,00481	0,00027	0	0,00142	0,00106	220,14	2,8	14,8	4,25	2,58	1,54	12,68	62,06	3,53	<1.51	18,34	13,74
Si	0,97	1,03	1,06	1,01	1,02	1	1,01	1	1,02	1	0,96	0,98	154857,8	164993,9	168919,7	161395	162595,1	159587	161045	160034,6	162646,9	160568,2	154318,1	157299,4
P	0,044	0,03	0,056	0,042	0,052	0,043	0,031	0,036	0,044	0,026	0,071	0,025	100,19	68,25	128,94	96,79	119,51	98,97	70,28	83,54	101,09	59,15	163,95	57,89
Ca	0	0	0,055	0	0	0	0	0	0	0	0	0,041	<405.10	<583.21	749,03	<509.99	<536.52	<538.94	<552.75	<551.50	<546.16	<538.60	<522.68	553,18
Ca	0	0	0	0,0132	0	0	0	0	0	0	0	0	<83.55	<121.84	<117.00	178,07	<108.61	<110.26	<114.53	<114.05	<109.37	<108.15	<107.10	<112.60
Sc	22,72	21,39	23,06	21,78	21,89	22,03	20,13	20,53	21,45	20,68	21,01	19,66	196,27	184,85	199,23	188,19	189,12	190,33	173,96	177,38	185,32	178,64	181,53	169,88
Ti	0,053	0,0278	0,066	0,051	0,06	0,055	0,038	0,045	0,058	0,0229	0,056	0,039	34,78	18,17	43,2	33,28	39,02	35,86	24,82	29,44	37,7	14,97	36,7	25,58
Mn	0,00031	0	0	0	0	0	0	0,00228	0	0	0	0	0,93	<0.64	<0.65	<0.56	<0.60	<0.60	<0.62	6,72	<0.62	<0.61	<0.58	<0.62
Fe	0,00019	0,00006	0	0	0,00002	0	0	0,00236	0,00007	0	0	0,00004	53,76	16,88	<6.00	<5.41	6,66	<5.69	<5.82	656,61	18,39	<5.60	<5.47	10,3
Co	0	0	0	0	0	0	0	0,00017	0	0,00008	0	0	<0.057	<0.124	<0.082	<0.065	<0.088	<0.074	<0.081	0,133	<0.080	0,061	<0.090	<0.089
Rb	0	0	0	0	0	0	0	0	0	0	0	0	<0.28	<0.37	<0.39	<0.35	<0.35	<0.37	<0.40	<0.40	<0.38	<0.38	<0.35	<0.37
Sr	0,0164	0,0097	0,0096	0,0106	0,0076	0,0213	0,0054	0,085	0,0177	0,0116	0,0167	0,0109	0,195	0,115	0,114	0,126	0,09	0,253	0,064	1,02	0,211	0,138	0,198	0,129
Y	294,43	136,08	271,75	167,3	313,59	309,19	79,34	106,28	263,45	204,48	224,1	77,55	662,46	306,17	611,43	376,41	705,57	695,68	178,5	239,14	592,75	460,08	504,23	174,48
Zr	89531,97	89531,96	89531,96	89531,97	89531,97	89531,97	89531,97	89531,97	89531,97	89531,96	89531,96	89531,95	496007,1	496007,1	496007,1	496007,1	496007,1	496007,1	496007,1	496007,1	496007,1	496007,1	496007,1	496007
Nb	2,87	3,18	2,54	2,89	2,21	2,58	2,71	3,3	2,2	2,99	3,23	2,19	1,07	1,19	0,95	1,08	0,83	0,97	1,02	1,24	0,83	1,12	1,21	0,82
Mo	2,37	2,61	1,97	2,13	1,88	2,36	2,27	2,2	1,82	1,67	1,71	1,95	3,28	3,6	2,72	2,93	2,6	3,26	3,14	3,03	2,51	2,31	2,36	2,69
Sn	0	0	0	0	0	0	0	0	0	0,35	0	0	<0.64	<0.88	<0.81	<0.79	<0.82	<0.88	<0.86	<0.88	<0.86	0,88	<0.84	<0.88
Sb	0	0	0	0	0	0	1,69	0	0	0	0	0	<0.17	<0.20	<0.24	<0.183	<0.223	<0.21	0,39	<0.21	<0.21	<0.20	<0.20	<0.25
Ba	0	0	0	0	0	0	0	1,38	0	0	0	0	<0.29	<0.46	<0.31	<0.37	<0.30	<0.24	<0.33	4,72	<0.49	<0.43	<0.28	<0.51
La	0,312	0,71	0,94	0,178	1,2	0,39	0	1,41	0,56	0	0,35	0	0,115	0,26	0,345	0,065	0,441	0,144	<0.048	0,52	0,206	<0.042	0,13	<0.048
Ce	48,13	33,42	47,73	36,63	48,27	51,68	29,54	33,12	41,97	34,71	47,19	27,8	46,06	31,98	45,68	35,05	46,2	49,46	28,27	31,69	40,16	33,22	45,16	26,6
Pr	7,93	1,25	9,71	2,56	12,84	12,13	0,67	2,55	7,58	1,29	8	1,01	1,09	0,172	1,33	0,35	1,76	1,66	0,092	0,349	1,04	0,177	1,1	0,138
Nd	21,91	2,79	24,87	8,06	29,25	28,53	1,64	3,46	17,57	3,47	20,75	2,72	15,58	1,99	17,68	5,73	20,8	20,29	1,17	2,46	12,49	2,47	14,75	1,93
Sm	79,8	14,04	72,32	39,33	89,17	90,44	10,24	15,92	59,63	24,2	55,29	12,6	18,43	3,24	16,71	9,08	20,6	20,89	2,37	3,68	13,77	5,59	12,77	2,91
Eu	81,53	19,58	68,63	36,48	77,03	82,34	12,82	19,35	57,09	28,89	64,67	13,95	7,09	1,7	5,97	3,17	6,7	7,16	1,11	1,68	4,97	2,51	5,63	1,21
Gd	153,93	44,18	132,65	74,33	157,97	155,48	28,08	35,68	122,2	70,94	111,92	27,64	47,1	13,52	40,59	22,74	48,34	47,58	8,59	10,92	37,39	21,71	34,25	8,46
Tb	180,27	65,92	159,83	94,61	185,31	198,92	35,25	57,39	152,45	95,18	136,46	36,3	10,46	3,82	9,27	5,49	10,75	11,54	2,04	3,33	8,84	5,52	7,91	2,11
Dy	232,93	84,42	193,39	110,33	228,35	225,46	47,93	67,65	182,85	127,87	160,01	48,57	88,75	32,16	73,68	42,04	87	85,9	18,26	25,78	69,67	48,72	60,96	18,5
Ho	256,86	122,78	250,27	150,56	284,47	279,61	70,59	91,43	243,25	168,53	203,32	68,38	21,86	10,45	21,3	12,81	24,21	23,79	6,01	7,78	20,7	14,34	17,3	5,82
Er	335,56	166,81	302,44	191,53	347,12	336,04	99,64	132	280,88	237,02	247,78	90,68	83,55	41,53	75,31	47,69	86,43	83,67	24,81	32,87	69,94	59,02	61,7	22,58
Tm	419,18	223,42	394,01	256,27	445,35	425,55	134,65	167,46	381,09	322,25	324,4	132,12	14,92	7,95	14,03	9,12	15,85	15,15	4,79	5,96	13,57	11,47	11,55	4,7
Yb	534,18	291,1	477,13	324,8	543,37	539,93	192,91	241	465,93	430,66	427,27	173,32	132,48	72,19	118,33	80,55	134,76	133,9	47,84	59,77	115,55	106,8	105,96	42,98
Lu	608,38	359,2	566,34	383,1	650,78	624,02	232,38	273	561	530,66	474,72	206,78	23,18	13,69	21,58	14,6	24,79	23,77	8,85	10,4	21,37	20,22	18,09	7,88
Hf	52391,55	56071,01	47286,66	48831,83	45828,37	49454,06	53411,76	53506,45	49321,8	57026,34	45585,73	51754,36	9378,09	10036,71	8464,31	8740,9	8203,28	8852,28	9560,71	9577,66	8828,6	10207,72	8159,85	9264,03
Ta	16,14	12,79	23,23	16,8	17,7	18,33	14,28	15,48	15,78	15,92	14,68	11,3	0,42	0,333	0,6	0,437	0,46	0,477	0,371	0,402	0,41	0,414	0,382	0,294
Pb	4,56	7,23	6,23	3,76	6,21	5,05	4,61	7	6,3	11,85	5,47	3,46	16,65	26,38	22,75	13,71	22,68	18,43	16,81	25,54	22,99	43,26	19,95	12,64
Pb	0,58	0,48	0,49	0,192	0,47	0,39	0,225	2,4	0,52	0,91	0,39	0,262	2,1	1,75	1,78	0,7	1,73	1,44	0,82	8,76	1,91	3,33	1,43	0,96
Pb	1,49	1,77	1,94	1,21	1,92	1,69	0,73	3,05	1,85	1,89	1,47	0,7	5,43	6,47	7,1	4,42	6,99	6,17	2,68	11,14	6,75	6,9	5,37	2,55
Th	2516,33	2509,96	2537,04	1521,73	2801,53	2406,42	1166,31	1405,57	2529,26	3232,26	2308,12	982,27	106,94	106,67	107,82	64,67	119,07	102,27	49,57	59,74	107,49	137,37	98,1	41,75
U	4467,12	5621,22	4726,65	3139,86	4725,75	3900,42	3448,66	4120,53	4493,11	9729,93	4026,22	2754,79	54,5	68,58	57,67	38,31	57,65	47,59	42,07	50,27	54,82	118,71	49,12	33,61

LA-ICP-MS results obtained for zircon– Sample PB-181

	LA-ICP-MS - Elementos Traço normalizado por Condrito - PB-181(LSS)										LA-ICP-MS - Concentração de Elementos Traço (Ppm) - PB-181 (LSS).									
Element	**Zr-1_b**	**Zr-1_c**	**Zr-1_a**	**Zr-2**	**Zr-3**	**Zr-4_b**	**Zr-4_c**	**Zr-5**	**Tit_06b**	**Tit_06c**	**Zr-1_b**	**Zr-1_c**	**Zr-1_a**	**Zr-2**	**Zr-3**	**Zr-4_b**	**Zr-4_c**	**Zr-5**	**Tit_06b**	**Tit_06c**
Li	1,142	1,27	0,238	0,502	1,77	0,328	0,52	0,212	0,084	0,719	2,74	3,06	0,57	1,2	4,25	0,79	1,25	0,508	0,202	1,73
Mg	0	0	0,00011	0,00002	0,00045	0,00001	0,00001	0,00004	0	0	0,49	<0.60	16,16	2,32	64,45	0,85	1	5,84	0,351	0,298
Al	0	0,00063	0,00108	0,00085	0,01173	0,00052	0,0005	0,00218	0,00007	0,00013	<7.28	8,16	13,91	10,93	151,28	6,65	6,48	28,11	0,88	1,71
Si	0,88	0,886	0,875	0,831	0,817	0,798	0,783	0,589	0,894	0,894	140783,7	141792,6	140054	133035,5	130661,6	127670,3	125288,4	94195,71	143036,4	143036,4
P	0,0244	0,0232	0,0132	0,019	0,0221	0,0197	0,0276	0,0128	0,0215	0,0206	56,14	53,33	30,37	43,69	50,79	45,26	63,37	29,38	49,51	47,33
Ca	0	0	0	0	0	0,051	0	0	0	0	<651.04	<601.87	<610.81	<579.96	<545.43	693,74	<514.86	<441.68	<104.33	<105.31
Ca	0	0	0	0	0,0485	0	0	0	0	0	<178.82	<167.14	<172.98	<163.71	655,11	<148.06	<147.60	<127.00	<28.62	<29.31
Sc	32,68	33,39	34,24	32,05	30,71	30,97	30,92	23,71	15,83	16,36	282,33	288,49	295,87	276,93	265,29	267,54	267,15	204,82	136,75	141,31
Ti	0,0531	0,0597	0,0255	0,0429	0,0506	0,0456	0,0449	0,0394	0,88	0,963	34,75	39,05	16,7	28,05	33,09	29,83	29,34	25,78	23,67	29,01
Mn	0	0	0	0	0,00279	0	0	0	0,0207	0,0118	<0.73	<0.74	<0.77	<0.69	8,19	<0.62	<0.61	<0.54	0,72	0,64
Fe	0	0	0,0001	0,00004	0,00021	0,00004	0,00005	0,00005	0	0	<8.51	<8.00	26,62	11,51	58,5	10,1	13,76	14,55	2,81	6,39
Co	0	0	0,0001	0	0	0	0	0	0,00024	0,00022	<0.139	<0.139	0,079	<0.100	<0.134	<0.085	<0.126	<0.060	<0.0205	<0.0168
Rb	0	0	0,108	0	0,079	0	0	0	0,00001	0,00002	<0.35	<0.34	0,37	<0.33	0,27	<0.30	<0.26	<0.235		
Sr	0,0171	0,0108	0,12	0,0618	3,19	0,0221	0,0366	0,181	0	0	0,203	0,128	1,43	0,735	37,92	0,263	0,435	2,15	0,173	0,134
Y	81,48	95,75	184,1	176,29	61,05	144,7	338,81	199,57	0,0146	0,0113	183,34	215,43	414,23	396,64	137,36	325,57	762,31	449,03	390,78	167,95
Zr	89131,06	89131,07	89131,08	89131,08	89131,08	89131,08	89131,08	89131,08	173,68	74,64	493786,1	493786,1	493786,2	493786,2	493786,2	493786,2	493786,2	493786,2	479746,5	494588,3
Nb	4,02	3,87	4,84	2,65	3,77	2,98	5,12	3,22	86596,84	89275,88	1,51	1,45	1,82	0,99	1,42	1,12	1,92	1,21	0,768	0,916
Mo	2,85	2,81	3,56	3,47	2,94	3,13	3,31	2,21	2,05	2,44	3,94	3,88	4,91	4,79	4,05	4,31	4,56	3,05		
Sn	0,41	0	0	0	0	0	0	0	0	0,103	1,04	<1.04	<1.27	<1.26	<1.19	<1.02	<1.14	<0.76	<0.27	0,26
Sb	0	0	0	0	0	0	0	0	0	0	<0.87	<0.64	<0.75	<0.84	<0.79	<0.62	<0.70	<0.66	<0.131	<0.147
Ba	0	0	0	0	0,57	0	0	0,78	0,087	0	<1.27	<1.51	<1.52	<1.11	1,95	<0.86	<1.21	2,65	0,298	<0.158
La	0	0	1,32	0,63	2,59	0,51	0,85	2,01	0,609	0,186	<0.239	<0.202	0,485	0,23	0,95	0,186	0,311	0,738	0,223	0,068
Ce	30,62	31,94	46,22	37,36	32,47	38,1	64,55	33,78	37,52	29,9	29,3	30,57	44,23	35,76	31,08	36,46	61,77	32,32	35,9	28,61
Pr	1,56	1,59	3,17	4,37	3,03	2,94	6,99	7,17	5,91	1,64	0,214	0,218	0,434	0,599	0,415	0,402	0,96	0,98	0,809	0,225
Nd	0	3,3	9,71	9,64	5,27	8,81	18,94	13,6	13,17	3,39	<1.91	2,35	6,91	6,85	3,75	6,27	13,47	9,67	9,36	2,41
Sm	10,24	18,2	27,12	30,96	9,93	22,95	65	32,78	38,25	12,69	2,37	4,2	6,26	7,15	2,29	5,3	15,02	7,57	8,84	2,93
Eu	18,24	19,09	37,37	46,89	12,06	40,84	88,92	51,26	52,44	16,82	1,59	1,66	3,25	4,08	1,05	3,55	7,74	4,46	4,56	1,463
Gd	24,47	35,78	50,6	68,47	16,56	45,85	122,56	70,86	66,62	22,76	7,49	10,95	15,48	20,95	5,07	14,03	37,5	21,68	20,38	6,97
Tb	34,15	41,93	72,47	77,03	25,16	66,89	152,22	91,8	80,31	32,55	1,98	2,43	4,2	4,47	1,46	3,88	8,83	5,32	4,66	1,888
Dy	47,22	58,81	105,09	106,62	38,86	83,97	199,69	126,51	106,17	42,5	17,99	22,41	40,04	40,62	14,81	31,99	76,08	48,2	40,45	16,19
Ho	58,58	73,56	142,84	145,63	49,84	119,64	269,75	171,33	140,14	58,18	4,98	6,26	12,16	12,39	4,24	10,18	22,96	14,58	11,93	4,95
Er	90,69	108,6	202,98	188,99	75,06	164,9	378,44	228,49	187,52	81,79	22,58	27,04	50,54	47,06	18,69	41,06	94,23	56,89	46,69	20,36
Tm	141,36	169,74	283,67	301,8	105,74	255,37	539,39	327,89	285,64	127,92	5,03	6,04	10,1	10,74	3,76	9,09	19,2	11,67	10,17	4,55
Yb	186,78	235,31	430,35	435,11	144,53	363,43	800,55	423,48	416,78	188,45	46,32	58,36	106,73	107,91	35,84	90,13	198,54	105,02	103,36	46,74
Lu	228,48	266,53	496,38	472,96	157,22	405,31	863,01	458,06	450,06	215,98	8,71	10,15	18,91	18,02	5,99	15,44	32,88	17,45	17,15	8,23
Hf	38318,39	38420,31	40128,32	39504,36	37814,89	37309,84	34247,49	26603,63	36287,91	36851,08	6858,99	6877,24	7182,97	7071,28	6768,87	6678,46	6130,3	4762,05	6495,54	6596,34
Ta	16,49	18,26	17,04	21,98	18,67	10,49	20,04	8,16	7,9	8,04	0,429	0,475	0,443	0,571	0,485	0,273	0,521	0,212	0,205	0,209
Pb	4,57	4,81	6,81	7,93	5,19	6,32	13,93	7,05	6,09	4,37	16,67	17,55	24,86	28,95	18,94	23,07	50,83	25,75	22,24	15,94
Pb	0	0	0,71	0,61	0	0,47	0,93	0,75	0,695	0,468	<1.20	<1.31	2,58	2,21	<1.06	1,71	3,41	2,73	2,54	1,71
Pb	1,01	1,12	1,85	2,26	1,17	1,58	5,09	2,13	1,869	1,136	3,7	4,08	6,77	8,26	4,27	5,76	18,59	7,76	6,82	4,14
Th	1835,39	2124,31	3003,52	3323,39	1647,54	2885,96	8567,28	3159,47	2485,61	1454,8	78	90,28	127,65	141,24	70,02	122,65	364,11	134,28	105,64	61,83
U	3855,13	4177,16	6783,14	6167,67	4614,53	4975,78	12438,09	6546,96	4683,49	3467,4	47,03	50,96	82,75	75,25	56,3	60,7	151,74	79,87	57,14	42,3

Appendix II – WDS and structural results

Pyroxene

WDS results for CPx– Sample PB-09

PB-09 CPx														
CPx 1-1		CPx 2-1	CPx 2-2	CPx 2-3	CPx 2-4	CPx 2-5	CPx 2-6	CPx 3-1	CPx 3-2	CPx 3-3	CPx 4-1	CPx 4-2	CPx 4-3	CPx 4-4
Element	Mass%	Mass%	Mass%	Mass%	Mass%	Mass%	Mass%	Mass%	Mass%	Mass%	Mass%	Mass%	Mass%	Mass%
SiO2	51,34	52,19	52,13	52,24	51,89	52,00	52,23	52,28	51,42	51,65	51,27	51,95	51,98	51,87
Al2O3	2,84	2,16	2,13	1,91	2,00	2,31	1,96	0,95	1,31	1,50	1,60	1,04	2,22	2,32
FeO	8,93	10,60	10,49	10,22	9,94	10,69	10,28	10,07	10,94	10,67	10,16	9,81	10,04	9,91
MnO	0,26	0,36	0,37	0,38	0,35	0,34	0,36	0,35	0,38	0,33	0,31	0,38	0,35	0,32
CaO	18,62	20,48	20,50	20,77	21,06	20,35	20,70	21,32	19,92	20,57	20,42	20,87	21,19	20,60
K2O	0,28	0,01	0,00	0,01	0,00	0,00	0,01	0,00	0,00	0,01	0,01	0,01	0,00	0,00
TiO2	0,40	0,35	0,40	0,28	0,30	0,43	0,35	0,26	0,59	0,48	0,40	0,27	0,42	0,41
Cr2O3	0,05	0,02	0,04	0,00	0,01	0,00	0,03	0,00	0,02	0,05	0,07	0,02	0,00	0,01
Na2O	0,77	0,66	0,64	0,65	0,75	0,69	0,62	0,65	0,64	0,69	0,72	0,65	0,71	0,68
MgO	14,93	13,26	13,41	13,43	13,23	13,40	13,50	13,84	13,50	13,14	13,00	13,59	13,26	13,54
Total	98,41	100,10	100,11	99,89	99,52	100,20	100,03	99,71	98,72	99,09	97,96	98,59	100,17	99,65
Fórm. Estr		Fórm. Estr	Fórm. Estr	Fórm. Estr	Fórm. Estr	Fórm. Estr	Fórm. Estr	Fórm. Estr	Fórm. Estr	Fórm. Estr	Fórm. Estr	Fórm. Estr	Fórm. Estr	Fórm. Estr
Si	1,924	1,947	1,944	1,951	1,943	1,937	1,948	1,954	1,948	1,949	1,954	1,964	1,935	1,938
Al	0,125	0,095	0,094	0,084	0,088	0,101	0,086	0,042	0,059	0,067	0,072	0,046	0,097	0,102
Fe2+	0,207	0,292	0,287	0,272	0,248	0,283	0,278	0,231	0,288	0,278	0,276	0,251	0,252	0,263
Fe3+	0,073	0,039	0,040	0,047	0,063	0,050	0,043	0,083	0,059	0,058	0,048	0,059	0,060	0,047
Mn	0,008	0,011	0,012	0,012	0,011	0,011	0,011	0,011	0,012	0,011	0,010	0,012	0,011	0,010
Ca	0,747	0,819	0,819	0,831	0,845	0,812	0,827	0,854	0,808	0,832	0,834	0,845	0,845	0,825
K	0,013	0,001	0,000	0,001	0,000	0,000	0,000	0,000	0,00	0,001	0,000	0,001	0,00	0,00
Ti	0,011	0,010	0,011	0,008	0,008	0,012	0,010	0,007	0,017	0,014	0,011	0,008	0,012	0,012
Cr	0,001	0,001	0,001	0,000	0,000	0,00	0,001	0,000	0,001	0,001	0,002	0,000	0,000	0,000
Na	0,056	0,048	0,046	0,047	0,054	0,050	0,045	0,047	0,047	0,051	0,053	0,048	0,051	0,049
Mg	0,834	0,738	0,746	0,748	0,739	0,744	0,751	0,771	0,762	0,739	0,739	0,766	0,736	0,754
Total	4,000	4,000	4,000	4,000	4,000	4,000	4,000	4,000	4,000	4,000	4,000	4,000	4,000	4,000
Membros-Finais		Membros-Finais	Membros-Finais	Membros-Finais	Membros-Finais	Membros-Finais	Membros-Finais	Membros-Finais	Membros-Finais	Membros-Finais	Membros-Finais	Membros-Finais	Membros-Finais	Membros-Finais
Wo	39,98	43,13	43,03	43,51	44,34	42,75	43,31	43,77	41,90	43,36	43,74	43,72	44,37	43,44
En	44,61	38,85	39,17	39,15	38,75	39,17	39,30	39,53	39,51	38,53	38,75	39,61	38,63	39,73
Fs	15,41	18,02	17,80	17,34	16,91	18,09	17,38	16,70	18,59	18,11	17,51	16,67	17,00	16,84
Ae	6,95	4,47	4,68	5,34	6,02	5,75	4,88	5,20	5,48	5,74	5,41	5,36	5,70	5,36
Jad	0,00	1,06	0,64	0,05	0,00	0,00	0,26	0,00	0,00	0,00	0,59	0,00	0,00	0,25
WEF	93,05	94,47	94,68	94,62	93,98	94,25	94,86	94,80	94,52	94,26	94,00	94,64	94,30	94,39
Q	1,79	1,85	1,85	1,85	1,83	1,84	1,86	1,86	1,86	1,85	1,85	1,86	1,83	1,84
J	0,11	0,10	0,09	0,09	0,11	0,10	0,09	0,09	0,09	0,10	0,11	0,10	0,10	0,10
Mg#	0,80	0,72	0,72	0,73	0,75	0,72	0,73	0,77	0,73	0,73	0,73	0,75	0,74	0,74
T (◦C)	**1098**	-	**1046**	**1044**	**1043**	**1043**	**1046**	**1060**	**1048**	**1043**	**1041**	**1047**	**1040**	**1050**

PB-09 Opx													
OPx 1-1	OPx 1-2	OPx 1-3	OPx 1-4	OPx 1-5	OPx 2-1	OPx 2-2	OPx 3-1	OPx 3-2	OPx 3-3	OPx 3-4	OPx 3-5	OPx 3-6	OPx 3-7
Mass%	Mass%	Mass%	Mass%	Mass%	Mass%	Mass%	Mass%	Mass%	Mass%	Mass%	Mass%	Mass%	Mass%
53,09	52,98	52,56	52,41	52,95	52,30	52,38	52,95	52,30	52,38	53,09	52,98	52,56	52,41
0,88	0,64	0,80	0,96	0,84	0,88	0,81	0,84	0,88	0,81	0,88	0,64	0,80	0,96
24,14	24,29	24,27	24,07	24,48	24,02	23,87	24,48	24,02	23,87	24,14	24,29	24,27	24,07
0,76	0,75	0,76	0,78	0,74	0,78	0,82	0,74	0,78	0,82	0,76	0,75	0,76	0,78
0,56	0,69	0,64	0,72	0,65	0,65	0,57	0,65	0,65	0,57	0,56	0,69	0,64	0,72
0,00	0,01	0,00	0,00	0,00	0,01	0,00	0,00	0,01	0,00	0,00	0,01	0,00	0,00
0,13	0,08	0,08	0,10	0,11	0,14	0,13	0,11	0,14	0,13	0,13	0,08	0,08	0,10
0,01	0,00	0,01	0,02	0,00	0,01	0,00	0,00	0,01	0,00	0,01	0,00	0,01	0,02
0,00	0,00	0,00	0,01	0,01	0,03	0,01	0,01	0,03	0,01	0,00	0,00	0,00	0,01
21,54	21,36	21,15	21,36	21,50	21,55	21,16	21,50	21,55	21,16	21,54	21,36	21,15	21,36
101,12	100,80	100,28	100,42	101,28	100,36	99,75	101,28	100,36	99,75	101,12	100,80	100,28	100,42
Fórm. Estr	Fórm. Estr	Fórm. Estr	Fórm. Estr	Fórm. Estr	Fórm. Estr	Fórm. Estr	Fórm. Estr	Fórm. Estr	Fórm. Estr	Fórm. Estr	Fórm. Estr	Fórm. Estr	Fórm. Estr
1,970	1,974	1,970	1,958	1,963	1,954	1,972	1,963	1,954	1,972	1,97	1,97	1,97	1,96
0,039	0,028	0,035	0,042	0,037	0,039	0,036	0,037	0,039	0,036	0,04	0,03	0,04	0,04
0,736	0,737	0,740	0,716	0,727	0,702	0,738	0,727	0,702	0,738	0,74	0,74	0,74	0,72
0,013	0,020	0,021	0,036	0,032	0,048	0,014	0,032	0,048	0,014	0,01	0,02	0,02	0,04
0,024	0,024	0,024	0,025	0,023	0,025	0,026	0,023	0,025	0,026	0,02	0,02	0,02	0,02
0,022	0,028	0,026	0,029	0,026	0,026	0,023	0,026	0,026	0,023	0,02	0,03	0,03	0,03
0,00	0,000	0,000	0,00	0,000	0,000	0,00	0,000	0,000	0,00	0,00	0,0003	0,00	0,00
0,004	0,002	0,002	0,003	0,003	0,004	0,004	0,003	0,004	0,004	0,004	0,002	0,002	0,003
0,000	0,00	0,000	0,001	0,00	0,000	0,00	0,00	0,000	0,00	0,0004	0,00	0,0001	0,001
0,00	0,000	0,000	0,001	0,001	0,002	0,001	0,001	0,002	0,001	0,00	0,00	0,00	0,001
1,192	1,187	1,182	1,190	1,188	1,200	1,187	1,188	1,200	1,187	1,19	1,19	1,18	1,19
4,000	4,000	4,000	4,000	4,000	4,000	4,000	4,000	4,000	4,000	4,00	4,00	4,00	4,00
Membros-Finais	Membros-Finais	Membros-Finais	Membros-Finais	Membros-Finais	Membros-Finais	Membros-Finais	Membros-Finais	Membros-Finais	Membros-Finais	Membros-Finais	Membros-Finais	Membros-Finais	Membros-Finais
1,11	1,39	1,30	1,43	1,29	1,30	1,16	1,29	1,30	1,16	1,11	1,39	1,30	1,43
59,97	59,48	59,31	59,63	59,52	59,97	59,73	59,52	59,97	59,73	59,97	59,48	59,31	59,63
38,91	39,13	39,40	38,93	39,19	38,73	39,11	39,19	38,73	39,11	38,91	39,13	39,40	38,93
0,00	0,78	0,28	2,94	3,50	6,51	2,77	3,94	6,51	3,27	0,00	0,78	0,28	2,94
0,00	0,00	0,00	0,00	0,00	0,00	0,00	0,00	0,00	0,00	0,00	0,00	0,00	0,00
100,00	99,22	99,72	97,06	96,50	93,49	97,23	96,49	93,49	97,24	100,00	99,22	99,72	97,05
1,95	1,95	1,95	1,93	1,94	1,93	1,95	1,94	1,93	1,95	1,95	1,95	1,95	1,93
0,00	0,00	0,00	0,00	0,00	0,00	0,00	0,00	0,00	0,00	0,00	0,00	0,00	0,00
0,62	0,62	0,61	0,62	0,62	0,63	0,62	0,62	0,63	0,62	0,62	0,62	0,61	0,62
-	-	-	-	-	-	-	-	-	-	-	-	-	-

WDS results for OPx– Sample PB-09

WDS results for CPx– Sample PB-06

PB-06 Piroxênios																				
CPx 1-1		CPx 1-3	CPx 1-4	CPx 1-6	CPx 1-8	CPx 1-9	CPx 2-1	CPx 2-2	CPx 2-4	CPx 3-1	CPx 3-2	CPx 3-3	CPx 3-4	CPx 3-5	CPx 3-6	CPx 4-1	CPx 4-2	CPx 4-3	CPx 4-4
Element	Mass%	Mass%	Mass%	Mass%	Mass%	Mass%	Mass%	Mass%	Mass%	Mass%	Mass%	Mass%	Mass%	Mass%	Mass%	Mass%	Mass%	Mass%	Mass%
SiO2	49,88	52,31	52,59	52,68	52,06	52,31	52,73	49,16	52,65	52,53	52,52	52,66	52,33	52,42	52,57	52,66	52,86	52,06	52,75
Al2O3	4,11	1,55	1,19	1,30	1,48	1,20	1,49	5,37	1,39	1,52	1,46	1,47	1,46	1,57	1,44	1,36	1,43	2,30	1,42
FeO	11,31	9,74	9,41	9,64	10,09	9,12	9,74	12,33	9,68	10,04	9,57	10,06	9,55	9,63	9,69	9,54	9,53	10,10	10,27
MnO	0,38	0,48	0,43	0,43	0,44	0,41	0,46	0,33	0,45	0,43	0,44	0,44	0,41	0,41	0,40	0,45	0,40	0,42	0,45
CaO	17,58	21,52	21,27	21,44	20,99	21,32	20,91	15,44	21,71	21,41	21,78	21,25	21,70	21,54	21,44	21,30	21,63	19,57	20,75
K2O	0,51	0,00	0,00	0,02	0,01	0,01	0,01	0,68	0,01	0,00	0,01	0,01	0,01	0,00	0,02	0,00	0,00	0,22	0,01
TiO2	0,71	0,25	0,18	0,22	0,21	0,14	0,15	0,80	0,09	0,23	0,17	0,12	0,26	0,30	0,24	0,20	0,14	0,30	0,19
Cr2O3	0,02	0,04	0,02	0,02	0,02	0,00	0,03	0,05	0,04	0,00	0,00	0,02	0,00	0,03	0,08	0,00	0,06	0,05	0,04
Na2O	1,39	0,90	0,91	0,90	0,87	0,89	0,94	1,76	0,87	0,94	0,91	0,99	0,88	0,89	0,89	0,92	0,97	1,18	1,02
MgO	13,37	13,14	13,06	13,17	13,17	13,29	12,98	13,25	13,11	12,88	12,89	12,85	12,69	12,76	12,97	12,85	12,79	13,49	12,71
Total	99,24	99,93	99,05	99,82	99,33	98,68	99,45	99,17	100,01	99,97	99,75	99,86	99,29	99,54	99,74	99,28	99,81	99,68	99,62
Fórm. Estr		Fórm. Estr	Fórm. Estr	Fórm. Estr	Fórm. Estr	Fórm. Estr	Fórm. Estr	Fórm. Estr	Fórm. Estr	Fórm. Estr	Fórm. Estr	Fórm. Estr	Fórm. Estr	Fórm. Estr	Fórm. Estr	Fórm. Estr	Fórm. Estr	Fórm. Estr	Fórm. Estr
Si	1,862	1,950	1,977	1,966	1,966	1,966	1,976	1,833	1,961	1,960	1,962	1,966	1,966	1,964	1,965	1,977	1,974	1,937	1,977
Ti	0,020	0,007	0,005	0,006	0,006	0,006	0,004	0,022	0,002	0,006	0,005	0,003	0,007	0,008	0,007	0,006	0,004	0,008	0,005
Al	0,181	0,068	0,053	0,057	0,057	0,057	0,066	0,236	0,061	0,067	0,064	0,064	0,065	0,069	0,064	0,060	0,063	0,101	0,063
Cr+3	0,001	0,001	0,001	0,000	0,000	0,000	0,001	0,001	0,001	0,000	0,000	0,001	0,000	0,001	0,002	0,000	0,002	0,001	0,001
Fe+3	0,180	0,082	0,049	0,064	0,064	0,064	0,043	0,212	0,074	0,069	0,069	0,068	0,054	0,049	0,055	0,042	0,050	0,101	0,047
Fe+2	0,173	0,222	0,247	0,236	0,236	0,236	0,263	0,173	0,228	0,245	0,230	0,246	0,246	0,253	0,247	0,258	0,247	0,213	0,275
Mn	0,012	0,015	0,014	0,013	0,013	0,013	0,015	0,011	0,014	0,013	0,014	0,014	0,013	0,013	0,013	0,014	0,013	0,013	0,014
Mg	0,744	0,730	0,732	0,733	0,733	0,733	0,725	0,736	0,728	0,716	0,718	0,715	0,711	0,713	0,723	0,719	0,712	0,748	0,710
Ca	0,703	0,860	0,857	0,857	0,857	0,857	0,839	0,617	0,866	0,856	0,872	0,850	0,873	0,865	0,859	0,857	0,865	0,780	0,833
Na	0,101	0,065	0,066	0,065	0,065	0,065	0,069	0,127	0,063	0,068	0,066	0,072	0,064	0,065	0,064	0,067	0,070	0,070	0,074
K	0,024	0,00	0,00	0,001	0,001	0,001	0,001	0,032	0,000	0,000	0,000	0,000	0,001	0,000	0,001	0,000	0,000	0,010	0,001
Tot.	4,000	4,000	4,000	4,000	4,000	4,000	4,000	4,000	4,000	4,000	4,000	4,000	4,000	4,000	4,000	4,000	4,000	4,000	4,000
Membros-Finais		Membros-Finais	Membros-Finais	Membros-Finais	Membros-Finais	Membros-Finais	Membros-Finais	Membros-Finais	Membros-Finais	Membros-Finais	Membros-Finais	Membros-Finais	Membros-Finais	Membros-Finais	Membros-Finais	Membros-Finais	Membros-Finais	Membros-Finais	Membros-Finais
Wo	38,80	45,04	45,13	45,02	45,02	45,02	44,55	35,28	45,36	45,07	45,82	44,90	46,04	45,70	45,27	45,34	45,84	42,04	44,33
En	41,06	38,26	38,56	38,48	38,48	38,48	38,48	42,13	38,11	37,73	37,74	37,78	37,46	37,67	38,10	38,06	37,72	40,32	37,78
Fs	20,14	16,70	16,31	16,50	16,50	16,50	16,98	22,59	16,53	17,21	16,44	17,33	16,50	16,63	16,63	16,61	16,44	17,65	17,88
Ae	12,52	7,05	5,29	6,99	6,99	6,99	4,68	17,10	6,79	7,36	7,06	7,37	5,73	5,27	6,01	4,53	5,38	8,22	5,16
Jad	0,00	0,00	1,89	0,10	0,10	0,10	2,87	0,00	0,00	0,00	0,00	0,40	1,14	1,70	0,96	2,74	2,10	0,00	3,03
WEF	87,48	92,95	92,81	92,91	92,91	92,91	92,45	82,90	93,21	92,64	92,94	92,22	93,13	93,04	93,03	92,73	92,52	91,78	91,81
Q	1,62	1,81	1,84	1,83	1,83	1,83	1,83	1,53	1,82	1,82	1,82	1,81	1,83	1,83	1,83	1,83	1,82	1,74	1,82
J	0,20	0,13	0,13	0,13	0,13	0,13	0,14	0,25	0,13	0,14	0,13	0,14	0,13	0,13	0,13	0,13	0,14	0,14	0,15
Mg#	0,81	0,77	0,75	0,76	0,76	0,76	0,73	0,81	0,76	0,75	0,76	0,74	0,74	0,74	0,74	0,74	0,74	0,78	0,72
T (°C)	**1080**	**1052**	**1047**	**1046**	**1047**	**1052**	**1043**	**1114**	**1052**	**1038**	**1041**	**1039**	**1036**	**1039**	**1043**	**1039**	**1039**	**1063**	**1039**

WDS results for CPx– Sample PB-22

PB-22 Piroxênios												
CPx 1-1		CPx 1-2	CPx 1-3	CPx 1-4	CPx 1-5	CPx 2-1	CPx 2-2	CPx 2-3	CPx 2-4	CPx 2-5	CPx 2-6	CPx 2-7
Element	Mass%	Mass%	Mass%	Mass%	Mass%	Mass%	Mass%	Mass%	Mass%	Mass%	Mass%	Mass%
SiO2	52,64	52,99	53,11	52,44	52,79	52,79	52,95	52,46	53,24	52,25	52,28	52,67
Al2O3	1,63	1,89	1,72	2,00	2,02	1,66	1,54	1,70	1,69	1,98	1,80	1,58
FeO	9,55	9,80	9,54	9,91	9,78	9,69	9,74	9,77	9,63	10,91	9,88	9,57
MnO	0,42	0,39	0,42	0,45	0,44	0,45	0,42	0,41	0,44	0,47	0,43	0,43
CaO	20,96	20,57	20,64	20,53	20,12	20,46	20,36	20,68	20,63	19,17	20,65	20,83
K2O	0,01	0,00	0,00	0,03	0,01	0,00	0,01	0,00	0,01	0,02	0,00	0,00
TiO2	0,16	0,23	0,27	0,28	0,21	0,24	0,24	0,27	0,18	0,24	0,25	0,20
Cr2O3	0,01	0,04	0,09	0,00	0,00	0,04	0,01	0,00	0,01	0,01	0,04	0,03
Na2O	0,85	0,91	0,96	0,85	0,89	0,86	0,84	0,82	0,92	0,84	0,92	0,85
MgO	13,43	13,28	13,34	13,26	13,48	13,46	13,57	13,38	13,33	13,84	13,34	13,34
Total	99,66	100,09	100,09	99,74	99,73	99,64	99,67	99,49	100,07	99,72	99,60	99,49
Fórm. Estr		Fórm. Estr	Fórm. Estr	Fórm. Estr	Fórm. Estr	Fórm. Estr	Fórm. Estr	Fórm. Estr	Fórm. Estr	Fórm. Estr	Fórm. Estr	Fórm. Estr
Si	1,965	1,971	1,974	1,958	1,969	1,972	1,977	1,963	1,980	1,951	1,954	1,971
Ti	0,004	0,007	0,008	0,008	0,006	0,007	0,007	0,007	0,005	0,007	0,007	0,006
Al	0,072	0,083	0,075	0,088	0,089	0,073	0,068	0,075	0,074	0,087	0,079	0,070
Cr+3	0,000	0,001	0,003	0,000	0,000	0,001	0,000	0,000	0,000	0,000	0,001	0,001
Fe+3	0,052	0,027	0,027	0,042	0,027	0,031	0,025	0,043	0,023	0,057	0,065	0,039
Fe+2	0,246	0,278	0,269	0,267	0,278	0,271	0,279	0,263	0,277	0,283	0,244	0,261
Mn	0,013	0,012	0,013	0,014	0,014	0,014	0,013	0,013	0,014	0,015	0,014	0,014
Mg	0,747	0,736	0,739	0,738	0,749	0,749	0,755	0,747	0,739	0,771	0,743	0,744
Ca	0,838	0,820	0,822	0,821	0,804	0,819	0,815	0,829	0,822	0,767	0,827	0,835
Na	0,061	0,065	0,069	0,061	0,064	0,062	0,060	0,059	0,066	0,060	0,067	0,061
K	0,001	0,000	0,000	0,001	0,001	0,000	0,000	0,000	0,000	0,001	0,000	0,000
Tot.	4,000	4,000	4,000	4,000	4,000	4,000	4,000	4,000	4,000	4,000	4,000	4,000
Membros-Finais		Membros-Finais	Membros-Finais	Membros-Finais	Membros-Finais	Membros-Finais	Membros-Finais	Membros-Finais	Membros-Finais	Membros-Finais	Membros-Finais	Membros-Finais
Wo	44,19	43,76	43,93	43,62	42,94	43,44	43,16	43,77	43,86	40,52	43,69	44,13
En	39,39	39,31	39,51	39,20	40,03	39,76	40,03	39,40	39,43	40,70	39,27	39,32
Fs	16,42	16,92	16,56	17,19	17,03	16,81	16,81	16,83	16,72	18,78	17,04	16,55
Ae	5,74	3,00	3,06	4,76	3,10	3,55	2,86	4,81	2,55	6,95	7,24	4,30
Jad	1,08	4,39	4,68	2,17	4,29	3,50	4,05	1,86	4,92	0,36	0,21	2,54
WEF	93,19	92,60	92,26	93,07	92,61	92,95	93,09	93,33	92,53	92,69	92,55	93,16
Q	1,83	1,83	1,83	1,83	1,83	1,84	1,85	1,84	1,84	1,82	1,81	1,84
J	0,12	0,13	0,14	0,12	0,13	0,12	0,12	0,12	0,13	0,12	0,13	0,12
Mg#	0,75	0,73	0,73	0,73	0,73	0,73	0,73	0,74	0,73	0,73	0,75	0,74
T (◦C)	**1052**	**1049**	**1054**	**1051**	**1058**	**1055**	**1058**	**1052**	**1052**	**1064**	**1050**	**1052**

PB-92B Piroxênios						
CPx 1-1		CPx 1-2	CPx 1-3	CPx 1-4	CPx 2-1	CPx 2-2
Element	Mass%	Mass%	Mass%	Mass%	Mass%	Mass%
SiO2	53,07	52,30	53,06	53,04	53,27	53,05
Al2O3	1,57	2,05	1,08	1,20	1,21	1,17
FeO	9,56	9,70	9,52	9,34	9,33	8,99
MnO	0,40	0,40	0,47	0,44	0,42	0,42
CaO	21,13	19,94	21,52	21,32	21,73	21,30
K2O	0,09	0,17	0,02	0,03	0,00	0,00
TiO2	0,24	0,35	0,17	0,13	0,18	0,18
Cr2O3	0,08	0,00	0,03	0,00	0,04	0,01
Na2O	1,09	1,19	0,98	1,02	0,99	1,00
MgO	13,15	13,43	13,37	13,25	13,01	13,04
Total	100,39	99,53	100,21	99,77	100,18	99,16
Fórm. Estr		Fórm. Estr	Fórm. Estr	Fórm. Estr	Fórm. Estr	Fórm. Estr
Si	1,966	1,949	1,970	1,976	1,980	1,990
Ti	0,007	0,010	0,005	0,004	0,005	0,005
Al	0,069	0,090	0,047	0,053	0,053	0,052
Cr+3	0,002	0,000	0,001	0,000	0,001	0,000
Fe+3	0,066	0,087	0,075	0,062	0,047	0,032
Fe+2	0,230	0,215	0,221	0,229	0,243	0,250
Mn	0,012	0,013	0,015	0,014	0,013	0,013
Mg	0,726	0,746	0,740	0,736	0,721	0,729
Ca	0,839	0,796	0,856	0,851	0,865	0,856
Na	0,078	0,086	0,071	0,074	0,071	0,073
K	0,004	0,008	0,001	0,001	0,000	0,000
Tot.	4,000	4,000	4,000	4,000	4,000	4,000
Membros-Finais		Membros-Finais	Membros-Finais	Membros-Finais	Membros-Finais	Membros-Finais
Wo	44,77	42,87	44,90	44,99	45,80	45,52
En	38,76	40,17	38,82	38,90	38,15	38,78
Fs	16,47	16,96	16,28	16,11	16,05	15,70
Ae	7,21	9,77	7,63	6,75	5,06	3,40
Jad	1,34	0,00	0,00	1,24	2,55	4,45
WEF	91,45	90,23	92,37	92,01	92,38	92,15
Q	1,79	1,76	1,82	1,82	1,83	1,84
J	0,16	0,17	0,14	0,15	0,14	0,15
Mg#	0,76	0,78	0,77	0,76	0,75	0,74
T (◦C)	**1036**	**1046**	**1040**	**1036**	**1030**	**1035**

DS

WDS results for CPx– Sample PB-92B

WDS results for CPx– Sample PB-123

PB-123 Piroxênios													
CPx 1-2		CPx 1-6	CPx 1-6-1	CPx 1-7	CPx 1-8	CPx 1-9	CPx 1-10	CPx 1-11	CPx 1-12	CPx 1-13	CPx 1-14	CPx 1-15	CPx 1-17
Element	Mass%	Mass%	Mass%	Mass%	Mass%	Mass%	Mass%	Mass%	Mass%	Mass%	Mass%	Mass%	Mass%
SiO2	52,41	52,69	52,45	52,57	52,47	52,38	52,15	52,54	52,31	52,40	52,39	52,38	52,13
Al2O3	1,70	1,51	1,83	1,68	1,70	1,75	1,82	1,69	1,76	1,84	1,68	1,73	1,88
FeO	10,81	10,25	10,85	10,71	10,02	10,52	10,43	10,11	10,06	10,72	11,04	10,57	10,28
MnO	0,41	0,44	0,41	0,40	0,40	0,40	0,41	0,41	0,40	0,40	0,41	0,40	0,37
CaO	21,32	21,69	21,51	21,31	21,68	21,55	21,18	21,34	21,41	21,45	21,20	20,86	21,26
K2O	0,00	0,01	0,01	0,00	0,00	0,02	0,01	0,00	0,00	0,00	0,00	0,00	0,00
TiO2	0,44	0,28	0,35	0,34	0,35	0,36	0,57	0,45	0,31	0,44	0,49	0,40	0,30
Cr2O3	0,02	0,06	0,00	0,00	0,00	0,03	0,02	0,00	0,00	0,04	0,03	0,00	0,01
Na2O	0,86	0,88	0,86	0,79	0,82	0,84	0,84	0,88	0,85	0,87	0,82	0,87	0,84
MgO	12,60	12,66	12,52	12,59	12,79	12,83	12,90	12,65	12,80	12,60	12,74	12,45	12,46
Total	100,57	100,47	100,79	100,39	100,24	100,67	100,33	100,06	99,89	100,75	100,80	99,67	99,53
Fórm. Estr		Fórm. Estr	Fórm. Estr	Fórm. Estr	Fórm. Estr	Fórm. Estr	Fórm. Estr	Fórm. Estr	Fórm. Estr	Fórm. Estr	Fórm. Estr	Fórm. Estr	Fórm. Estr
Si	1,951	1,961	1,949	1,961	1,955	1,945	1,943	1,962	1,955	1,947	1,947	1,967	1,959
Ti	0,012	0,008	0,010	0,010	0,010	0,010	0,016	0,012	0,009	0,012	0,014	0,011	0,008
Al	0,075	0,066	0,080	0,074	0,075	0,076	0,080	0,075	0,077	0,081	0,073	0,076	0,083
Cr+3	0,000	0,002	0,000	0,000	0,000	0,001	0,001	0,000	0,000	0,001	0,001	0,000	0,000
Fe+3	0,060	0,059	0,065	0,042	0,055	0,074	0,063	0,039	0,057	0,063	0,064	0,029	0,043
Fe+2	0,277	0,260	0,272	0,292	0,257	0,252	0,262	0,277	0,258	0,270	0,279	0,303	0,280
Mn	0,013	0,014	0,013	0,013	0,013	0,013	0,013	0,013	0,013	0,012	0,013	0,013	0,012
Mg	0,699	0,702	0,693	0,700	0,710	0,710	0,716	0,704	0,713	0,698	0,706	0,697	0,698
Ca	0,850	0,865	0,856	0,852	0,866	0,857	0,845	0,854	0,857	0,854	0,844	0,839	0,856
Na	0,062	0,063	0,062	0,057	0,059	0,061	0,061	0,064	0,062	0,062	0,059	0,063	0,061
K	0,000	0,000	0,000	0,000	0,000	0,001	0,000	0,000	0,000	0,000	0,000	0,000	0,000
Tot.	4,000	4,000	4,000	4,000	4,000	4,000	4,000	4,000	4,000	4,000	4,000	4,000	4,000
Membros-Finais		Membros-Finais	Membros-Finais	Membros-Finais	Membros-Finais	Membros-Finais	Membros-Finais	Membros-Finais	Membros-Finais	Membros-Finais	Membros-Finais	Membros-Finais	Membros-Finais
Wo	44,78	45,51	45,07	44,86	45,53	44,96	44,50	45,26	45,18	45,00	44,29	44,62	45,32
En	36,82	36,96	36,50	36,88	37,37	37,25	37,71	37,33	37,59	36,78	37,03	37,05	36,96
Fs	18,40	17,52	18,43	18,26	17,10	17,79	17,79	17,42	17,23	18,21	18,68	18,33	17,73
Ae	6,55	6,34	6,72	4,62	5,93	6,60	6,70	4,27	6,18	6,80	6,57	3,25	4,71
Jad	0,26	0,49	0,00	1,65	0,49	0,00	0,00	2,65	0,51	0,00	0,00	3,77	1,93
WEF	93,20	93,17	93,28	93,73	93,58	93,40	93,30	93,08	93,30	93,20	93,43	92,98	93,36
Q	1,83	1,83	1,82	1,84	1,83	1,82	1,82	1,84	1,83	1,82	1,83	1,84	1,83
J	0,12	0,13	0,12	0,11	0,12	0,12	0,12	0,13	0,12	0,12	0,12	0,13	0,12
Mg#	0,72	0,73	0,72	0,71	0,73	0,74	0,73	0,72	0,73	0,72	0,72	0,70	0,71
T (°C)	**1028**	**1027**	**1024**	**1027**	**1033**	**1032**	**1036**	**1033**	**1035**	**1024**	**1030**	**1029**	**1030**

WDS results for CPx– Sample PB-181

PB-181 Piroxênios															
CPx 1-1		CPx 1-2	CPx 1-3	CPx 1-4	CPx 1-5	CPx 2-1	CPx 2-2	CPx 2-3	CPx 2-4	CPx 2-5	CPx 3-1	CPx 3-2	CPx 3-3	CPx 3-4	CPx 3-5
Element	Mass%	Mass%	Mass%	Mass%	Mass%	Mass%	Mass%	Mass%	Mass%	Mass%	Mass%	Mass%	Mass%	Mass%	Mass%
SiO2	52,89	52,50	52,43	51,43	52,30	52,54	53,08	52,37	52,88	52,37	52,38	52,31	51,99	52,52	52,10
Al2O3	1,19	1,59	1,57	3,00	1,44	1,78	1,33	1,49	1,36	1,60	1,45	1,58	1,69	1,65	1,45
FeO	12,05	13,38	12,62	11,81	11,85	11,63	12,10	11,46	11,24	12,06	11,62	11,80	11,55	11,68	12,32
MnO	0,40	0,33	0,37	0,37	0,39	0,38	0,44	0,38	0,39	0,37	0,38	0,39	0,39	0,40	0,39
CaO	18,77	15,51	18,63	14,75	19,24	19,21	19,27	19,68	19,37	19,68	19,79	19,97	19,23	19,51	19,58
K2O	0,00	0,35	0,02	0,51	0,01	0,00	0,05	0,01	0,01	0,00	0,00	0,00	0,00	0,00	0,00
TiO2	0,23	0,29	0,48	0,42	0,45	0,59	0,34	0,51	0,34	0,57	0,38	0,69	0,53	0,53	0,51
Cr2O3	0,00	0,01	0,02	0,01	0,05	0,04	0,03	0,03	0,07	0,05	0,04	0,07	0,06	0,00	0,02
Na2O	2,87	3,66	2,90	3,39	2,60	2,50	2,61	2,46	2,63	2,50	2,50	2,42	2,49	2,65	2,70
MgO	10,72	10,83	10,48	13,70	10,91	11,13	10,81	11,26	11,20	11,20	10,92	11,19	10,99	10,77	10,93
Total	99,12	98,45	99,51	99,38	99,24	99,81	100,07	99,65	99,48	100,40	99,46	100,42	98,92	99,71	100,00
Fórm. Estr		Fórm. Estr	Fórm. Estr	Fórm. Estr	Fórm. Estr	Fórm. Estr	Fórm. Estr	Fórm. Estr	Fórm. Estr	Fórm. Estr	Fórm. Estr	Fórm. Estr	Fórm. Estr	Fórm. Estr	Fórm. Estr
Si	1,986	1,974	1,965	1,889	1,963	1,961	1,979	1,956	1,975	1,944	1,962	1,943	1,958	1,962	1,941
Ti	0,006	0,008	0,013	0,012	0,013	0,017	0,010	0,014	0,010	0,016	0,011	0,019	0,015	0,015	0,014
Al	0,053	0,070	0,069	0,130	0,064	0,078	0,058	0,065	0,060	0,070	0,064	0,069	0,075	0,072	0,063
Cr+3	0,000	0,000	0,001	0,000	0,002	0,001	0,001	0,001	0,002	0,001	0,001	0,002	0,002	0,000	0,001
Fe+3	0,172	0,249	0,186	0,335	0,172	0,147	0,156	0,171	0,159	0,189	0,170	0,180	0,160	0,166	0,219
Fe+2	0,206	0,172	0,210	0,028	0,200	0,216	0,222	0,187	0,192	0,186	0,194	0,187	0,204	0,199	0,164
Mn	0,013	0,011	0,012	0,012	0,012	0,012	0,014	0,012	0,012	0,012	0,012	0,012	0,012	0,013	0,013
Mg	0,600	0,607	0,585	0,750	0,611	0,619	0,601	0,627	0,624	0,620	0,610	0,619	0,617	0,600	0,619
Ca	0,755	0,625	0,748	0,580	0,774	0,768	0,770	0,788	0,775	0,783	0,794	0,795	0,776	0,781	0,796
Na	0,209	0,267	0,211	0,241	0,189	0,181	0,189	0,178	0,190	0,180	0,182	0,174	0,182	0,192	0,199
K	0,000	0,017	0,001	0,024	0,000	0,000	0,003	0,000	0,000	0,000	0,000	0,000	0,000	0,000	0,000
Tot.	4,000	4,000	4,000	4,000	4,000	4,000	4,000	4,000	4,000	4,000	4,000	4,000	4,000	4,000	4,000
Membros-Finais		Membros-Finais	Membros-Finais	Membros-Finais	Membros-Finais	Membros-Finais	Membros-Finais	Membros-Finais	Membros-Finais	Membros-Finais	Membros-Finais	Membros-Finais	Membros-Finais	Membros-Finais	Membros-Finais
Wo	43,24	37,57	42,97	34,05	43,75	43,59	43,69	44,13	43,99	43,76	44,62	44,32	43,86	44,41	43,96
En	34,36	36,50	33,64	44,00	34,52	35,14	34,10	35,13	35,39	34,65	34,26	34,56	34,88	34,11	34,15
Fs	22,40	25,93	23,39	21,95	21,73	21,27	22,21	20,73	20,62	21,59	21,12	21,12	21,26	21,48	21,89
Ae	17,87	27,89	19,37	29,38	17,88	15,49	16,24	17,70	16,49	18,69	17,45	17,99	16,72	17,04	19,97
Jad	3,80	2,03	2,61	0,00	1,77	3,57	3,44	0,75	3,24	0,00	1,16	0,00	2,26	2,69	0,00
WEF	78,33	70,08	78,02	70,62	80,35	80,94	80,31	81,55	80,28	81,31	81,39	82,01	81,02	80,27	80,03
Q	1,56	1,40	1,54	1,36	1,58	1,60	1,59	1,60	1,59	1,59	1,60	1,60	1,60	1,58	1,58
J	0,42	0,53	0,42	0,48	0,38	0,36	0,38	0,36	0,38	0,36	0,36	0,35	0,36	0,38	0,40
Mg#	0,74	0,78	0,74	0,96	0,75	0,74	0,73	0,77	0,76	0,77	0,76	0,77	0,75	0,75	0,79
T (°C)	**1003**	**1030**	**994**	**1127**	**1006**	**1013**	**1002**	**1013**	**1017**	**1009**	**1001**	**1008**	**1012**	**1003**	**1003**

WDS results for CPx– Sample PB-185

PB-185 Piroxênios																															
CPx 1-1		CPx 1-2	CPx 1-3	CPx 1-4	CPx 1-5	CPx 1-6	CPx 1-7	CPx 1-8	CPx 1-9	CPx 1-10	CPx 2-1	CPx 2-2	CPx 2-3	CPx 2-4	CPx 2-5	CPx 2-6	CPx 2-7	CPx 5-1	CPx 5-2	CPx 5-3	CPx 5-4	CPx 5-5	CPx 5-6	CPx 5-7	CPx 6-1	CPx 6-2	CPx 6-3	CPx 6-4	CPx 6-5
Element	Mass%	Mass%	Mass%	Mass%	Mass%	Mass%	Mass%	Mass%	Mass%	Mass%	Mass%	Mass%	Mass%	Mass%	Mass%	Mass%	Mass%	Mass%	Mass%	Mass%	Mass%	Mass%	Mass%	Mass%	Mass%	Mass%	Mass%	Mass%	Mass%
SiO2	49,36	52,80	52,37	52,58	52,90	52,63	52,62	52,51	52,87	52,44	52,46	52,49	52,46	52,41	52,95	52,14	52,33	52,17	52,18	52,65	52,67	57,42	52,12	52,42	52,83	52,48	52,42	52,43	52,42
Al2O3	5,43	1,38	1,36	1,30	1,30	1,36	1,43	1,30	1,06	1,33	1,23	1,32	1,38	1,30	1,20	1,40	1,45	1,40	1,30	1,16	1,31	1,25	1,26	1,20	1,30	1,31	1,35	1,34	1,28
FeO	11,02	11,53	11,46	11,18	11,44	11,38	11,58	11,21	11,82	11,10	11,03	11,77	11,73	11,17	11,23	11,29	11,38	11,37	11,37	10,55	11,46	10,05	11,22	11,57	11,30	11,10	11,03	11,08	10,74
MnO	0,34	0,41	0,39	0,36	0,44	0,34	0,38	0,37	0,38	0,38	0,37	0,38	0,42	0,41	0,40	0,39	0,39	0,39	0,41	0,38	0,41	0,34	0,39	0,37	0,38	0,38	0,39	0,37	0,37
CaO	18,40	20,13	20,73	20,17	20,08	20,37	20,21	20,28	20,23	20,60	20,87	20,59	20,18	20,53	20,56	20,23	20,22	20,31	19,85	20,66	20,08	18,19	20,06	20,24	20,20	19,98	19,93	20,55	20,73
K2O	0,01	0,01	0,01	0,00	0,01	0,00	0,00	0,00	0,01	0,00	0,00	0,01	0,00	0,00	0,01	0,00	0,02	0,00	0,02	0,00	0,00	0,03	0,00	0,01	0,00	0,00	0,01	0,00	0,01
TiO2	0,58	0,58	0,57	0,60	0,34	0,60	0,53	0,48	0,25	0,55	0,67	0,50	0,55	0,59	0,42	0,43	0,55	0,55	0,41	0,65	0,49	0,63	0,54	0,42	0,63	0,54	0,52	0,64	0,63
Cr2O3	0,00	0,00	0,00	0,17	0,04	0,00	0,02	0,06	0,04	0,01	0,00	0,03	0,00	0,00	0,00	0,01	0,00	0,00	0,02	0,02	0,00	0,00	0,05	0,01	0,04	0,00	0,00	0,02	0,00
Na2O	1,68	1,83	1,72	1,77	1,92	1,83	1,89	1,88	1,85	1,72	1,69	1,83	1,88	1,72	1,94	1,95	1,91	1,76	1,96	1,49	1,80	1,42	1,78	1,89	1,66	1,81	1,74	1,70	1,57
MgO	11,45	11,42	11,57	11,53	11,57	11,70	11,51	11,64	11,59	11,62	11,92	11,49	11,49	11,71	11,63	11,63	11,56	11,58	11,37	11,98	11,52	10,40	11,57	11,73	11,69	11,50	11,64	11,78	12,10
Total	98,27	100,08	100,17	99,66	100,03	100,21	100,17	99,73	100,10	99,75	100,24	100,40	100,09	99,84	100,35	99,46	99,81	99,53	98,90	99,54	99,75	99,73	98,99	99,85	100,03	99,11	99,02	99,90	99,85
Fórm. Estr		Fórm. Estr	Fórm. Estr	Fórm. Estr	Fórm. Estr	Fórm. Estr	Fórm. Estr	Fórm. Estr	Fórm. Estr	Fórm. Estr	Fórm. Estr	Fórm. Estr	Fórm. Estr	Fórm. Estr	Fórm. Estr	Fórm. Estr	Fórm. Estr	Fórm. Estr	Fórm. Estr	Fórm. Estr	Fórm. Estr	Fórm. Estr	Fórm. Estr	Fórm. Estr	Fórm. Estr	Fórm. Estr	Fórm. Estr	Fórm. Estr	Fórm. Estr
Si	1,867	1,974	1,956	1,973	1,975	1,962	1,963	1,965	1,975	1,965	1,955	1,956	1,960	1,962	1,969	1,955	1,958	1,959	1,970	1,977	1,975	2,170	1,968	1,960	1,976	1,978	1,977	1,961	1,960
Ti	0,017	0,016	0,016	0,017	0,009	0,017	0,015	0,014	0,007	0,016	0,019	0,014	0,015	0,016	0,012	0,012	0,015	0,016	0,012	0,018	0,014	0,018	0,015	0,012	0,018	0,015	0,015	0,018	0,018
Al	0,242	0,061	0,060	0,057	0,057	0,060	0,063	0,057	0,047	0,059	0,054	0,058	0,061	0,057	0,053	0,062	0,064	0,062	0,058	0,051	0,058	0,056	0,056	0,053	0,057	0,058	0,060	0,059	0,056
Cr+3	0,000	0,000	0,000	0,005	0,001	0,000	0,001	0,002	0,001	0,000	0,000	0,001	0,000	0,000	0,000	0,000	0,000	0,000	0,001	0,000	0,000	0,000	0,001	0,000	0,001	0,000	0,000	0,001	0,000
Fe+3	0,114	0,092	0,122	0,086	0,112	0,115	0,117	0,119	0,123	0,105	0,122	0,134	0,124	0,111	0,126	0,146	0,129	0,117	0,122	0,067	0,096	0,000	0,107	0,141	0,074	0,086	0,083	0,107	0,103
Fe+2	0,235	0,268	0,236	0,264	0,245	0,240	0,244	0,232	0,246	0,242	0,222	0,233	0,242	0,239	0,223	0,208	0,227	0,241	0,237	0,264	0,263	0,318	0,247	0,221	0,279	0,264	0,265	0,240	0,232
Mn	0,011	0,013	0,012	0,012	0,014	0,011	0,012	0,012	0,012	0,012	0,012	0,012	0,013	0,013	0,013	0,012	0,012	0,012	0,013	0,012	0,013	0,011	0,013	0,012	0,012	0,012	0,012	0,012	0,012
Mg	0,646	0,636	0,644	0,645	0,644	0,650	0,640	0,650	0,645	0,649	0,662	0,638	0,640	0,653	0,645	0,650	0,645	0,648	0,640	0,670	0,644	0,586	0,651	0,654	0,652	0,646	0,655	0,657	0,674
Ca	0,746	0,806	0,829	0,811	0,803	0,814	0,808	0,813	0,810	0,827	0,833	0,822	0,808	0,823	0,819	0,813	0,810	0,817	0,803	0,831	0,807	0,737	0,811	0,811	0,810	0,807	0,806	0,823	0,830
Na	0,123	0,133	0,125	0,129	0,139	0,132	0,137	0,136	0,134	0,125	0,122	0,132	0,136	0,125	0,140	0,142	0,139	0,128	0,143	0,108	0,131	0,104	0,130	0,137	0,120	0,132	0,127	0,123	0,114
K	0,000	0,000	0,000	0,000	0,000	0,000	0,000	0,000	0,001	0,000	0,000	0,000	0,000	0,000	0,001	0,000	0,001	0,000	0,001	0,000	0,000	0,002	0,000	0,000	0,000	0,000	0,000	0,000	0,001
Tot.	4,000	4,000	4,000	4,000	4,000	4,000	4,000	4,000	4,000	4,000	4,000	4,000	4,000	4,000	4,000	4,000	4,000	4,000	4,000	4,000	4,000	4,000	4,000	4,000	4,000	4,000	4,000	4,000	4,000
Membros-Finais		Membros-Finais	Membros-Finais	Membros-Finais	Membros-Finais	Membros-Finais	Membros-Finais	Membros-Finais	Membros-Finais	Membros-Finais	Membros-Finais	Membros-Finais	Membros-Finais	Membros-Finais	Membros-Finais	Membros-Finais	Membros-Finais	Membros-Finais	Membros-Finais	Membros-Finais	Membros-Finais	Membros-Finais	Membros-Finais	Membros-Finais	Membros-Finais	Membros-Finais	Membros-Finais	Membros-Finais	Membros-Finais
Wo	42,59	44,39	44,99	44,60	44,18	44,47	44,35	44,55	44,09	45,04	45,02	44,70	44,20	44,76	44,87	44,43	44,45	44,54	44,24	45,05	44,25	44,62	44,35	44,11	44,31	44,45	44,25	44,79	44,83
En	36,88	35,04	34,94	35,47	35,42	35,54	35,15	35,58	35,15	35,35	35,78	34,70	35,02	35,52	35,31	35,54	35,36	35,33	35,26	36,34	35,32	35,49	35,60	35,57	35,68	35,60	35,96	35,73	36,41
Fs	20,53	20,57	20,08	19,93	20,41	19,98	20,50	19,87	20,76	19,60	19,21	20,60	20,78	19,72	19,82	20,03	20,20	20,13	20,50	18,61	20,43	19,89	20,05	20,32	20,01	19,95	19,79	19,48	18,76
Ae	13,13	9,83	12,76	9,19	11,91	12,18	12,37	12,57	13,07	11,07	12,73	13,85	13,18	11,69	13,14	14,85	13,62	12,32	12,92	7,15	10,27	0,00	11,36	14,45	7,98	9,19	8,93	11,25	10,94
Jad	1,05	4,30	0,29	4,51	2,84	1,80	2,10	1,80	1,13	2,05	0,05	0,00	1,24	1,48	1,44	0,00	0,98	1,23	2,24	4,39	3,69	12,38	2,48	0,00	4,97	4,89	4,72	1,77	1,11
WEF	85,82	85,87	86,95	86,30	85,25	86,02	85,53	85,63	85,80	86,87	87,22	86,15	85,57	86,83	85,42	85,15	85,40	86,44	84,84	88,46	86,04	87,62	86,16	85,55	87,05	85,92	86,36	86,98	87,95
Q	1,63	1,71	1,71	1,72	1,69	1,70	1,69	1,69	1,70	1,72	1,72	1,69	1,69	1,72	1,69	1,67	1,68	1,71	1,68	1,77	1,71	1,64	1,71	1,69	1,74	1,72	1,72	1,72	1,74
J	0,25	0,27	0,25	0,26	0,28	0,26	0,27	0,27	0,27	0,25	0,24	0,26	0,27	0,25	0,28	0,28	0,28	0,26	0,29	0,22	0,26	0,21	0,26	0,27	0,24	0,26	0,25	0,25	0,23
Mg#	0,73	0,70	0,73	0,71	0,72	0,73	0,72	0,74	0,72	0,73	0,75	0,73	0,73	0,73	0,74	0,76	0,74	0,73	0,73	0,72	0,71	0,65	0,72	0,75	0,70	0,71	0,71	0,73	0,74
T (°C)	1078	1048	1049	1053	1053	1051	1050	1054	1044	1049	1057	1048	1048	1053	1052	1053	1052	1046	1051	1058	1051	1059	1055	1054	1052	1048	1055	1055	1063

Apatite

WDS results for Apatite– Sample PB-09

PB-09 Apatita																				
AP 2a.1		AP 2a.2	AP 2a.3	AP 2a.4	AP 2a.5	AP 2a.6	AP 3.1	AP 3.2	AP 3.3	AP 3.4	AP 4.1	AP 4.2	AP 4.3	AP 13.1	AP 13.2	AP 13.3	AP 10.1	AP 10.2	AP 10.3	AP 10.4
Element	Mass%	Mass%	Mass%	Mass%	Mass%	Mass%	Mass%	Mass%	Norm%	Mass%	Mass%	Mass%	Mass%	Mass%	Mass%	Mass%	Mass%	Mass%	Mass%	Mass%
Na2O	0,14	0,14	0,21	0,18	0,23	0,24	0,16	0,21	0,20	0,18	0,23	0,188	0,14	0,22	0,16	0,14	0,11	0,17	0,08	0,12
SiO2	0,38	0,62	0,35	0,43	0,50	0,36	0,51	0,57	0,57	0,47	0,40	0,518	1,06	0,41	0,71	0,50	0,59	0,57	0,66	0,74
Y2O3	0,00	0,00	0,00	0,00	0,00	0,00	0,00	0,00	0,00	0,00	0,00	0	0,00	0,00	0,00	0,00	0,00	0,00	0,00	0,00
Fe2O3	0,13	0,12	0,13	0,11	0,22	0,12	0,07	0,14	0,14	0,08	0,12	0,056	0,49	0,11	0,10	0,12	0,24	0,27	0,37	0,18
MnO	0,06	0,06	0,02	0,03	0,03	0,04	0,05	0,06	0,06	0,05	0,04	0,039	0,03	0,04	0,07	0,06	0,07	0,09	0,04	0,04
La2O3	0,16	0,32	0,28	0,27	0,23	0,25	0,31	0,24	0,24	0,29	0,20	0,305	0,37	0,15	0,42	0,21	0,34	0,35	0,46	0,46
SO3	0,25	0,33	0,38	0,43	0,59	0,48	0,33	0,48	0,48	0,32	0,39	0,361	0,37	0,48	0,34	0,35	0,20	0,35	0,39	0,22
P2O5	41,06	40,42	40,76	40,52	40,37	40,71	40,26	39,86	39,53	39,85	40,78	40,42	40,02	40,44	39,84	40,76	40,40	39,94	39,90	40,07
SrO	0,20	0,20	0,20	0,22	0,19	0,21	0,15	0,18	0,18	0,16	0,22	0,169	0,12	0,16	0,11	0,18	0,21	0,25	0,13	0,19
TiO2	0,00	0,00	0,00	0,00	0,00	0,00	0,00	0,00	0,00	0,00	0,00	0	0,03	0,00	0,00	0,00	0,01	0,01	0,05	0,00
Cl	0,30	0,33	0,31	0,32	0,33	0,32	0,28	0,29	0,29	0,27	0,25	0,333	0,33	0,29	0,31	0,28	0,31	0,33	0,30	0,29
CaO	54,02	53,67	54,05	53,92	54,11	54,27	54,03	53,47	53,02	53,35	54,15	53,61	52,95	53,83	53,11	54,02	52,85	53,36	53,48	53,57
Ce2O3	0,97	1,65	0,97	1,56	1,41	1,00	1,31	1,40	1,39	1,31	1,03	1,92	2,55	1,21	2,22	1,20	1,96	1,75	2,09	2,27
F	3,48	3,36	3,12	3,67	3,44	3,66	3,76	3,94	3,91	3,99	3,78	4,07	3,13	3,29	3,29	3,67	3,63	3,60	3,50	4,10
MgO	0,00	0,00	0,00	0,00	0,00	0,00	0,00	0,00	0,00	0,00	0,00	0	0,00	0,00	0,00	0,00	0,00	0,00	0,00	0,00
Al2O3	0,00	0,00	0,00	0,00	0,00	0,02	0,00	0,01	0,01	0,01	0,00	0,007	0,03	0,02	0,04	0,02	0,01	0,01	0,01	0,02
Total	101,15	101,22	100,77	101,65	101,65	101,67	101,21	100,84	100,00	100,31	101,60	101,993	101,62	100,65	100,71	101,49	100,94	101,05	101,46	102,27
Formula		Formula	Formula	Formula	Formula	Formula	Formula	Formula	Formula	Formula	Formula	Formula	Formula	Formula	Formula	Formula	Formula	Formula	Formula	Formula
Ca	9,498	9,491	9,570	9,506	9,557	9,544	9,545	9,503	9,507	9,510	9,461	9,422	9,374	9,565	9,477	9,495	9,362	9,484	9,484	9,409
Na	0,044	0,045	0,068	0,058	0,072	0,076	0,051	0,066	0,058	0,073	0,051	0,060	0,043	0,070	0,052	0,043	0,036	0,054	0,027	0,038
Mn	0,008	0,008	0,003	0,003	0,005	0,005	0,006	0,008	0,006	0,006	0,004	0,005	0,004	0,006	0,010	0,008	0,010	0,012	0,006	0,005
Fe	0,016	0,014	0,016	0,013	0,027	0,015	0,008	0,017	0,009	0,015	0,019	0,007	0,061	0,014	0,012	0,015	0,030	0,034	0,046	0,022
La	0,010	0,019	0,017	0,017	0,014	0,015	0,019	0,015	0,018	0,012	0,018	0,018	0,023	0,009	0,026	0,013	0,021	0,022	0,028	0,028
Ce	0,058	0,100	0,058	0,094	0,085	0,060	0,079	0,085	0,080	0,062	0,114	0,115	0,154	0,073	0,135	0,072	0,119	0,106	0,127	0,136
P	5,705	5,648	5,703	5,645	5,634	5,657	5,620	5,598	5,611	5,659	5,693	5,613	5,598	5,678	5,617	5,661	5,655	5,609	5,591	5,562
Si	0,062	0,103	0,057	0,071	0,083	0,060	0,083	0,095	0,078	0,066	0,086	0,085	0,175	0,068	0,119	0,081	0,097	0,095	0,109	0,121
Cl	0,083	0,093	0,088	0,088	0,092	0,088	0,078	0,082	0,076	0,070	0,087	0,093	0,093	0,081	0,087	0,079	0,088	0,092	0,084	0,081
F	1,806	1,754	1,631	1,910	1,793	1,900	1,961	2,067	2,099	1,959	1,613	2,111	1,635	1,726	1,733	1,904	1,898	1,888	1,832	2,126
S	0,031	0,041	0,047	0,053	0,072	0,059	0,041	0,060	0,040	0,048	0,043	0,044	0,046	0,059	0,043	0,043	0,025	0,044	0,048	0,027
Sr	0,019	0,019	0,019	0,021	0,018	0,020	0,014	0,017	0,015	0,021	0,018	0,016	0,012	0,016	0,010	0,017	0,021	0,024	0,013	0,018
OH	-0,889	-0,847	-0,718	-0,998	-0,886	-0,988	-1,039	-1,148	-1,174	-1,029	-0,701	-1,204	-0,729	-0,807	-0,820	-0,983	-0,986	-0,980	-0,916	-1,207
Total	16,531	16,598	16,676	16,609	16,739	16,652	16,571	16,608	16,525	16,588	16,622	16,497	16,634	16,694	16,617	16,554	16,461	16,609	16,625	16,457

WDS results for Apatite– Sample PB-06

PB-06 Apatita										
AP. 1-1		AP. 1-2	AP. 3-1	AP. 3-2	AP.1-1-1	AP.1-1-2	AP.1-1-3	AP.11-1	AP.11-2	AP.11-3
Element	Mass%	Mass%	Mass%	Mass%	Mass%	Mass%	Mass%	Mass%	Mass%	Mass%
Na2O	0,37	0,30	0,06	0,22	0,29	0,20	0,32	0,08	0,16	0,24
SiO2	0,48	0,51	0,48	0,35	0,52	0,63	0,44	0,65	0,55	0,70
Y2O3	0,00	0,00	0,00	0,00	0,00	0,00	0,00	0,00	0,00	0,00
Fe2O3	0,08	0,08	0,00	0,01	0,07	0,02	0,04	0,09	0,30	0,06
MnO	0,06	0,10	0,02	0,02	0,05	0,05	0,04	0,03	0,06	0,10
La2O3	0,38	0,45	0,28	0,19	0,39	0,23	0,33	0,24	0,20	0,46
SO3	0,64	0,57	0,21	0,38	0,53	0,46	0,72	0,35	0,38	0,51
P2O5	40,38	40,18	40,55	41,28	39,67	40,72	40,05	40,93	40,32	39,56
SrO	0,29	0,26	0,26	0,21	0,27	0,22	0,31	0,24	0,24	0,29
TiO2	0,00	0,04	0,01	0,00	0,00	0,00	0,00	0,00	0,00	0,00
Cl	0,59	0,58	0,31	0,37	0,58	0,40	0,53	0,46	0,40	0,52
CaO	52,64	52,74	53,66	53,52	53,66	54,62	54,37	54,60	54,66	53,91
Ce2O3	2,02	2,09	1,66	1,38	1,97	1,00	1,34	1,49	1,26	2,17
F	3,28	3,24	3,36	3,37	3,33	3,10	3,24	3,13	3,15	2,95
MgO	0,00	0,00	0,00	0,00	0,00	0,00	0,00	0,00	0,00	0,00
Al2O3	0,01	0,01	0,00	0,00	0,01	0,05	0,02	0,00	0,02	0,02
Total	101,20	101,13	100,86	101,31	101,34	101,69	101,75	102,29	101,69	101,49
Formula		Formula	Formula	Formula	Formula	Formula	Formula	Formula	Formula	Formula
Ca	9,380	9,415	9,518	9,421	9,585	9,616	9,659	9,564	9,654	9,638
Na	0,118	0,095	0,018	0,068	0,094	0,064	0,104	0,025	0,051	0,076
Mn	0,009	0,014	0,002	0,003	0,006	0,007	0,006	0,004	0,008	0,014
Fe	0,010	0,010	0,000	0,001	0,008	0,003	0,005	0,011	0,037	0,008
La	0,023	0,028	0,017	0,011	0,024	0,014	0,020	0,014	0,012	0,028
Ce	0,123	0,127	0,101	0,083	0,120	0,060	0,081	0,089	0,076	0,133
P	5,686	5,668	5,684	5,742	5,599	5,665	5,622	5,665	5,627	5,589
Si	0,080	0,086	0,080	0,058	0,087	0,103	0,072	0,106	0,091	0,117
Cl	0,166	0,163	0,088	0,104	0,164	0,112	0,148	0,128	0,111	0,147
F	1,725	1,707	1,759	1,751	1,756	1,611	1,699	1,618	1,642	1,557
S	0,080	0,071	0,026	0,047	0,066	0,056	0,090	0,043	0,047	0,064
Sr	0,027	0,025	0,024	0,020	0,026	0,021	0,030	0,023	0,023	0,028
OH	-0,891	-0,870	-0,847	-0,855	-0,920	-0,723	-0,847	-0,747	-0,753	-0,703
Total	16,699	16,684	16,524	16,550	16,754	16,722	16,872	16,636	16,737	16,827

WDS results for Apatite– Sample PB-22

PB-22 Apatita										
AP. 1		AP. 2	AP. 3	AP. 4	AP. 5	AP. 6	AP. 7	AP. 8	AP. 9	AP. 10
Element	Mass%	Mass%	Mass%	Mass%	Mass%	Mass%	Mass%	Mass%	Mass%	Mass%
Na2O	0,08	0,08	0,16	0,16	0,25	0,12	0,24	0,18	0,23	0,28
SiO2	0,43	0,39	0,35	0,40	0,34	0,42	0,39	0,41	0,37	0,36
Y2O3	0,00	0,00	0,00	0,00	0,00	0,00	0,00	0,00	0,00	0,00
Fe2O3	0,06	0,05	0,03	0,07	0,09	0,01	0,15	0,05	0,06	0,22
MnO	0,05	0,05	0,05	0,07	0,06	0,03	0,02	0,05	0,04	0,05
La2O3	0,16	0,20	0,24	0,20	0,19	0,24	0,15	0,27	0,22	0,21
SO3	0,15	0,18	0,46	0,24	0,39	0,18	0,52	0,31	0,30	0,47
P2O5	41,19	40,76	40,89	41,14	40,98	40,57	40,84	40,84	40,26	40,12
SrO	0,27	0,21	0,20	0,23	0,26	0,27	0,30	0,25	0,25	0,29
TiO2	0,01	0,00	0,01	0,00	0,00	0,00	0,00	0,01	0,00	0,00
Cl	0,29	0,24	0,28	0,26	0,31	0,30	0,30	0,34	0,29	0,22
CaO	54,76	55,01	55,14	55,03	54,70	54,73	54,40	54,66	54,04	54,65
Ce2O3	1,27	1,18	1,05	1,23	1,29	1,64	0,97	1,64	1,76	1,46
F	3,24	3,68	3,19	3,49	3,32	3,49	3,88	3,40	3,66	3,23
MgO	0,00	0,00	0,00	0,00	0,00	0,00	0,00	0,00	0,00	0,00
Al2O3	0,00	0,02	0,00	0,01	0,00	0,00	0,02	0,00	0,00	0,00
Total	101,95	102,06	102,04	102,54	102,18	101,99	102,18	102,41	101,48	101,55
Formula		Formula	Formula	Formula	Formula	Formula	Formula	Formula	Formula	Formula
Ca	9,583	9,633	9,683	9,592	9,592	9,625	9,528	9,582	9,567	9,698
Na	0,024	0,025	0,051	0,052	0,080	0,039	0,077	0,057	0,074	0,088
Mn	0,007	0,007	0,007	0,010	0,008	0,004	0,003	0,007	0,005	0,006
Fe	0,008	0,006	0,003	0,009	0,011	0,001	0,018	0,006	0,007	0,028
La	0,010	0,012	0,015	0,012	0,012	0,014	0,009	0,017	0,014	0,013
Ce	0,076	0,071	0,063	0,073	0,077	0,099	0,058	0,098	0,106	0,089
P	5,696	5,640	5,674	5,666	5,679	5,638	5,652	5,657	5,632	5,626
Si	0,071	0,064	0,057	0,065	0,056	0,069	0,064	0,066	0,062	0,059
Cl	0,080	0,068	0,076	0,073	0,085	0,083	0,082	0,093	0,081	0,061
F	1,674	1,902	1,653	1,796	1,718	1,812	2,006	1,759	1,912	1,692
S	0,018	0,022	0,056	0,029	0,048	0,022	0,064	0,038	0,037	0,058
Sr	0,025	0,020	0,019	0,022	0,025	0,026	0,029	0,024	0,024	0,028
OH	-0,754	-0,970	-0,730	-0,868	-0,804	-0,894	-1,088	-0,853	-0,993	-0,753
Total	16,556	16,547	16,741	16,593	16,688	16,581	16,641	16,632	16,606	16,823

WDS results for Apatite– Sample PB-92B

PB-92B Apatita										
AP. 1-1		AP. 1-2	AP. 1-3	AP. 1-4	AP. 9-1	AP. 9-2	AP. 9-3	AP. 9-4	AP. 9-5	AP. 9-6
Element	Mass%	Mass%	Mass%	Mass%	Mass%	Mass%	Mass%	Mass%	Mass%	Mass%
Na2O	0,10	0,02	0,16	0,11	0,15	0,09	0,07	0,11	0,16	0,30
SiO2	0,73	0,65	0,83	0,84	0,75	0,74	0,66	0,64	0,83	0,69
Y2O3	0,00	0,00	0,00	0,00	0,00	0,00	0,00	0,00	0,00	0,00
Fe2O3	0,04	0,21	0,27	0,11	0,04	0,04	0,19	0,21	0,23	0,29
MnO	0,02	0,01	0,01	0,03	0,06	0,04	0,01	0,06	0,06	0,09
La2O3	0,27	0,25	0,35	0,28	0,40	0,39	0,18	0,41	0,42	0,51
SO3	0,29	0,17	0,29	0,28	0,30	0,31	0,23	0,22	0,42	0,39
P2O5	40,41	40,29	40,40	39,42	40,23	40,02	39,27	39,10	40,42	39,02
SrO	0,24	0,26	0,23	0,26	0,26	0,21	0,18	0,29	0,34	0,30
TiO2	0,00	0,01	0,00	0,01	0,00	0,00	0,01	0,01	0,00	0,00
Cl	0,21	0,18	0,21	0,19	0,46	0,37	0,32	0,37	0,39	0,47
CaO	54,67	54,48	54,39	53,69	54,23	54,09	53,64	53,73	53,76	53,13
Ce2O3	2,28	1,88	2,45	2,32	2,45	2,68	1,80	2,47	2,61	3,36
F	3,84	3,92	3,82	3,95	3,26	3,24	3,14	3,76	2,88	3,34
MgO	0,00	0,00	0,00	0,00	0,00	0,00	0,00	0,00	0,00	0,00
Al2O3	0,00	0,00	0,02	0,02	0,01	0,00	0,01	0,00	0,02	0,00
Total	103,09	102,32	103,43	101,50	102,58	102,21	99,71	101,39	102,52	101,88
Formula	Formula	Formula	Formula	Formula	Formula	Formula	Formula	Formula	Formula	Formula
Ca	9,548	9,555	9,480	9,541	9,551	9,568	9,675	9,604	9,486	9,526
Na	0,030	0,005	0,051	0,035	0,047	0,029	0,021	0,035	0,050	0,097
Mn	0,003	0,001	0,001	0,004	0,008	0,005	0,002	0,009	0,008	0,013
Fe	0,005	0,026	0,033	0,014	0,005	0,005	0,024	0,027	0,028	0,036
La	0,016	0,015	0,021	0,017	0,024	0,024	0,011	0,025	0,025	0,031
Ce	0,136	0,113	0,146	0,141	0,147	0,162	0,111	0,151	0,157	0,206
P	5,577	5,584	5,564	5,536	5,598	5,594	5,597	5,523	5,635	5,529
Si	0,119	0,106	0,135	0,140	0,123	0,122	0,110	0,107	0,136	0,115
Cl	0,059	0,049	0,059	0,053	0,127	0,103	0,090	0,104	0,107	0,132
F	1,979	2,029	1,965	2,072	1,695	1,692	1,672	1,984	1,500	1,768
S	0,035	0,020	0,036	0,035	0,037	0,038	0,030	0,028	0,052	0,049
Sr	0,022	0,025	0,022	0,025	0,025	0,020	0,017	0,028	0,033	0,029
Total	16,563	16,504	16,578	16,563	16,641	16,645	16,669	16,605	16,728	16,746

WDS results for Apatite– Sample PB-92B - Continuation

PB-92B Apatita											
AP. 13-1		AP. 13-2	AP. 13-3	AP. 13-4	AP. 13-6	AP. 13-7	AP. 13-8	AP. 13-9	AP. 13-10	AP. 13-11	AP. 13-12
Element	Mass%	Mass%	Mass%	Mass%	Mass%	Mass%	Mass%	Mass%	Mass%	Mass%	Mass%
Na2O	0,14	0,24	0,17	0,26	0,19	0,14	0,13	0,21	0,27	0,13	0,12
SiO2	0,69	0,69	1,17	0,87	0,83	0,82	0,80	0,80	0,73	0,78	0,72
Y2O3	0,00	0,00	0,00	0,00	0,00	0,00	0,00	0,00	0,00	0,00	0,00
Fe2O3	0,62	0,53	0,67	0,44	0,14	0,06	0,03	0,16	0,06	0,12	0,08
MnO	0,07	0,06	0,09	0,07	0,06	0,05	0,03	0,03	0,08	0,05	0,01
La2O3	0,39	0,50	0,50	0,53	0,58	0,33	0,42	0,38	0,55	0,41	0,33
SO3	0,31	0,28	0,34	0,29	0,37	0,45	0,33	0,29	0,38	0,40	0,36
P2O5	40,48	40,01	39,44	39,92	40,42	39,94	40,23	39,48	40,46	39,44	39,94
SrO	0,25	0,31	0,32	0,27	0,26	0,28	0,26	0,24	0,27	0,24	0,26
TiO2	0,02	0,03	0,01	0,04	0,00	0,01	0,00	0,00	0,00	0,00	0,01
Cl	0,40	0,35	0,27	0,39	0,44	0,38	0,23	0,26	0,27	0,19	0,18
CaO	54,10	53,99	52,86	52,93	53,48	54,20	54,19	54,04	53,93	54,22	54,54
Ce2O3	2,37	2,86	3,82	3,31	3,45	2,68	2,73	2,98	3,06	2,44	2,34
F	3,76	3,86	3,40	3,30	3,41	3,65	3,36	3,32	3,43	3,20	3,56
MgO	0,00	0,00	0,00	0,00	0,00	0,00	0,00	0,00	0,00	0,00	0,00
Al2O3	0,00	0,00	0,01	0,00	0,01	0,01	0,01	0,01	0,02	0,00	0,00
Total	103,61	103,71	103,09	102,62	103,64	103,00	102,75	102,19	103,49	101,62	102,45
Formula		Formula	Formula	Formula	Formula	Formula	Formula	Formula	Formula	Formula	Formula
Ca	9,426	9,450	9,349	9,364	9,370	9,536	9,535	9,600	9,447	9,668	9,619
Na	0,045	0,077	0,055	0,082	0,060	0,046	0,040	0,066	0,086	0,043	0,040
Mn	0,010	0,009	0,013	0,010	0,008	0,008	0,004	0,005	0,011	0,007	0,001
Fe	0,075	0,065	0,083	0,055	0,017	0,007	0,004	0,019	0,007	0,015	0,010
La	0,024	0,030	0,031	0,032	0,035	0,020	0,025	0,023	0,033	0,025	0,020
Ce	0,141	0,171	0,231	0,200	0,207	0,161	0,164	0,181	0,183	0,149	0,141
P	5,573	5,534	5,512	5,581	5,596	5,553	5,593	5,542	5,601	5,557	5,566
Si	0,113	0,112	0,194	0,143	0,136	0,135	0,132	0,133	0,119	0,130	0,119
Cl	0,111	0,097	0,074	0,110	0,121	0,106	0,063	0,073	0,074	0,053	0,051
F	1,934	1,994	1,775	1,723	1,763	1,895	1,745	1,741	1,774	1,684	1,853
S	0,038	0,035	0,042	0,036	0,046	0,055	0,041	0,036	0,046	0,050	0,045
Sr	0,023	0,029	0,031	0,026	0,025	0,027	0,025	0,023	0,025	0,023	0,024
Total	16,581	16,613	16,666	16,630	16,599	16,661	16,646	16,711	16,655	16,774	16,678

WDS results for Apatite– Sample PB-92B - Continuation

PB-92B Apatita										
AP. 20-1		AP. 20-2	AP. 20-3	AP. 20-5	AP. 20-6	AP. 20-7	AP. 7-1	AP. 7-2	AP. 7-3	AP. 7-4
Element	Mass%	Mass%	Mass%	Mass%	Mass%	Mass%	Mass%	Mass%	Mass%	Mass%
Na2O	0,12	0,14	0,24	0,09	0,27	0,19	0,22	0,23	0,20	0,19
SiO2	0,74	0,77	0,82	0,82	0,77	0,77	0,85	0,81	0,86	0,83
Y2O3	0,00	0,00	0,00	0,00	0,00	0,00	0,00	0,00	0,00	0,00
Fe2O3	0,02	0,02	0,05	0,11	0,08	0,07	0,10	0,15	0,27	0,13
MnO	0,04	0,04	0,07	0,00	0,08	0,05	0,05	0,04	0,05	0,05
La2O3	0,28	0,34	0,61	0,33	0,63	0,49	0,52	0,41	0,44	0,49
SO3	0,30	0,44	0,31	0,31	0,37	0,28	0,40	0,34	0,32	0,35
P2O5	40,30	40,44	40,55	40,22	39,77	40,58	40,13	40,01	39,78	40,87
SrO	0,25	0,26	0,25	0,21	0,25	0,21	0,32	0,26	0,28	0,26
TiO2	0,00	0,00	0,00	0,00	0,00	0,02	0,00	0,00	0,05	0,00
Cl	0,26	0,33	0,36	0,27	0,43	0,37	0,25	0,27	0,27	0,34
CaO	54,76	54,34	53,44	54,42	53,41	54,01	53,92	54,10	53,44	53,84
Ce2O3	1,99	2,66	3,59	2,44	3,39	2,88	3,39	3,11	3,05	3,19
F	4,20	4,09	3,51	3,77	3,66	3,52	3,69	3,67	3,67	3,69
MgO	0,00	0,00	0,00	0,00	0,00	0,00	0,00	0,00	0,00	0,00
Al2O3	0,01	0,02	0,04	0,01	0,02	0,02	0,01	0,01	0,04	0,01
Total	103,27	103,88	103,82	102,99	103,14	103,45	103,84	103,40	102,73	104,22
Formula		Formula	Formula	Formula	Formula	Formula	Formula	Formula	Formula	Formula
Ca	9,542	9,455	9,342	9,528	9,429	9,436	9,442	9,493	9,437	9,343
Na	0,036	0,044	0,075	0,029	0,085	0,059	0,069	0,071	0,065	0,058
Mn	0,006	0,005	0,010	0,000	0,012	0,006	0,007	0,005	0,007	0,007
Fe	0,003	0,002	0,006	0,013	0,010	0,008	0,012	0,018	0,034	0,016
La	0,017	0,021	0,037	0,020	0,038	0,029	0,031	0,025	0,027	0,029
Ce	0,118	0,158	0,214	0,146	0,204	0,172	0,203	0,186	0,184	0,189
P	5,549	5,560	5,601	5,564	5,548	5,602	5,553	5,548	5,551	5,604
Si	0,120	0,125	0,133	0,134	0,128	0,125	0,139	0,133	0,142	0,134
Cl	0,070	0,089	0,101	0,074	0,121	0,101	0,069	0,076	0,077	0,092
F	2,160	2,101	1,811	1,948	1,907	1,815	1,907	1,901	1,913	1,890
S	0,037	0,054	0,037	0,038	0,046	0,035	0,049	0,042	0,040	0,043
Sr	0,024	0,025	0,023	0,020	0,024	0,020	0,030	0,025	0,027	0,024
Total	16,526	16,558	16,556	16,575	16,621	16,566	16,638	16,638	16,610	16,541

WDS results for Apatite– Sample PB-123

PB-123 Apatita															
AP. 1-1		AP. 1-2	AP. 1-3	AP. 1-4	AP. 1-5	AP. 1-6	AP. 1-7	AP. 1-8	AP. 4-1	AP. 4-2	AP. 4-3	AP. 4-4	AP. 4-5	AP. 4-6	AP. 4-7
Element	Mass%	Mass%	Mass%	Mass%	Mass%	Mass%	Mass%	Mass%	Mass%	Mass%	Mass%	Mass%	Mass%	Mass%	Mass%
Na2O	0,19	0,22	0,22	0,08	0,13	0,14	0,15	0,17	0,20	0,12	0,15	0,15	0,12	0,26	0,20
SiO2	0,84	0,94	1,14	0,66	0,62	0,81	0,66	0,64	0,90	0,90	0,85	0,79	0,92	0,96	0,85
Y2O3	0,00	0,00	0,00	0,00	0,00	0,00	0,00	0,00	0,00	0,00	0,00	0,00	0,00	0,00	0,00
Fe2O3	0,07	0,05	0,22	0,03	0,03	0,05	0,04	0,10	0,08	0,02	0,02	0,07	0,03	0,10	0,17
MnO	0,05	0,09	0,03	0,06	0,07	0,06	0,06	0,03	0,02	0,05	0,04	0,03	0,04	0,05	0,08
La2O3	0,41	0,55	0,43	0,37	0,43	0,43	0,33	0,40	0,50	0,49	0,48	0,34	0,39	0,52	0,37
SO3	0,50	0,53	0,68	0,25	0,30	0,30	0,38	0,46	0,48	0,26	0,39	0,38	0,44	0,65	0,62
P2O5	39,53	39,41	38,96	40,57	39,93	40,20	40,39	40,41	40,22	39,55	39,55	39,79	39,45	39,44	39,55
SrO	0,23	0,24	0,25	0,27	0,21	0,28	0,29	0,26	0,28	0,25	0,27	0,29	0,24	0,27	0,23
TiO2	0,02	0,02	0,00	0,00	0,01	0,01	0,02	0,00	0,00	0,02	0,00	0,00	0,00	0,03	0,02
Cl	0,36	0,33	0,32	0,26	0,28	0,31	0,31	0,27	0,30	0,29	0,29	0,25	0,32	0,35	0,33
CaO	54,02	53,51	53,38	54,53	54,53	54,27	54,45	54,51	53,67	53,74	53,77	54,11	53,59	53,55	54,06
Ce2O3	3,09	3,21	2,73	2,14	2,29	2,56	2,07	1,58	2,99	3,22	2,85	2,29	3,19	3,13	2,37
F	3,41	3,58	3,21	3,72	3,49	3,39	3,37	3,86	3,39	3,71	3,64	4,22	3,70	3,31	3,45
MgO	0,00	0,00	0,00	0,00	0,00	0,00	0,00	0,00	0,00	0,00	0,00	0,00	0,00	0,00	0,00
Al2O3	0,01	0,01	0,08	0,00	0,01	0,02	0,01	0,01	0,02	0,00	0,01	0,00	0,00	0,00	0,00
Total	102,72	102,67	101,64	102,94	102,32	102,82	102,53	102,69	103,04	102,61	102,31	102,70	102,43	102,62	102,29
Formula		Formula	Formula	Formula	Formula	Formula	Formula	Formula	Formula	Formula	Formula	Formula	Formula	Formula	Formula
Ca	9,574	9,494	9,564	9,531	9,632	9,541	9,577	9,548	9,441	9,506	9,534	9,513	9,504	9,517	9,589
Na	0,060	0,069	0,070	0,025	0,042	0,045	0,047	0,052	0,063	0,037	0,049	0,048	0,039	0,082	0,063
Mn	0,007	0,012	0,005	0,008	0,009	0,009	0,008	0,005	0,002	0,007	0,005	0,005	0,005	0,007	0,012
Fe	0,008	0,006	0,028	0,003	0,003	0,006	0,004	0,012	0,010	0,003	0,003	0,008	0,003	0,012	0,021
La	0,025	0,033	0,027	0,022	0,026	0,026	0,020	0,024	0,030	0,030	0,029	0,021	0,024	0,032	0,023
Ce	0,187	0,195	0,167	0,128	0,138	0,154	0,124	0,095	0,180	0,195	0,173	0,138	0,193	0,190	0,144
P	5,536	5,525	5,516	5,603	5,573	5,585	5,613	5,593	5,591	5,528	5,542	5,528	5,529	5,539	5,543
Si	0,138	0,156	0,191	0,108	0,103	0,132	0,109	0,104	0,148	0,149	0,141	0,130	0,153	0,160	0,140
Cl	0,101	0,092	0,090	0,071	0,077	0,086	0,086	0,075	0,083	0,081	0,081	0,069	0,090	0,098	0,092
F	1,784	1,875	1,698	1,919	1,819	1,759	1,749	1,996	1,760	1,937	1,905	2,190	1,937	1,736	1,806
S	0,063	0,066	0,085	0,031	0,037	0,036	0,047	0,057	0,060	0,032	0,048	0,047	0,054	0,080	0,077
Sr	0,022	0,023	0,024	0,026	0,020	0,027	0,028	0,025	0,026	0,023	0,026	0,027	0,023	0,026	0,022
OH	-0,884	-0,967	-0,788	-0,990	-0,897	-0,845	-0,835	-1,070	-0,843	-1,018	-0,986	-1,259	-1,027	-0,834	-0,899
Total	16,749	16,715	16,858	16,548	16,658	16,637	16,674	16,633	16,675	16,575	16,648	16,463	16,527		16,632

WDS results for Apatite– Sample PB-181

PB-181 Apatita															
AP. 1		AP. 2	AP. 3	AP. 4	AP. 5	AP. 6	AP. 7	AP. 8	AP. 9	AP. 10	AP. 11	AP. 12	AP. 13	AP. 14	AP. 15
Element	Mass%	Mass%	Mass%	Mass%	Mass%	Mass%	Mass%	Mass%	Mass%	Mass%	Mass%	Mass%	Mass%	Mass%	Mass%
Na2O	0,31	0,32	0,22	0,30	0,35	0,31	0,39	0,31	0,35	0,29	0,34	0,37	0,33	0,36	0,28
SiO2	0,69	0,76	0,53	0,55	0,53	0,65	0,82	0,65	0,43	0,36	0,71	0,61	1,04	0,69	0,68
Y2O3	0,00	0,00	0,00	0,00	0,00	0,00	0,00	0,00	0,00	0,00	0,00	0,00	0,00	0,00	0,00
Fe2O3	0,01	0,02	0,09	0,06	0,00	0,00	0,00	0,00	0,02	0,07	0,02	0,09	0,12	0,22	0,22
MnO	0,03	0,00	0,03	0,03	0,02	0,04	0,06	0,02	0,02	0,03	0,02	0,04	0,03	0,05	0,06
La2O3	0,46	0,52	0,44	0,40	0,44	0,50	0,55	0,50	0,36	0,32	0,50	0,39	0,43	0,42	0,38
SO3	0,82	0,78	0,46	0,94	0,75	0,85	0,85	0,79	0,89	0,50	0,85	0,87	0,76	0,81	0,84
P2O5	39,53	39,58	40,12	39,71	39,81	39,69	39,07	39,59	40,27	40,44	39,62	38,81	38,75	38,99	39,89
SrO	1,30	1,16	1,12	1,29	1,20	1,81	1,82	1,41	1,41	1,44	1,38	1,59	1,81	1,42	1,75
TiO2	0,00	0,00	0,00	0,00	0,00	0,00	0,00	0,00	0,00	0,01	0,01	0,00	0,00	0,00	0,02
Cl	0,03	0,03	0,02	0,01	0,02	0,047	0,051	0,04	0,04	0,02	0,03	0,05	0,02	0,05	0,05
CaO	53,56	53,35	53,60	53,47	53,28	52,95	52,65	53,35	53,71	53,86	53,29	52,88	52,70	53,54	53,58
Ce2O3	1,72	1,92	1,37	1,58	1,41	1,98	2,51	2,00	1,16	1,22	2,31	2,12	1,66	1,61	1,40
F	3,31	3,37	3,45	3,59	4,64	3,60	3,76	3,69	3,83	3,95	3,77	4,19	3,47	4,21	3,87
MgO	0,00	0,00	0,00	0,00	0,00	0,00	0,00	0,00	0,00	0,00	0,00	0,00	0,00	0,00	0,00
Al2O3	0,00	0,01	0,00	0,01	0,02	0,00	0,00	0,00	0,01	0,00	0,00	0,01	0,07	0,00	0,01
Total	101,75	101,82	101,43	101,95	102,47	102,43	102,54	102,35	102,50	102,51	102,85	102,01	101,18	102,36	103,02
Formula	Formula	Formula	Formula	Formula	Formula	Formula	Formula	Formula	Formula	Formula	Formula	Formula	Formula	Formula	Formula
Ca	9,615	9,559	9,559	9,573	9,442	9,489	9,474	9,538	9,531	9,522	9,498	9,535	9,558	9,578	9,510
Na	0,100	0,104	0,070	0,098	0,113	0,101	0,126	0,099	0,111	0,091	0,110	0,119	0,107	0,117	0,089
Mn	0,004	0,000	0,004	0,005	0,003	0,005	0,009	0,003	0,003	0,003	0,003	0,006	0,004	0,008	0,008
Fe	0,001	0,002	0,011	0,008	0,000	0,001	0,000	0,000	0,003	0,009	0,003	0,012	0,015	0,027	0,028
La	0,029	0,032	0,027	0,025	0,027	0,031	0,034	0,031	0,022	0,020	0,030	0,024	0,027	0,026	0,023
Ce	0,106	0,118	0,083	0,097	0,085	0,121	0,154	0,122	0,070	0,074	0,141	0,131	0,103	0,098	0,085
P	5,607	5,604	5,654	5,618	5,575	5,620	5,555	5,593	5,647	5,649	5,580	5,530	5,554	5,512	5,595
Si	0,115	0,128	0,088	0,092	0,088	0,108	0,138	0,109	0,072	0,059	0,119	0,102	0,176	0,116	0,113
Cl	0,008	0,009	0,005	0,004	0,005	0,013	0,015	0,012	0,010	0,006	0,008	0,013	0,005	0,014	0,014
F	1,754	1,782	1,816	1,897	2,427	1,904	1,997	1,947	2,006	2,061	1,983	2,230	1,858	2,223	2,027
S	0,103	0,097	0,057	0,118	0,092	0,107	0,107	0,099	0,110	0,062	0,106	0,110	0,097	0,101	0,105
Sr	0,126	0,113	0,108	0,125	0,115	0,176	0,177	0,136	0,135	0,138	0,133	0,155	0,178	0,137	0,168
OH	-0,761	-0,792	-0,821	-0,901	-1,432	-0,918	-1,012	-0,959	-1,016	-1,067	-0,991	-1,243	-0,862	-1,237	-1,042
Total	16,805	16,757	16,661	16,758	16,542	16,759	16,776	16,730	16,704	16,628	16,723	16,724	16,818	16,720	16,723

WDS results for Apatite– Sample PB-185

PB-185 Apatita									
AP. 1-1		AP. 2-1	AP. 2-2	AP. 2-5	AP. 8-1	AP. 8-2	AP. 19-1	AP. 19-2	AP. 19-3
Element	Mass%	Mass%	Mass%	Mass%	Mass%	Mass%	Mass%	Mass%	Mass%
Na2O	0,39	0,23	0,37	0,31	0,28	0,22	0,23	0,26	0,36
SiO2	0,63	0,50	0,45	0,49	0,76	0,66	1,01	0,79	0,54
Y2O3	0,00	0,00	0,00	0,00	0,00	0,00	0,00	0,00	0,00
Fe2O3	0,01	0,05	0,02	0,04	0,04	0,07	0,10	0,20	0,12
MnO	0,06	0,08	0,09	0,04	0,05	0,07	0,09	0,06	0,05
La2O3	0,54	0,40	0,33	0,38	0,56	0,48	0,68	0,50	0,35
SO3	0,78	0,54	0,74	0,78	0,61	0,58	0,77	0,80	0,71
P2O5	38,40	38,96	39,20	39,40	38,05	38,75	38,57	38,55	39,15
SrO	2,91	2,75	2,81	2,13	2,77	2,82	2,64	3,08	2,51
TiO2	0,00	0,00	0,01	0,00	0,00	0,00	0,00	0,00	0,01
Cl	0,10	0,11	0,10	0,07	0,07	0,06	0,10	0,08	0,05
CaO	51,57	52,78	52,38	53,04	51,46	51,95	51,52	51,85	52,43
Ce2O3	1,42	1,22	1,18	1,22	2,15	1,52	2,65	1,97	1,26
F	4,28	4,08	4,16	3,83	4,26	4,14	3,63	3,93	4,63
MgO	0,00	0,00	0,00	0,00	0,00	0,00	0,00	0,00	0,00
Al2O3	0,00	0,00	0,01	0,02	0,00	0,00	0,03	0,01	0,01
Total	101,09	101,70	101,84	101,75	101,05	101,32	102,02	102,08	102,17
Formula	Formula	Formula	Formula	Formula	Formula	Formula	Formula	Formula	Formula
Ca	9,451	9,566	9,484	9,563	9,452	9,463	9,393	9,454	9,433
Na	0,131	0,074	0,120	0,102	0,093	0,072	0,075	0,087	0,117
Mn	0,008	0,012	0,013	0,005	0,007	0,010	0,013	0,009	0,007
Fe	0,002	0,006	0,003	0,005	0,005	0,009	0,013	0,025	0,015
La	0,034	0,025	0,020	0,023	0,035	0,030	0,042	0,031	0,022
Ce	0,089	0,076	0,073	0,075	0,135	0,095	0,165	0,123	0,077
P	5,561	5,580	5,609	5,613	5,523	5,577	5,556	5,554	5,566
Si	0,108	0,084	0,076	0,082	0,130	0,113	0,172	0,135	0,090
Cl	0,028	0,032	0,029	0,021	0,019	0,018	0,029	0,022	0,013
F	2,315	2,183	2,223	2,038	2,310	2,226	1,953	2,115	2,459
S	0,100	0,069	0,094	0,098	0,078	0,074	0,098	0,102	0,090
Sr	0,289	0,270	0,275	0,208	0,275	0,278	0,260	0,304	0,244
OH	-1,343	-1,215	-1,252	-1,059	-1,329	-1,244	-0,982	-1,137	-1,471
Total	16,771	16,762	16,766	16,775	16,734	16,720	16,788	16,825	16,661

Amphibole

WDS results for Amphibole– Sample PB-09

PB-09							
ANF 1-1		ANF 1-2	ANF 1-3	ANF 1-4	ANF 1-5	ANF 1-6	ANF 1-7
Element	Mass%	Mass%	Mass%	Mass%	Mass%	Mass%	Mass%
SiO2	44,98	45,09	45,16	45,53	44,87	44,99	45,24
Al2O3	9,81	9,90	10,31	9,78	10,11	10,01	9,89
FeO	12,89	12,64	12,89	12,23	12,98	12,99	12,54
MnO	0,16	0,16	0,18	0,18	0,18	0,20	0,20
Cl	0,10	0,11	0,11	0,07	0,11	0,10	0,08
CaO	11,02	11,09	11,17	11,06	11,06	11,01	11,22
K2O	1,39	1,34	1,34	1,31	1,38	1,44	1,40
TiO2	1,79	1,84	1,70	1,70	1,83	1,88	1,78
Cr2O3	0,02	0,00	0,01	0,04	0,01	0,00	0,01
F	0,86	0,84	0,78	0,97	0,89	0,86	0,96
Na2O	1,87	1,78	1,82	1,74	1,96	1,88	1,88
MgO	14,31	14,17	13,88	14,46	13,98	13,95	14,14
Total	99,20	98,95	99,35	99,07	99,37	99,31	99,34
Formula		Formula	Formula	Formula	Formula	Formula	Formula
Si	6,486	6,515	6,507	6,555	6,480	6,497	6,536
Ti	0,194	0,200	0,184	0,184	0,199	0,204	0,193
Al	1,667	1,686	1,751	1,659	1,721	1,703	1,684
Cr	0,002	0,000	0,002	0,005	0,001	0,000	0,002
Fe(iii)	0,787	0,705	0,662	0,721	0,696	0,697	0,597
Fe(ii)	0,768	0,822	0,891	0,751	0,871	0,872	0,918
Mn	0,020	0,020	0,022	0,022	0,023	0,024	0,024
Mg	3,076	3,052	2,982	3,103	3,010	3,003	3,046
Ca	1,702	1,717	1,724	1,706	1,711	1,703	1,737
Na	0,523	0,499	0,508	0,486	0,549	0,526	0,527
K	0,256	0,247	0,246	0,241	0,254	0,265	0,258
Zr	0,000	0,000	0,000	0,000	0,000	0,000	0,000
TOTAL	15,481	15,462	15,479	15,432	15,514	15,495	15,521
T©	802,3	808,5	791,5	791,3	807,3	813,0	801,6

WDS results for Amphibole– Sample PB-06

PB-06																
ANF 1-1		ANF 1-2	ANF 1-3	ANF 1-4	ANF 1-5	ANF 2-1	ANF 2-2	ANF 2-3	ANF 2-4	ANF 2-5	ANF 2-6	ANF 2-7	ANF 2-8	ANF 2-9	ANF 2-10	ANF 2-11
Element	Mass%	Mass%	Mass%	Mass%	Mass%	Mass%	Mass%	Mass%	Mass%	Mass%	Mass%	Mass%	Mass%	Mass%	Mass%	Mass%
SiO2	45,27	45,59	45,46	46,04	45,10	45,47	45,29	45,69	45,32	45,97	45,79	45,83	45,87	45,33	45,46	45,79
Al2O3	9,35	9,49	9,25	8,93	9,59	9,17	8,91	9,08	9,21	8,94	8,99	8,96	9,23	9,27	9,28	9,24
FeO	14,41	14,45	14,39	14,04	14,35	14,20	14,40	14,21	14,13	13,76	14,03	13,96	14,14	14,19	14,16	14,44
MnO	0,26	0,28	0,29	0,29	0,26	0,29	0,26	0,30	0,28	0,26	0,30	0,27	0,28	0,25	0,30	0,27
Cl	0,26	0,28	0,24	0,27	0,24	0,22	0,21	0,25	0,21	0,25	0,21	0,21	0,24	0,21	0,21	0,23
CaO	10,99	11,03	11,18	11,28	10,64	11,03	10,78	10,89	10,90	10,95	11,00	10,97	11,05	10,91	11,05	10,96
K2O	1,30	1,30	1,22	1,22	1,29	1,24	1,20	1,22	1,24	1,24	1,21	1,23	1,27	1,30	1,30	1,21
TiO2	1,48	1,54	1,52	1,49	1,69	1,63	1,83	1,67	1,99	1,62	1,76	1,95	1,81	1,74	1,82	1,75
Cr2O3	0,01	0,01	0,00	0,00	0,00	0,00	0,03	0,00	0,03	0,00	0,00	0,00	0,00	0,04	0,00	0,04
F	0,64	0,77	0,72	0,74	0,70	0,75	0,69	0,69	0,76	0,68	0,88	0,84	0,82	0,71	0,74	0,74
Na2O	2,14	2,09	2,22	1,98	2,15	2,19	2,24	2,17	2,12	2,22	2,15	2,21	2,24	2,13	2,22	2,15
MgO	13,13	13,12	13,46	13,52	12,73	13,19	13,31	13,41	13,27	13,62	13,62	13,48	13,14	13,20	13,26	13,31
Total	99,24	99,94	99,95	99,79	98,74	99,39	99,15	99,57	99,46	99,51	99,94	99,91	100,09	99,27	99,80	100,13
Formula		Formula	Formula	Formula	Formula	Formula	Formula	Formula	Formula	Formula	Formula	Formula	Formula	Formula	Formula	Formula
Si	6,594	6,599	6,578	6,663	6,597	6,620	6,594	6,617	6,581	6,658	6,614	6,631	6,644	6,596	6,594	6,601
Ti	0,162	0,168	0,165	0,162	0,186	0,179	0,200	0,181	0,217	0,176	0,191	0,212	0,197	0,190	0,199	0,190
Al	1,605	1,619	1,577	1,523	1,653	1,573	1,529	1,550	1,576	1,526	1,530	1,528	1,575	1,590	1,586	1,570
Cr	0,001	0,001	0,000	0,000	0,000	0,000	0,003	0,000	0,003	0,000	0,000	0,000	0,000	0,004	0,000	0,004
Fe(iii)	0,607	0,601	0,624	0,547	0,595	0,539	0,661	0,640	0,607	0,554	0,630	0,539	0,450	0,590	0,530	0,635
Fe(ii)	1,148	1,147	1,117	1,152	1,160	1,189	1,092	1,080	1,109	1,113	1,065	1,150	1,263	1,136	1,188	1,106
Mn	0,032	0,035	0,036	0,035	0,032	0,036	0,031	0,036	0,035	0,032	0,037	0,033	0,034	0,030	0,036	0,033
Mg	2,851	2,831	2,903	2,917	2,776	2,863	2,889	2,895	2,873	2,941	2,933	2,907	2,837	2,863	2,867	2,861
Ca	1,715	1,710	1,733	1,749	1,667	1,720	1,681	1,689	1,696	1,699	1,702	1,700	1,715	1,701	1,717	1,693
Na	0,604	0,586	0,623	0,556	0,610	0,618	0,632	0,609	0,597	0,623	0,602	0,620	0,629	0,601	0,624	0,601
K	0,242	0,240	0,225	0,225	0,241	0,230	0,223	0,225	0,230	0,229	0,223	0,227	0,235	0,241	0,241	0,223
Zr	0,000	0,000	0,000	0,000	0,000	0,000	0,000	0,000	0,000	0,000	0,000	0,000	0,000	0,000	0,000	0,000
TOTAL	15,561	15,537	15,581	15,530	15,518	15,569	15,537	15,524	15,522	15,552	15,527	15,547	15,578	15,543	15,582	15,516
T©	765,39	772,35	769,18	765,85	793,36	785,15	809,00	788,37	826,47	782,73	799,15	821,26	805,58	798,29	807,05	797,56

ANF 3-1		ANF 3-2	ANF 3-3	ANF 3-4	ANF 3-5	ANF 3-6	ANF 3-7	ANF 3-8	ANF 3-9
Element	Mass%	Mass%	Mass%	Mass%	Mass%	Mass%	Mass%	Mass%	Mass%
SiO2	46,11	46,10	45,48	45,71	41,03	45,35	45,47	45,85	45,14
Al2O3	9,14	8,93	8,94	9,02	7,88	9,22	9,04	8,99	9,05
FeO	14,33	14,81	14,13	13,96	14,02	14,09	13,82	14,27	14,28
MnO	0,27	0,30	0,30	0,30	0,29	0,29	0,27	0,28	0,24
Cl	0,22	0,19	0,23	0,22	0,21	0,19	0,25	0,24	0,21
CaO	10,98	10,82	10,93	11,00	10,46	10,88	10,84	10,75	10,65
K2O	1,23	1,22	1,21	1,17	1,25	1,22	1,29	1,25	1,28
TiO2	1,56	1,66	1,65	1,71	1,52	1,62	1,46	1,52	1,58
Cr2O3	0,02	0,01	0,04	0,02	0,00	0,01	0,01	0,00	0,05
F	0,76	0,63	0,71	0,67	0,73	0,79	0,86	0,78	0,80
Na2O	2,08	2,20	2,16	2,18	2,19	2,14	2,13	2,10	2,18
MgO	13,42	13,27	13,41	13,16	13,42	13,34	13,45	13,21	13,32
Total	100,11	100,12	99,18	99,11	93,00	99,15	98,90	99,24	98,77
Formula		Formula	Formula	Formula	Formula	Formula	Formula	Formula	Formula
Si	6,639	6,637	6,618	6,663	6,393	6,597	6,636	6,663	6,591
Ti	0,169	0,179	0,180	0,187	0,178	0,177	0,161	0,166	0,173
Al	1,551	1,515	1,533	1,550	1,447	1,581	1,555	1,540	1,557
Cr	0,002	0,001	0,004	0,002	0,000	0,001	0,002	0,000	0,006
Fe(iii)	0,637	0,675	0,625	0,477	1,009	0,647	0,617	0,631	0,721
Fe(ii)	1,089	1,108	1,094	1,224	0,817	1,067	1,070	1,103	1,023
Mn	0,033	0,036	0,036	0,036	0,039	0,036	0,033	0,035	0,030
Mg	2,881	2,848	2,909	2,860	3,117	2,893	2,927	2,862	2,900
Ca	1,694	1,669	1,704	1,718	1,746	1,696	1,695	1,674	1,666
Na	0,581	0,614	0,609	0,616	0,661	0,604	0,603	0,592	0,617
K	0,226	0,224	0,225	0,218	0,248	0,226	0,240	0,232	0,238
Zr	0,000	0,000	0,000	0,000	0,000	0,000	0,000	0,000	0,000
TOTAL	15,500	15,507	15,538	15,552	15,656	15,526	15,538	15,497	15,522
T©	773,75	785,97	787,25	795,07	784,87	783,62	764,18	770,43	778,83

WDS results for Amphibole– Sample PB-06 - Continuation

WDS results for Amphibole– Sample PB-92B

PB-92B - Anf													
ANF 1-3		ANF 1-4	ANF 1-5	ANF 1-6	ANF 1-3	ANF 1-4	ANF 1-5	ANF 1-6	ANF 1-1	ANF 1-2	ANF 1-4	ANF 1-5	ANF 1-6
Element	Mass%	Mass%	Mass%	Mass%	Mass%	Mass%	Mass%	Mass%	Mass%	Mass%	Mass%	Mass%	Mass%
SiO2	46,38	45,9	45,78	46,05	47,39	47,12	47,39	46,99	47,25	47,11	47,09	46,63	46,87
Al2O3	8,06	8,38	8,39	8,25	8,07	8,27	8,44	8,06	7,77	8,27	7,94	8,15	8,26
FeO	12,77	12,52	12,5	12,82	12,90	12,68	12,41	13,93	12,14	12,06	12,05	12,43	12,34
MnO	0,319	0,32	0,238	0,268	0,28	0,28	0,25	0,27	0,28	0,29	0,29	0,31	0,27
Cl	0,198	0,176	0,179	0,182	0,21	0,22	0,21	0,24	0,14	0,17	0,19	0,21	0,22
CaO	11,1	11,01	11,03	11,22	10,85	10,78	10,90	10,37	11,06	10,85	10,93	10,98	10,77
K2O	1,204	1,27	1,175	1,25	1,16	1,15	1,15	1,14	1,19	1,19	1,15	1,22	1,16
TiO2	1,241	1,238	0,973	1,131	1,33	1,46	0,93	1,19	1,31	1,60	1,22	1,05	1,28
Cr2O3	0,018	0,002	0,033	0,021	0,03	0,02	0,00	0,03	0,01	0,01	0,02	0,00	0,00
F	1,11	1,11	1,19	1,11	1,11	1,14	1,18	1,10	1,32	1,14	1,05	1,11	1,20
Na2O	2,34	2,3	2,38	2,36	2,36	2,25	2,32	2,44	2,27	2,35	2,31	2,24	2,32
MgO	15,07	15,01	15,04	14,68	14,91	14,85	14,94	14,22	15,17	14,73	14,79	14,71	14,69
Total	99,811	99,237	98,908	99,342	100,60	100,22	100,12	99,99	99,90	99,76	99,02	99,05	99,37
Formula		Formula	Formula	Formula	Formula	Formula	Formula	Formula	Formula	Formula	Formula	Formula	Formula
Si	6,681	6,643	6,650	6,691	6,757	6,734	6,778	6,751	6,795	6,778	6,821	6,764	6,769
Ti	0,134	0,135	0,106	0,124	0,142	0,157	0,100	0,129	0,141	0,173	0,133	0,115	0,139
Al	1,368	1,429	1,436	1,413	1,356	1,393	1,423	1,365	1,317	1,402	1,355	1,393	1,406
Cr	0,002	0,000	0,004	0,002	0,004	0,003	0,000	0,004	0,001	0,001	0,002	0,000	0,000
Fe(iii)	0,697	0,721	0,728	0,566	0,663	0,688	0,628	0,791	0,550	0,477	0,481	0,579	0,582
Fe(ii)	0,841	0,794	0,790	0,991	0,875	0,827	0,856	0,882	0,909	0,974	0,978	0,928	0,908
Mn	0,039	0,039	0,029	0,033	0,033	0,034	0,030	0,033	0,034	0,035	0,035	0,038	0,033
Mg	3,237	3,239	3,257	3,180	3,169	3,164	3,185	3,046	3,252	3,160	3,194	3,181	3,163
Ca	1,713	1,707	1,716	1,747	1,657	1,651	1,670	1,596	1,704	1,672	1,696	1,706	1,666
Na	0,654	0,645	0,670	0,665	0,652	0,623	0,643	0,680	0,633	0,656	0,649	0,630	0,650
K	0,221	0,234	0,218	0,232	0,211	0,210	0,210	0,209	0,218	0,218	0,213	0,226	0,214
Zr	0,000	0,000	0,000	0,000	0,000	0,000	0,000	0,000	0,000	0,000	0,000	0,000	0,000
TOTAL	15,588	15,587	15,604	15,643	15,521	15,484	15,524	15,485	15,555	15,546	15,557	15,562	15,530
T©	730,597	730,997	689,510	715,472	740,903	759,055	679,269	722,671	739,804	778,398	728,488	702,883	736,022

WDS results for Amphibole– Sample PB-123

PB-123 - Anf						
ANF 1-1		ANF 1-6	ANF 1-7	ANF 1-8	ANF 1-9	ANF 1-10
Element	Mass%	Mass%	Mass%	Mass%	Mass%	Mass%
SiO2	46,66	45,97	45,84	46,14	46,30	46,13
Al2O3	8,91	8,71	8,91	9,08	8,83	8,99
FeO	12,55	12,71	12,83	12,64	13,14	12,68
MnO	0,21	0,26	0,26	0,25	0,24	0,25
Cl	0,22	0,17	0,17	0,17	0,16	0,15
CaO	11,32	11,20	10,96	11,08	11,06	11,13
K2O	1,24	1,36	1,49	1,44	1,45	1,41
TiO2	0,98	1,38	1,48	1,50	1,35	1,58
Cr2O3	0,05	0,01	0,02	0,03	0,03	0,01
F	1,43	1,54	1,42	1,51	1,44	1,40
Na2O	2,12	2,22	2,16	2,16	2,24	2,13
MgO	14,98	14,80	14,51	14,63	14,60	14,62
Total	100,66	100,32	100,05	100,63	100,84	100,48
Formula		Formula	Formula	Formula	Formula	Formula
Si	6,670	6,626	6,618	6,622	6,636	6,624
Ti	0,105	0,149	0,161	0,162	0,145	0,171
Al	1,501	1,480	1,516	1,536	1,492	1,521
Cr	0,005	0,001	0,002	0,003	0,004	0,001
Fe(iii)	0,662	0,639	0,656	0,621	0,659	0,612
Fe(ii)	0,839	0,893	0,893	0,896	0,916	0,910
Mn	0,025	0,032	0,032	0,030	0,029	0,031
Mg	3,193	3,180	3,123	3,130	3,120	3,130
Ca	1,734	1,730	1,695	1,704	1,698	1,712
Na	0,588	0,620	0,605	0,601	0,622	0,593
K	0,226	0,250	0,274	0,264	0,265	0,258
Zr	0,000	0,000	0,000	0,000	0,000	0,000
TOTAL	15,547	15,600	15,574	15,568	15,586	15,563
T©	687,705	749,887	764,433	765,775	744,532	775,994

WDS results for Amphibole– Sample PB-181

PB-181																									
ANF 1-1		ANF 1-2	ANF 1-3	ANF 1-4	ANF 2-1	ANF 2-2	ANF 2-3	ANF 2-4	ANF 1-1	ANF 1-2	ANF 1-3	ANF 1-4	ANF 1-5	ANF 1-6	ANF 1-7	ANF 1-8	ANF 2-1	ANF 2-2	ANF 2-3	ANF 2-4	ANFb 1-1	ANFb 1-2	ANFb 1-3	ANFb 1-4
Element	Mass%	Mass%	Mass%	Mass%	Mass%	Mass%	Mass%	Mass%	Mass%	Mass%	Mass%	Mass%	Mass%	Mass%	Mass%	Mass%	Mass%	Mass%	Mass%	Mass%	Mass%	Mass%	Mass%	Mass%
SiO2	48,61	48,07	48,34	48,73	47,83	48,23	48,40	48,02	49,88	48,60	48,81	50,45	48,82	48,96	49,18	48,73	54,50	52,64	53,37	53,42	52,16	52,04	49,05	50,90
Al2O3	6,62	6,74	6,76	6,47	6,83	6,68	6,59	6,36	5,87	6,53	6,43	5,62	6,74	6,84	6,22	6,63	2,36	4,04	3,33	2,86	4,37	4,40	6,21	4,27
FeO	11,51	11,44	11,24	12,36	11,45	12,48	11,75	11,96	11,77	11,28	12,44	12,00	11,47	11,49	12,13	12,13	10,45	11,21	11,00	10,19	11,62	11,42	12,46	11,50
MnO	0,31	0,32	0,32	0,35	0,33	0,37	0,33	0,31	0,38	0,32	0,36	0,48	0,34	0,35	0,34	0,36	0,38	0,40	0,37	0,35	0,39	0,33	0,36	0,36
Cl	0,02	0,04	0,02	0,09	0,04	0,03	0,02	0,03	0,00	0,05	0,02	0,01	0,04	0,02	0,06	0,03	0,01	0,05	0,03	0,02	0,03	0,03	0,07	0,04
CaO	9,55	9,53	9,59	9,01	9,33	9,06	9,23	9,27	9,07	9,42	9,18	9,15	9,46	9,60	9,26	9,18	8,04	8,46	8,15	8,17	8,58	8,45	9,01	8,45
K2O	1,67	1,52	1,63	1,52	1,74	1,59	1,70	1,66	1,43	1,34	1,55	1,43	1,31	1,38	1,32	1,49	0,97	1,05	1,08	1,02	1,21	1,23	1,49	1,24
TiO2	1,14	1,32	1,17	0,64	1,50	0,90	1,26	1,04	0,45	0,82	1,11	0,39	0,91	1,08	1,10	0,74	0,17	0,18	0,19	0,28	0,23	0,29	0,67	0,23
Cr2O3	0,04	0,07	0,07	0,04	0,01	0,02	0,05	0,04	0,04	0,03	0,00	0,02	0,00	0,00	0,00	0,04	0,01	0,01	0,03	0,01	0,02	0,01	0,01	0,03
F	1,90	1,97	2,02	1,93	1,91	1,94	2,09	2,07	1,82	1,99	1,80	1,82	1,93	1,89	1,64	2,04	1,99	1,93	1,93	1,97	2,02	2,32	1,87	2,16
Na2O	3,58	3,58	3,53	3,88	3,58	3,80	3,63	3,66	3,55	3,73	3,82	3,65	3,73	3,86	3,64	3,82	4,01	4,14	3,95	4,07	4,03	4,13	3,97	4,19
MgO	15,92	15,59	16,02	15,29	15,36	15,02	15,47	15,50	16,32	16,32	15,32	16,03	15,95	15,89	15,29	15,71	17,64	16,75	17,32	17,64	16,43	16,60	15,49	16,78
Total	100,88	100,18	100,70	100,31	99,91	100,12	100,52	99,92	100,59	100,43	100,85	101,04	100,70	101,36	100,17	100,89	100,53	100,87	100,74	100,01	101,09	101,25	100,66	100,15
Formula		Formula	Formula	Formula	Formula	Formula	Formula	Formula	Formula	Formula	Formula	Formula	Formula	Formula	Formula	Formula	Formula	Formula	Formula	Formula	Formula	Formula	Formula	Formula
Si	6,950	6,933	6,933	7,016	6,927	6,972	6,967	6,96	7,074	6,945	6,990	7,151	6,966	6,962	7,060	6,962	7,637	7,420	7,477	7,538	7,367	7,351	7,031	7,266
Ti	0,123	0,143	0,143	0,069	0,163	0,098	0,136	0,11	0,048	0,088	0,120	0,041	0,098	0,115	0,118	0,079	0,018	0,019	0,020	0,030	0,024	0,031	0,072	0,025
Al	1,115	1,146	1,146	1,098	1,166	1,138	1,118	1,09	0,981	1,100	1,085	0,939	1,133	1,146	1,052	1,116	0,390	0,671	0,550	0,476	0,727	0,732	1,049	0,718
Cr	0,004	0,008	0,008	0,005	0,001	0,002	0,005	0,00	0,005	0,003	0,000	0,002	0,000	0,000	0,000	0,004	0,001	0,001	0,003	0,001	0,003	0,001	0,001	0,003
Fe(iii)	0,512	0,468	0,468	0,586	0,432	0,557	0,500	0,55	0,778	0,669	0,534	0,634	0,577	0,461	0,488	0,658	0,624	0,575	0,740	0,619	0,569	0,592	0,602	0,727
Fe(ii)	0,864	0,911	0,911	0,902	0,955	0,951	0,914	0,90	0,617	0,679	0,956	0,788	0,792	0,906	0,968	0,791	0,600	0,746	0,549	0,583	0,803	0,757	0,892	0,646
Mn	0,038	0,038	0,038	0,042	0,041	0,046	0,040	0,04	0,046	0,039	0,044	0,057	0,041	0,042	0,041	0,043	0,045	0,048	0,043	0,042	0,047	0,040	0,044	0,044
Mg	3,393	3,352	3,352	3,282	3,316	3,237	3,320	3,35	3,451	3,477	3,271	3,387	3,393	3,368	3,272	3,346	3,685	3,520	3,618	3,711	3,460	3,496	3,310	3,571
Ca	1,463	1,473	1,473	1,390	1,448	1,403	1,423	1,44	1,378	1,442	1,408	1,389	1,446	1,462	1,424	1,405	1,207	1,277	1,223	1,235	1,298	1,279	1,384	1,292
Na	0,992	1,001	1,001	1,083	1,005	1,065	1,013	1,03	0,976	1,033	1,061	1,003	1,032	1,064	1,013	1,058	1,089	1,131	1,073	1,113	1,104	1,131	1,103	1,160
K	0,305	0,280	0,280	0,279	0,321	0,293	0,312	0,31	0,259	0,244	0,283	0,259	0,238	0,250	0,242	0,272	0,172	0,189	0,192	0,184	0,218	0,222	0,272	0,226
Zr	0,000	0,000	0,000	0,000	0,000	0,000	0,000	0,00	0,000	0,000	0,000	0,000	0,000	0,000	0,000	0,000	0,000	0,000	0,000	0,000	0,000	0,000	0,000	0,000
TOTAL	15,760	15,753	15,753	15,752	15,774	15,761	15,748	15,77	15,613	15,720	15,752	15,651	15,716	15,777	15,679	15,735	15,469	15,598	15,489	15,533	15,620	15,631	15,759	15,678
T©	714,490	741,776	741,776	622,098	767,402	676,002	732,783	700,596	573,587	659,473	710,265	553,942	675,335	703,161	707,995	642,574	462,247	467,332	474,788	514,666	492,353	519,524	627,948	493,950

WDS results for Amphibole– Sample PB-185

PB-185 - ANF					
ANF 1-1		ANF 1-2	ANF 1-3	ANF 1-4	ANF 1-5
Element	Mass%	Mass%	Mass%	Mass%	Mass%
SiO2	56,69	55,79	55,72	55,03	56,35
Al2O3	0,89	1,68	1,38	2,13	0,95
FeO	9,06	9,45	9,75	9,94	9,67
MnO	0,42	0,37	0,41	0,40	0,42
Cl	0,00	0,02	0,00	0,02	0,03
CaO	9,71	9,95	9,07	9,75	9,86
K2O	0,48	0,41	0,66	0,36	0,47
TiO2	0,07	0,13	0,11	0,33	0,04
Cr2O3	0,00	0,02	0,00	0,00	0,02
F	1,26	1,24	1,46	1,10	1,04
Na2O	2,04	2,17	2,73	2,25	1,98
MgO	18,67	17,96	18,02	17,48	17,83
Total	99,29	99,19	99,30	98,79	98,66
Formula		Formula	Formula	Formula	Formula
Si	7,877	7,809	7,807	7,734	7,916
Ti	0,007	0,013	0,011	0,035	0,004
Al	0,146	0,277	0,227	0,353	0,157
Cr	0,000	0,002	0,000	0,000	0,002
Fe(iii)	0,560	0,429	0,554	0,495	0,408
Fe(ii)	0,493	0,677	0,588	0,673	0,728
Mn	0,049	0,044	0,048	0,048	0,050
Mg	3,868	3,748	3,764	3,662	3,734
Ca	1,445	1,492	1,361	1,468	1,484
Na	0,550	0,589	0,742	0,613	0,539
K	0,085	0,073	0,118	0,065	0,085
Zr	0,000	0,000	0,000	0,000	0,000
TOTAL	15,080	15,154	15,221	15,146	15,108
T©	380,103	434,869	417,440	533,430	345,032

Titanite

WDS results for Amphibole– Sample PB-92B

PB-92B Titanite																		
Element	Tit 1.1		Tit 1.2		Tit 1.3		Tit 1.4		Tit 1.5		Tit 1.6		Tit 2-1		Tit 2-2		Tit 2-3	
	Mass%	Form. Est	Mass%	Form. Est	Mass%	Form. Est	Mass%	Form. Est	Mass%	Form. Est	Mass%	Form. Est	Mass%	Form. Est	Mass%	Form. Est	Mass%	Form. Est
SiO2	29,16	**1,00**	29,04	**1,00**	29,87	**1,02**	29,24	**1,01**	29,46	**1,01**	29,19	**1,01**	29,05	**1,00**	29,61	**1,00**	33,23	**1,13**
Al2O3	1,51	**0,06**	1,48	**0,06**	1,57	**0,06**	1,60	**0,07**	1,53	**0,06**	1,57	**0,06**	1,59	**0,06**	1,37	**0,05**	2,61	**0,10**
Y2O3	0,07	**0,001**	0,06	**0,001**	0,08	**0,001**	0,09	**0,002**	0,10	**0,002**	0,13	**0,002**	0,04	**0,001**	0,00	**0,000**	0,00	**0,000**
Fe2O3	2,45	**0,06**	2,65	**0,07**	2,64	**0,07**	2,07	**0,05**	2,22	**0,06**	2,44	**0,06**	2,43	**0,06**	2,66	**0,07**	4,80	**0,12**
MnO	0,10	**0,003**	0,09	**0,003**	0,10	**0,003**	0,07	**0,002**	0,11	**0,00**	0,07	**0,00**	0,09	**0,00**	0,11	**0,00**	0,11	**0,00**
La2O3	0,44	**0,01**	0,45	**0,01**	0,39	**0,005**	0,41	**0,01**	0,45	**0,01**	0,49	**0,01**	0,45	**0,01**	0,38	**0,00**	0,31	**0,00**
CaO	26,00	**0,96**	25,91	**0,96**	25,61	**0,93**	26,00	**0,97**	26,09	**0,96**	26,01	**0,97**	26,20	**0,97**	26,07	**0,95**	22,93	**0,83**
K2O	0,02	**0,001**	0,03	**0,001**	0,03	**0,001**	0,01	**0,000**	0,00	**0,000**	0,00	**0,000**	0,01	**0,000**	0,06	**0,002**	0,32	**0,014**
Nb2O5	0,11	**0,002**	0,13	**0,002**	0,11	**0,002**	0,11	**0,002**	0,17	**0,003**	0,12	**0,002**	0,12	**0,002**	0,19	**0,003**	0,12	**0,002**
ZrO2	0,03	**0,0005**	0,11	**0,002**	0,12	**0,002**	0,00	**0,00**	0,03	**0,001**	0,08	**0,001**	0,03	**0,001**	0,02	**0,000**	0,05	**0,001**
TiO2	34,70	**0,90**	34,30	**0,89**	34,96	**0,89**	34,09	**0,89**	34,47	**0,89**	33,92	**0,88**	34,28	**0,89**	35,61	**0,91**	26,68	**0,68**
Ce2O3	1,51	**0,02**	1,62	**0,02**	1,50	**0,02**	1,49	**0,02**	1,50	**0,02**	1,59	**0,02**	1,45	**0,02**	1,28	**0,02**	0,90	**0,01**
F	0,17	**0,02**	0,17	**0,02**	0,17	**0,02**	0,12	**0,01**	0,17	**0,02**	0,14	**0,02**	0,17	**0,02**	0,13	**0,01**	0,21	**0,02**
Na2O	0,05	**0,003**	0,07	**0,004**	0,05	**0,003**	0,06	**0,004**	0,07	**0,005**	0,02	**0,001**	0,05	**0,003**	0,04	**0,003**	0,42	**0,027**
MgO	0,00	**0,000**	0,00	**0,000**	0,00	**0,000**	0,00	**0,000**	0,00	**0,000**	0,00	**0,000**	0,00	**0,000**	0,00	**0,000**	3,14	**0,159**
Total	96,29	**3,02**	96,11	**3,02**	97,20	**3,01**	95,35	**3,02**	96,36	**3,02**	95,76	**3,02**	95,94	**3,03**	97,54	**3,01**	95,84	**3,09**

WDS results for Amphibole– Sample PB-181

PB - 181 Titanite																																														
Element	Tit 1.1		Tit 1.2		Tit 1.3		Tit 1.4		Tit 1.5		Tit 1.7		Tnt 1.8		Tnt 1.9		Tnt 1.10		Tnt 1.11		Tnt 2-1		Tnt 2-2		Tnt 2-3		Tnt 2-4		Tnt 2-5		Tnt 3-5		Tnt 3-6		Tnt 3-7		Tnt 3-8		Tnt 3-9		Tnt 3-10		Tnt 3-11		Tnt 3-12	
	Mass%	Form. Est		Form. Est		Form. Est		Form. Est		Form. Est		Form. Est		Form. Est		Form. Est		Form. Est		Form. Est		Form. Est		Form. Est		Form. Est		Form. Est		Form. Est		Form. Est		Form. Est		Form. Est		Form. Est		Form. Est		Form. Est		Form. Est		Form. Est
SiO2	29,52	1,02	29,39	1,01	29,03	1,01	29,53	1,01	29,55	1,02	29,23	1,01	29,32	1,01	29,49	1,02	29,06	1,00	29,28	1,01	29,49	1,01	29,53	1,01	29,37	1,01	29,47	1,01	29,54	1,02	29,74	1,01	29,58	1,01	29,23	1,01	29,39	1,01	29,82	1,02	29,86	1,00	29,63	1,00	30,01	1,01
Al2O3	0,99	0,04	1,13	0,05	1,10	0,05	1,04	0,04	1,11	0,05	1,02	0,04	1,04	0,04	1,10	0,04	1,00	0,04	1,01	0,04	1,13	0,05	1,16	0,05	1,01	0,04	1,10	0,04	1,12	0,05	1,13	0,04	1,07	0,04	0,94	0,04	0,89	0,04	0,97	0,04	0,80	0,03	0,74	0,03	0,90	0,04
Y2O3	0,00	0,000	0,00	0,000	0,00	0,000	0,00	0,000	0,00	0,000	0,00	0,000	0,00	0,000	0,00	0,000	0,00	0,000	0,00	0,000	0,00	0,000	0,00	0,000	0,00	0,000	0,00	0,000	0,01	0,000	0,00	0,000	0,00	0,000	0,00	0,000	0,00	0,000	0,00	0,000	0,00	0,000	0,00	0,000	0,00	0,000
Fe2O3	3,10	0,08	3,11	0,08	3,28	0,09	3,10	0,08	3,08	0,08	3,07	0,08	3,28	0,08	3,35	0,09	3,09	0,08	3,05	0,08	3,11	0,08	3,29	0,08	3,48	0,09	3,18	0,08	2,89	0,07	2,91	0,07	2,95	0,08	2,80	0,07	2,72	0,07	3,00	0,08	2,91	0,07	3,24	0,08	3,08	0,08
MnO	0,10	0,00	0,08	0,00	0,12	0,00	0,08	0,00	0,09	0,00	0,11	0,00	0,11	0,00	0,10	0,00	0,11	0,00	0,09	0,00	0,09	0,00	0,10	0,00	0,10	0,00	0,09	0,00	0,09	0,00	0,10	0,00	0,08	0,00	0,10	0,00	0,10	0,00	0,11	0,00	0,11	0,00	0,10	0,00	0,10	0,00
La2O3	0,23	0,00	0,23	0,00	0,27	0,00	0,21	0,00	0,18	0,00	0,27	0,00	0,22	0,00	0,25	0,00	0,25	0,00	0,22	0,00	0,27	0,00	0,23	0,00	0,22	0,00	0,24	0,00	0,23	0,00	0,10	0,00	0,27	0,00	0,26	0,00	0,28	0,00	0,17	0,00	0,02	0,00	0,04	0,00	0,04	0,00
CaO	26,62	0,98	26,71	0,98	26,59	0,99	26,58	0,98	26,94	1,00	26,56	0,98	26,91	0,99	26,85	0,99	26,68	0,98	26,68	0,99	26,60	0,97	26,51	0,97	26,69	0,99	26,67	0,98	27,01	0,99	27,72	1,00	26,89	0,99	27,02	1,00	26,84	0,99	27,39	1,00	27,48	0,99	27,36	0,99	27,71	1,00
K2O	0,01	0,000	0,01	0,000	0,00	0,000	0,12	0,005	0,04	0,002	0,00	0,000	0,01	0,000	0,00	0,000	0,01	0,0003	0,02	0,001	0,00	0,000	0,00	0,000	0,00	0,000	0,00	0,000	0,04	0,002	0,01	0,000	0,00	0,000	0,00	0,000	0,00	0,000	0,01	0,000	0,00	0,000	0,02	0,001	0,00	0,000
Nb2O5	0,12	0,002	0,15	0,002	0,06	0,001	0,15	0,002	0,10	0,002	0,18	0,003	0,16	0,002	0,10	0,001	0,11	0,002	0,13	0,002	0,09	0,001	0,13	0,002	0,13	0,002	0,10	0,001	0,04	0,001	0,04	0,001	0,06	0,001	0,07	0,001	0,06	0,001	0,07	0,001	0,09	0,001	0,06	0,001	0,01	0,000
ZrO2	0,57	0,010	0,64	0,011	0,86	0,015	0,70	0,012	0,59	0,010	0,74	0,012	0,67	0,011	0,65	0,011	0,70	0,012	0,76	0,013	0,53	0,009	0,56	0,009	0,58	0,010	0,62	0,010	0,50	0,008	0,29	0,005	0,77	0,013	0,38	0,006	0,44	0,007	0,34	0,006	0,62	0,010	0,49	0,008	0,33	0,005
TiO2	33,95	0,88	34,02	0,88	33,22	0,87	34,26	0,88	33,22	0,86	33,82	0,88	33,76	0,87	33,34	0,86	34,32	0,89	33,68	0,88	34,66	0,89	34,19	0,88	33,62	0,87	34,17	0,88	33,85	0,88	35,09	0,89	34,09	0,88	34,46	0,89	34,85	0,90	34,22	0,88	35,79	0,91	36,07	0,91	35,25	0,89
Ce2O3	0,64	0,01	0,70	0,01	0,74	0,01	0,73	0,01	0,56	0,01	0,68	0,01	0,70	0,01	0,72	0,01	0,64	0,01	0,83	0,01	0,78	0,01	0,74	0,01	0,60	0,01	0,66	0,01	0,69	0,01	0,11	0,00	0,69	0,01	0,63	0,01	0,80	0,01	0,50	0,01	0,08	0,00	0,07	0,00	0,07	0,00
F	0,19	0,02	0,21	0,02	0,24	0,03	0,22	0,02	0,22	0,02	0,23	0,03	0,22	0,02	0,22	0,02	0,21	0,02	0,19	0,02	0,23	0,02	0,19	0,02	0,22	0,02	0,20	0,02	0,23	0,02	0,21	0,02	0,21	0,02	0,21	0,02	0,23	0,02	0,28	0,03	0,26	0,03	0,22	0,02	0,26	0,03
Na2O	0,12	0,008	0,10	0,007	0,10	0,007	0,10	0,006	0,10	0,007	0,14	0,009	0,09	0,006	0,12	0,008	0,14	0,009	0,13	0,008	0,11	0,007	0,10	0,007	0,11	0,007	0,10	0,007	0,12	0,008	0,11	0,007	0,13	0,009	0,11	0,008	0,13	0,009	0,10	0,007	0,13	0,009	0,10	0,007	0,11	0,007
MgO	0,00	0,000	0,00	0,000	0,00	0,000	0,00	0,000	0,01	0,000	0,00	0,000	0,00	0,000	0,00	0,000	0,02	0,001	0,00	0,000	0,02	0,001	0,00	0,000	0,00	0,000	0,00	0,000	0,00	0,000	0,00	0,000	0,00	0,000	0,00	0,000	0,00	0,000	0,00	0,000	0,00	0,000	0,00	0,000	0,00	0,000
Total	96,16	3,03	96,48	3,03	95,61	3,04	96,81	3,03	95,79	3,04	96,04	3,03	96,48	3,04	96,27	3,04	96,32	3,03	96,05	3,03	97,11	3,03	96,73	3,03	96,12	3,03	96,60	3,03	96,35	3,04	97,56	3,04	96,81	3,03	96,22	3,04	96,73	3,03	96,97	3,04	98,14	3,03	98,14	3,03	97,87	3,04

Appendix III – Thermometry

Ti in zircon temperature calculations

Parameters used and zircon temperatures obtained for sample PB-09

PB-09	Cálculo da Temperatura														
	aTiO2	0,5													
	aSiO2	0,8													
		Zr-1	Zr-2	Zr-3	Zr-4	Zr-5	Zr-6	Zr-7	Zr-8	Zr-9	Zr-10	Zr-11	Zr-12	Zr-13	Zr-15
	Ti (ppm)	48,06	25,92	34,61	28,86	24,31	41,48	33,33	36,25	28,53	48,95	39,01	28,12	43,82	43,25
	T (K)	1255	1173	1210	1186	1165	1234	1205	1216	1185	1257	1226	1183	1242	1240
	T (C)	982	900	937	913	892	961	932	943	912	984	953	910	969	967
	1/T	0,000797	0,000853	0,000827	0,000843	0,000859	0,00081	0,00083	0,000822	0,000844	0,000795	0,000816	0,000845	0,000805	0,000806

Parameters used and zircon temperatures obtained for sample PB-22

PB-22	Cálculo da Temperatura										
	aTiO2	0,7									
	aSiO2	0,8									
		Zr-2	Zr-3	Zr-4	Zr-5	Zr-6	Zr-7	Zr-8	Zr-9	Zr-10	Zr-12
	Ti (ppm)	9,03	32,87	35,99	35,13	39,2	30,12	25,44	22,72	23,74	45,32
	T (K)	1022	1160	1172	1169	1182	1150	1130	1117	1122	1201
	T (C)	749	887	898	895	909	877	857	844	849	928
	1/T	0,000979	0,000862	0,000854	0,000856	0,000846	0,00087	0,000885	0,000895	0,000891	0,000833

Parameters used and zircon temperatures obtained for sample PB-92B

PB-92b	Cálculo da Temperatura										
	aTiO2	0,7									
	aSiO2	0,8									
		Zr5	Zr-6	Zr-9	Zr-10	Zr-13	Zr-14	Zr-15	Zr-17	Zr-18	Zr-20
	Ti (ppm)	13,2	29,51	21,6	23,58	17,82	27,84	31	33,02	12,24	26,51
	T (K)	1059	1147	1111	1121	1090	1141	1153	1161	1051	1135
	T (C)	786	874	838	848	817	867	880	888	778	862
	1/T	0,000944	0,000871	0,0009	0,000892	0,000917	0,000877	0,000867	0,000861	0,000951	0,000881

Parameters used and zircon temperatures obtained for sample PB-123

PB-123	Cálculo da Temperatura												
	aTiO2	0,7											
	aSiO2	0,8											
		ZR-01	ZR-02	ZR-03	ZR-04	ZR-05	ZR-06	ZR-07	ZR-08b	ZR-08c	ZR-09	ZR-10	ZR-11
	Ti (ppm)	34,78	18,17	43,2	33,28	39,02	35,86	24,82	29,44	37,7	14,97	36,7	25,58
	T (K)	1167	1092	1195	1162	1182	1171	1127	1147	1177	1072	1174	1131
	T (C)	894	819	922	889	909	898	854	874	904	799	901	858
	1/T	0,000857	0,000915	0,000837	0,000861	0,000846	0,000854	0,000887	0,000872	0,000849	0,000933	0,000852	0,000884

Parameters used and zircon temperatures obtained for sample PB-181

PB-181	Cálculo da Temperatura										
	aTiO2	0,9									
	aSiO2	0,5									
		Zr-1_b	Zr-1_c	Zr-1_a	Zr-2	Zr-3	Zr-4_b	Zr-4_c	Zr-5	Tit_06b	Tit_06c
	Ti (ppm)	34,75	39,05	16,7	28,05	33,09	29,83	29,34	25,78	23,67	29,01
	T (K)	1085	1097	1012	1062	1079	1069	1067	1054	1045	1066
	T (C)	812	824	739	789	806	796	794	781	772	793
	1/T	0,000922	0,000911	0,000988	0,000941	0,000926	0,000936	0,000937	0,000949	0,000957	0,000938

Zr in Titanite temperature calculations

Parameters used and titanite temperatures obtained for sample PB-92B

PB-92b	Parâmetros										
	P(GPa)	0,38									
	aTiO2	0,7									
	aSiO2	0,8									
	Element	Tit-1	Tit-4	Tit-5	Tit-6	Tit-7	Tit-8	Tit-10	Tit-11	Tit-12	Tit-13
	Zr	435,0	708,3	653,3	474,9	681,2	475,9	694,8	516,7	652,7	639,3
	T (C)	720	746	742	724	744	724	745	729	742	740
	T (K)	993	1019	1015	997	1017	997	1018	1002	1015	1014
	1/T	0,001007	0,000981	0,000985	0,001003	0,000983	0,001003	0,000982	0,000998	0,000986	0,000987

Parameters used and titanite temperatures obtained for sample PB-123

PB-123	Parâmetros								
	P(GPa)	0,38							
	aTiO2	0,7							
	aSiO2	0,8							
	Element	Tit_1	Tit_2	Tit_3	Tit_4	Tit_5	Tit_6	Tit_7	Tit_8
	Zr (ppm)	1400,9	1062,6	1229,9	1343,3	1319,6	1468,1	1427,0	1120,3
	T (C)	786	769	778	783	782	789	787	772
	T (K)	1059	1042	1051	1056	1055	1062	1060	1046
	1/T	0,000944	0,000959	0,000951	0,000947	0,000948	0,000942	0,000943	0,000956

Parameters used and titanite temperatures obtained for sample PB-08A

PB-08A	Parâmetros									
	P(GPa)	0,38								
	aTiO2	0,9								
	aSiO2	0,5								
	Element	Tit_1	Tit_2	Tit_3	Tit_4	Tit_5n	Tit_5b	Tit_6	Tit_7	Tit_8
	Zr	5360,5	4837,9	5047,0	4648,0	5262,6	4850,5	6768,5	6132,5	5780,8
	T (C)	858	851	854	848	857	851,2	874	867	863
	T (K)	1131	1124	1127	1121	1130	1124	1147	1141	1136
	1/T	0,000884	0,00089	0,000887	0,000892	0,000885	0,000889	0,000871	0,000877	0,00088

Parameters used and titanite temperatures obtained for sample PB-181

PB-181	Parâmetros						Pop. 1	1,5,7,03TF,04TF,05TF,09TF,15TF,16TF,2TF												
	P(GPa)	0,38					Pop 2	2,4,6,8,9,01TF,11TF												
	aTiO2	0,9																		
	aSiO2	0,5																		
	Element	Tit-1	Tit-2	Tit-3	Tit-4	Tit-5	Tit-6-px	Tit-7	Tit-8	Tit-9	Tit_01_TF	Tit_03_TF	Tit_04_TF	Tit_05_TF	Tit_09_TF	Tit_11_TF	Tit_15_TF	Tit_16_TF	Tit_2c_TF	
	Zr	1705,51	995,42	2665,43	976,87	1639,87	975,69	4115,47	1016,82	1134,73	3533,64	2302,02	2964,84	2151,86	3514,48	2499,48	5235	5008,97	3924,43	
	T (C)	784	753	812	752	782	752	840	754	760	830	803	819	799	830	808	856	853	837	
	T (K)	1058	1026	1085	1025	1055	1025	1113	1027	1034	1103	1076	1092	1072	1103	1081	1130	1127	1110	
	1/T	0,000946	0,000975	0,000922	0,000976	0,000948	0,000976	0,000898	0,000973	0,000968	0,000906	0,000929	0,000916	0,000933	0,000907	0,000925	0,000885	0,000888	0,000901	

Parameters used and titanite temperatures obtained for sample PB-185

PB-185	Parâmetros																			
	P(GPa)	0,38																		
	aTiO2	0,9																		
	aSiO2	0,5																		
	Element	Tit_01	Tit_02	Tit_04	Tit_05c	Tit_05b	Tit_06	Tit_07	Tit_14	Tit_15_1	Tit_15_2	Tit_15_3	Tit_16	Tit_17	Tit_18c	Tit_18b	Tit_19	Tit_20c	Tit_20b	Média
	Zr	3904,58	3726,27	3897,85	3480,65	3415,99	5571,88	3633,41	3708,04	6363,22	3985,46	2918,52	4148,23	3554,8	4033,14	3268,38	3548,15	4143,1	3540,56	3935,679
	T (C)	837	834	837	829	828	861	832	833	870	838	818	841	830	839	825	830	840,6	830,2	837
	T (K)	1110	1107	1110	1102	1101	1134	1105	1106	1143	1111	1091	1114	1104	1112	1098	1103	1114	1103	1110
	1/T	0,000901	0,000904	0,000901	0,000907	0,000908	0,000882	0,000905	0,000904	0,000875	0,0009	0,000917	0,000898	0,000906	0,000899	0,000911	0,000906	0,000898	0,000906	0,000901

Appendix IV – SEM Images and Mineral Maps

Sample – PB 09

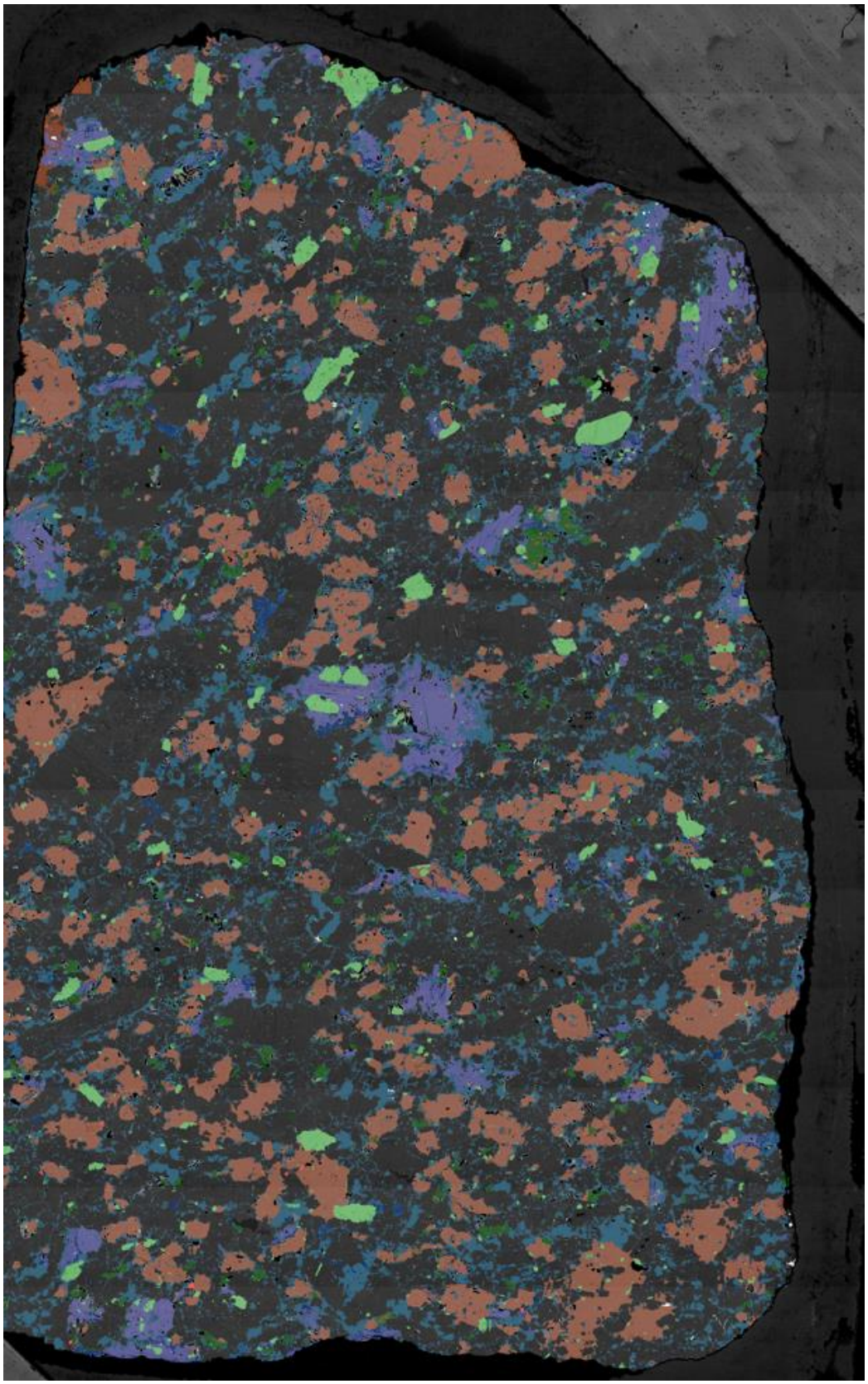

	Name	Area %	Particles
	K-feldspato	57,45%	125
	px_anf_CaMgFe	15,88%	129
	plagioclasio_NaCa	14,84%	114
	biotita	3,56%	117
	apatita	2,56%	110
	FeMg_SiO	1,83%	119
	ilmenita	1,27%	110
	Ti-magnetita	1,23%	110
	quartzo	1,03%	114
	Unknown	0,28%	178
	zircao	0,03%	35
	magnetita	0,03%	76
	titanita	0,00%	10
	Low_Counts	0,00%	10
	No_XRay	0,00%	47
	Background	0,00%	0

Legend for sample PB-09

Sample – PB 181

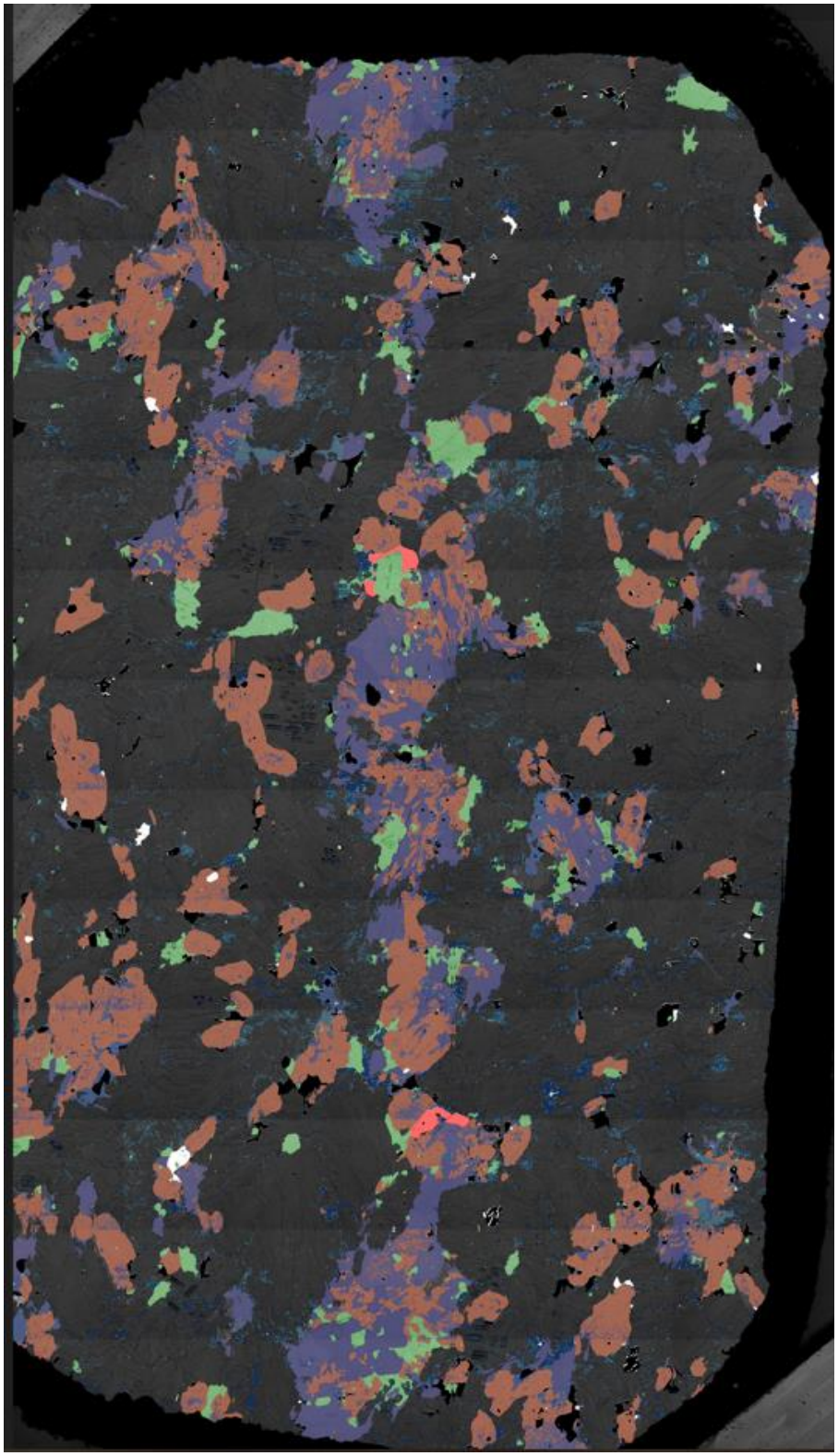

	Name	Area %	Particles
	K-feldspato	66,84%	98
	px_anf_CaMgFe	12,78%	92
	biotita	9,27%	92
	plagioclasio_NaCa	2,96%	97
	apatita	2,80%	95
	quartzo	1,83%	98
	Ti-magnetita	1,81%	95
	titanita	0,92%	85
	magnetita	0,29%	74
	ilmenita	0,19%	70
	Unknown	0,15%	116
	zircao	0,14%	9
	FeMg_SiO	0,01%	58
	No_XRay	0,00%	11
	Low_Counts	0,00%	1
	Background	0,00%	0

Legend for sample PB-181

APPENDIX V – CSD Files

CSD Files depicting the obtained apatite crystals contours for each analyzed sample

Sample – PB 09

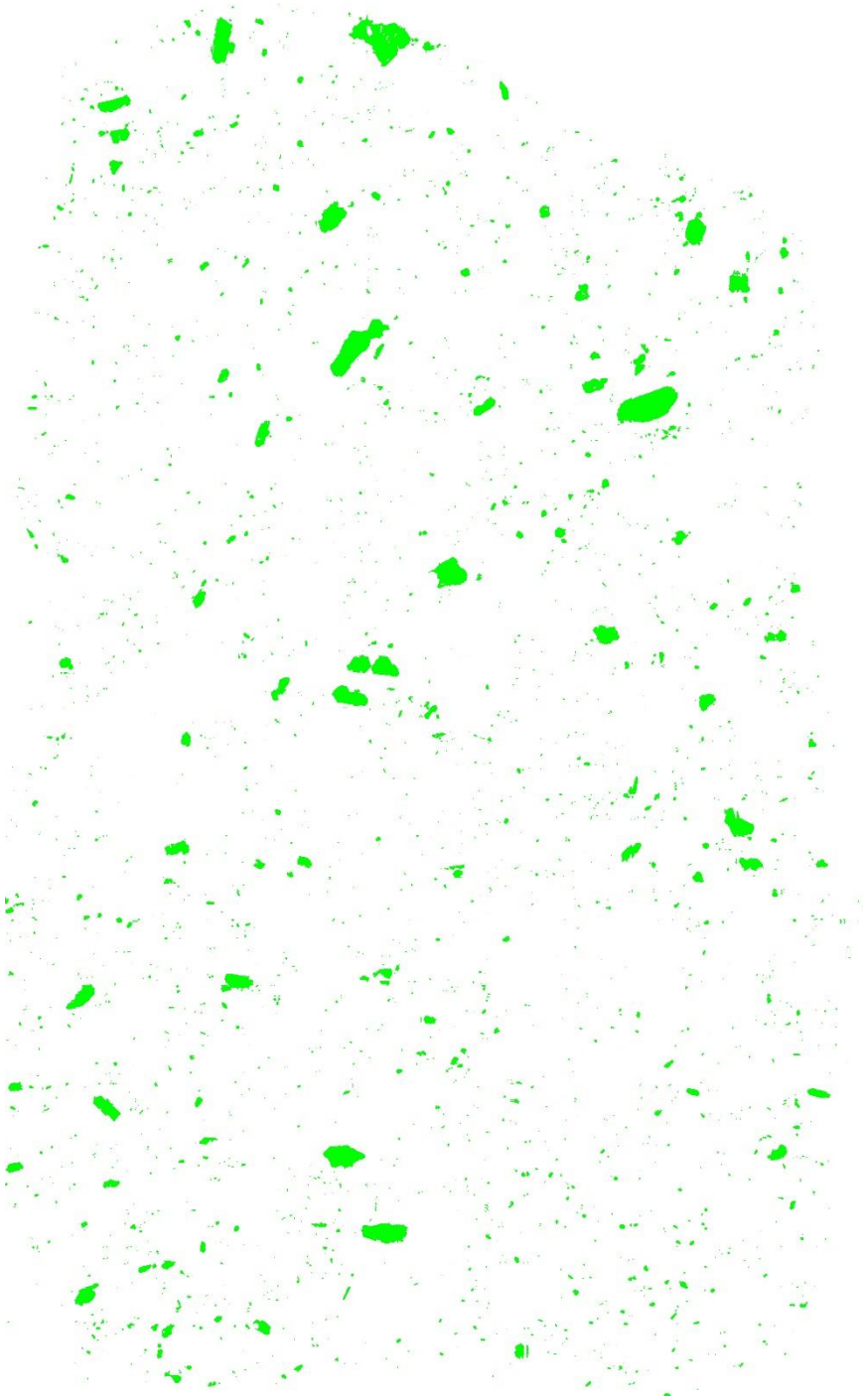

Sample PB-181